



UNIVERSITY OF
PLYMOUTH



School of Geography, Earth and Environmental Sciences Theses
Faculty of Science and Engineering Theses

2017

Tectono-stratigraphic evolution of the offshore Benin Basin, SW Nigeria

Israel Aruoriwo Abiodun Etobro

Let us know how access to this document benefits you

General rights

All content in PEARL is protected by copyright law. Author manuscripts are made available in accordance with publisher policies. Please cite only the published version using the details provided on the item record or document. In the absence of an open licence (e.g. Creative Commons), permissions for further reuse of content should be sought from the publisher or author.

Take down policy

If you believe that this document breaches copyright please [contact the library](#) providing details, and we will remove access to the work immediately and investigate your claim.

Follow this and additional works at: <https://pearl.plymouth.ac.uk/gees-theses>

Recommended Citation

Etobro, I. (2017) *Tectono-stratigraphic evolution of the offshore Benin Basin, SW Nigeria*. Thesis. University of Plymouth. Retrieved from <https://pearl.plymouth.ac.uk/gees-theses/27>

This Thesis is brought to you for free and open access by the Faculty of Science and Engineering Theses at PEARL. It has been accepted for inclusion in School of Geography, Earth and Environmental Sciences Theses by an authorized administrator of PEARL. For more information, please contact openresearch@plymouth.ac.uk.



UNIVERSITY OF
PLYMOUTH

PEARL

PHD

Tectono-stratigraphic evolution of the offshore Benin Basin, SW Nigeria

Etobro, Israel Aruoriwo Abiodun

Award date:
2017

Awarding institution:
University of Plymouth

[Link to publication in PEARL](#)

All content in PEARL is protected by copyright law.

The author assigns certain rights to the University of Plymouth including the right to make the thesis accessible and discoverable via the British Library's Electronic Thesis Online Service (EThOS) and the University research repository (PEARL), and to undertake activities to migrate, preserve and maintain the medium, format and integrity of the deposited file for future discovery and use.

Copyright and Moral rights arising from original work in this thesis and (where relevant), any accompanying data, rests with the Author unless stated otherwise*.

Re-use of the work is allowed under fair dealing exceptions outlined in the Copyright, Designs and Patents Act 1988 (amended), and the terms of the copyright licence assigned to the thesis by the Author.

In practice, and unless the copyright licence assigned by the author allows for more permissive use, this means,

That any content or accompanying data cannot be extensively quoted, reproduced or changed without the written permission of the author / rights holder

That the work in whole or part may not be sold commercially in any format or medium without the written permission of the author / rights holder

* Any third-party copyright material in this thesis remains the property of the original owner. Such third-party copyright work included in the thesis will be clearly marked and attributed, and the original licence under which it was released will be specified. This material is not covered by the licence or terms assigned to the wider thesis and must be used in accordance with the original licence; or separate permission must be sought from the copyright holder.

Copyright statement

This copy of the thesis has been supplied on condition that anyone who consults it is understood to recognise that its copyright rests with its author and that no quotation from the thesis and no information derived from it may be published without the author's prior consent.

**Tectono-stratigraphic evolution of the offshore Benin
Basin, SW Nigeria**

by

ISRAEL ARUORIWO ABIODUN ETOBRO

**A thesis submitted to the University of Plymouth
in partial fulfilment for the degree of**

DOCTOR OF PHILOSOPHY

School of Geography, Earth and Environmental Sciences

November 2017

Abstract

This thesis presents an evaluation of the tectonic and stratigraphic evolution of the offshore Benin Basin based on the analysis of 2D and 3D seismic data, in addition to exploration well data of four closely-spaced wells. To date, little has been published on this part of the African Equatorial Atlantic margin because of the lack of publicly available datasets, and this is the first academic study to be provided with 3D seismic data from this basin. The aims of the study were to establish a tectono-sequence stratigraphic framework for the basin, and to establish the timing, distribution, and nature of tectonic and gravity-driven deformation events. This tectono-stratigraphic evolution was then compared to adjacent and formerly adjacent basins to better understand their significance in relation to the opening of the Equatorial Atlantic and its post-drift history.

Five megasequences have been identified which relate to key tectonic phases in the basin history, and/or major changes in its genetic stratigraphic behaviour. These sequences have been subdivided into seismic sequences. The megasequences are MS1 - pre-rift (Precambrian - Barremian); MS2 - syn-rift (Barremian - late Aptian); MS3 - Cretaceous post-rift (late Aptian - latest Maastrichtian), MS4 - transgressive (latest Maastrichtian - middle Miocene) and MS5 - regressive (Middle Miocene - Holocene).

Rifting by N-S orientated orthogonal extension took place in the Barremian to late Aptian. This led to the formation of two synchronous asymmetrical half-grabens named the northern and southern half-grabens. The rifting ceased in the offshore Benin Basin in the late Aptian (MSB3). This syn-rift megasequence is subdivided into three sequences which can be interpreted to represent rift onset, and rift climax phases, probably associated with the growth, linkage, and abandonment of normal fault systems. There is no evidence in these sequences for transform-related tectonics.

Several short-lived episodes of contractional deformation probably occurred from late Aptian/early Albian to Cenozoic, with the Cretaceous events studied in detail in this thesis. The localised late Aptian/early Albian deformation is restricted to the northern half-graben, and immediately postdates the syn-rift phase. The late Aptian/early Albian deformation formed four structures: Elo thrust, Oga fold, Iro transfer and Ore thrust structures. The E-W striking basin-bounding normal faults (F1 and F2) were not reactivated. However, a NE-SW striking rifts transfer fault was probably reactivated by NW-SE shortening. The late Aptian/early Albian event immediately post-dated rifting and suggests a shift in regional stresses, which may be related to a change from N-S extension to the NE-SW shearing that led to the final separation of plates along the Equatorial Atlantic margin.

The second deformation event occurred in the Santonian (SB3F), and led to the development of the Eji anticline. Despite their age differences, their structures strike in the same NE-SW direction. The late Aptian/early Albian contraction resulted in mild inversion causing intense buckling of the roll-over anticlines associated with the basin-bounding normal fault (F1). Deformation was accommodated by thrusting and folding on the hanging-wall of the basin-bounding normal fault that remains in net extension after the deformation. Contractional deformation propagated to the south in the Santonian (SB3F) reactivating new thrusts and folds. The Santonian event is basement-involved (thick-skinned). Both deformations were probably caused by the reactivation of pre-existing zones of lithospheric weakness due to change in plate motion. A change in motion of the Nubian block from originally N-S to NE-SW direction towards the European Plate has been suggested as the cause of these structures. Both extensional and contractional structures in the study area can serve as potential traps for petroleum.

The data presented in this dissertation are consistent with a two-stage opening model (as proposed by Fairhead et al., 2013) rather than an oblique model (e.g. Heine and Brune, 2014) for the Equatorial Atlantic. This involved an initial phase of N-S orthogonal extension (Barremian-Aptian) which extended into the Central African Rift System and Portuguar Basin (Brazil) and a later NE-SW tranpressional movement, accommodated along evolving transform faults, in the post-Aptian.

Table of Contents

Copyright statement	i
Title page.....	ii
Abstract	iii
Table of contents.....	vi
List of Figures	xii
List of Tables	xxvii
Author's Declaration.....	xxix
Acknowledgments.....	xxx
Chapter One	1
1.0 Introduction.....	1
1.1 General statement.....	1
1.2 Aims and objectives	2
1.2.1 Aims.....	2
1.2.2 Objectives.....	5
1.2.3 Importance of this study.....	5
1.3 Geographical location of the study area	6
1.3.1 The offshore Benin Basin.....	7
1.3.2 Seafloor physiography and bathymetry of southwestern Nigerian margin.....	7
1.3.3 Continent-ocean boundary (COB).....	9
1.4 Precambrian geology and basement reactivation	10
1.5 Regional geological setting of the South Atlantic margin	13
1.6 Opening of the South Atlantic Ocean.....	16
1.7 Rifting of the African intraplate basins	18
1.7.1 Syn-rift phase 1 (142-120 Ma).....	18
1.7.2 Syn-rift phase 2 (119-101 Ma).....	19
1.8 Tectonic evolution of the Equatorial Atlantic margin.....	21
1.9 Existing models for the opening of the Equatorial Atlantic Ocean.....	25
1.9.1 One-stage opening model.....	28
1.9.2 Two-stage opening model.....	29
1.10 Basin architecture of rifted versus transform margins	31

1.11 Previous tectono-stratigraphic studies in the Benin Basin	35
1.12 Stratigraphy of the offshore Benin Basin.....	36
1.12.1 Ise Formation (Early Barremian- Late Aptian).....	37
1.12.2 Albian Sandstone.....	38
1.12.3 Abeokuta Formation (Turonian).....	39
1.12.4 Awgu Formation (Coniacian-Maastrichtian).....	39
1.12.5 Araromi Formation (Maastrichtian-Palaeocene).....	40
1.12.6 Imo Shale (Palaeocene-Eocene).....	40
1.12.7 Oshoshun Formation (Middle Eocene).....	40
1.12.8 Afowo Formation (Early to Middle Miocene.....	41
1.12.9 Benin-Ijebu Formation (Pliocene-Holocene).....	41
1.13 Petroleum systems of the Equatorial Atlantic.....	42
1.13.1 History of petroleum exploration in the offshore Benin Basin.....	43
1.14 Thesis structure.....	44
Chapter Two	46
2.0 Structural and stratigraphic framework of the offshore Benin Basin	46
2.1 Introduction	46
2.2 Aims and objectives	49
2.3 Datasets	49
2.3.1 2D seismic reflection data.....	49
2.3.2 3D seismic reflection data.....	50
2.2.3 Polarity and quality of the seismic data.....	52
2.3.4 Well data.....	55
2.3.5 Biostratigraphic datasets.....	56
2.3.6 Other datasets.....	58
2.4 Explanation of the abbreviations and definitions of terminology used in this study.....	59
2.5 Methodology	63
2.5.1 Seismic stratigraphic interpretation.....	64
2.5.2 Seismic facies analysis.....	70
2.5.3 Well-log analysis.....	71
2.5.4 Structural analysis.....	72
2.6 Seismic stratigraphic framework of the offshore Benin Basin.....	74
2.6.1 Pre-rift megasequence (MS1), Precambrian – Barremian.....	75
2.6.2 Syn-rift megasequence (MS2), Barremian (MSB2) – Aptian (MSB3).....	78

2.6.3 Post-rift stratigraphy (MS3, MS4, and MS5).....	80
2.7 Structural framework in the offshore Benin Basin.....	87
2.8 Tectonic structures	88
2.8.1 Northern and southern half-grabens and their basin-bounding normal faults (F1 and F2).....	88
2.8.2 Transfer structure (F5).....	89
2.9 Tectonic contractional structures.....	89
2.9.1 Inverted structures.....	91
2.9.2 Reverse and thrust faults.....	91
2.9.3 Anticlinal structures.....	92
2.10 Gravity-induced structures	92
2.11 Problems of correlating across the northern and southern half-grabens	95
2.12 Regional correlation of the megasequence boundaries (MSB2-MSB5)	95
Chapter Three	100
3.0 Tectono-stratigraphy and structure of the syn-rift megasequence MS2, offshore Benin Basin.....	100
3.1 Introduction	100
3.2 Aims and objectives	101
3.3 Review of rift models and rift stratigraphy	102
3.3.1 The models of lithospheric extension.....	102
3.3.2 Basin development and geometry.....	107
3.4 Rift tectono-stratigraphy.....	111
3.5 Methodology	112
3.5.1 Structural analysis.....	114
3.6 Detailed syn-rift stratigraphy and structure of the offshore Benin Basin.....	115
3.6.1 Early rift sequence S2A (Early Barremian, MSB2 - late Barremian/early Aptian, SB2B).....	117
3.6.2 Rift-climax sequence S2B (late Barremian/early Aptian - middle Aptian...)	121
3.6.3 Late rift sequence, S2C, (middle Aptian, SB2C – late Aptian, MSB3).....	124
3.7 Analysis of the basin-bounding normal faults (F1 and F2) and their orientation	127
3.8 Structural styles in the offshore Benin Basin	131
3.9 Benin Basin: an extensional or a transform basin?	132
3.10 Discussion	134
3.10.1 Evolution of the offshore Benin Basin.....	134
3.11 Conclusions	143

Chapter Four	146
4.0 Cretaceous post-rift megasequence MS3 (late Aptian – latest Maastrichtian)	146
4.1 Introduction	146
4.2 Aims and objectives	147
4.3 Methodology	148
4.4 Post-rift stratigraphy	148
4.4.1 Breakup unconformity and breakup sequence concepts.....	148
4.5 Seismic Stratigraphy of the Cretaceous post-rift megasequence MS3 (late Aptian, MSB3 - latest Maastrichtian, MSB4)	151
4.5.1 Immediate post-rift sequence, S3A (late Aptian - early Albian).....	151
4.5.2 Parallel reflection sequence S3B (middle Albian).....	151
4.5.3 High amplitude parallel reflections, S3C (late Albian - Cenomanian)..	153
4.5.4 Parallel reflection sequence (S3D) (Cenomanian - late Turonian).....	156
4.5.5 Transparent reflections sequence (S3E) (Turonian - Santonian).....	156
4.5.6 Parallel reflection sequence (S3F) (late Santonian).....	158
4.5.7 High amplitude reflection sequence (S3G) (Maastrichtian).....	158
4.6 Post-rift contractional deformation in offshore Benin Basin	161
4.7 Late Aptian/early Albian deformation	161
4.7.1 Elo thrust (late Aptian/early Albian).....	164
4.7.2 Oga fold (late Aptian/early Albian).....	166
4.7.3 Ore thrust (late Aptian/early Albian).....	169
Timing of the late Aptian/early Albian deformation.....	171
4.7.4 Iro transfer zone (middle Aptian).....	172
4.8 Santonian deformation (SB3F).....	174
4.8.1 Location of the Eji anticline (Santonian, SB3F) in megasequence MS3.....	175
4.9 Relationship in timing between the Santonian deformation and slumping.....	178
4.10 Young deformation event (?Miocene).....	181
4.11 Mechanisms/causes of the contractional deformation in the offshore Benin Basin	181
4.12 Influence of the deformation events on stratigraphy and depositional systems in the offshore Benin Basin.....	186
4.13 Discussion	188
4.13.1 Significance of the breakup sequence in the offshore Benin Basin.....	188
4.13.2 Post-rift deformation and petroleum systems in the offshore Benin Basin.....	191

4.14 Conclusions.....	195
Chapter Five	197
5.0 Cenozoic Geology of the offshore Benin Basin	197
5.1 Introduction.....	197
5.2 Aims and objectives.....	198
5.3 Terminology applied in this chapter.....	199
5.3.1 Mass-transport complexes (MTCs).....	200
5.4 Methodology.....	201
5.4.1 Sequence stratigraphic analysis.....	201
5.4.2 Structural analysis.....	203
5.5 Sequence stratigraphy of the Cenozoic offshore Benin Basin.....	203
5.5.1 The transgressive megasequence (MS4).....	203
5.5.2 The regressive megasequence (MS5) (MSB5, middle Miocene to MSB6, Holocene).....	208
5.6 Analysis of relative changes in sea level.....	212
5.6.1 Neal and Abreu (2009) model.....	214
5.7 Structural setting of the Cenozoic offshore Benin Basin.....	217
5.7.1 Late Miocene-Pliocene slump event.....	218
5.8 Mass-transport complexes (MTCs) of the offshore Benin Basin.....	219
5.8.1 Recognition of the mass-transport complexes (MTCs) on seismic data.....	219
5.9 Mass-transport complexes of the offshore Benin Basin.....	221
5.9.1 Mass-transport complex 1 (MTC1) (late Miocene-Pliocene).....	223
5.9.2 Mass-transport complex 2 (MTC2) (Pleistocene).....	225
5.10 Discussion.....	227
5.11 Conclusions.....	228
Chapter Six	229
6.0 Discussion	229
6.1 Introduction.....	229
6.2. Early Barremian (MSB2) to Late Aptian (MSB3) continental rifting.....	230
6.2.1 Lack of evidence for transform tectonics.....	230
6.2.2 Rifting of the offshore Benin Basin.....	230
6.2.3 Significance of north-dipping normal faults.....	233
6.2.4 Significance of the breakup sequence.....	236
6.3 Late Aptian (MSB3) to Santonian (SB3F) tectonics.....	236
6.4 Santonian basin inversion.....	240

6.5 Opening models for the Equatorial Atlantic.....	241
6.6 Cenozoic sedimentation	242
6.7 Implications of tectonics for the hydrocarbon entrapment in the offshore Benin Basin.....	243
Chapter Seven	245
7.0 Summary, Conclusions, and Recommendations	245
7.1 Summary	245
7.2 Conclusions	248
7.3 Recommendations	249
7.3.1 Limitations of this study.....	249
7.3.2 Future Work.....	251
References	253

List of Figures

Chapter One

Figure 1.1: The Equatorial Atlantic segment displays its characteristic fracture zones (St Paul, Romanche and Chain Fracture Zones). Both margins of the Northeast Brazil and West Africa are characterised by alternating E-W and NE-SW conjugate basins. The basin of the present study (Benin Basin and its conjugated divergent basin- Mundaú Basin, both generally trend E-W) (modified after Basile et al., 2005).....3

Figure 1.2: Oil and Gas fields in the Equatorial Atlantic region between Côte d'Ivoire and Cameroun. The concentration of these activities in the Cenozoic Niger Delta Basin while the Cretaceous basins are marked by fewer discoveries, and the Benin Basin being one of the least explored basins along the Equatorial Atlantic margin 4

Figure 1.3: Bathymetric map of Southern Nigeria showing submarine features such as submarine canyons and fans extending from the Nigerian part of the Benin Basin to the offshore Niger Delta to the east. Note the study area lies between the continental shelf and continental slope (after Olabode and Adekoya, 2008)..... 8

Figure 1.4: Gravimetric map of the Equatorial Atlantic showing the study area (small red rectangle). Line AA' is an N-S oriented seismic section shown in Figure 2.3. The continent-ocean boundary (COB) is indicated by the heavy red line. Note that the study area, offshore Benin Basin occurs some distance away from a major fracture zone (i.e. Chain fracture zone). The fracture zone occurs obliquely to the approximately E-W striking Benin Basin. Gravity anomaly values are in milliGal (mGal). (modified after Sandwell and Smith, 1997; Davies et al., 2005)..... 11

Figure 1.5: Major fault zones of Gondwana that may reactivate under stresses such as those related to change in plate motion. Gondwana reconstruction and apparent Archaean and Palaeoproterozoic cratons (in grey) after Rogers et al. (1995). Note these fault zones became weak zones that controlled ocean opening and intraplate deformation changes in the stress field were recorded, especially between South America and Africa. Where: Ag. = Agulhas; C = Central; CAFZ = Central African Fault Zone; Ch. = Chain; Dam. = Damara; Fal. = Falkland; GNL = Guinean-Nubian Lineaments; H. = Hodna; Hog. = Hoggar; Moz. = Mozambique; N-S = Narmada Son; N. Taoud, = North Taoudenni Lineament; R. = Rukwa; Tanz. = Tanzania; TB = Trans-Brasiliano; Tib. = Tibesti; TL = Tibesti Lineament.

Apparent curvature of the Tibesti Lineament is due to the map's projection (from Guiraud et al., 2000).....	12
Figure 1.6: The South Atlantic is subdivided into four segments from the south to north: the Falkland, South, Central and Equatorial segments. Note that the study area is located on the Equatorial segment of the South Atlantic at its eastern border (the Chain Fracture Zone). The study area occurs some distance away from the Continent-Oceanic Boundary (COB) (after Moulin et al., 2010).....	14
Figure 1.7: 117 Ma reconstruction (Heine et al., 2013). Note that the northernmost segment of South Atlantic Rift System (SARS) is already in seafloor spreading mode in the Equatorial Atlantic (EqRS), the breakup is incipient. Minor rigid plates: BPB - Borborema province block (northeast Brazil), Jos - Jos subplate (northern Nigeria), SLC - São Luís Craton. Basins (B): BeT - Benue Trough, FdA - Foz do Amazonas Basin, GG - Gurupi Graben, IuB - Iullemmeden Basin, MarB - Marajó Basin, MB - Maranhão Basin, PotB - Potiguar Basin; SAf - South African block; Sam - South American block; NWA - Northwestern African block; WARS - West African Rift System; CARS - Central African Rift System (after Heine and Brune, 2014).....	16
Figure 1.8: Regional index map of the West and Central African Rift systems (WCARS). Note that most of the intraplate basins in these regions evolved through NE-SW continental extension. The southern Sudan rift is also called Muglad rift. The east Niger basins (Niger rift) are a complex rift zone with the Termit Basin as its major element. Some of the basins cited in the text: DS = Doseo; BG = Bongor; BR = Borno; MG = Muglad; TN = Tenéré (after Warren, 2009; Fairhead et al., 2013).....	20
Figure 1.9: Models of transform continental margin evolution. Note that the opening of the Equatorial Atlantic margin demonstrates a one-stage model from the intracontinental stage to the post-transform stage (after Mercier de Lépinay et al., 2016).....	25
Figure 1.10: Schematic Cretaceous stages in the Mesozoic breakup of Africa and South America highlighting the tectonic evolution of the Equatorial Atlantic, and showing the approximate location of the Bové, Benin, Ivory Coast, Keta, Senegal, Volta Basins and the Benue Trough of Africa, and the Para-Maranhão Basin of Brazil. A, Hauterivian, 125 Ma; B, early Albian, 110 Ma; C, late Albian, 100 Ma; D, Santonian, 85 Ma (from Mascle et al., 1988; Brownfield and Charpentier, 2006).....	26

Figure 1.11: Line drawings of seismic reflection profiles perpendicular to Côte d'Ivoire-Ghana transform margin. Note that the continental slope is steeply-dipping (after Basile et al., 1998; 2005; Antobreh et al., 2009; Mercier de Lépinay et al., 2016).....27

Figure 1.12: A one-stage opening model of the Equatorial Atlantic Ocean involving the African Plate moving dominantly northeast in the Albian. A solely NE movement of the African Plate initiated through the re-activation of the Central African Shear Zone (CASZ; red line indicates active shear zone) (i.e. intraplate rifting; e.g. Heine and Brune, 2014)..... 29

Figure 1.13: A two-stage opening model resulted in the opening of the Equatorial Atlantic Ocean. A) An initial opening involved the northward movement of the African Plate relative to the South American Plate in Barremian. A northward movement of the African Plate occurred due to movement along the re-activated N-S Sobral Fault (the red line indicates active fault) (e.g. Moulin et al., 2010). B) A stage 2 NE-SW movement as a consequence of change in the direction of movement of the African Plate in the Albian. The NE movement occurred through the re-activation of the Central African Shear Zone (red line) (CASZ; e.g. Fairhead et al., 2013).....30

Figure 1.14: Examples of seismic sections obtained from different locations (B) in the Equatorial Atlantic margin. A) Seismic section (A-A') across the NE-SW trending Côte d'Ivoire-Ghana Transform Margin showing some characteristic features of a transform margin such as a sharp gradation from the continental shelf to basin floor (after Clift et al., 1997; Bird, 2001). B) Physiographic map of Gulf of Guinea in the Equatorial Atlantic region showing the study area (blue box) and locations of seismic sections (after Delteil et al., 1974). C) Seismic section (C-C') representing the E-trending Keta Basin and showing a relatively gradual change from continental shelf through continental slope to continental rise. D) Seismic section (D-D') across the (E-W) trending Benin Basin showing a gradual change in slope gradient from continental shelf to the slope and a rise (after Delteil et al., 1974). 33

Figure 1.15: Stratigraphy of the offshore Benin Basin. Both the ages (for the Barremian-Aptian rift episode) and tectonic stages have been modified to reflect this study (modified after Omotsola and Adegoke, 1981; Brownfield and Charpentier, 2006 and Kaki et al., 2012)..... 37

Chapter Two

- Figure 2.1: Basemap of the study area showing the location of the interpreted datasets; well data, 2D, and 3D seismic data. Note the four wells are located within the Aje Field in the 3D survey area (dashed rectangle). The vertical and horizontal lines represent 2D dip and strike lines. The continuous vertical lines are the 2D lines used in conjunction with 3D seismic data. Red lines indicate locations of some of the seismic sections used in this chapter..... 47
- Figure 2.2: Seismic section (crossline 3802) containing plots of GR-log and some of the biozones and formation tops at well B-04 (the referenced well). Good ties exist amongst most of the interpreted seismic horizons, the formation tops (biozones) and well-logs. Some of the spikes on the GR-log tie with reflection terminations or horizons. See Figure 2.1 for the location of the seismic section..... 48
- Figure 2.3: 2D seismic section showing the area extent of the 3D survey (red rectangle). Two half-grabens and their characteristic basin-bounding normal faults (F1 and F2) interpreted in the study area. CSB5B refers to a second composite sequence boundary within MS5. Location of the seismic section is shown in Figure 2.1.....54
- Figure 2.4: Different well-logs (Velocity, Sonic, and Density) of Well B-04 cross-plotted with the synthetic seismograph on Kingdom Workstation. Formation Tops that were provided correlate and tie with some spikes. Reflection terminations (onlap, downlap, toplap and erosional truncations) identified in this study correlate and tie with these Formation Tops..... 58
- Figure 2.5A) Uninterpreted 3D seismic section (crossline 4342). See Figure 2.5B for the interpretation of the seismic section..... 68
- Figure 2.6: Line diagram showing a characteristic wedge-shaped geometry (yellow) of the syn-rift phase of basin development. The syn-rift phase consists of reflections diverging away from the main fault (the basin-bounding normal fault). The dips also increase downwards because of progressive rotation in the hanging-wall. Note that both pre-rift and post-rift phases comprise parallel reflections. However, the pre-rift may sometimes show chaotic reflections. Reflections of the wedge geometry progressively onlap the rift-onset unconformity, while the post-rift reflections onlap the post-rift unconformity. Red arrows point to stratal onlap (modified after Leeder and Gawthorpe, 1987; Prosser, 1993)..... 70
- Figure 2.7: Reflection terminations used to define seismic sequence and megasequence boundaries (from Mitchum et al., 1977).....71

Figure 2.8: Some examples of reflection configurations used for the identification of seismic facies. They often describe the internal components of a seismic sequence (after Vail et al., 1977 and Mitchum et al., 1977).....	72
Figure 2.9: Log patterns for palaeoenvironmental reconstructions (after Nyantakyi et al., 2013).....	73
Figure 2.10: Fault interpretation on a seismic section (crossline 3828) based on the discontinuity and displacement of seismic reflections. See Figure 2.1 for the location of the seismic section.....	76
Figure 2.11: Measurement of fault dips (e.g. reverse fault, F3). The dip (θ) of the fault was taken using the horizontal line (black broken line) as reference. See Figure 2.1 for the location of the seismic section (Inline 1344).....	77
Figure 2.12: Interpretation of a fold on a seismic section (inline 1329); a flexure of a seismic horizon often indicates a fold. The pre-rift megasequence (MS1) has been displaced by the reverse fault (F3). Strata that were deposited before the Santonian are all folded, whereas younger strata above the Santonian unconformity appear to be nearly horizontal and sub-parallel. Reflections overlying the Santonian onlap these later strata (red arrows indicate onlap). See Figure 2.1 for the location of the seismic section.....	79
Figure 2.13: Megasequences (MS2-MS5) interpreted based on well-log data (GR and resistivity logs) from well B-04. The pre-rift megasequence (MS1) was interpreted as crystalline basement on the basis of its reflection character. The base (MSB2) of the syn-rift megasequence (MS2) was not penetrated by the well. The early-rift sequence (S2A) was partly penetrated.....	80
Figure 2.14: A) Crossline 4342 showing the two half-grabens referenced to in the text with their characteristic wedge geometries. The seismic reflections of the syn-rift megasequence (MS2) thicken toward the basin-bounding normal faults (F1 and F2) in both half-grabens. The syn-rift megasequence (MS2) is subdivided into three sequences early rift sequence (S2A), rift-climax sequence (S2B), and late rift sequence (S2C). See Figure 2.17 for the location of the seismic section.....	81
Figure 2.15: A) Uninterpreted seismic section (crossline 4608). B) Line interpretation of the pre-rift, syn-rift, and parts of the post-rift megasequences. The wedge geometry of the syn-rift megasequence (MS2) is overlain by parallel reflectors. TBS = Top of breakup sequence; BS = breakup sequence. See Figure 2.17 for the location of the seismic section.....	83

Figure 2.16: Crossline 2482 summarises the Cenozoic geology in the offshore Benin Basin. Cenozoic strata are grouped into two megasequences in this study: a transgressive megasequence (MS4) and a regressive megasequence (MS5). Gravity-induced faults and some other mass-transport complexes (MTCs) are associated with both megasequences. Red arrows indicate reflection terminations. CSB = composite sequence boundary. See Figure 2.17 for the location of the seismic section..... 84

Figure 2.17: A composite structural element map showing the main tectonic structures (the main basin-bounding normal faults, F1 and F2; transfer fault, F5; thrust and reverse faults) in the study area. The location of some of the figures cited in this chapter are also indicated..... 90

Figure 2.18: 3D seismic section (crossline 3940) displaying the two main contractional deformation phases analysed in this thesis (late Aptian/early Albian and Santonian). See Figure 2.17 for the location of the seismic section.....93

Figure 2.19: A regional correlation of the megasequence boundaries interpreted for the offshore Benin Basin (OBB), highlighting the continental rifting episodes in the intraplate basins of West and Central African rift system (WCARS). Note that the rift onset (MSB2) and post-rift (MSB3) unconformities in the offshore Benin Basin correlate with on-going rifting in the WCARS. Other megasequence boundaries (base of transgressive megasequence MSB4, and base of regressive megasequence MSB5), despite their non-tectonic origin, correlate respectively with end-of- and on-going-rifting in the WCARS. Vertical thick lines indicate rifting events whereas wavy red lines denote unconformities. Shaded areas show erosion or much-reduced sedimentation, i.e. condensed sections (modified after Fairhead et al., 2013)..... 99

Chapter Three

Figure 3.1: Schematic representation of the principal modes of lithospheric extension, A) Wide rift mode B) narrow rift mode, C) core complex mode (after Buck, 1991; Rosenbaum et al., 2008)..... 104

Figure 3.2: Schematic models of continental lithospheric extension: A) McKenzie pure shear model, B) Wernicke simple shear model, C) delamination model (after Lister et al., 1986)..... 105

Figure 3.3: Detachment-fault model for passive continental margins with A) lower-plate or upper-plate characteristics. The lower-plate margin has complex structure; tilt

blocks are remnants from the upper plate, above bowed-up detachment faults. B) The upper-plate margin is relatively unstructured. Uplift of the adjacent continent is caused by underplating of igneous rocks. Multiple detachments have led to two generations of tilt blocks in the diagram shown. Opposing passive margin pairs exhibit marked but complementary asymmetry (after Lister, 1986)..... 106

Figure 3.4: Basin development and characteristic geometry of rift basins (after Ravnas and Steel, 1998)..... 109

Figure 3.5: A) Half-graben morphology and rift-interior sediment dispersal pattern. B) Dip section through rifted terrains showing accommodation, intrabasinal drainage, and sediment dispersal direction in: (I) a solitary half-graben, (II) a series of half-grabens with simple basin-bounding master faults, and (III) a series of half-grabens with segmented fault-complex or collapsed footwall as basin-bounding structures (after Ravnâs and Steel, 1998)..... 110

Figure 3.6: Line diagram showing the different configurations of pre-rift, syn-rift and post-rift strata in both lateral (A) and cross-section (B) views. ET = erosional truncation; PRU: post-rift unconformity. Modified after Williams (1993)..... 114

Figure 3.7: a) The three principal stresses and the three planes of zero shear stress on which they act. B) The three stress ellipsoid, defined by the three principal stresses (after Rowland et al., 2007)..... 116

Figure 3.8: Block diagram and equal area plots of the three classes of faults predicted by Anderson (1942). The equal area stereograms show typical fault and slickenside orientation data for each set of faults within each of Anderson's (1942) classes. For normal faults (a) and thrust faults (c), the arrows on the great circles of the stereograms point in the direction of the hanging-wall motion. For strike-slip faults, the arrows on the great circles indicate the sense of shear (after Rowland et al., 2007)..... 117

Figure 3.9: 3D seismic section (crossline 3940) showing syn-rift megasequence MS2 (S2A, S2B, and S2C) comprising thickening of strata towards the main basin-bounding normal fault (F1) in spite of the late Aptian/early deformation in the northern half-graben. See Figure 2.17 for the location of the seismic section..... 120

Figure 3.10: Relay structure with synthetic normal faults and its stratigraphy. See Figure 3.14 for the seismic section location..... 121

Figure 3.11: Crossline 4328 showing a syn-rift megasequence (MS2) comprising the three sequences S2A, S2B, and S2C. Note the reflection divergence that characterises the syn-rift megasequence. The post-rift unconformity (PRU), MSB3,

shows onlap, erosional truncation, and offlap (red arrows). TBS = Top of breakup sequence. See Figure 3.14 for the location of the seismic section.....	122
Figure 3.12: Lithologic interpretation of the syn-rift megasequence, MS2 (S2A+S2B+S2C) Barremian to late Aptian and the overlying breakup sequence (early to middle Albian, part of the Cretaceous post-rift megasequence, MS3. The syn-rift megasequence is composed of both fining- (FU) and coarsening-upward (CU) patterns. Whereas the breakup sequence is made up of the cylindrical pattern.....	123
Figure 3.13: Vertical profile (crossline 4640) showing the southern half-graben and its characteristic wedge geometry consisting of three sequences (S2A, S2B, and S2C) which have been classified as the syn-rift megasequence (MS2). S2A = early rift sequence; S2B = rift-climax sequence, and S2C = late rift sequence. Red arrows indicate the reflection terminations. Figure 3.14 shows the location of seismic section.....	126
Figure 3.14: TWT structural map of the base of the rift-climax stage (early Aptian) showing the strike of the main structures (fault and anticline) as E-W to ENE-WSW. The basin-bounding normal fault (F2) of the southern half-graben was not fully covered by the 3D survey. The southern half-graben, however, maintains a similar strike to the northern half-graben.....	129
Figure 3.15: Seismic section (crossline 4328) interpreted and flattened along the top of the breakup sequence (TSB). Note that the two half-grabens retained their wedge geometries below MSB3 (i.e. the post-rift unconformity, PRU). The basin-bounding normal faults (F1 and F2 appear steeper after the flattening is applied, see also on Figure 3.11. MSB2= rift onset. See Figure 3.14 for the location of the seismic section.....	135
Figure 3.16: Gawthorpe and Leeder (2000) models modified for the study area. Schematic diagram showing that the 3D evolution of normal fault arrays can enhance the formation of a major basin-bounding normal fault. A) Fault initiation stage in the study area was characterised by a large number of small-displacement normal fault segments (Fi-Fvii) in the Barremian. B) Fault interaction and linkage stage; at this stage small-displacement normal faults (Fii, Fiii, and Fiv) were linked together C) Through-going fault zone stage, where deformation is localised along major border fault zone 1; a final linkage to the remaining small faults give rise to the evolution of two basin-bounding normal faults (F1 and F2).....	138

Figure 3.17: Schematic diagram of the stages of evolution of the offshore Benin Basin during the Barremian-Aptian rifting episode.....139

Figure 3.18 A): Uninterpreted seismic section (on preceding page). B): Schematic representation of the tectonic evolution of the offshore Benin Basin in the Barremian-Aptian. A localised inversion post-dated continental rifting in the northern half-graben in the late Aptian/early Albian.....142

Chapter Four

Figure 4.1: Development of Atlantic-type or rifted continental margins from their initial doming' to an incipient rift, widening rift valley and continental breakup. Seafloor spreading and subsidence of the new continental margin occur after continental breakup (after Falvey, 1974)..... 149

Figure 4.2: Crossline 3968 showing main seismic sequences and at least two phases of deformation events in the late Aptia/early Albian, and Santonian (SB3F). Red arrows show onlap onto fold limb in both phases. Apt. = Aptian, Alb. = Albian, E. = early, M. = middle, L. = late, PRU = post-rift unconformity. See Figure 4.8 for the location of the seismic section.....152

Figure 4.3: Crossline 4646 showing the seismic sequences in the syn-rift megasequence with a characteristic wedge pattern. The post-rift phase developed a parallel to sub-parallel reflection geometry. Note the propagation of the basin-bounding normal fault (F1) above the post-rift unconformity (PRU) in the northern half-graben. Sequence S3A comprising parallel reflections passively filled an inherited 'wedge geometry' in both half-grabens. See Figure 4.8 for the location of the seismic section..... 155

Figure 4.4: Uninterpreted (A). Interpreted inline 1100 (B) showing erosional features (forced regression) at MSB3 forming an erosional 'canyon' into MS2). This has been draped by a series of sequences that correlate to the breakup sequence (S3A and S3B). See Figure 4.8 for location of the seismic section..... 157

Figure 4.5: Vertical profile (crossline 3808) highlighting the upper part of the post-rift succession within a folded megasequence MS3. See Figure 4.8 for the location of the seismic section..... 159

Figure 4.6: Crossline 3762 showing the internal seismic characters of sequences of megasequences M2 and MS3. Well signatures of the megasequence MS3 are also shown. See Figure 4.8 for the location of the seismic section.....160

Figure 4.7: Crossline 3884 highlighting the relationship between the Santonian (SB3F) contractional deformation, Campanian slumping and the Miocene/Pliocene slumping observed in the study area. SB3F cuts down through sequences S3E and S3D. The erosion of these sequences is not related to slumping because they are not translated downslope. Red arrows and yellow dots show onlapping reflections. See Figure 4.8 for the location of crossline 3884.....	162
Figure 4.8: TWT isochron map of the top of breakup sequence, S3A (early Albian). Some of the figures cited in this chapter are indicated in this figure.....	163
Figure 4.9: Arbitrary line (NW-SE) seismic section uninterpreted (A) and interpreted section (B). Elo thrust (F6) is located close to the main basin-bounding normal fault (F1). The roll-over structure of the main fault (F1) and the wedge pattern associated with F1 are still preserved. Fault F1 is still in net extension, suggesting it was not inverted. The thrust fault (F6) offsets the early Aptian. Onlap of parallel reflections onto the fold limb of fold (late Aptian/early Albian. See Figure 4.10 for the location of the seismic section.....	165
Figure 4.10: Isochron map of the top of the late Aptian/early Albian fold onset unconformity. Location of seismic sections shown in this chapter indicated in this figure.....	167
Figure 4.11: Dip line (crossline 3968) depicting the Oga fold in the northern half-graben. Note the onlapping seismic reflections on the forelimb of the fold. Seismic reflections were truncated by the post-rift unconformity (MSB3, Late Aptian). See Figure 4.10 for the location of the seismic section.....	169
Figure 4.12: Arbitrary line (NW-SE) displaying the relationship between the Ore thrust and the Iro transfer in time of formation. See Figure 4.10 for the location of the seismic section.....	170
Figure 4.13: An arbitrary line (NW-SE) showing the Iro relay structure. See Figure 4.10 for the location of the seismic section.....	172
Figure 4.14: Association of some small faults (relay) and the basin-bounding normal fault (F1) in the northern half-graben, compared to the less deformed southern half-graben (see Figure 4.10 for the location of crossline 2698 shown in this figure).	174
Figure 4.15: Inline 1398 showing the Eji anticline and the characteristic thinning of the sequence (S3F) at the fold hinge. In contrast, sequence S3F thickens at the backlimb and forelimb of the fold. Red arrows indicate where the canyon cuts to the north. Note the thick sediment to the SE as a result of Santonian deformation. See Figure 4.16 for the location of the seismic section.....	177

Figure 4.16: Time-structural map of the top Santonian (SB3F) in the study area. Note the high relief in the northeastern part of the map marking the position of the Eji anticline. A hinge line that may mark the Santonian palaeo-shelf edge occurs roughly along the thick blue line. Black arrows point to a NW-SE shortening direction. The locations of some of the seismic sections cited in the main text are indicated in this figure..... 179

Figure 4.17: Coast-parallel line (inline 1380) showing the Eji anticline as formed by a basement-involved reverse fault (F3). Note the onlapping of parallel reflections on top of the forelimb of the anticline in SB3F (Santonian). Red arrows indicate the onlap of parallel reflections onto the forelimb of the anticline. The basement appears deformed by other subordinate small faults. See Figure 4.16 for the location of the seismic section.....180

Figure 4.18: Crossline 3906 shows the relationship between the Santonian deformation, submarine erosion and slumping. See Figure 4.16 for the location of the seismic section..... 182

Figure 4.19: Schematic diagrams of the development of the Santonian deformation, submarine erosion and slumping..... 183

Figure 4.20: Crossline 3208 highlighting the folding of post-Santonian sequences. A possible ?Miocene folding event indicated by strata (red arrows) onlap, is proposed for this deformation. See Figure 4.16 for the location of the seismic section..... 184

Figure 4.21: During the late Aptian/early Albian, a NW-SE oriented stress probably caused the mild inversion of the transfer fault F5..... 185

Figure 4.22: Structural elemental map showing the major tectonic features in the offshore Benin Basin. The major features are the E-W to ENE-WSW striking basin-bounding normal faults (F1 and F2) of Barremian-Aptian age. The later ones include NE-SW transfer structure (F5) (middle Aptian); the late Aptian/early Albian deformation (Elo thrust, Oga fold and Ore thrust). The last tectonic event recorded in the study area was in the Santonian (Eji anticline). Note how the later tectonic events (e.g. transfer fault F5; the reverse fault F3) offset the main basin-bounding normal fault F1 in the north. The locations of some of the seismic sections cited in the main text are indicated in this figure.....187

Figure 4.23: Lithologic analysis of sequence S3F based on the GR log of B-04. Sequence S3F consists of sandstone and shale. See Figure 4.22 for the location of the seismic section (crossline 3786)..... 188

Figure 4.24: A) Uninterpreted NW-SE arbitrary seismic section. B) Interpreted section showing how contractional structures (folds and faults) may enhance accumulation of hydrocarbons in the offshore Benin Basin. See Figure 4.22 for the location of the seismic section..... 193

Figure 4.25: Summarised implications of the Santonian deformation for petroleum systems in the offshore Benin Basin. A) Interpreted seismic section (inline 1407) showing the seismic character of potential source rocks, reservoir rocks, petroleum seal and a possible migration pathway (F3) for the offshore Benin Basin. B) Petroleum systems of the basin as interpreted from seismic data. Note that the major reverse fault (F3) serves as migration pathway for hydrocarbons. See Figure 4.16 for the location of the seismic section. See Figure 4.22 for the location of the seismic section..... 194

Chapter Five

Figure 5.1: Schematic classification of MTCs based on causal mechanisms and pre-failure conditions. (a) Slope attached mass-transport complex. (b) Shelf-attached mass-transport complex. (c) Detached mass-transport from collapsing flank of a mud-volcano ridge. (d) Detached mass-transport complex formed through oversteepening of one of the margin. (e) Detached mass-transport complex derived from a levee-channel complex (from Moscardelli and Wood, 2008)..... 202

Figure 5.2: Interpretation procedure of shoreline trajectories (after Christie-Blicke, 1991)..... 204

Figure 5.3: Crossline 3858 displaying slumping in megasequence MS4. The deformed MS4 mainly comprises extensional faults; reverse/thrust faults were probably eroded by canyon. See Figure 5.11 for the location of the seismic section..... 206

Figure 5.4 Crossline 3836 showing the internal character of transgressive megasequence MS4. See Figure 5.11 for the location of the seismic section..... 207

Figure 5.5: 2D line (N06) highlighting some of the stratigraphic features of the regressive megasequence MS5. A) Uninterpreted seismic profile. B) Regressive megasequence MS5 showing some of the diagnostic features for the recognition of seismic sequence. C) Line interpretation of the regressive megasequence MS5. Coastal onlaps define for the sequences. Red arrows indicate seismic reflection terminations. See Figure 5.11 for the location of the seismic section..... 210

Figure 5.6: 2D line (N08) showing discrete sequences within the regressive megasequence MS5. See Figure 5.11 for the location of the seismic section.....	213
Figure 5.7: Sea level curve obtained for the Cenozoic Benin Basin (offshore) on the basis of the mapping of coastal onlaps. It shows a relative rise in sea level for the transgressive megasequence (MS4, Latest Maastrichtian to middle Miocene), and a relative fall in sea level for the regressive megasequence (MS5, middle Miocene to Holocene). See Figure 5.11 for the location of the seismic section. Modified after Vail et al. (1977) and Christie-Blick (1991). Geological time scale obtained from International Chronostratigraphic Chart, 2017.....	216
Figure 5.8: Crossline 4240 showing the Miocene-Pliocene slump and its diagnostic features. See Figure 5.11 for the location of the seismic section.	220
Figure 5.9: Diagnostic criteria of mass-transport complexes (MTCs) (after different authors indicated on them).....	222
Figure 5.10: Examples of some MTCs in the study area. See Figure 5.11 for the location of the seismic section.....	224
Figure 5.11: Isochron map to base of the transgressive megasequence boundary (MSB4, latest Maastrichtian). Evidence of the slumping and some ancient submarine canyons are eminent. The locations of some of the seismic sections cited in this chapter are indicated in this figure.....	226

Chapter Six

Figure 6.1: Palaeogeographic reconstruction of the Equatorial Atlantic Ocean. The figure shows, on each plate, gravity data from Sandwell and Smith (1997) between the coast and the area of continental breakup. The heavy red line shows the breakup separation between the plates by incipient seafloor spreading. Note the remarkable alignment of the conjugate pre-breakup fault systems (in blue: Kandi/Sobral, Patos/Ngaoundere, Pernambuco/Sanaga lineaments and Demerara/Guinea plateaus). After Moulin et al. (2010).....	232
Figure 6.2: Paleogeographic reconstruction of the Equatorial Atlantic prior to the Aptian. African and South American Plates separation was dominantly in a N-S direction due to movement along the Sobral Fault (red line) in the South American Plate. Here, the southern South American block moved southward relatively to a fixed northern South American block. Note the remarkable alignment of the	

conjugate pre-breakup fault lineaments: Sobral Fault / Kandi (1); Patos (4) / Ngaoundere (2); Pernambuco (5) / Sanaga (3). After Moulin et al. (2010)..... 234

Figure 6.3: Geodynamic evolution of the Equatorial Atlantic margin based on the Benin Basin (offshore) during the Pre-Aptian times. A) Note that the Sobral Fault was active during the pre-Aptian. The southward movement of the southern South American block relatively to the northern South American block. The West African remains fixed (modified after Moulin et al., 2010)..... 235

Figure 6.4: Reconstruction of the Early Cretaceous breakup of western Gondwana. Intraplate deformation emanating from the NE movement of the Arabian-Nubian block towards Eurasia, resulting in plate collision. The late Aptian/early Albian deformation recorded in the study area was possibly due to this collision. Blue dashed line rectangle is shown in Figure 6.5 (after Guiraud and Bellion, 1995; Bumby and Guiraud, 2005)..... 238

Figure 6.5: Geodynamic evolution of the Equatorial Atlantic margin based on the late Aptian/early Albian deformation in the Benin Basin (offshore). African Plate motion changed as the Nubian Block moved NE and was now stretching in the ENE-WSW direction. C1: West African craton; C2: Eburnean shield; C3: São Francisco craton; C4: São Luis craton; C5: Guyana craton. S1: Kandi lineament; S2: Guinean-Nubian lineaments; S3: South Adamaoua shear zone; S4: Sanaga shear zone; S5: Patos shear zone; S6: Pernambuco shear zone; S7: Trans-Brazilian fault zone. Conjugate divergent basins: b1 (Liberia) and b2 (Caciporè); b3 (deep Ivorian basin) and b4 (Barreirinhas); b5 (Benin) and b6 (Mundaú). Intracontinental divergent basins: b7 (Solimoes), b8 (Amazonas), b9 (Marajó), b10 (Tacutu). Conjugate transform continental margins: b11 (Côte d'Ivoire) and b12 (Pará-Maranhão); b13 (Ghana-Togo) and b14 (Ceará). Strike-slip basins: b15 (Benue), b16 (Potiguar) (after Basile et al., 2005)..... 239

Figure 6.6: Santonian deformation of the study area thought to result from right-lateral transpression. Continued movement of the Arabian-Nubian block towards the European block in the Santonian. See legend used for Figure 6.5 (after Basile et al., 2005)..... 241

Figure 6.7: A two-stage opening model resulted in the opening of the Equatorial Atlantic Ocean. A) An initial opening involved the northward movement of the African Plate relative to the South American Plate in the Barremian. A northward movement of the African Plate occurred due to movement along the re-activated N-S Sobral Fault (the red line indicates active fault) (e.g. Moulin et al., 2010). B)

Stage 2 NE-SW movement due to a change in the direction of movement of the African Plate in the Albian. The NE movement occurred through the reactivation of the Central African Shear Zone (red line) (CASZ; e.g. Fairhead et al., 2013). 242

List of Tables

Chapter One

Table 1.1: Summary of characteristics of transform and divergent margins (Brownfield and Charpentier, 2006; Antobreh et al., 2009; Fairhead et al., 2013; Allen and Allen 2013; Heine and Brune, 2014).....	35
---	----

Chapter Two

Table 2.1: Summary of the 2D seismic data acquisition and processing.....	50
Table 2.2: Summary of 3D seismic data acquisition and processing.....	51
Table 2.3: Typical rock velocities and densities (after Bourbié et al., 1987).....	53
Table 2.4: Summary table of attributes from available well data in the offshore Benin Basin.....	56
Table 2.5: Well co-ordinates used for the plotting of the four wells provided into Kingdom suite.....	57
Table 2.6: Formation tops, biozones and their relative ages as estimated from Cenozoic calcareous Nannofossils in well B-04 (after Mosunmolu, 2008).....	61
Table 2.7: Biozones and their relative ages as estimated from Cretaceous calcareous Nannofossils in well B-04 (Du Chene and Adegoke, 2006).....	62
Table 2.8: Formation tops, biozones and their ages extracted from the biostratigraphic reports for well B-03.....	63
Table 2.9: Formation tops extracted from the well reports that accompanied the datasets in this study.....	64
Table 2.10: Depth-time data uploaded into Kingdom software and used to tie the seismic to well data. Depth-time data for well B-02.....	65
Table 2.11: Depth-time data uploaded into Kingdom software and used to tie the seismic to well data. Depth-time data for well B-03.....	66
Table 2.12: Depth-time data uploaded into Kingdom software and used to tie the seismic to well data. Depth-time data for well B-04.....	67
Table 2.13: Reflection characteristics of the five megasequences studied in this thesis. Lithologic interpretation was based on both well-log interpretation and seismic character. However, megasequence MS1 and sequence S2A in megasequence MS2 were based on seismic character because they have not been drilled.....	86

Chapter Three

Table 3.1: Thickness of the syn-rift megasequence MS2, and its sequences S2A, S2B, and S2C, in both the northern and the southern half-grabens.....	118
Table 3.2: Summary of the principal features of syn-rift megasequence MS2 in the offshore Benin Basin.....	125
Table 3.3: Measurements of the maximum displacements of basin-bounding normal faults (F1 and F2) and their corresponding lengths, in both the northern and southern half-grabens.....	130

Chapter Four

Table 4.1: Reflection characteristics and interpretations for discrete seismic sequences in megasequence MS3.....	154
---	-----

Author's Declaration

At no time during the registration for the degree of Doctor of Philosophy has the author been registered for any other University award without prior agreement of the Graduate School Sub-Committee.

Work submitted for this degree at the Plymouth University has not formed part of any other degree either at Plymouth University or at another establishment.

This study was financed by Tertiary Education Trust fund (TETFund) under the Ministry of Education, Nigeria in collaboration with the Delta State University, Abraka, Nigeria.

Relevant scientific seminars and conferences were regularly attended at which work was often presented.

Presentation and Conference Attended:

1. American Association of Petroleum Geologists International Conference
Pittsburgh, USA May 2013 (Poster Presentation)
2. The Nigerian Association of Petroleum Explorationists (NAPE) International
Conference Lagos Nigeria November 2013 (Oral Presentation)
3. Geological Society London - (Petroleum Group), September 2014 (Oral
Presentation)
4. Plymouth University CRES Seminar, December 2014

Word count of the main thesis: 48,287.

Signed: A. A. I. Etobro

Date: 29/11/2017

Acknowledgments

I wish to acknowledge God for His favour, mercy, and kindness for the success of my Ph.D. thesis.

I want to especially thank my supervisory team – Dr. M. P. Watkinson (Director of Studies) and Prof M. Anderson (Second Supervisor) for their supervisory supports in bringing this thesis to a huge success.

I am indebted to Delta State University, Abraka, under the administration of Prof Eric A. Arubayi and Prof Victor F. Peretomode (former and present Vice-Chancellors respectively) for this opportunity to carry out my research in the United Kingdom. I also want to thank the Federal Government of Nigeria for funding this research through the Tertiary Education Trust Fund (TETFund) scheme. All my colleagues at the Department of Geology, Delta State University, Abraka are not left out- “a big thank you”. I wish to acknowledge the Department of Petroleum Resources (DPR), Lagos, Nigeria for the provision of the datasets used for this study. I want to thank all my Ph.D. student colleagues and many friends whom I came across during my research work for their support. I thank all who contributed to the success of this research such as Pastors (Drs) B. Morakinyo, A. Alademomi, Drs E. Chinwendu and S. Chaanda.

The Body of Christ to mention but a few Our Saviour’s Chapel DELSU, Abraka, Nigeria for prayerfully supporting my family during my stay in the UK. I want to thank the Deeper Life Church, Plymouth, and the Bristol Region, as well as the Overcomers Fellowship, Plymouth United Kingdom for the fellowship that we had together. I also appreciate the Etobro’s, Okpidi’s and Arubayi’s families for all their wonderful love and assistance.

I want to appreciate my lovely and amiable sweetheart - Ejiroghene Etobro, for being so wonderful to me. You are indeed a virtuous woman. Thank you for your sacrifice, supports and for being there for me and our children. Our wonderful children including Elo-Oghenezino, Oghale-Oghene, Iruo-Oghene, and Oreva-Oghene - thank you for your understanding and love. I also want to appreciate my mother (Mrs. Ruth Etobro), brothers (Dr. Benjamin, Messrs Isaac, Bartholomew) sisters (Mrs. Olotu and Onoja), nephews, and nieces. God bless you all.

Chapter One

1.0 Introduction

1.1 General statement

This Ph.D. dissertation presents the first detailed tectono-stratigraphic analysis of the offshore part of the Benin Basin, Nigeria. Understanding the tectonic and stratigraphic evolution of this basin is important because it is located in a key location at the eastern end of the West African margin, Equatorial Atlantic (Figure 1.1), where the continental margin is orientated perpendicular to the Atlantic spreading axis. It represents one of a series of basins thought to have been affected by transform tectonics (Mascle et al., 1996; Clift et al., 1997; Matos, 1992; 2000; Bird, 2001; MacGregor et al., 2003; Basile et al., 2005; Brownfield and Charpentier, 2006; Antobreh et al., 2009; Moulin et al., 2010; Nemčok et al., 2013a and 2013b; Heine and Brune, 2014; Basile, 2016). Yet, the evolution of this segment of the Atlantic margin is still very much debated in the literature (e.g. Basile et al., 2005; Moulin et al., 2010; Fairhead et al., 2013; Heine and Brune, 2014).

To the east of the Benin Basin are the Niger Delta and its prolific petroleum systems (Figure 1.2), as well as a series of Mesozoic failed rift basins that extend into the African Plate interior (e.g. the Benue Basin, see Figure 1.1). To the southeast of the Benue Trough is the N-S oriented South Atlantic Province, from where the Atlantic opening is thought to have propagated northwards in the Early Cretaceous (e.g. Moulin et al., 2010; Fairhead et al., 2013). As a result of its location, a better understanding of the timing and nature of tectonic events in the Benin Basin, and their influence on

stratigraphic and petroleum system development, is of scientific and economic importance.

A preliminary analysis of both the 2D and 3D seismic data used in this study shows the occurrence of both extensional and contractional structures. Extensional structures include major basin-bounding normal faults, while contractional structures comprise a basement-involved reverse fault and (its associated propagation fold), inverted structures, local/shallow thrusts, and folds. These structures will be analysed to ascertain whether they are of a tectonic or non-tectonic origin. The significance of this study is to critically evaluate fault geometries in 2D and 3D seismic data in order to deduce whether the offshore Benin Basin is a passive or transform margin. Contractional structures identified in this study will be analysed to evaluate whether they are of tectonic origin; and whether they are of local or regional significance. The results will be discussed in the wider scale of the African/American tectonic plates, and in relation to how the African-South American Plates moved during the opening of the Equatorial Atlantic.

1.2 Aims and objectives

1.2.1 Aims

The aims of this research project are:

- ❖ To determine the tectono-stratigraphic evolution of the offshore Benin Basin.
- ❖ To evaluate the timing and nature of tectonic events that occurred in the offshore Benin Basin since its evolution.
- ❖ To investigate the implications of tectonics (extensional, contractional and strike-slip deformation) for the geodynamic evolution of southwest Nigeria.

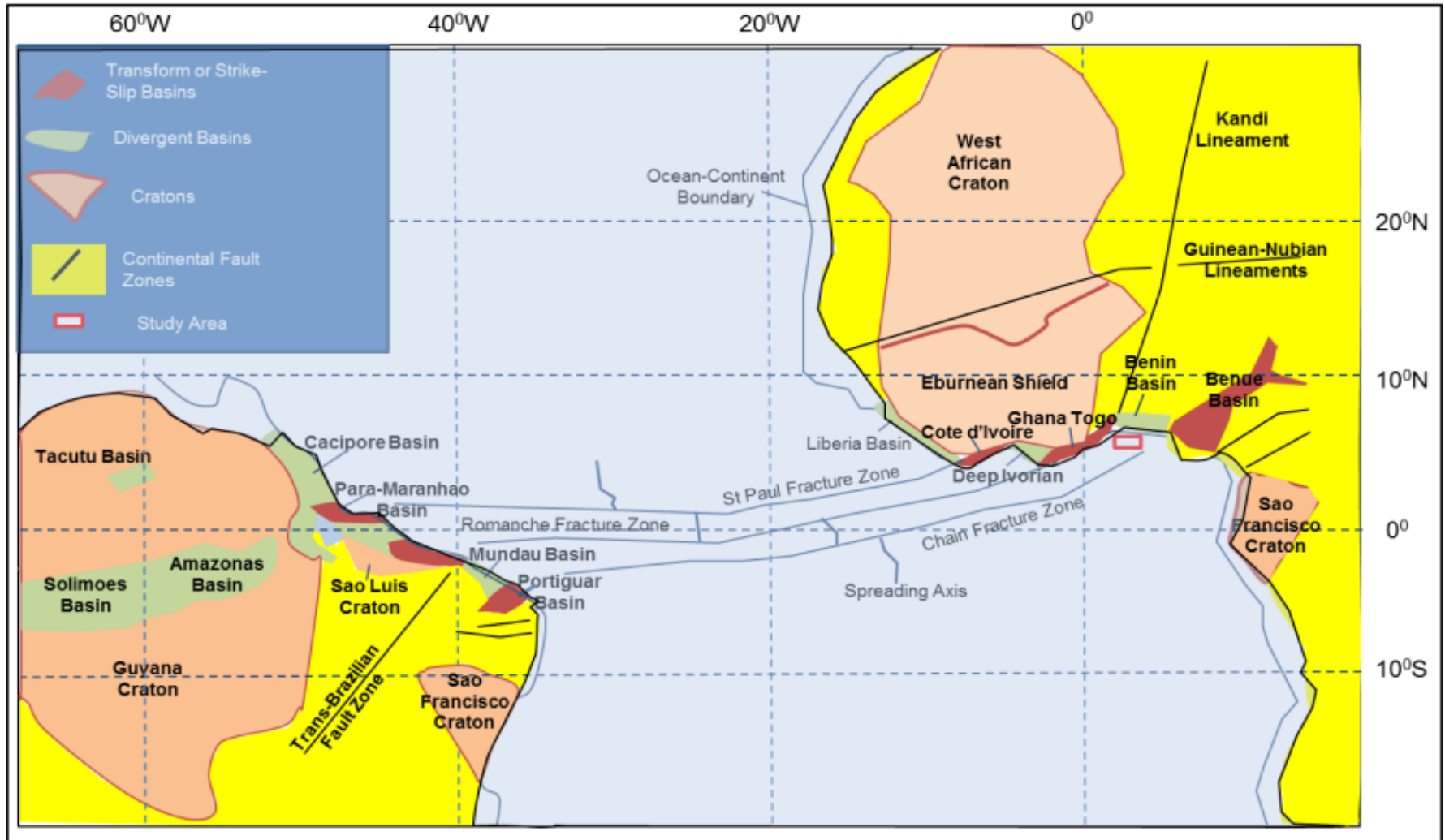


Figure 1.1: The Equatorial Atlantic segment displays its characteristic fracture zones (St Paul, Romanche and Chain Fracture Zones). Both margins of the Northeast Brazil and West Africa are characterised by alternating E-W and NE-SW conjugate basins. The basin of the present study (Benin Basin and its conjugated divergent basin- Mundaú Basin, both generally trend E-W) (modified after Basile et al., 2005).

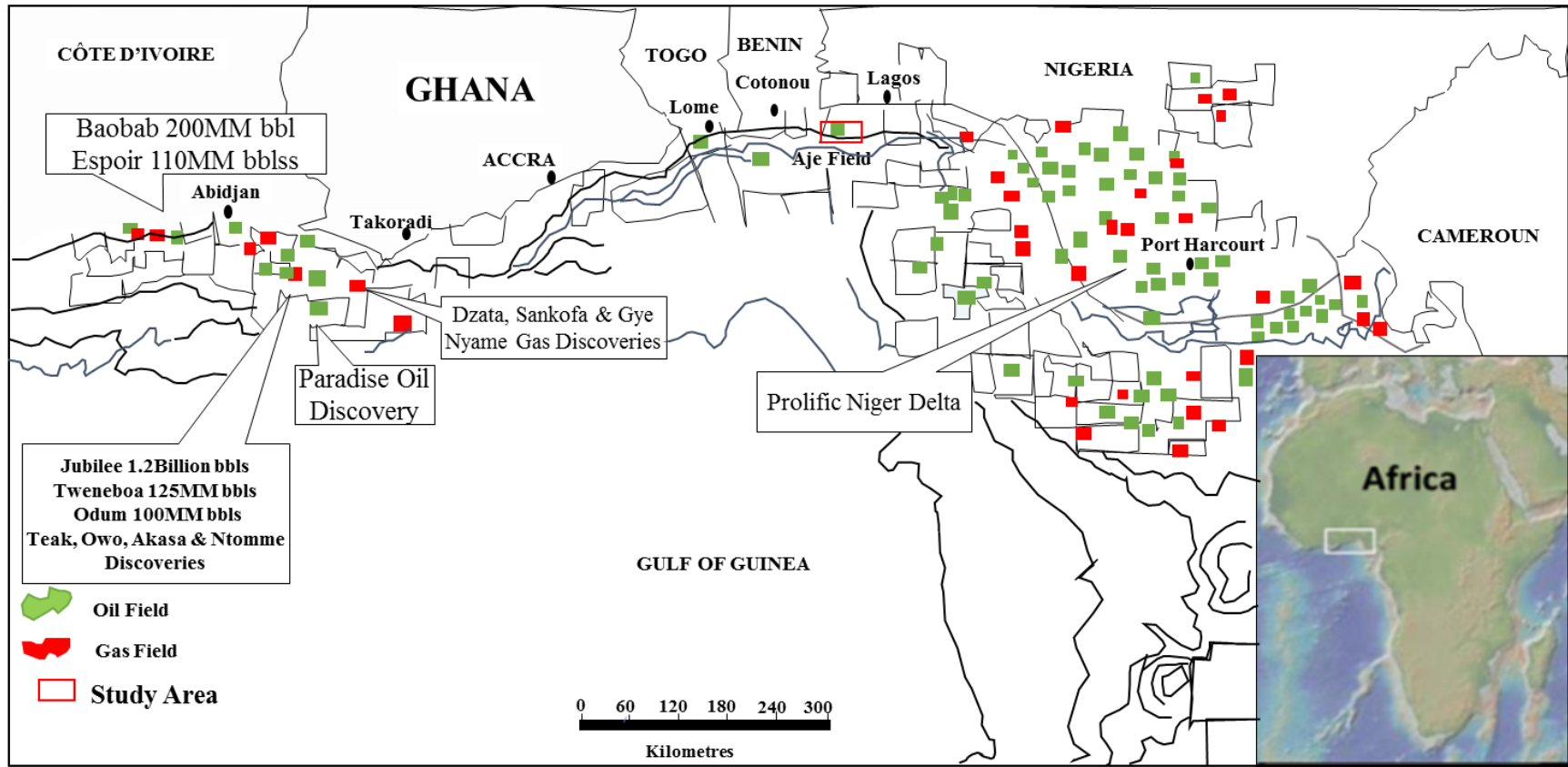


Figure 1.2: Oil and Gas fields in the Equatorial Atlantic region between Côte d'Ivoire and Cameroun. The concentration of these activities in the Cenozoic Niger Delta Basin while the Cretaceous basins are marked by fewer discoveries, and the Benin Basin being one of the least explored basins along the Equatorial Atlantic margin.

1.2.2 Objectives

To achieve these aims, the following objectives were addressed and presented in this study:

- ❖ To critically review models for the tectonic and stratigraphic evolution of the Equatorial Atlantic, and how these relate to surrounding regions.
- ❖ To develop an integrated seismic stratigraphic and structural framework for the offshore Benin Basin based on the analysis of the datasets available.
- ❖ To map out the fault geometries observed on the seismic data in order to interpret regional kinematics and mechanisms for their formation.
- ❖ To examine growth stratigraphic sequences (i.e. syn-compressional) associated with folding in order to constrain the timing of regional deformational events.
- ❖ To use these analyses to help better constrain the relative motions of the African and South American Plates during and after rifting.

1.2.3 Importance of this study

The study of continental margins has received increasing attention in recent years because of the interest of the oil and gas industry in the exploration of deep-water plays (e.g. Manatschal, 2004; Alves et al., 2006; Kaki et al., 2012). Understanding how the African Plate separated from the South American Plate, and the subsequent drifting history of both plates, is of paramount importance to palaeogeographic reconstructions of the Atlantic (Moulin et al., 2010). Since the Equatorial Atlantic forms the connection between the Central and the South Atlantic, it is important to understand how and when rifting and the initial opening occurred. The Benin Basin, which displays both

extensional and contractional structures, offers opportunities to evaluate and further refine models for the opening of the Equatorial Atlantic.

Following an initial review of the data, this study aimed at answering these outstanding questions:

- ❖ Are the existing tectono-stratigraphic models for the Equatorial Atlantic consistent with the tectonic evolution of the offshore Benin Basin?
- ❖ Is the Benin Basin a rifted or a typical transform-margin basin?
- ❖ What is the significance of the geometry of syn-rift structural elements and rift architecture?
- ❖ How has structural (tectonic) deformation influenced deposition in this basin?
- ❖ What mechanisms formed the thrusts and folds in this basin?
- ❖ Did the Benin Basin undergo inversion tectonics during its evolution?
- ❖ What relationship does post-rift compression have with gravity-driven structures in offshore Benin Basin?

1.3 Geographical location of the study area

The Benin Basin covers about 40,000 km² (Figure 1.2; Kaki et al., 2012). It stretches from south-eastern Ghana through Togo, Benin Republic, to the south-western parts of Nigeria (Allen, 1964; Adeleye, 1975; Omatsola and Adegoke, 1981; Whiteman, 1982; Okosun, 1990; 1998; Ala and Selley, 1997; Akinmosin and Osinowo, 2010; Akinmosin et al., 2011). The Nigerian part of the basin is separated from the Cenozoic Niger Delta Basin (to the east) by the Okitipupa Ridge (Onuoha, 1999). The surface area of the onshore Benin Basin probably does not exceed 19,000 km² (Whiteman, 1982). The basin is grouped as part of the Gulf of Guinea Province according to the U.S. Geological Survey (USGS) (Brownfield and Charpentier, 2006). It lies within the Equatorial segment of the South Atlantic Ocean, between the Romanche and the Chain

fracture zones (Figure 1.1; Basile et al., 2005; Brownfield and Charpentier, 2006; Moulin et al., 2010; Kaki et al., 2012). The basin is sometimes referred to as Dahomey Embayment (e.g. Opara, 2011).

1.3.1 The offshore Benin Basin

The offshore Benin Basin has been studied by relatively few workers, in which are included Delteil et al. (1974); Delteil et al. (1976); MacGregor et al. (2003); Brownfield and Charpentier (2006); Olabode and Adekoya (2008); Opara (2011); and Kaki et al. (2012). Offshore Nigeria, the Neogene strata were analysed by authors such as Pacht et al. (1994); Lang et al. (1995); Olabode and Adekoya (2008). Kaki et al. (2012) studied the petroleum geology of this basin using a sequence stratigraphic approach in which they defined eleven seismo-stratigraphic units. These units range from the Mid-Cretaceous to Mid-Miocene in age. This shows that Kaki et al. (2012) were able to date strata as old as the Mid-Cretaceous. The study of Kaki et al. (2012), in the western part of the study area, has revealed an older age for strata up to the early Aptian. The offshore part of the basin was studied by the above authors during regional studies of the Gulf of Guinea.

1.3.2 Seafloor physiography and bathymetry of southwestern Nigerian margin

The present-day seafloor comprises prominent topographic features such as the continental shelf, shelf-break, a steep continental slope, continental rise, ocean floor, mid-oceanic ridges (MOR), seamounts and trenches. The physiography of any ocean or sea is dependent on the types of boundaries associated with it. Rifted basins and passive margins generally have a gently-dipping continental slope, whereas the continental slope is often steeply-dipping on transform margins.

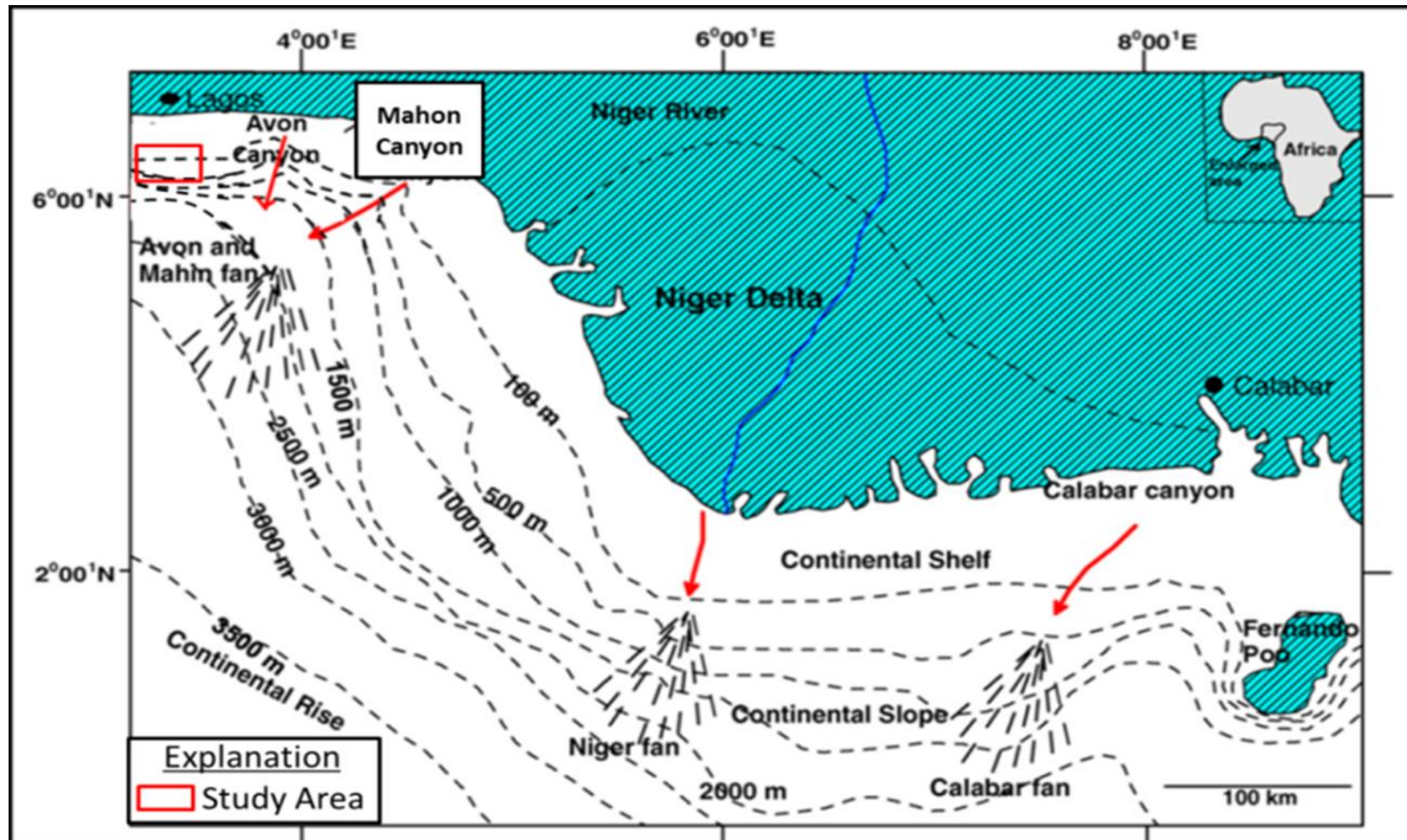


Figure 1.3: Bathymetric map of Southern Nigeria showing submarine features such as submarine canyons and fans extending from the Nigerian part of the Benin Basin to the offshore Niger Delta to the east. Note the study area lies between the continental shelf and continental slope (after Olabode and Adekoya, 2008).

Previous studies of Delteil et al. (1974), and Brownfield and Charpentier (2006) revealed that the physiography of the offshore Benin Basin is typical of Atlantic-type continental margins as described by Heezen (1974). The bathymetric map of the southwestern Nigerian margin (Figure 1.3) shows the water gradient gradually changing from a shallow depth of 100 m on the continental shelf through the 500 m depth contour to a maximum of 2000 m. This contrasts the bathymetry in the eastern part around the Ghana-Togo region (Clift et al., 1997; Bird, 2001; Antobreh et al., 2009) where there is a sharp change in depth from less than 200 m to a depth of over 2000 m (Figure 1.3). Such a physiography is particular to/diagnostic of regions where transform movements have taken place, whereas the southwestern Nigerian margin is typical of regions where divergent motion prevailed. In some localities of southwestern Nigeria, submarine canyon incision may occur, e.g. the Avon Canyon cutting into the seafloor (Allen, 1964; Olabode and Adekoya, 2008; Figure 1.3). Such physiographic features are non-tectonic, formed by the erosional effects of rivers as they flow downslope into the deep waters (Pratson et al., 1994; Pratson, 2001). The seismic data provided for this study will be analysed for the possible occurrence of submarine canyons in the Benin Basin (see Chapter 5).

1.3.3 Continent-ocean boundary (COB)

The continent-ocean boundary (COB) is the line of maximum extent of continental lithosphere and marks a change from continental to oceanic crust. The location of the COB may be ambiguous due to tectonic complexity associated with the transform margin. For example, it has been defined for the Ghana and Ivorian Basins by Faleide et al. (1993) and Antobreh et al. (2009), although these authors observed that it was difficult to map it because of tectonic complexity. They also observed that at the

sheared margin segment, the COB was extensive and it tends to decimate (Figure 1.4; Austin and Uchui, 1982; Faleide et al., 1993).

The identification of the COB is important because it helps to constrain the thermodynamic modelling of petroleum systems in a sedimentary basin (Dickson et al., 2003). The oceanic regimes are generally known to be characterised by high heat flow; this, therefore, means that only 50% of the sediment blanket necessary for source rock maturation on the continental crust is required in abyssal environments. This condition may be attained during the continental breakup stage of margin development.

1.4 Precambrian geology and basement reactivation

The reactivation of the pre-existing structures in basement rocks is thought to have a major control on the evolution of geological structures during subsequent tectonic events (Etheridge, 1986; Letouzey et al., 1990). In Africa, the evolution of Phanerozoic rift basins is strongly controlled by pre-existing basement structures inherited from Precambrian tectonics (Daly et al., 1989; Smith and Mosley, 1993). Understanding the onshore Precambrian geology and basement fabric is, therefore, important when considering the evolution of the offshore Benin basin. Phanerozoic tectonism and magmatism within the African Plate are thought to have taken place along broad lineaments, which reflect reactivation and exploitation of earlier, Late Proterozoic Pan-African-Braziliano sutures, formed generally between 720 and 550 Ma (Stern, 1994; Unrug, 1996, 1997; Bumby and Guiraud, 2005). Both the Precambrian cratons and the Pan-African Belts are crosscut by large fault zones (Figure 1.5). Cratonic regions are thought to be relatively stable, and are not involved in significant basement reactivation. Pre-existing zones of weakness generally occur in the fault zones, suture zones, failed rifts, and other tectonic boundaries, especially near the continental margins (Sykes, 1978).

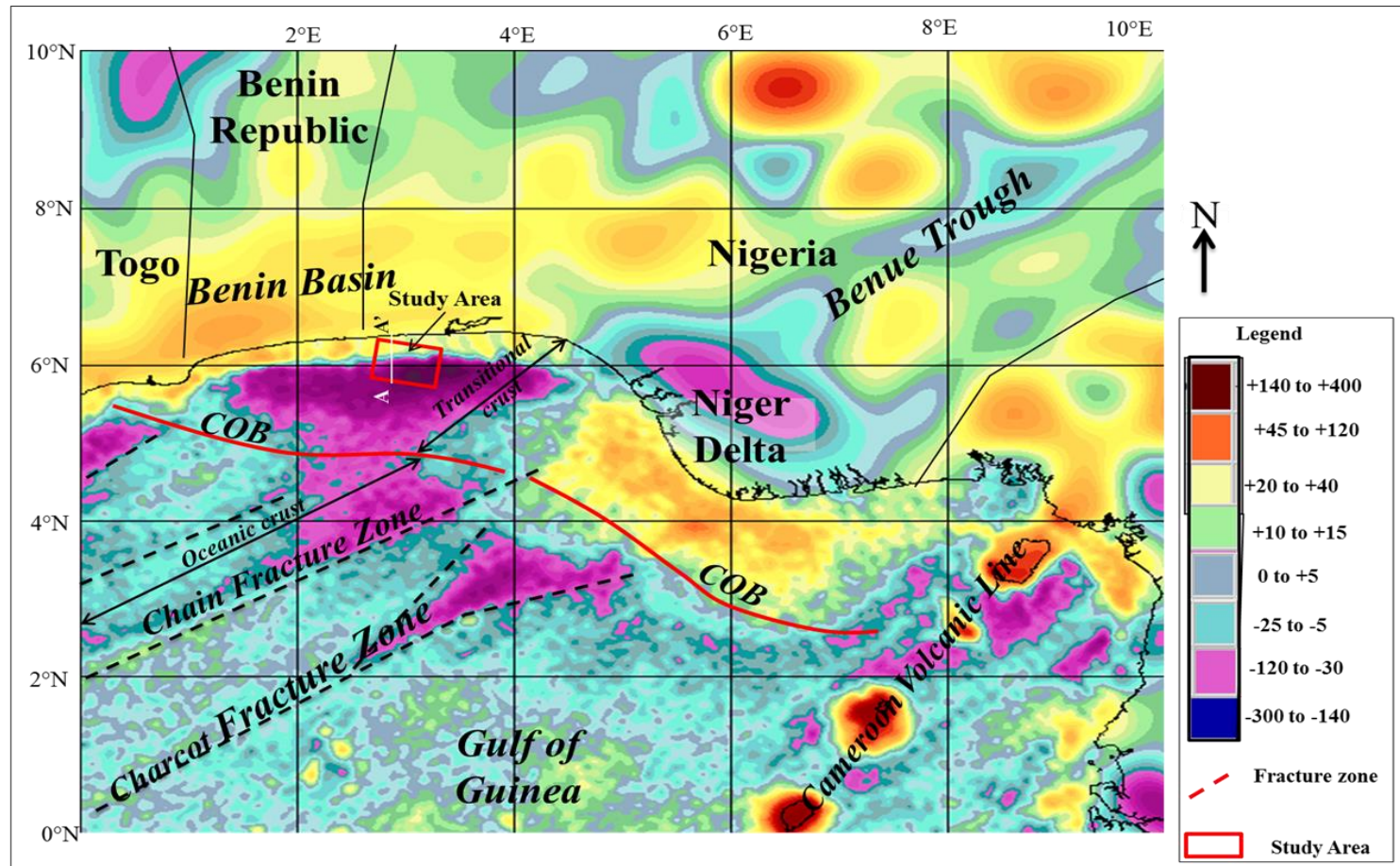


Figure 1.4: Gravimetric map of the Equatorial Atlantic showing the study area (small red rectangle). Line AA' is an N-S oriented seismic section shown in Figure 2.3. The continent-ocean boundary (COB) is indicated by the heavy red line. Note that the study area, offshore Benin Basin occurs some distance away from a major fracture zone (i.e. Chain fracture zone). The fracture zone occurs obliquely to the approximately E-W striking Benin Basin. Gravity anomaly values are in milliGal (mGal). (modified after Sandwell and Smith, 1997; Davies et al., 2005).

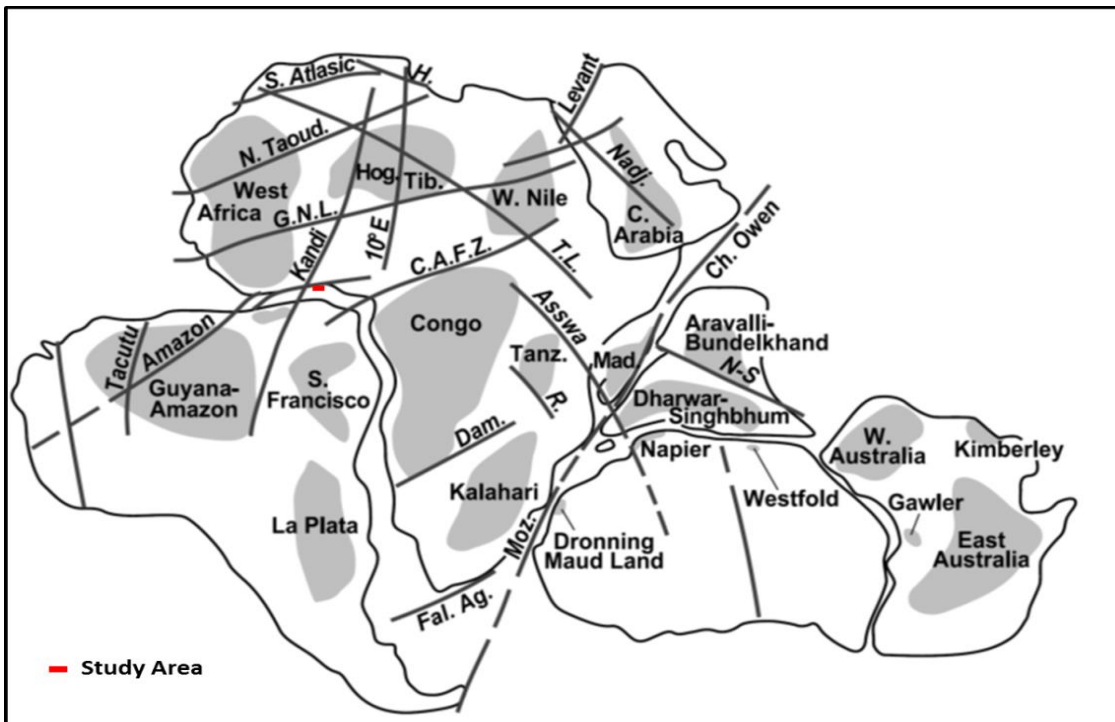


Figure 1.5: Major fault zones of Gondwana that may reactivate under stresses such as those related to change in plate motion. Gondwana reconstruction and apparent Archaean and Palaeoproterozoic cratons (in grey) after Rogers et al. (1995). Note these fault zones became weak zones that controlled ocean opening and intraplate deformation changes in the stress field were recorded, especially between South America and Africa. Where: Ag. = Agulhas; C = Central; CAFZ = Central African Fault Zone; Ch. = Chain; Dam. = Damara; Fal. = Falkland; GNL = Guinean–Nubian Lineaments; H. = Hodna; Hog. = Hoggar; Moz. = Mozambique; N-S = Narmada Son; N. Taoud. = North Taoudenni Lineament; R. = Rukwa; Tanz. = Tanzania; TB = Trans-Brasiliano; Tib. = Tibesti; TL = Tibesti Lineament. Apparent curvature of the Tibesti Lineament is due to the map’s projection (from Guiraud et al., 2000).

Many of such pre-existing weak zones are thought to have been reactivated during the early phases of the continental separation (Sykes, 1978; Guiraud et al., 1992; 2000; 2010; Moulin et al., 2010; Fairhead et al., 2013). During the Pan-African stages, these faults mainly acted as sub-vertical strike-slip faults. The major fault zones recognised in North and Central Africa are shown in Figure 1.1. These faults may reactivate depending on the stress orientation; movement will likely be along pre-existing faults (Sykes, 1978; Hammuda et al., 1992).

The Equatorial Atlantic margins extend over an assemblage of Proterozoic to earliest Palaeozoic tectonic domains that were formed during the Pan African-Brazilian Orogeny (Black, 1984; Caby, 2003; Basile et al., 2005; Guiraud et al., 1985; 1987; 2005). The Pan African-Brazilian orogeny is represented by a fold-thrust belt formed around the West African Craton, the Guyana Craton, the São Luis Craton-Eburnean shield and the São Francisco Craton. Major pre-existing zones of weakness that trend subparallel to the WSW-ENE direction of relative continental separation exert control on the locations of transform faults that develop into a new ocean (Skyes, 1978; Daly et al., 1989). The weak fault zones include the Central African Fracture Zone (CAFZ), the Kandi-Transbrazilian fracture zone, and the Guinea-Nubian lineaments during the Phanerozoic times (Figure 1.5; Black, 1984; Guiraud et al., 1985; 2005; Caby, 1989; Keller et al., 1995; Kroner and Stern, 2004; Basile et al., 2005; Bumby and Guiraud, 2005). Strike-slip reactivation of pre-existing structures is both transpressional and transtensional, depending largely on orientation (e.g. Basile et al., 2005).

During continental rifting, the African-South American Plate has been considered to have been made up of three blocks, or sub-plates (Burke and Dewey, 1974; Guiraud and Maurin, 1992; Fairhead et al., 2013; Heine and Brune, 2014), named the Nubian-Arabian, the Western and southern Austral blocks. Each block is bordered by a zone of weakness (mobile zone) that became reactivated under stress fields initiated when a change in direction of plate movement occurred (Burke and Dewey, 1974; Guiraud and Maurin, 1992; Guiraud et al., 2005).

1.5 Regional geological setting of the South Atlantic margin

The South Atlantic margin is subdivided into four segments which are, from south to north, the Falklands, the Austral, the Central and Equatorial Atlantic segments (Figure 1.6; Moulin et al., 2010). Rifting is thought to have started at the Falkland segment

(Figure 1.6) in the Late Jurassic, and propagated to the north in the Early Cretaceous (Moulin et al., 2010). The opening of the South Atlantic is itself linked to the breakup of the Gondwana supercontinent in the Late Carboniferous to Middle Jurassic (Guiraud and Bellion, 1995; Guiraud and Bosworth, 1999; Bumby and Guiraud, 2005). It is thought to have occurred in three different phases. The first phase of rifting of the Gondwana supercontinent probably spanned the Late Carboniferous to Middle Jurassic.

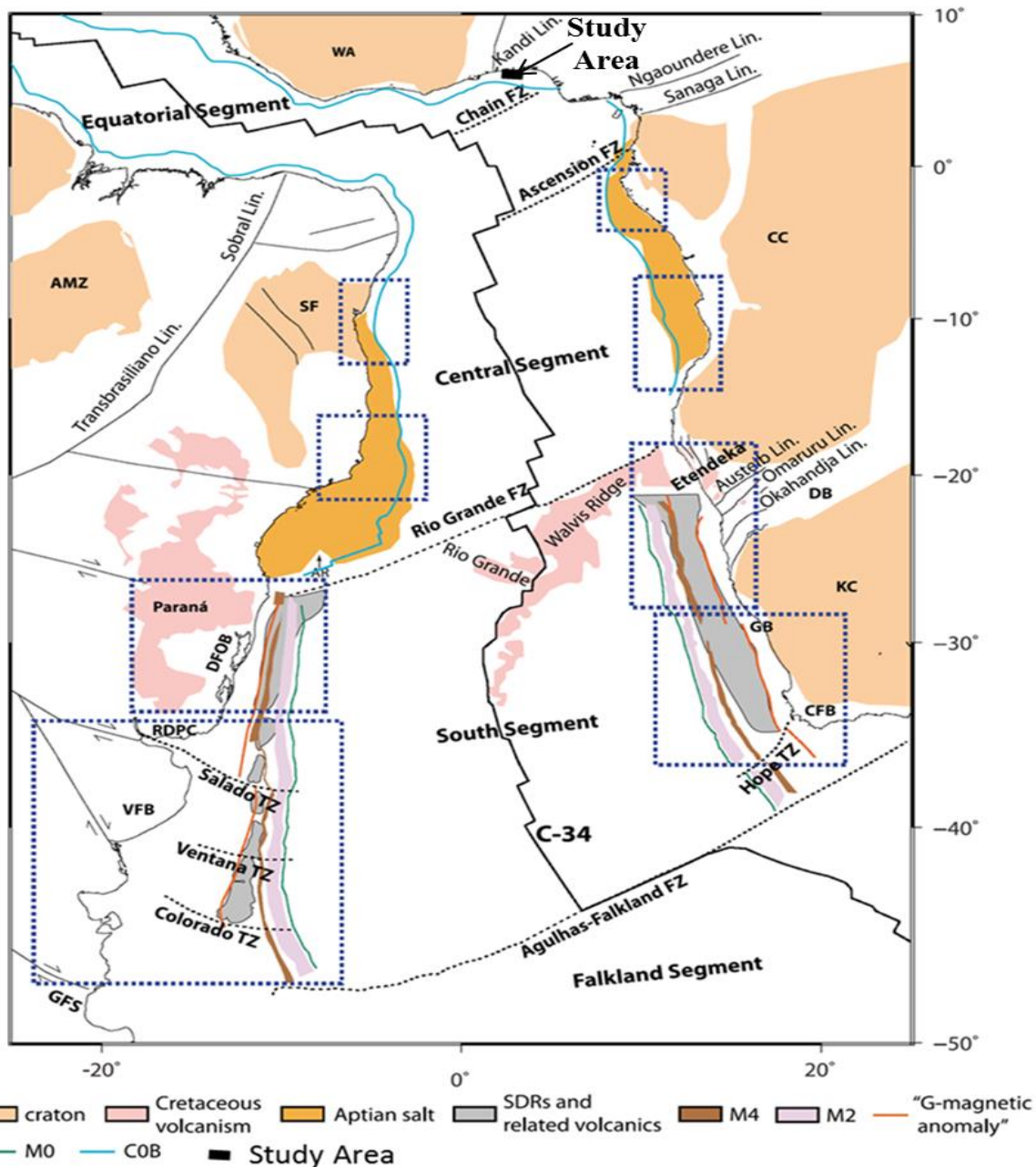


Figure 1.6: The South Atlantic is subdivided into four segments from the south to north: the Falkland, South, Central and Equatorial segments. Note that the study area is located on the Equatorial segment of the South Atlantic at its eastern border (the Chain Fracture Zone). The study area occurs some distance away from the Continent-Oceanic Boundary (COB) (after Moulin et al., 2010).

The first phase affected the Central Atlantic province, the north and east margins of Africa and Arabia (Bumby and Guiraud, 2005), resulting in the opening of the Neotethys during the Permian and Triassic. The opening propagated westwards from the northeastern Arabian margin towards Morocco (Guiraud, 1998; Bumby and Guiraud, 2005). It has been reported by Bumby and Guiraud (2005) that rifting was accompanied by alkaline basalts. Important basins that developed during this rifting phase include the Atlas and Karoo Basins; these basins were not located in the Neotethyan oceanic realm (Bumby and Guiraud, 2005).

The second phase of rifting of the Gondwana supercontinent took place in the Late Jurassic-Early Cretaceous (Nüremberg and Müller, 1991). This is the most widespread rifting phase affecting Gondwana (Guiraud and Bellion, 1995; Bumby and Guiraud, 2005). Sedimentary basins along the South Atlantic margin, the Equatorial Atlantic margin, as well as the East African and West Central African Rift Systems (Figure 1.7), evolved during this phase. These two later intraplate rift systems reflect aborted breakup events within the African Plate (Binks and Fairhead, 1992; Basile et al., 2005; Bumby and Guiraud, 2005; Guiraud et al., 2005; Moulin et al., 2010; Fairhead et al., 2013; Heine and Brune, 2014; Basile, 2016). This phase of rifting of the Gondwana supercontinent is further discussed in the following sections.

The third phase of rifting of Gondwana occurred between the Late Eocene and Early Miocene (Bumby and Guiraud, 2005). This phase is generally associated with continued rifting between the African and the Arabian Plates. It also marks the onset of seafloor spreading in the Red Sea from about 41 Ma to 34 Ma (Girdler and Styles, 1973; Rihm and Henke, 1998). Examples of basins formed during this rifting phase include the Dead Sea-Red Sea-Gulf of Aden, as well as basins in the East African Rift, which continued their development into the Holocene (Eyal and Reches, 1983). These rifting events are

thought to be associated with the onset of magmatism associated with the Afar Plume at 31 Ma (Burke et al., 2003; Bumby and Guiraud, 2005).

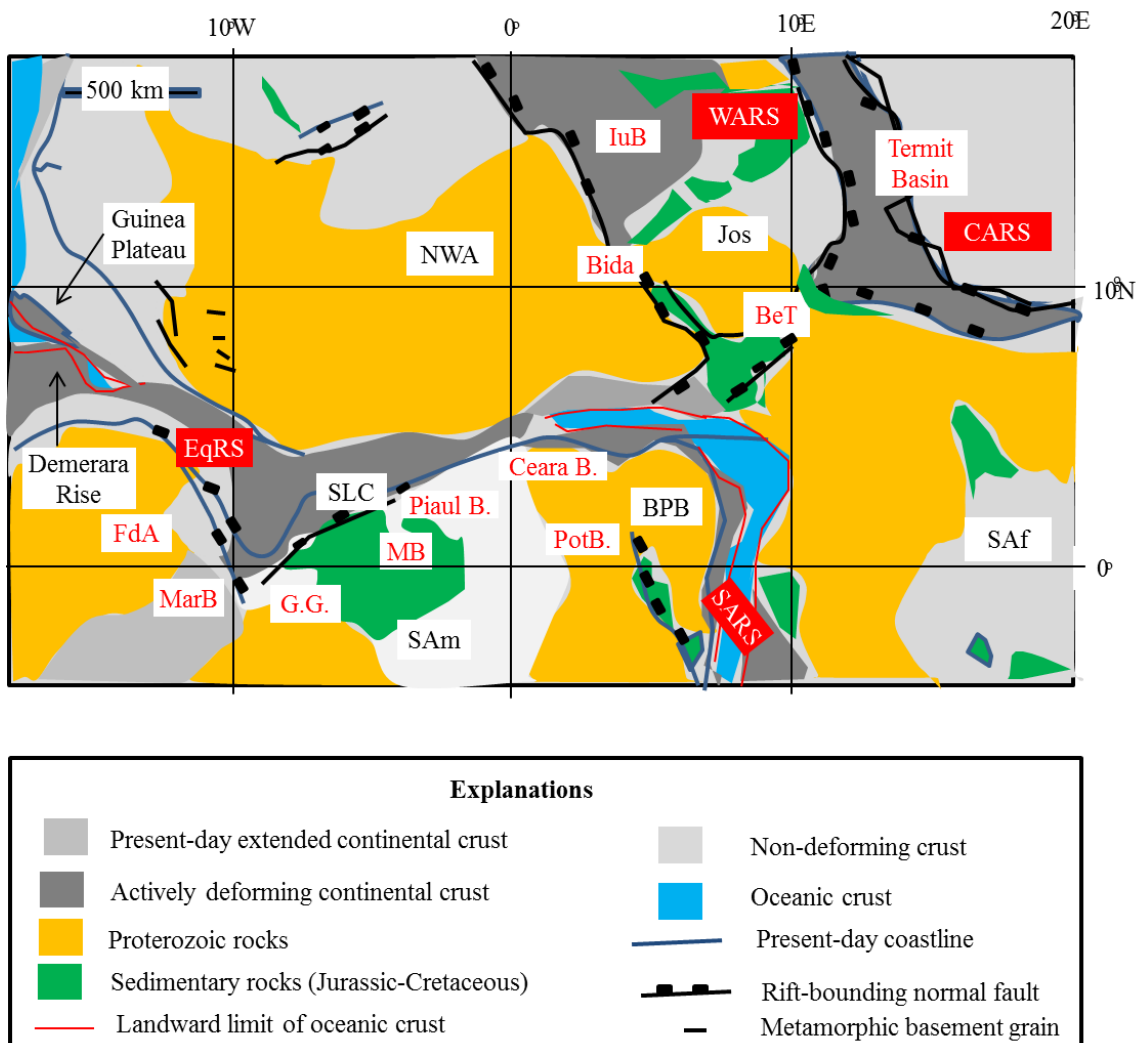


Figure 1.7: 117 Ma reconstruction (Heine et al., 2013). Note that the northernmost segment of South Atlantic Rift System (SARS) is already in seafloor spreading mode in the Equatorial Atlantic (EqRS), the breakup is incipient. Minor rigid plates: BPB - Borborema province block (northeast Brazil), Jos - Jos subplate (northern Nigeria), SLC - São Luís Craton. Basins (B): BeT - Benue Trough, FdA - Foz do Amazonas Basin, GG - Gurupi Graben, IuB - Iullemmeden Basin, MarB - Marajó Basin, MB - Maranhão Basin, PotB - Potiguar Basin; SAf - South African block; Sam - South American block; NWA - Northwestern African block; WARS - West African Rift System; CARS - Central African Rift System (after Heine and Brune, 2014).

1.6 Opening of the South Atlantic Ocean

Lithospheric extension leading to the final breakup of the western Gondwana started in the Early Cretaceous with the formation of large intracontinental rift systems within

(and between) the African and South American Plates (Burke and Dewey, 1974; Untemehr et al., 1988; Blaich et al., 2011; Granot et al., 2015). Four extensional domains are associated with the lithospheric extension in the Early Cretaceous (Heine et al., 2013; Heine and Brune, 2014):

- ❖ The Central African Rift System (CARS) extends from Sudan to the eastern part of the Benue Trough (Figure 1.8; Fairhead, 1986).
- ❖ The West African Rift System (WARS) extends northwards from the eastern part of the Benue Trough to southern Libya (Figure 1.8; Burke and Dewey, 1974; Winterer and Bosellini, 1981; Genik, 1992; 1993).
- ❖ The South Atlantic Rift System (SARS) consists of the present day conjugate South Atlantic marginal basins, with the Benue Trough–northeast Brazil at its northernmost extent (Nürnberg and Müller, 1991).
- ❖ The Equatorial Atlantic Rift System (EqRS) covers the conjugate West African and South American margins from the Guinea Plateau–Demerara Rise in the west to the Benue Trough – northeasternmost Brazil in the east (Figure 1.7; Basile et al., 2005).

Extension in both the South Atlantic rift system (SARS) and the Equatorial Atlantic rift system (EqRS) ultimately led to the opening of the South Atlantic and the Equatorial Atlantic Oceans respectively. Their modes of opening generally differ (Nürnberg and Müller, 1991; Torsvik et al., 2009; Moulin et al., 2010; Heine et al., 2013; Heine and Brune, 2014; Basile, 2016). The Late Jurassic-Early Cretaceous extension that led to the subsequent opening of the South Atlantic Ocean is thought to be related to orthogonal rifting (Guiraud et al., 2005; Moulin et al., 2010; Fairhead et al., 2013). The rift basins along the South Atlantic margins are characterised by wedge geometries with divergent reflections that thin away from their basin-bounding normal faults.

1.7 Rifting of the African intraplate basins

The development of the West and Central African Rift Systems in the Early Cretaceous is related to the build-up of intraplate tensional stresses during the fragmentation of Gondwana. Extensional basins of the West and Central African rift system opened under the influence of NE–SW oriented extensional palaeostresses (West Africa: Benue, Douala, Rio Muni, Gabon, Congo) and became part of the South Atlantic coastal rift system (Teisserenc and Villemin, 1990; Guiraud, 1986; Matos, 1992; Maurin and Guiraud, 1993). Rift segments characterised by different extensional and subsidence histories are limited by major NE-striking transfer structures (Francheteau and Le Pichon, 1972; Matos, 1992; Mounquengui and Guiraud, 2009).

The Cretaceous rifting in the WARS and CARS is thought to have occurred in two phases that took place contemporaneously with the opening of the South Atlantic Ocean (e.g. Seranne and Anka, 2005; Mounquengui and Guiraud, 2009):

- ❖ Syn-rift phase 1 (142-120 Ma)
- ❖ Syn-rift phase 2 (119-101 Ma)

1.7.1 Syn-rift phase 1 (142-120 Ma)

Rifting was initiated in the Early Cretaceous through orthogonal extension along the West and Central African Rift Systems (Mounquengui and Guiraud, 2009; Guiraud et al., 2010; Fairhead et al., 2013). The start of rifting is generally identified as Late Hauterivian to earliest Aptian in age, although an older (Neocomian and Berriasian) may exist (e.g. Fairhead et al., 2013). This phase of rifting led to the formation of asymmetrical half-graben basins trending E-W along this margin.

Rifting is thought to have started on the Equatorial Atlantic margin during syn-rift phase 1 probably in the Barremian-Aptian (e.g. Moulin et al., 2010; Fairhead et al., 2013).

This rift phase is thought to be similar to N-S extension between the African and South American Plates that led to the opening of the southern South Atlantic Ocean between the Late Jurassic and Early Cretaceous (e.g. Guiraud et al., 1992; Moulin et al., 2010; Fairhead et al., 2013). This initial phase of rifting probably led in the evolution of E to ENE striking basins along the Equatorial Atlantic margin such as the Benin and Keta Basins (Basile et al., 2005).

1.7.2 Syn-rift phase 2 (119-101 Ma)

Rifting is thought to have continued in some basins within the African Plate from the earliest Aptian to Late Albian. This continued rifting possibly led to the evolution of Benue Trough, Sudan, Kenya and in the Termit and south Ténéré Basins. These basins generally strike NE-SW, therefore, providing evidence for strike-slip extension (Fairhead et al., 2013). The end of rifting is often indicated by a regional unconformity that can be observed in the entire WARS/CARS (Genik, 1993), as well as along margins of the Equatorial Atlantic (Masclé et al., 1988). This unconformity represents the cessation of rifting in these regions and it has varying ages ranging from the Albian-Cenomanian boundary (Masclé et al., 1995) to between the mid- and Late Albian (Genik, 1993). The Central African Rift System (CARS) extends from Sudan to the eastern part of the Benue Trough while the West African Rift System (WARS) stretches from the eastern part of part of the Benue Trough northward toward southern Libya (Guiraud and Maurin, 1992; Guiraud et al., 1992).

A new rifting episode began at the end of early Aptian that affected rifts located along the Equatorial Atlantic margin, within the WCARS (from Benue to southern Chad) and in northern Libya, while the Sudanese rifts, the east Niger Ténéré Trough and the Gao Trough of eastern Mali also remained active.

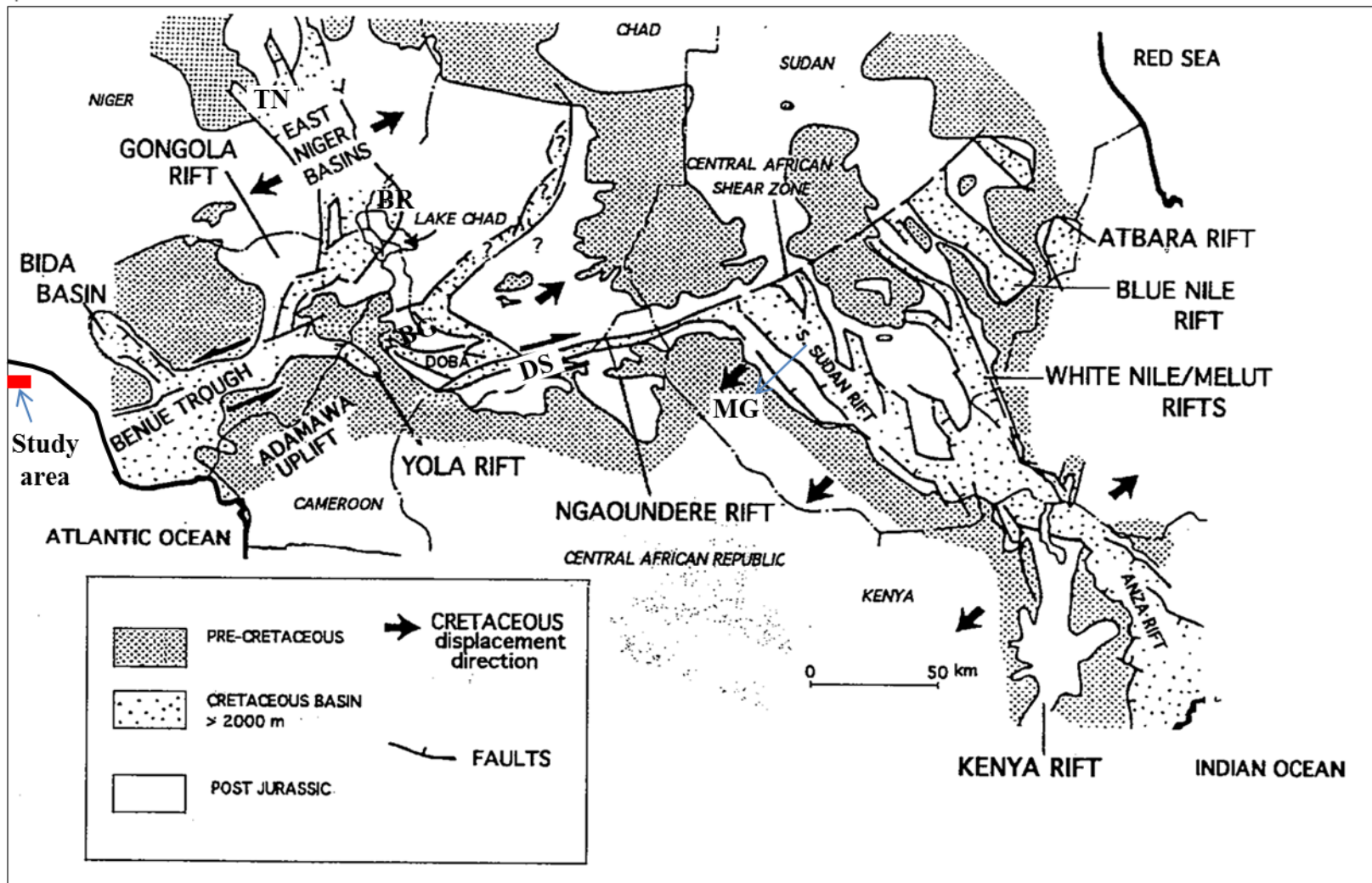


Figure 1.8: Regional index map of the West and Central African Rift systems (WCARS). Note that most of the intraplate basins in these regions evolved through NE-SW continental extension. The southern Sudan rift is also called Muglad rift. The east Niger basins (Niger rift) are a complex rift zone with the Termit Basin as its major element. Some of the basins cited in the text: DS = Doseo; BG = Bongor; BR = Borno; MG = Muglad; TN = Tenéré (after Warren, 2009; Fairhead et al., 2013).

This rifting phase ended in the Late Albian (Guiraud et al., 1992; Moulin et al., 2010; Fairhead et al. 2013; Heine and Brune, 2014). Structurally, the basins along the WCARS trend in either a NW-SE or E-W/ENE-WSW direction. The NW-SE trending basins are thought to evolve in response to an approximate NE-SW crustal extension, while the E-W/ENE-WSW striking elongated pull-apart basins developed in response to dextral (Cameroon to Sudan) and sinistral (Niger Delta to Lake Chad) strike-slip movements (e.g. Guiraud et al., 1992; Destro et al., 2003). An orthogonal extensional strain in the basins of the Southern Sudan and East Niger was taken up along the dextral Central African and the sinistral Benue fracture zones, respectively, therefore providing a link to the Gulf of Guinea (Figure 1.8). The simultaneous rapid opening of the Equatorial Atlantic Ocean (Masclé et al., 1988; Guiraud et al., 1992) resulted in the connection of the Central and South Atlantic mid-oceanic spreading ridges via the Equatorial fracture zones. Differential rates of seafloor spreading in the Central and South Atlantic provide an explanation for the rejuvenation of crustal weakness zones in Africa and the important lateral displacements recorded along them (Fairhead and Binks, 1991).

1.8 Tectonic evolution of the Equatorial Atlantic margin

The early tectonic history of the Equatorial Atlantic margin is different from that of the central segment of the South Atlantic margin or “Aptian salt basin” (Emery et al., 1975a; 1975b; Masclé, 1976; Blarez and Masclé, 1988; Masclé et al., 1988; Basile et al. 1993; 1998; MacGregor et al., 2003; Brownfield and Charpentier, 2006; Moulin et al., 2010). The tectonic evolution of these “Aptian salt basins” is characterised by a continental rifting stage dominated by extensional or block faulting, forming grabens filled with lacustrine and fluvial sediments. This rifting was followed by deposition of

regional evaporites, and subsequent halokinesis (Teisserenc and Villemin, 1990; McHargue et al., 1992; Seranne and Anka, 2005).

The Equatorial Atlantic is characterised by continent-ocean fracture zones (COFZs). COFZ often marks the transition between extended continental crust, consisting of multiple half-grabens, and oceanic crust with a characteristic pervasive seafloor-spreading fabric (Figure 1.1; Davies et al., 2005). The COFZ preserves a history of continent-continent shearing, followed by oceanic crust accretion and continent-ocean shearing during the inception of the Equatorial Atlantic rifting (Guiraud et al., 1997; Davies et al., 2005; Basile et al., 2005; Moulin et al., 2010; Basile, 2016). Transform margins are typified by sharp continent to ocean transitions (Sage et al., 2000), and show definite bathymetric features, including steep slopes and marginal ridges (e.g. Mercier de Lépinay et al., 2016). Transform faulting along the Equatorial Atlantic margins has been identified by many workers especially along the region between Nigeria and Liberia in West Africa (Harland, 1971; Mascle and Blarez, 1987; Basile et al., 1993; 2005; Edwards et al., 1997; Mohriak and Rosendahl, 2003; Moulin et al., 2010; Fairhead et al., 2013; Basile, 2016). The main fracture zones in the Equatorial Atlantic include (from south to north): the Chain, Romanche, and St. Paul Fracture Zones (Figure 1.1). These fracture zones trend ENE-WSW and are known to bound east-west to east northeast-west southwest pull-apart basins. The continental basins that trend parallel to these transform faults include the Benue and Potiguar Basins (Chain), Togo-Ghana and Ceará Basins (Romanche), the Côte d'Ivoire and Pará-Maranhão Basins (Saint Paul). Some short segments of conjugated divergent margins also occur between these transform faults (Benin-Mundáú, deep Ivorian Basin-Barreirinhas, Libéria-Cassipore (Figure 1.1; Da Costa et al., 1990; De Caprona, 1992; Basile and Brun, 1999; Basile et al., 2005; Moulin et al., 2010; Basile, 2016).

Both margins of West Africa and northeast Brazil possess complex tectonic histories compared to basins elsewhere along both sides of the southern South Atlantic margin (Heine and Brune, 2014). Their complexity is associated with the influence of transform faulting during the tectonic evolution of basins along the West African and northeast Brazilian margins (Fox and Gallo, 1984; Benkhelil et al., 1988; 1995; Matos 2000, Moulin et al., 2010; Fairhead et al., 2013; Austin et al., 2013; Heine and Brune, 2014). Conventional processes of rifting cannot explain kinematics and rift geometry of sedimentary basins along the Equatorial Atlantic margin (e.g. Matos, 2000; Moulin et al., 2010; Basile, 2016). This is because the tectonic evolution of these basins is influenced by transform faulting (Matos, 2000; Basile et al., 2005; Moulin et al., 2010; Fairhead et al., 2013; Heine and Brune, 2014; Basile, 2016; Mercier de Lépinay et al., 2016). These basins along the Equatorial Atlantic margin are typically characterised by both shearing and pull-apart features. Despite these characteristic features, their magnitude and basin architecture depend on distance from the major transform faults (Aydin and Nur, 1982; Mann et al., 1983; 2003; Matos, 2000; Basile et al., 2005).

The Phanerozoic tectonic evolution of the Equatorial Atlantic has been condensed into four stages (stages I to IV) (Figure 1.9; Mohriak and Rosendahl, 2003; Attoh et al., 2004; Brownfield and Charpentier, 2006; Antobreh et al., 2009; Basile, 2016; Mercier de Lépinay et al., 2016). These stages include oblique rifting, continent-continent transform, ocean accretion, and the connection between West African and Brazilian was broken (e.g. Heine and Brune, 2014).

The intracontinental stage is characterised by oblique rifting that led to the evolution of pull-apart basins (Mann et al., 1983; Mann, 2007). The width of the pull-apart basins is dependent on the initial fault geometry while their lengths increase with increasing fault displacement. These basins developed as a result of displacements along lithospheric-scale strike-slip faults (Figures 1.9 and 1.10). During the Berriasian syn-rift

sedimentation occurred in intracontinental basins such as in the Potiguar Basin (Araripe and Feijó, 1994) and probably along the Patos Lineament in the Araripe (Baudin and Berthou, 1996) and Rio do Peixe Basins (Senant and Popoff, 1991; Françolin et al., 1994; Basile et al., 2005).

The signatures of the rifting stage are often destroyed by the subsequent syn-transform processes and the wedge geometry that signifies the rifting stage may generally be rare in most transform margins (Figures 1.9B and 1.10B; e.g. Matos, 2000). Sedimentation started in the early Barremian in the Benue Trough (Brunet et al., 1988), the Ghanaian Keta Basin (Doyle et al., 1982) and Foz do Amazonas (Brandão and Feijó, 1994). During this phase of rifting, the Niger Delta area acts as a triple junction between the South Atlantic rift, the Benue transtensional rift and the transform zone of en echelon Equatorial basins (Basile et al., 2005).

The syn-transform stage involves the formation of oceanic lithosphere along a spreading centre to establish an active ocean-continent transform (Figures 1.9C and 1.10C). The contact between the new, hot oceanic lithosphere and the old, cold continental lithosphere is such that thermal exchange is predicted to cause heating and uplift of the continental crust, especially near the continental-oceanic boundary (COB). This uplift due to thermal expansion results in subaerial erosion near the COB (Basile et al., 2005; Basile, 2016).

The post-transform stage is the passive margin stage when transform motion ceases as the oceanic ridge passes beyond the unstretched West African continental lithosphere (Figures 1.9D and 1.10D). This stage is typified by slow thermal subsidence on the Côte D'Ivoire Ghana transform margin (CIGTM) (Attoh et al., 2004). The CIGTM formed along the paleo-Romanche transform fault coincides with the most prominent fracture zone in the Equatorial Atlantic, with an offset on the Mid-Atlantic Ridge approaching 900 km (Figure 1.11; Attoh et al., 2004; Antobreh et al., 2009).

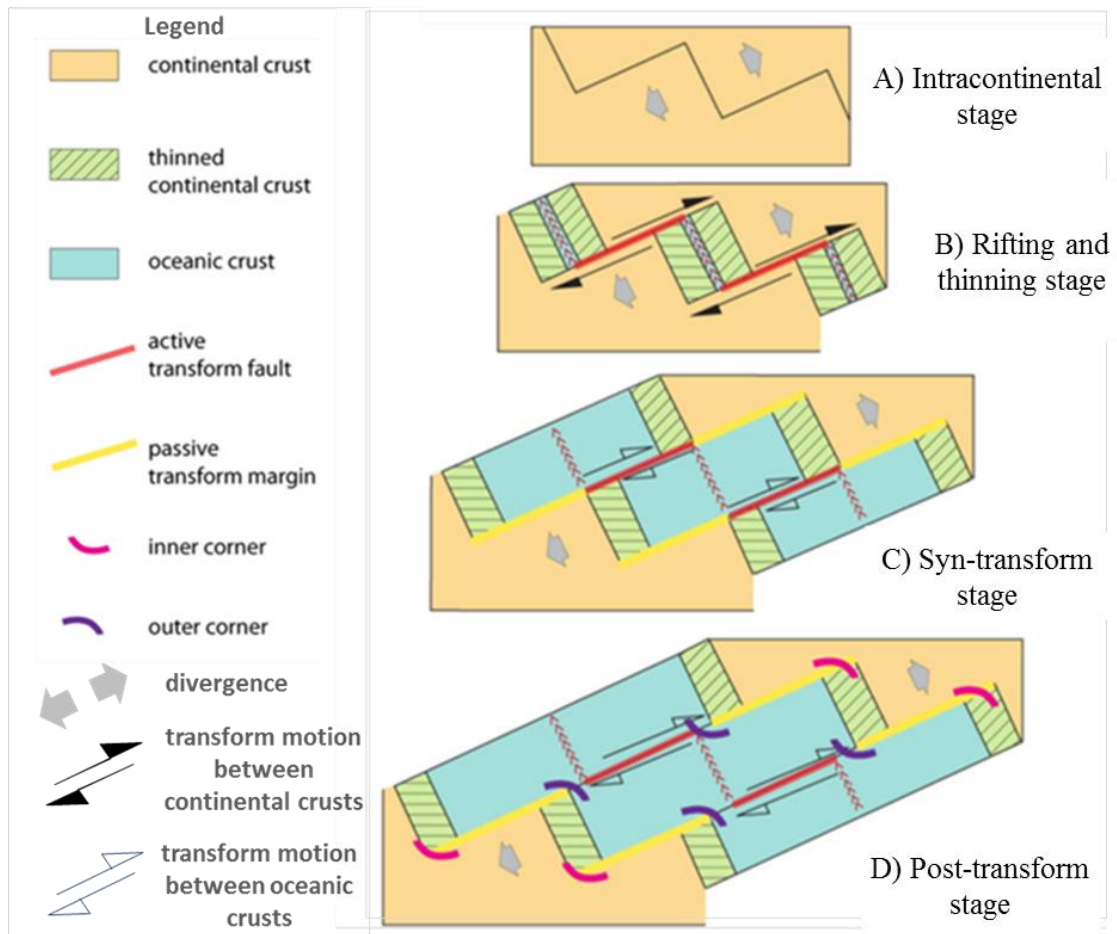


Figure 1.9: Models of transform continental margin evolution. Note that the opening of the Equatorial Atlantic margin demonstrates a one-stage model from the intracontinental stage to the post-transform stage (after Mercier de Lépinay et al., 2016).

1.9 Existing models for the opening of the Equatorial Atlantic Ocean

The timing and mechanisms for the opening of the South Atlantic, and especially its Equatorial segment are controversial (e.g. Færseth and Lien, 2002; Moulin et al., 2010; Fairhead et al., 2013; Heine and Brune, 2014; Basile, 2016; Mercier de Lépinay et al., 2016). The Cretaceous quiet zone is seafloor that formed during the Cretaceous Normal Superchron (CNS), i.e. during a long period of stable polarity in the geomagnetic field (e.g. Channell et al., 1995).

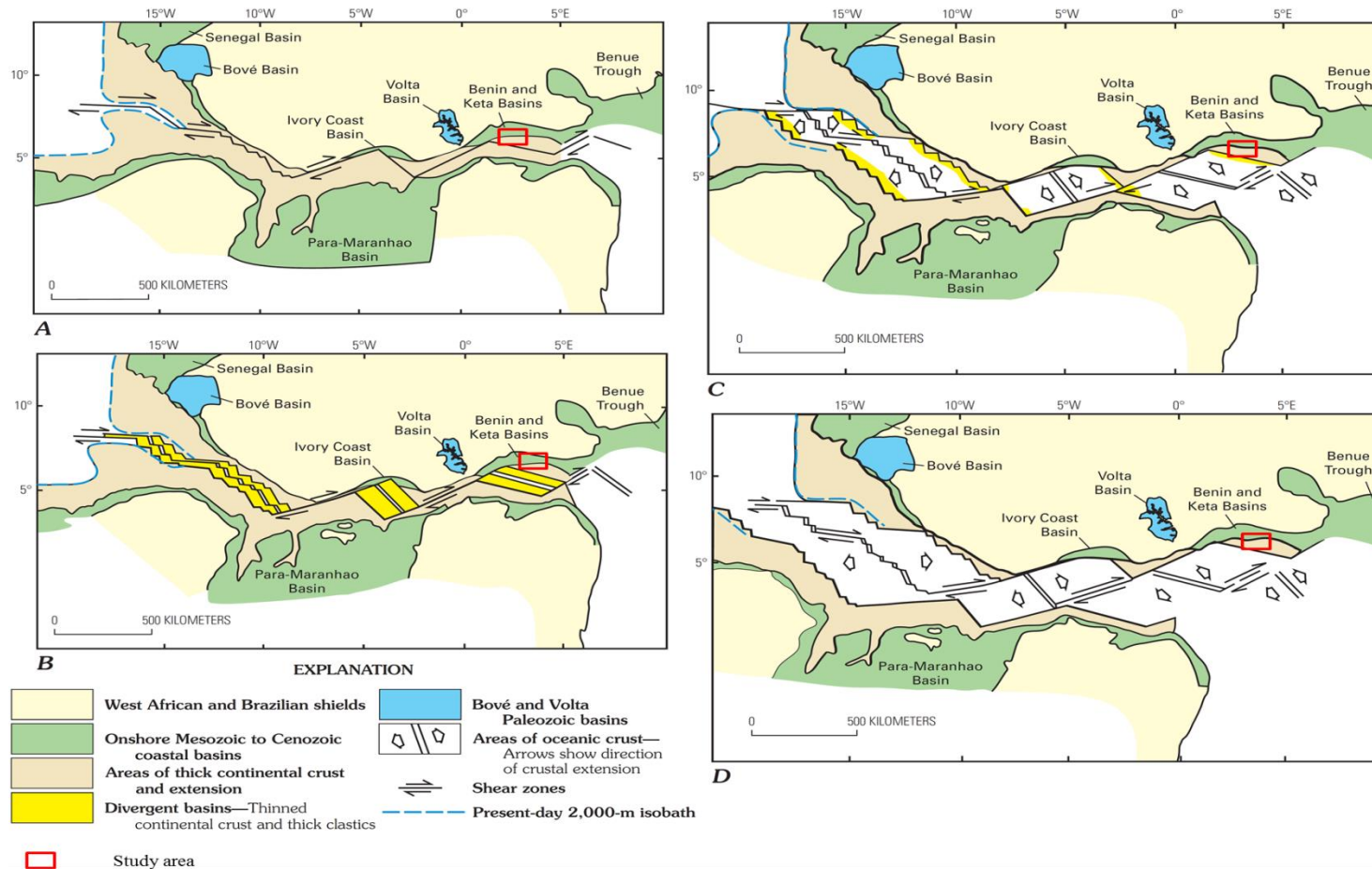


Figure 1.10: Schematic Cretaceous stages in the Mesozoic breakup of Africa and South America highlighting the tectonic evolution of the Equatorial Atlantic, and showing the approximate location of the Bové, Benin, Ivory Coast, Keta, Senegal, Volta Basins and the Benue Trough of Africa, and the Para-Maranhão Basin of Brazil. A, Hauterivian, 125 Ma; B, early Albian, 110 Ma; C, late Albian, 100 Ma; D, Santonian, 85 Ma (from Mascle et al., 1988; Brownfield and Charpentier, 2006).

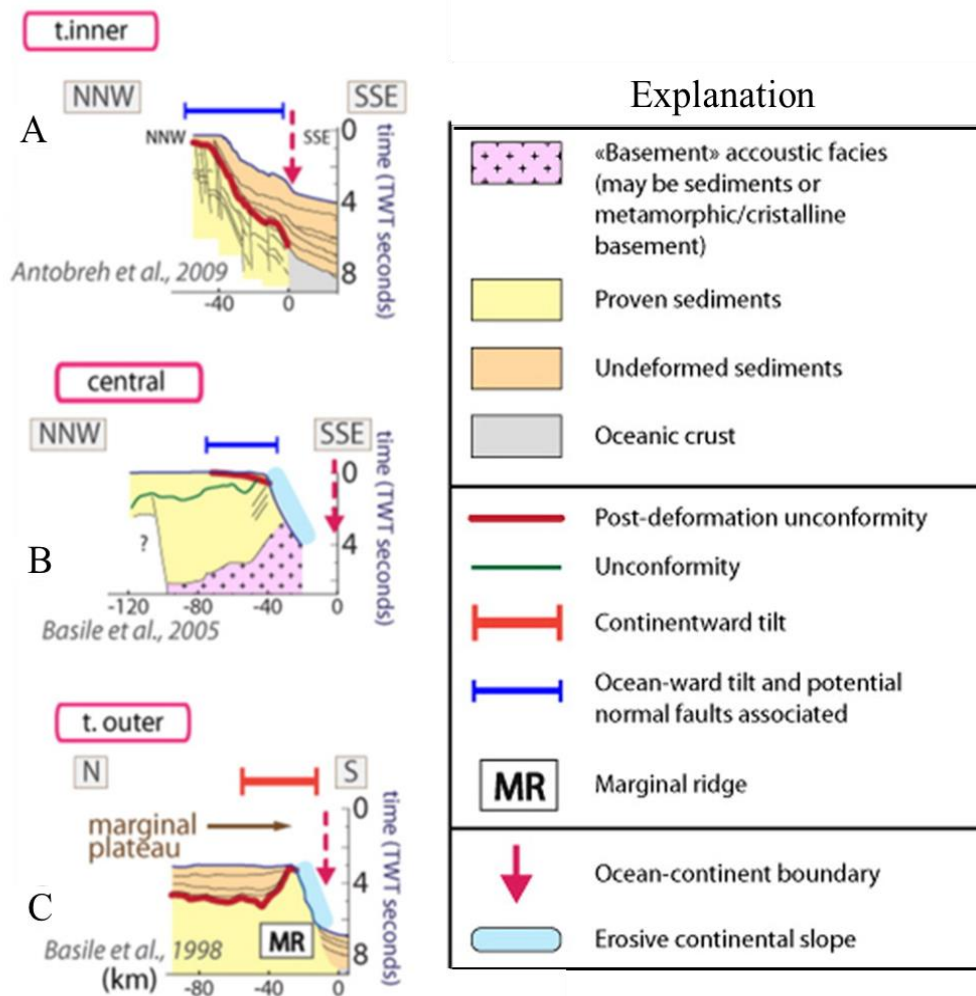


Figure 1.11: Line drawings of seismic reflection profiles perpendicular to Côte d'Ivoire-Ghana transform margin. Note that the continental slope is steeply-dipping (after Basile et al., 1998; 2005; Antobreh et al., 2009; Mercier de Lépinay et al., 2016).

The ocean crust adjacent to the Equatorial Atlantic margin is dominated by the Cretaceous Quiet Zone, formed during a period without geomagnetic reversals. The Cretaceous Quiet Zone may also occur when the original magnetization has been destroyed by the effects of thermal blanketing by later sediments. It is marked by anomaly 34 corresponding from the Aptian (124 Ma) to Santonian (84 Ma), therefore, making the dating of events related to its opening difficult, coupled with an inability to drill to the basement in order to recover fossils for dating it.

Many kinematic models have been postulated to explain the opening of the Equatorial Atlantic (Mohriak et al., 2000; Mohriak and Talwani, 2000; Moulin et al., 2010; Fairhead et al., 2013; Heine and Brune, 2014; Basile, 2016). These models are based on a series of constraints including seafloor isochrons (Müller et al., 2008), flow lines or fracture zones (Rabinowitz and Labrecque, 1979; Cande et al., 1988; Fidalgo, 2001; Labails, 2007), a linkage between stratigraphic unconformities and fracture zones (i.e. azimuth-age plot; Fairhead et al., 2013); numerical models (Brune et al., 2012; Brune and Austin, 2013; Heine and Brune, 2014); analogue models (Chemenda et al., 2002); continental and oceanic homologous structures, and radiometric dating of igneous rocks (Basile, 2016).

Reviews of the opening of the Equatorial Atlantic Ocean show that the existing models fall into two main schools of thought:

- ❖ One-stage opening model
- ❖ Two-stage opening model

1.9.1 One-stage opening model

The one-stage model is more widely accepted than the two-stage model by many authors (e.g. Heine and Brune, 2014; Mercier de Lépinay et al., 2016). These authors believe that the opening of the Equatorial Atlantic Ocean has been solely due to a one-stage movement of the African Plate away from the South American Plate (e.g. Heine and Brune, 2014; Mercier de Lépinay et al., 2016). This was probably due to the role of fracture zones in this region. It is also thought that the African Plate had moved northeastward relatively to the South American Plate (Figure 1.12). This model holds that tectonic evolution of the Equatorial Atlantic through the pre-transform (syn-rift), the syn-transform, to the post-transform (passive) stages involved rifting by oblique

extension since the Aptian to Santonian (e.g. Mercier de Lépinay et al., 2016; Figures 1.9 and 1.10). The movement was initiated through shearing along the Central African Shear Zone (CASZ) and later continued along the oceanic fracture zones. This, therefore, suggests an NE-SW extension for the Equatorial Atlantic through syn-rift, syn-transform to drifting phases (Figure 1.12). This one-stage opening of the Equatorial Atlantic will be tested in the offshore Benin Basin in Chapter 6 of this study.

Model 1: One-stage opening of Equatorial Atlantic

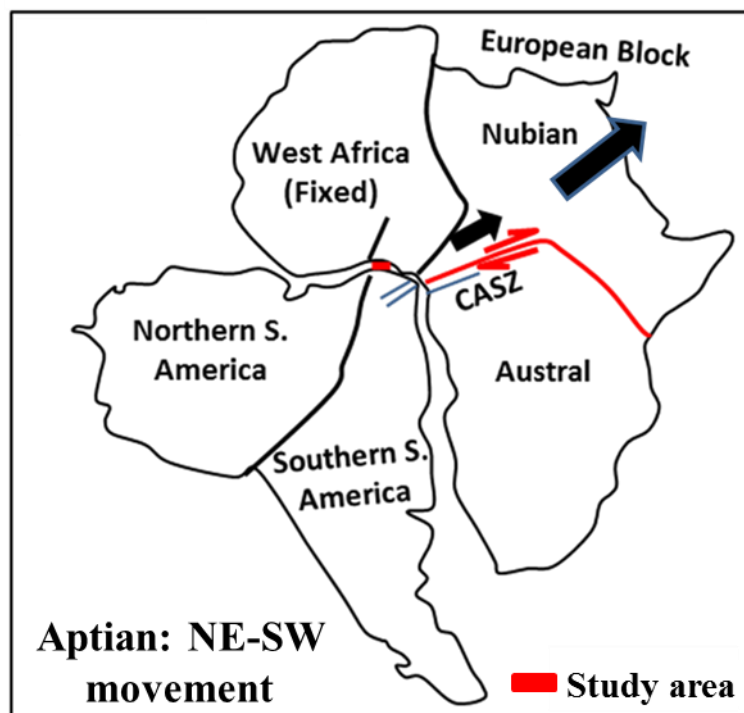


Figure 1.12: A one-stage opening model of the Equatorial Atlantic Ocean involving the African Plate moving dominantly northeast in the Albian. A solely NE movement of the African Plate initiated through the re-activation of the Central African Shear Zone (CASZ; red line indicates active shear zone) (i.e. intraplate rifting; e.g. Heine and Brune, 2014).

1.9.2 Two-stage opening model

The two-stage model postulates that the opening of the Equatorial Atlantic Ocean occurred in two stages involving:

- ❖ An initial N-S rifting by orthogonal extension of the African-South American Plate during the Barremian (Figure 1.13A; Moulin et al., 2010; Fairhead et al., 2013)
- ❖ A later NE-SW rifting of African Plate in the earliest Aptian - Albian (Figure 1.13B; Fairhead et al., 2013).

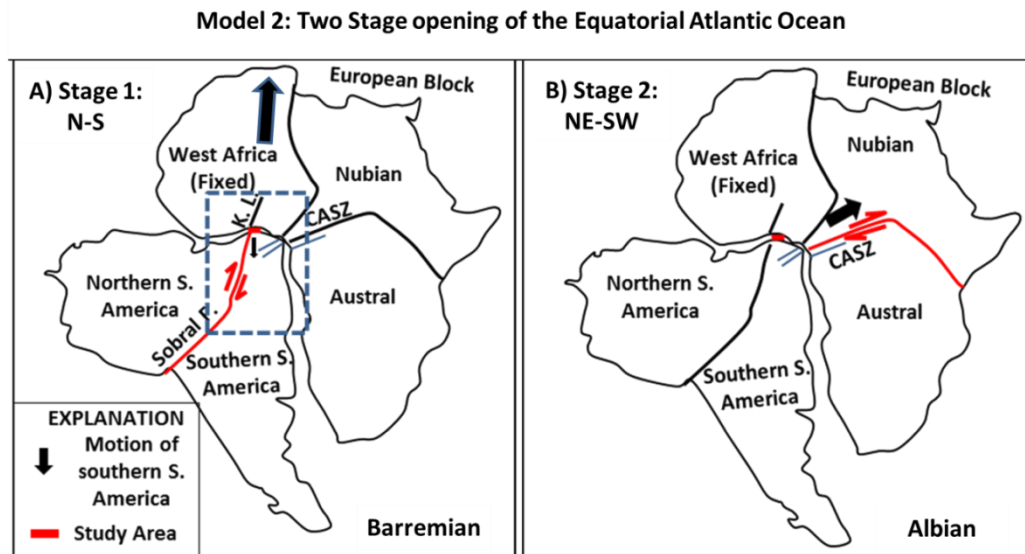


Figure 1.13: A two-stage opening model resulted in the opening of the Equatorial Atlantic Ocean. A) An initial opening involved the northward movement of the African Plate relative to the South American Plate in Barremian. A northward movement of the African Plate occurred due to movement along the re-activated N-S Sobral Fault (the red line indicates active fault) (e.g. Moulin et al., 2010). B) A stage 2 NE-SW movement as a consequence of change in the direction of movement of the African Plate in the Albian. The NE movement occurred through the re-activation of the Central African Shear Zone (red line) (CASZ; e.g. Fairhead et al., 2013).

The first stage is associated with the syn-rift 1 phase of rifting of the West and Central African Rift Systems (WCARS) from the Barremian to earliest Aptian. This initial rifting is coeval with orthogonal extension on the Equatorial Atlantic margin. A northward movement of the African-Arabian block with respect to other blocks (Guiraud et al., 1992; Guiraud and Maurin, 1992) was proposed to be responsible for the tectonic evolution of WCARS. In contrast Genik (1992) and Binks and Fairhead (1992) favour a more northeasterly movement of the Arabian-Nubian block. In the

review of the opening of the Equatorial Atlantic, Moulin et al. (2010) proposed an N-S movement involving the reactivation of the Sobral Fault that led to the northward movement of the northern South American block while the southern South American block moved southward (Figure 1.13A).

The N-S opening of the Equatorial Atlantic was followed by a second stage of opening that is thought to result from changes in relative African-South American Plate motion from the initial N-S to NE-SW direction during the Aptian-Albian. The change in motion led to change stress field that subsequently caused the reactivation of pre-existing structures (i.e. the Central African shear zone, CASZ; Figure 13B). This Aptian-Albian phase of movement can account for the evolution of intra-continental basins in WCARS. This phase of movement in the WCARS was linked to wrenching and strike-slip deformation (Guiraud et al., 1992; Guiraud and Maurin, 1992; Fairhead et al., 2013).

1.10 Basin architecture of rifted versus transform margins

Extensional passive continental margins and sheared continental margins (characterised by transform faults and strike-slip motion; e.g. Christie-Blick and Biddle, 1985) are typified by very different geological and geophysical signatures, reflecting fundamentally different tectonic processes (Mohriak and Rosendahl, 2003). Rift basins are found in all passive continental margins especially along the Atlantic and they may be referred to as Atlantic-type rifts. They provide a history of the early stages of the breakup of the continents and the super-continents. Their architecture and basin-fill are controlled by the basin-bounding normal fault systems. The displacement of these fault systems generally creates accommodation space where sediments accumulate. Their architecture is such that records of the evolution their faults in terms of fault nucleation, propagation and linkages can be obtained from their rock record. Their architecture may

also permit the accumulation of lacustrine deposits and petroleum (Gibson et al., 1989; Katz, 1990; Schlische and Olsen, 1990; Schlische, 1993; Bonini et al., 1997; Olsen and Kent, 1999; Ebinger et al., 2002).

Extensional passive margins are often characterised by broad zones of thinned crust (100 - 200 km) close to the continent-ocean transition, at least in the magma-poor case (Boillot et al., 1988; Clift and Lorenzo, 1999). Sheared passive margins, however, show sharp (<30 km) continent-ocean transitions, with deformation focused close to the former plate boundary (Masclé et al., 1995; Clift and Lorenzo, 1999). Structurally, the sheared margins are often complex and narrow while the rifted passive margins are relatively simpler (Figures 1.11 and 1.14).

Sheared margins are often associated with a ridge formed when the seafloor spreading axis moves along the margin, whereas ridges may be rare on rifted passive margin. Sheared margins are less volcanic than rifted margins (Benkhelil et al., 1995; 2002; Geoffroy, 2005; Jammes et al., 2010).

Extensional passive margins are typically characterised by a fault-bounded feature known as half-grabens (Steel and Ravnâs, 1998). The half-graben has a triangular geometry in cross-sections viewed perpendicular to their bounding faults. The half-graben is directly dependent on the deformation field surrounding the bounding fault. The displacement is often such that it is greatest at the centre of the fault and decreases to zero at the fault tips. This often results in a syncline-shaped basin in longitudinal sections (Gawthorpe and Leeder, 2000).

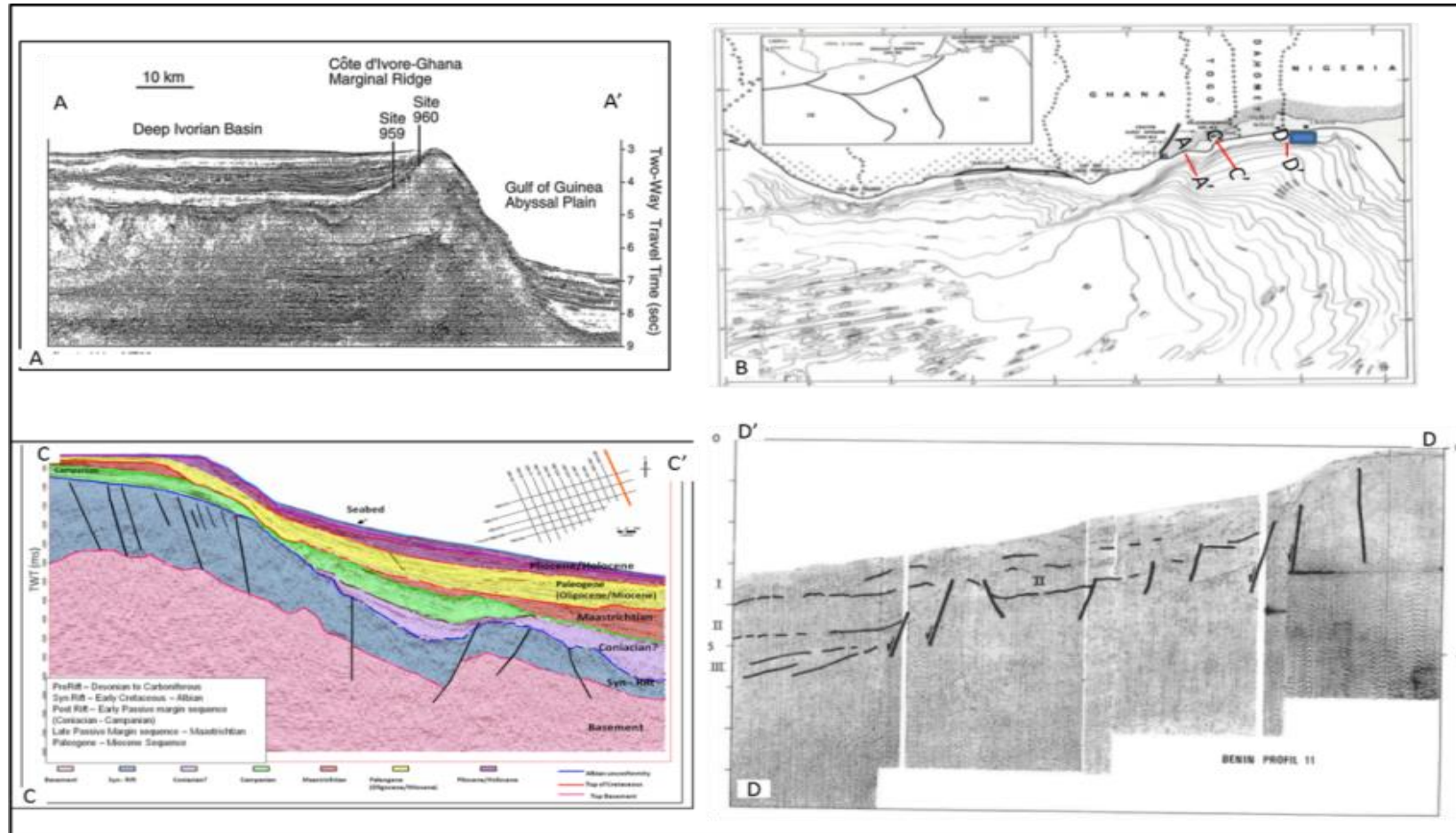


Figure 1.14: Examples of seismic sections obtained from different locations (B) in the Equatorial Atlantic margin. A) Seismic section (A-A') across the NE-SW trending Côte d'Ivoire-Ghana Transform Margin showing some characteristic features of a transform margin such as a sharp gradation from the continental shelf to basin floor (after Clift et al., 1997; Bird, 2001). B) Physiographic map of Gulf of Guinea in the Equatorial Atlantic region showing the study area (blue box) and locations of seismic sections (after Delteil et al., 1974). C) Seismic section (C-C') representing the E-trending Keta Basin and showing a relatively gradual change from continental shelf through continental slope to continental rise. D) Seismic section (D-D') across the (E-W) trending Benin Basin showing a gradual change in slope gradient from continental shelf to the slope and a rise (after Delteil et al., 1974).

Fault-propagation folds tend to form in contractional settings. The main folds in extensional settings are roll-overs (Withjack et al., 1990; Gawthorpe et al., 1997; Ford et al., 2007).

Stratigraphically, most non-marine rift basins have a tripartite stratigraphy comprising a basin-wide fluvial deposit that is overlain by a relatively abrupt deepening-upward lacustrine succession followed by a gradual shallowing-upward lacustrine and fluvial succession (Lambiase, 1990; Schlische and Olsen, 1990; Carroll and Bohacs, 1999).

Transform faults in oceanic lithosphere generally behave according to the plate-tectonic model. However, strike-slip faults in continental lithosphere are extremely complex and difficult to fit into a model involving rigid plates. This is because they are thought to have possibly experienced alternating periods of extension and contraction as slip directions adjust along major crustal faults. They are, therefore, formed through transtension (by extension along a strike-slip fault), transpression (by compression along a strike-slip fault), or transrotation (by rotation of the crustal blocks about vertical axes within strike-slip fault) (Ingersoll, 1988; Dewey, 1989, 1998; Park, 1997; Fossen and Tikoff, 1998; Fossen, 2012; Allen and Allen, 2013).

Because strike-slip movement is often involved in sheared passive margins there is no net addition or subtraction (i.e. conservative plate boundary) to the crust, whereas during the development of extensional passive margins new oceanic crust is formed (i.e. constructive plate boundary). Table 1.1 summarises some of the differences in basin architecture between basins along transform and extensional passive margins.

Table 1.1: Summary of characteristics of transform and divergent margins (Brownfield and Charpentier, 2006; Antobreh et al., 2009; Fairhead et al., 2013; Allen and Allen 2013; Heine and Brune, 2014).

<i>Criteria</i>	<i>Transform Margin</i>	<i>Divergent Margin</i>
Fault type	Strike-slip with normal or reverse sense	Normal fault
Angle of Dip	Oblique	30 ⁰ - 60 ⁰
Geometry	Wedge not often well-preserved	Wedge pattern often well-preserved
Seafloor physiography	Highly steeply-dipping seafloor with little continental shelf	Gently-dipping seafloor, with characteristic continental shelf that graded into gently to slope to rise
Fault shape	Planar or curvilinear in both plan (map) and cross-sectional views	Planar or listric in cross-section Planar or curvilinear in map view
Volcanism	May sometimes lack volcanic rocks; for example, the Equatorial Atlantic	May sometimes have volcanic rocks, for example, the SW Africa margin
Evaporite	May lack evaporite	May contain evaporite
Examples of basins	Togo-Ghana margin, Red Sea, Gulf of Aden, Gulf of Guinea	Tenéré, Kenya, Sudan, Syte Basins

1.11 Previous tectono-stratigraphic studies in the Benin Basin

The tectono-stratigraphic evolution of the offshore Benin Basin is not yet fully understood because of the poor dating of the syn-rift and pre-rift phases in this region (MacGregor et al., 2003; Brownfield and Charpentier, 2006; Nemçok et al., 2013a; Kaki et al, 2012). For example, the entire syn-rift succession is yet to be drilled and so cannot be directly dated. This study, however, uses well data that have dated strata up to the rift-climax stage (this will be discussed further in Chapter 3). For the purposes of this dissertation, the dating of the remaining part of syn-rift and pre-rift successions was undertaken by correlation with adjacent basins along the Equatorial and South Atlantic margins, as well as with those in intra-continental basins in Africa (Guiraud et al., 1992; Guiraud and Maurin, 1992; Basile et al., 2005; Moulin et al., 2010; Fairhead et al., 2013). Another problem with dating the timing of drift onset and the end of the syn-rift succession is the absence of magnetic anomalies offshore, within the Cretaceous magnetic

quiet zone. The pre-rift succession in the conjugate Mundáu-Ceará Basin in the northeastern Brazil has also not been dated (Matos, 1992; Matos, 2000).

1.12 Stratigraphy of the offshore Benin Basin

As noted earlier, most historical studies carried out on the Benin Basin have been limited to its onshore parts (Jones and Hockey, 1964; Reyment, 1965; Adegoke, 1969; Ogbe, 1970; Adeleye, 1975; Ako et al., 1980; Whiteman, 1982; Billman, 1992; Ala and Selley, 1997; Olabode, 2006; Adekeye and Akande, 2010; Akinmosin and Osinowo, 2010; Akinmosin et al., 2011). Few studies have regionally been carried out in the offshore part of the basin (Burke et al., 1971; Burke, 1976; MacGregor et al., 2003; Brownfield and Charpentier, 2006; Olabode and Adekoya, 2008; Opara, 2011; Kaki et al., 2012; Nemçok et al., 2013a). The stratigraphy of the offshore Benin Basin has been established (e.g. MacGregor et al., 2003; Brownfield and Charpentier, 2006; and Kaki et al., 2012; Figure 1.15), but there are disparities in the nomenclature used and in age assignments. For example, the Palaeocene Ewekoro Formation was described as overlying the Cretaceous Abeokuta Group onshore (Jones and Hockey, 1964; Burke, 1972; Whiteman, 1982, Elueze and Nton, 2004; Olabode, 2006). These latter authors classified all the Cretaceous stratigraphic units as Abeokuta Group. Another controversy is the age assignment of Late Jurassic-Early Cretaceous to the Ise Formation undertaken by early authors (e.g. Brownfield and Charpentier, 2006; Kaki et al., 2012) comprising both the pre-rift and syn-rift phases. The Late Jurassic-Early Cretaceous age seems to be ‘over-exaggerated’ because continental rifting propagated to the Equatorial Atlantic in the Barremian-Aptian (e.g. Moulin et al 2010).

sandstone, shale, and conglomerates deposited under fluvial, lacustrine and deltaic environments (MacGregor et al., 2003; Brownfield and Charpentier, 2006; Kaki et al., 2012, D’Almeida et al., 2016). D’Almeida et al. (2016) pointed out that the Ise Formation is folded. The nature and cause of the folding of the Ise Formation will be evaluated in Chapter 4 of this dissertation. As noted above, the pre-rift phase has yet to be drilled. The timing of rifting in this basin will be tested in Chapter 3. It is, however, thought to range from Upper Jurassic to Neocomian (Brownfield and Charpentier, 2006). The pre-rift phase of this formation was assigned to the Late Jurassic, while the syn-rift phase has been assigned to the Lower Cretaceous (Brownfield and Charpentier, 2006; Kaki et al., 2012, D’Almeida et al., 2016). These ages were based on correlations with the associated volcanic intrusive that accompanied initial block faulting in eastern Ghana during the Late Jurassic, in the Benin Basin (MacGregor et al., 2003; Brownfield and Charpentier, 2006; Kaki et al., 2012). The strike of volcanic rocks suggests that the initial crustal faulting and graben evolution were sub-parallel to the present-day coastline (Eagles, 2007; Eagles and Konig, 2008; Moulin et al., 2010; Kaki et al., 2012). This also implies that the age assigned to the pre-rift is uncertain. The formation is unconformably overlain by the transgressive Albian Sandstone (Brownfield and Charpentier, 2006; Kaki et al., 2012).

1.12.2 Albian Sandstone

The Albian Sandstone consists of white, grey, and dark brown fine- to coarse-grained, well to poorly-sorted sandstone, and interbedded shale (Brownfield and Charpentier, 2006; Kaki et al., 2012). The interbedded shale is black and it is rich in organic matter. It has a variable thickness ranging between 234 m and 403 m in the Benin Republic (Kaki et al., 2012). Its environment of deposition is

interpreted to be marginal marine (Kaki et al., 2012). According to Brownfield and Charpentier (2006), the Albian Sandstone is regarded as part of the syn-rift unit, with its upper limit forming the post-rift unconformity. This unconformity separates the Albian Sandstone from marine rocks of the uppermost Albian-Cenomanian age (MacGregor et al., 2003; Brownfield and Charpentier, 2006). The breakup sequence defined in this study for this basin (see Chapter 4) correlates with this Albian Sandstone.

1.12.3 Abeokuta Formation (Turonian)

This unit unconformably overlies the Albian Sandstone offshore and the crystalline basement rock onshore (Jones and Hockey, 1964; Kogbe, 1974, 1989; Ako et al., 1980; Whiteman, 1982). The Abeokuta Formation is composed of two stratigraphic units, the ‘Cenomanian Shale’ and ‘Turonian Sandstone’ (Brownfield and Charpentier, 2006). The Cenomanian Shale is composed of shales. The Turonian Sandstone is made up of grey to white coarse-grained sandstones interbedded with shale beds. It occasionally overlies a shale and siltstone sequence (Kaki et al., 2012). The thickness of the Abeokuta Formation may be about 1000 m, but it tends to thin to the north and west. Its environment of deposition may range from marginal marine to inner shelf (Kaki et al., 2012).

1.12.4 Awgu Formation (Coniacian-Maastrichtian)

This formation is unconformable over the Turonian Sandstone (Brownfield and Charpentier, 2006). It consists of dark-grey calcareous shale, interbedded with calcareous siltstone, and fine-grained sandstone deposited under anoxic marine conditions. It fills a graben formed below the Senonian unconformity (Brownfield and Charpentier, 2006). Its age ranges from Coniacian to Maastrichtian.

1.12.5 Araromi Formation (Maastrichtian-Palaeocene)

This formation comprises two members: the upper and lower Araromi Members. It is generally composed of black to dark laminated carbonaceous shales with pyrite and pyritised microfauna (Kaki et al., 2012). The two members are demarcated by a change in colour. The upper Araromi member is of Palaeocene age, while the lower Araromi is Maastrichtian. The formation also contains limestone layers (Kaki et al., 2012).

1.12.6 Imo Shale (Palaeocene-Eocene)

The Imo Shale conformably overlies the Araromi Formation. It comprises light greenish to blueish, grey to dark grey, non-calcareous hard shales and macro-crystalline limestones (Kaki et al., 2012). The Imo Shale is described as the lateral equivalent to the Eocene Akata Formation, the main source interval in the prolific Niger Delta (Short and Stauble, 1967). Its age ranges from Palaeocene to Eocene. It was deposited in an upper bathyal to outer sub-littoral marine, well-oxygenated environment. It is separated from the overlying Oshoshun Formation by a major unconformity dated as Oligocene (Brownfield and Charpentier, 2006).

1.12.7 Oshoshun Formation (Middle Eocene)

This formation comprises marine sandy shales of Middle Eocene age. It contains abundant phosphatic material (Kaki et al., 2012). It occurs throughout the shelf area. Its environment of deposition is marine, outer sub-littoral.

1.12.8 Afowo Formation (Early to Middle Miocene)

The Afowo Formation is considered as the main petroliferous formation, consisting of coarse- to medium-grained sandstones with thick intercalations of shale, siltstone and pyritised clay (D'Almeida et al., 2016).

In the offshore Benin Republic, the Afowo Formation is, however, thought to consist of two units separated by a Miocene unconformity (Brownfield and Charpentier, 2006; D'Almeida et al., 2016). The lower unit comprises light grey siltstone that grades upwards into fine-grained sandstone, while the upper unit consists of a sequence of silty clay, coarse-grained sandstone with glauconite, pyrite and shell debris (Kaki et al., 2012). The unit is thought to have been deposited in marine, outer sub-littoral to the upper bathyal well-oxygenated environment. Its age ranges from Early to Middle Eocene (Figure 1.14; Brownfield and Charpentier, 2006; Kaki et al., 2012). In Benin Republic, some authors regarded the Turonian Abeokuta Formation, as the lateral equivalent of the Miocene Afowo Formation in southwestern Nigeria, because the Abeokuta Formation has been applied for the Afowo Formation (e.g. Omatsola and Adegoke, 1981; D'Almeida et al., 2016). This is misleading, and a unified stratigraphy needs be established for the basin (Omatsola and Adegoke, 1981; D'Almeida et al., 2016).

1.12.9 Benin-Ijebu Formation (Pliocene-Holocene)

This is the uppermost stratigraphic unit in the offshore Benin Basin. It is composed of marine shelf sands that coarsen upwards. It also consists of argillaceous sandstone and siltstone. Its age is Pliocene to Holocene. This stratigraphic unit is capped by very young marine sediments that prograde

southward (Brownfield and Charpentier, 2006; Kaki et al., 2012; Olabode and Mohammed, 2016).

1.13 Petroleum systems of the Equatorial Atlantic

The West African part of the Equatorial Atlantic can generally be described as underdeveloped as exploration for hydrocarbon only recently intensified as a result of the discovery of Jubilee Field. The reason may be connected with the nature of the transform margin that characterises this region unlike the passive margin to the south of Niger Delta.

The source rock for hydrocarbon generation in the Equatorial Atlantic is generally considered as not mature due to the absence of a syn-rift phase that can easily enhance hydrocarbon generation. However, Early Cretaceous source rocks have been identified in the Abidjan, Tano and Benin Basins, while the proven source rocks in the Ghana Platform are Palaeozoic strata (Brownfield and Charpentier, 2006; Kaki et al., 2012).

The reservoir rocks are much developed in the West African part of the Equatorial Atlantic; they include the clastics of Albian age in the Côte d'Ivoire-Ghana transform margin and in the Benin Basin (Figure 1.2). Other hydrocarbon reservoirs include Upper Cretaceous (Turonian-Senonian) strata.

Seal intervals consist of mudstone and shale in many parts of the Equatorial Atlantic margin. Both structural and stratigraphic traps occur in the Tano, Benin, Keta Basins and the Ghana-Togo Transform margin. Main structural traps include block traps and anticlinal traps. Post-transform anticlinal traps also occur in the Ghana-Togo margin.

1.13.1 History of petroleum exploration in the offshore Benin Basin

Petroleum exploration in the Benin Basin dates back to 1908 near Okitipupa, east of Lagos, where bituminous sands outcrop (Coker and Ejedawe, 1987). This was championed by the Nigerian Bitumen Company and the British Colonial Petroleum. The discovery of hydrocarbon at Oloibiri (Niger Delta), in 1956, led to a shift in focus from the eastern Benin Basin to the Niger Delta. This discovery was made by the then Shell D'Arcy Petroleum (now Shell Petroleum Development Company). Few of the wells drilled in the onshore part of the Benin Basin during this period were later tagged 'dry' and abandoned (Nton, et al., 2009). In the early 1990s, the Federal Government of Nigeria attempted to involve local oil companies (for example, the Yinka Folawiyo Nigeria Limited) in the exploration of this basin and other frontier areas such as the Anambra Basin, Borno Basin, Bida Basin, and Benue Trough. Thus, there has been a resurgence of interest in exploration activity in the Benin Basin. This then led to the acquisition of 2D seismic data in the 1990s and later 3D in the early 2000s. Some of the discovered fields in the Benin Basin include the Aje, and the north and south Seme Fields. The study area covers the Aje Field, which is the most explored field in the Nigerian part of the basin. The Aje field was discovered in 1996, but only four wells (B-01 to B-04) have so far been drilled in it. About 156 mmbbls of crude oil and 1.5 tcf of gas have been discovered in the Aje Field (DPR, 2003). However, production is yet to commence in the Nigerian portion of the Benin Basin.

1.14 Thesis structure

The remainder of this dissertation has been structured into a further six chapters (Chapters 2-7). The role of each chapter in addressing the research questions identified in this introductory chapter is outlined briefly below.

Chapter 2 is titled: “Structural and stratigraphic framework of the offshore Benin Basin”. This chapter describes five major megasequences (MS1-MS5) and their corresponding boundaries (MSB1-MSB5). These boundaries were identified on the basis of reflection terminations and geometries on seismic data, tied to biostratigraphic data. Each of these unconformities denotes the onset (or end) of major geological events that may be tectonic or non-tectonic in origin. It also includes the structural analysis of the seismic data on the basis of the geometries observed on the seismic. Some of the main structures recognised include basin-bounding normal faults (F1 and F2), reverse fault (F3), and associated folds, half-grabens and gravity-induced normal faults.

Chapter 3 has been titled “Tectono-stratigraphy and structure of the syn-rift megasequence, offshore Benin Basin”. It uses a similar procedure to that in Chapter 2 to describe the syn-rift phase of the basin evolution. This involves the identification of wedge-shaped growth geometries on the seismic data. Growth geometries often characterise the syn-rift phase of basin development (Prosser, 1993). Unconformities representing both the onset and end of rifting are identified and dated. The seismic geometry indicated two synchronous asymmetric half-grabens; one in the northern and the other in the southern part of the study area.

Chapter 4 is titled “Cretaceous post-rift megasequence MS3 (late Aptian – latest Maastrichtian)”. This chapter examines the seismic stratigraphy of the first post-

rift megasequence and its tectonically-induced structures. The seismic data were also analysed for the presence of breakup sequence and its possible implication for the opening of the Equatorial Atlantic and spreading of the ocean floor. The chapter concentrates on the contractional structures with the aim of predicting the kinematics and mechanisms for their evolution. Onlapping of seismic reflections on fold limb was used to date them. The importance/impact of these structures on sediment distribution in the basin is also discussed.

Chapter 5 is named “Cenozoic Geology of the offshore Benin Basin”. It covers the Cenozoic strata that include both the transgressive megasequence (MS4) and the regressive megasequence (MS5). These are characterised by slumping and regressive sedimentation, respectively. Associated submarine canyons and channels were studied for their evolution and influence on sediment distribution. Their implications to the petroleum systems of the basin were also considered. The regressive megasequence (MS5) was tested for its conformity to the existing sequence-stratigraphic models of Vail et al. (1977) and Neal and Abreu (2009).

Chapter 6 discusses the overall results obtained in this thesis with the objective of addressing the control of the extensional structures on sedimentation. The implication of tectonics for petroleum systems in the Benin Basin was also considered, including implications of both the extensional and contractional structures to the geodynamic evolution of southwestern Nigeria and the Equatorial Atlantic.

Chapter 7 summarises the major contribution of this research project and explores the general implications of these results to future studies, it also reviews our new understanding of the Benin Basin.

Chapter Two

2.0 Structural and stratigraphic framework of the offshore Benin Basin

This chapter describes the datasets (2D and 3D seismic data, well data (well-logs and biostratigraphic data) and methodologies used for this study. It also presents a new seismic stratigraphic and structural framework for the offshore Benin Basin which has been developed from analysis of this data.

2.1 Introduction

Megasequences are composed of a series of higher-order sequences and their bounding sequence boundaries. According to Hubbard (1988), megasequence boundaries separate the major phases of basin evolution (e.g. change in basin subsidence mechanism including syn-rift to post-rift). However, in this study, Hubbard (1988) definition has been slightly modified to include other major unconformities of the regional extent where there is a significant change in stratigraphic behaviour (e.g. a change from transgressive to regressive phase). The age of the megasequences was constrained by tying the megasequences to well data from the four wells (Figure 2.1) that have been biostratigraphically dated during oil exploration (Du Chene and Adegoke, 2006; Mosumolu, 2008). The ages of megasequences covering the deeper, undrilled, part of the stratigraphy section were interpreted by correlation to adjacent basins in the region (e.g. Guiraud et al., 1992; Guiraud and Maurin, 1992; Moulin et al., 2010; Fairhead et al., 2013).

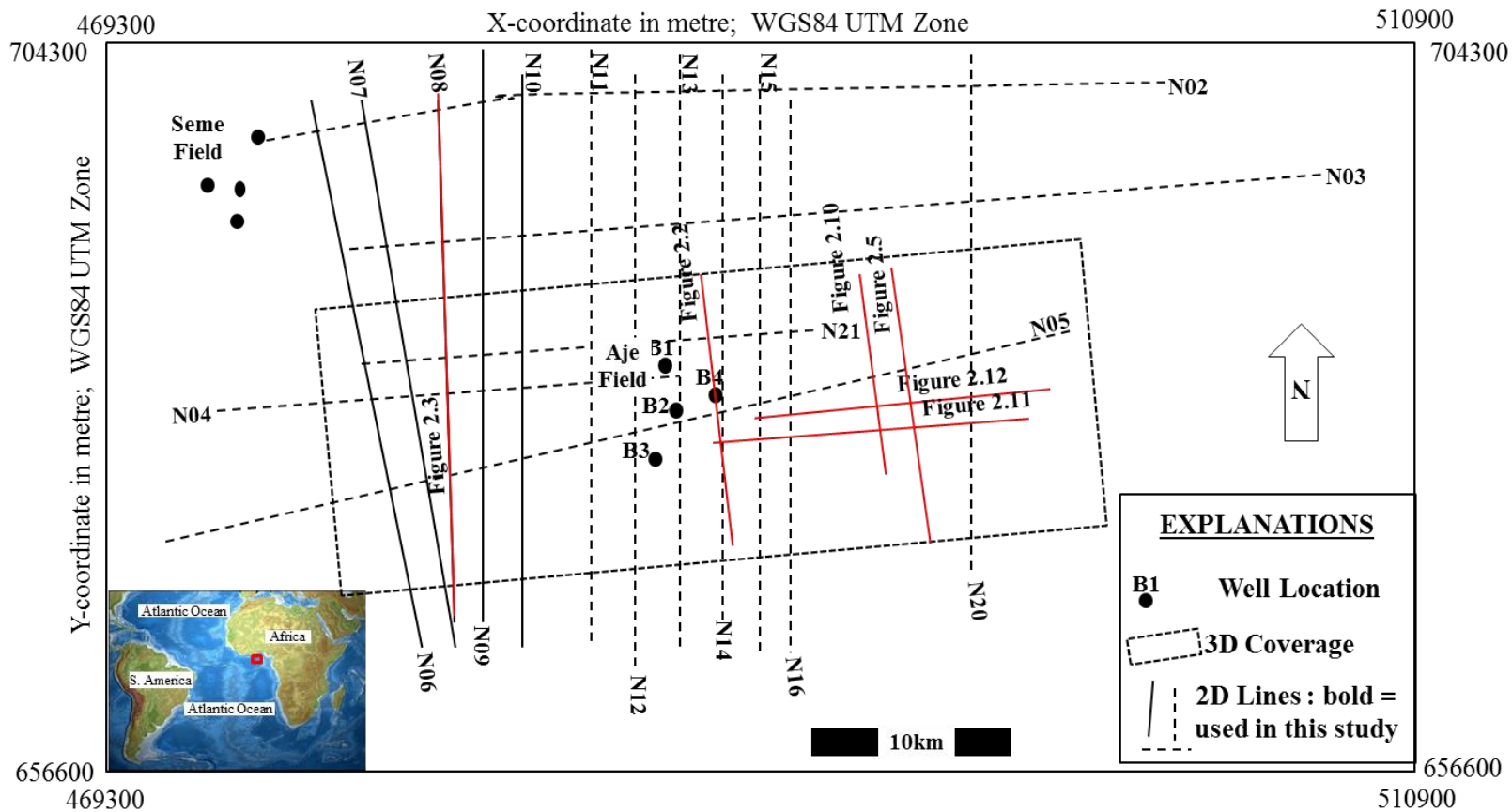


Figure 2.1: Basemap of the study area showing the location of the interpreted datasets; well data, 2D, and 3D seismic data. Note the four wells are located within the Aje Field in the 3D survey area (dashed rectangle). The vertical and horizontal lines represent 2D dip and strike lines. The continuous vertical lines are the 2D lines used in conjunction with 3D seismic data. Red lines indicate locations of some of the seismic sections used in this chapter.

The aims were achieved through the analysis of both 2D and 3D seismic data, in the search for major reflection terminations that helped in the identification of major unconformities bounding megasequences or sequences. Key structural elements were established by identifying structures such as faults, folds, and half-grabens.

The three datasets (seismic, well-log and biostratigraphic data) used in this study show good ties and correlation (Figure 2.2). One of the four wells (B-04) crosses the rift-climax (S2B) and the entire late rift (S2C) sequences in the southern half-graben. It provides robust biostratigraphic data that were later applied in this study. This makes this study the first academic research to correlate the syn-rift phase to well data in the offshore Benin Basin.

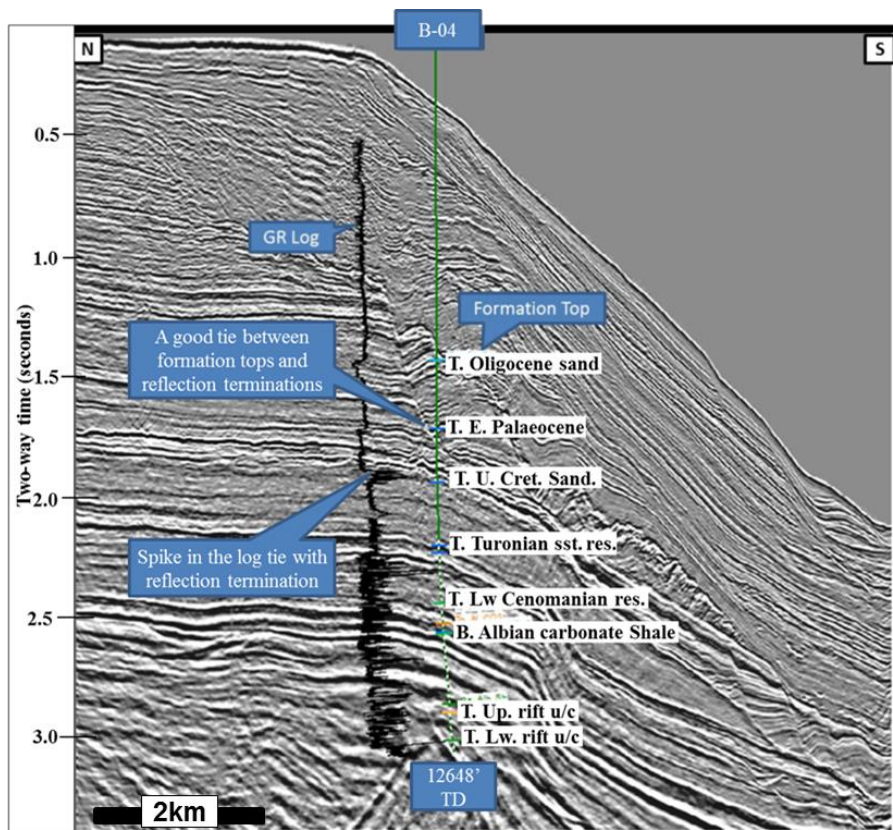


Figure 2.2: Seismic section (crossline 3802) containing plots of GR-log and some of the biozones and formation tops at well B-04 (the referenced well). Good ties exist amongst most of the interpreted seismic horizons, the formation tops (biozones) and well-logs. Some of the spikes on the GR-log tie with reflection terminations or horizons. See Figure 2.1 for the location of the seismic section.

2.2 Aims and objectives

The aim of this chapter is to provide a summary of the seismic stratigraphy and main structural elements present in the study area, and which have been identified as a result of this research project. The analysis and interpretation of particular stratigraphic and structural elements will be investigated in depth in subsequent chapters.

The main objective of this chapter is to define and describe key seismic megasequences, as well as their key structural features, establish their ages and relative distribution, and correlate them to published studies (Binks and Fairhead, 1992; MacGregor et al., 2003; Bumby and Guiraud, 2005; Brownfield and Charpentier, 2006; Moulin et al., 2010; Kaki et al., 2012; Fairhead et al., 2013; Heine and Brune, 2014). It also involves predictions of depositional environments interpreted on seismic data for the offshore Benin Basin. Seismic megasequences were established by defining their bounding surfaces, or major unconformities (Vail et al., 1977). The methods of Vail et al. (1977); Hubbard (1988); Christie-Blick (1991); Prosser, (1993); Driscoll et al. (1995); Catuneanu et al. (2009); (2012); Neal and Abreu (2009); and Abreu et al. (2010) involving the analysis of the major unconformities, followed by the identification of the minor unconformities, will be applied in this chapter.

2.3 Datasets

2.3.1 2D seismic reflection data

The 2D seismic data were acquired between 1994 and 1995 by Abacan Resources of Canada (Table 2.1). Five 2D dip lines were provided. These make about 400 km of 2D located offshore Benin Basin (Figure 2.1). Imaging depth reaches a

maximum of 6.0 seconds TWT across the study area for both the 2D and 3D seismic surveys.

Table 2.1: Summary of the 2D seismic data acquisition and processing

Company	Abacan-Geco-Prakla
Measurement System	Metric
Number of Lines	13
Acquisition Date	1994
Sample Interval	2 milliseconds
CPD Fold	192
Data Trace /Record	394
Auxiliary Trace/Record	-
Maximum Distance	4788 m
Group Distance	12.5 m
Amplitude Recovery	None
Spread	Offset 138 m
Byte/Sample	4
Bits/In	-
Sample/Trace	3500
Recording Format	SEGD
Format this Reel	SEGY

2.3.2 3D seismic reflection data

The 3D seismic data were acquired and processed by PGS in 1997. The 3D survey covers a surface area of about 1,200 km². The survey consists of 3080 crosslines N-S and 762 E-W inlines (Table 2.2). The 3D seismic data were pre-stack time-migrated (PSTM) in 2004 by Applied Geophysical Services (AGS). About 750 km² of the 3D seismic data were re-processed to provide post-stack depth migrated (PSDM) volumes by GeoCentre Incorporation, Houston, in 2006. The interpreted 3D seismic data used for this study are the re-processed pre-stack time-migrated volumes. Conventional 3D seismic data interpretation includes the application of synthetic seismograms using well-logs to provide reliable correlations between seismic reflections and well data (Brown, 2004).

Table 2.2: Summary of 3D seismic data acquisition and processing

<i>Company</i>	<i>GeoCentre</i>	
<i>Grid</i>	<i>25 X 25 m</i>	
<i>Inline</i>	<i>1001-1763</i>	
<i>Crossline</i>	<i>1858-5200</i>	
<i>Mid-Point</i>	<i>X</i>	
<i>Mid-Point</i>	<i>Y</i>	
<i>PreSTM Processing (May, 2006)</i>	<i>PreSTM with GVRA Processing (August 2006)</i>	<i>Depth Migration (September 2006)</i>
<i>PSTM Gathers</i>	<i>PSTM Gathers</i>	<i>Depth Migration</i>
<i>CVS Interactive Velocity</i>	<i>PSTM Gathers</i>	<i>Mute</i>
<i>Radon Multiple Attenuation</i>	<i>Radon Multiple Attenuation</i>	<i>Stack</i>
<i>NMO, Mute</i>	<i>NMO, Mute (Merged velocity GRVA regular half km grid velocity)</i>	<i>Filter, TV Scale</i>
<i>Stack</i>	<i>Stack</i>	
<i>FXYDN Noise Attenuation</i>	<i>FXYDN Noise Attenuation</i>	
<i>Filter 3/6-60/70 Hz</i>	<i>FXYDN Noise Attenuation</i>	
<i>TV Scale expanding windows</i>	<i>TV Scale expanding windows</i>	

Where; PreSTM: Pre-Stack Time Migration; NMO: normal move out

IHS-Kingdom suite was the main interactive tool used for the seismic data interpretation. It has been used to identify sequence boundaries, facies, and tectonic structures (i.e. faults, and folds). Kingdom suite was also applied for the construction of two-way time (TWT) structural and isochron maps.

As sound waves propagate through the rocks, their velocity is accelerated or slowed, and the transition between distinct rock units of different nature and their boundaries in space are often recorded. This, therefore, makes seismic data suitable for the investigation of the continuity of geological strata (Emery and Myers, 1996; Kearey et al., 2002). These surfaces (seismic reflections) are then thought to represent relatively concise periods of time and can be used as time lines bounding seismic packages with identical signals.

Seismic reflection data are generally reliable tools for stratigraphic studies because they provide high lateral resolution, while well-logs provide high vertical resolution. The two tools combined can be important in sequence stratigraphic

studies, especially when well-logs are tied to biostratigraphic markers or lithological horizons. With the combination of the 2D, 3D seismic, well-log, and biostratigraphic data, this research project intends to improve our understanding of the opening of the Equatorial Atlantic.

2.2.3 Polarity and quality of the seismic data

The polarity of seismic data needs to be determined before they are interpreted. There are generally two international standards to the polarity, the American and European standards. The European standard involves an increase in impedance that often results in positive amplitudes; it is normally displayed as a red intensity depending on the colour used. The American (SEG) standard shows negative amplitude when there is an increase in impedance and a blue intensity in colour (Brown, 2004; 2008).

One of the important issues that were addressed before the interpretation of these seismic data has to do with the quality of the data. It is always necessary for a seismic interpreter to have a dataset of high quality (Brown, 2004; 2008). The interpreter should be able to distinguish between good and bad data. A geologist should be able to differentiate noise-related features from geological features.

The vertical resolution of seismic data is in the range of tens of meters. The frequencies used in seismic surveys are usually from 10 – 100 Hz. Higher frequencies are often implying higher resolution. The minimum vertical thickness (d_{min}) of a layer that could be interpreted using the formula:

$$d_{min} = \lambda / 4 \text{ and } \lambda = v/f$$

Where λ is the wavelength of the seismic wave; f is the frequency; and v is the seismic velocity (e.g. Brown, 2012; Table 2.3).

This formula can be used to calculate the minimum interpretable thickness of a layer that makes up the subsurface. The frequency of the seismic data used for this study is 50 Hz and the velocity of most sandy and muddy layers is 2000 m/s. The vertical resolution would be 10 m.

Table 2.3: Typical rock velocities and densities (after Bourbié et al., 1987).

Type of formation	P wave velocity (m/s)	S wave velocity (m/s)	Density (g/cm ³)	Density of constituent crystal (g/cm ³)
Scree, vegetal soil	300-700	100-300	1.7-2.4	-
Dry sands	400-1200	100-500	1.5-1.7	2.65 quartz
Wet sands	1500-2000	400-600	1.9-2.1	2.65 quartz
Saturated shales and clays	1100-2500	200-800	2.0-2.4	-
Marls	2000-3000	750-1500	2.1-2.6	-
Saturated shale and sand sections	1500-2200	500-750	2.1-2.4	-
Porous and saturated sandstones	2000-3500	800-1800	2.1-2.4	2.65 quartz
Limestones	3500-6000	2000-3300	2.4-2.7	2.71 calcite
Chalk	2300-2600	1100-1300	1.8-3.1	2.71 calcite
Salt	4500-5500	2500-3100	2.1-2.3	2.1 halite
Anhydrite	4000-5500	2200-3100	2.9-3.0	-
Dolomite	3500-6500	1900-3600	2.5-2.9	(Ca, Mg) CO ₃ 2.8-2.9
Granite	4500-6000	2500-3300	2.5-2.7	-
Basalt	5000-6000	2800-3400	2.7-3.1	-
Gneiss	4400-5200	2700-3200	2.5-2.7	-
Coal	2200-2700	1000-1400	1.3-1.8	-
Water	1450-1500	-	1.0	-
Ice	3400-3800	1700-1900	0.9	-
Oil	1200-1250	-	0.6-0.9	-

The available data for this thesis are the re-processed post-stack time migrated data. The 2D and 3D seismic data are presented in two-way travel time (TWT) in seconds (Figure 2.3) i.e. the time that the P-wave takes to travel to a boundary and back again.

Since the seismic data were not depth-converted, the fault displacement in TWT was depth-converted by reading its corresponding seismic velocity on the well-log.

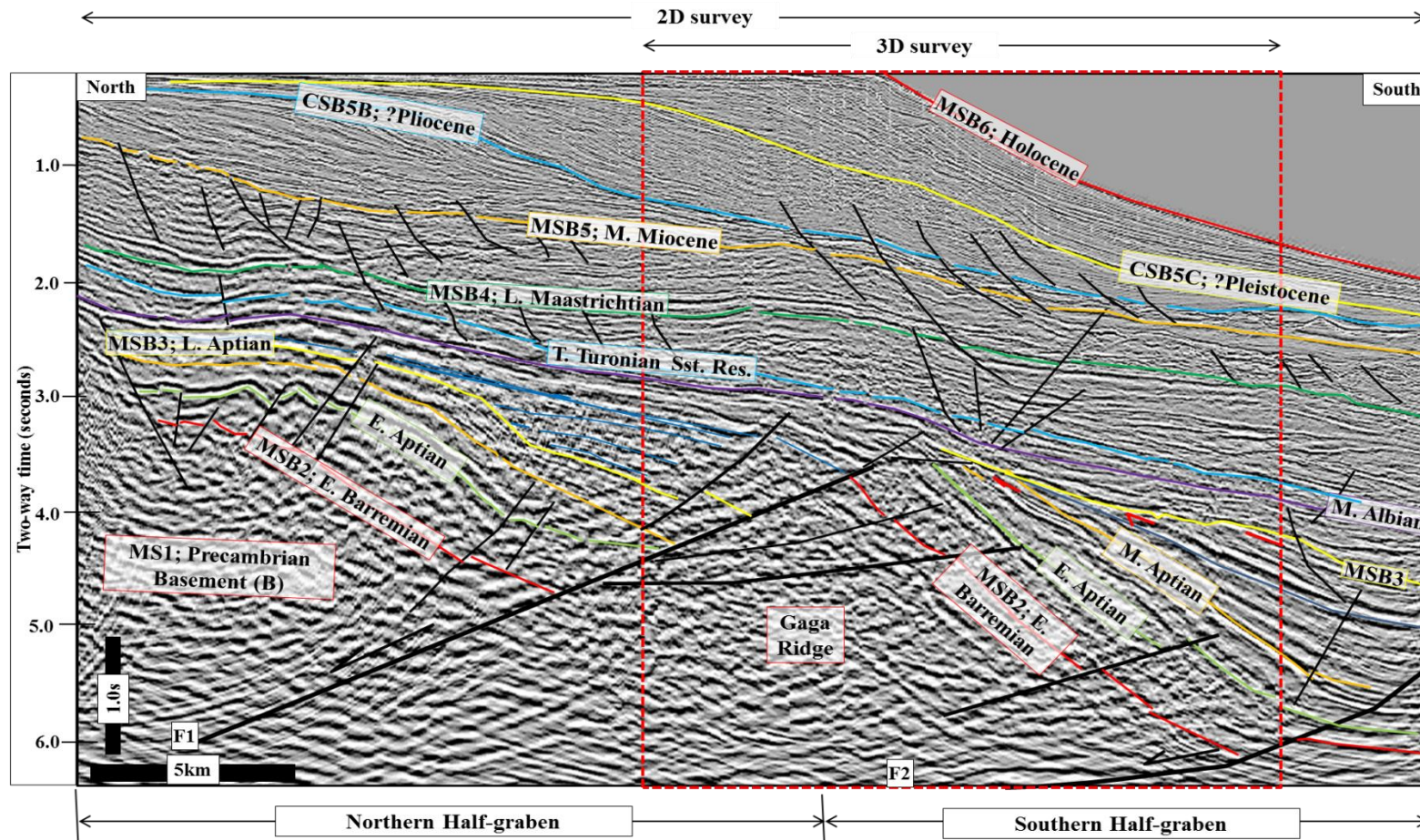


Figure 2.3: 2D seismic section showing the area extent of the 3D survey (red rectangle). Two half-grabens and their characteristic basin-bounding normal faults (F1 and F2) interpreted in the study area. CSB5B refers to a second composite sequence boundary within MS5. Location of the seismic section is shown in Figure 2.1.

The following formula was applied:

$$D = \text{TWT}/2 * V$$

Where D = Depth (m), TWT = Two-way-time (s) and V = Velocity in m/s.

The data quality is generally poor to good. The poor quality occurs in the deeper parts of the seismic sections. The good quality of the data allows good analysis of the seismic data for their reflection characteristics and strata geometry. Integration between seismic and well data permits correlations between megasequence units and dating of smaller units based on the biostratigraphic data provided for this study. The available 3D seismic data do not cover the entire area of the 2D survey (Figures 2.1 and 2.3), thus, it limits the application of 3D seismic data.

2.3.4 Well data

Well data include four exploration wells (B-01 to B-04) located in the central part of the study area. The wells are closely-spaced and located within the 3D seismic volume (Figure 2.1). Geophysical logs, biostratigraphic and lithological information from the four wells (Table 2.4) were also integrated into this study. All the wells are deviated, except for well B-03. The wells were uploaded into Kingdom suite using the deviation survey data provided and are summarised as Table 2.5.

The wells drilled through sedimentary units ranging from the Lower Cretaceous to the Cenozoic (Tables 2.6 to 2.9). Well data for three of the wells (B-02 to B-04) provided for this study include typical industry datasets:

- ❖ Caliper log (CALI)
- ❖ Gamma Ray (GR)
- ❖ Spontaneous Potential (SP)
- ❖ Resistivity logs (include shallow, medium and deep)

- ❖ Density log (RHOB)
- ❖ Neutron (NPHI)
- ❖ Sonic (DT)
- ❖ Synthetic seismograms

Formation tops were re-assessed in order to permit correlation with the existed chronostratigraphy for offshore Benin Basin (Brownfield and Charpentier, 2006; Kaki et al., 2012). The 3D seismic volume allowed for the correlation of key horizons from adjacent wells into the 2D lines. Well B-01 has the poorest quality biostratigraphic and lithological information, whereas well B-04 has the best data and served as the reference well for this study.

Table 2.4: Summary table of attributes from available well data in the offshore Benin Basin

Well	Year Drilled	Total Depth (m)	Time/Depth	GR Log	Resist. Log	Sonic Log	Density Log	Biostrat. Info.	Litho. Info.	Well Report
B-01	1996	4041.6							Yes	Yes
B-02	1996	4918.9	Yes	Yes	Yes	Yes	Yes	Yes	Yes	Yes
B-03	2005	2585.3	Yes	Yes	Yes	Yes	Yes	Yes	Yes	Yes
B-04	2008	3848.1	Yes	Yes	Yes	Yes	Yes	Yes	Yes	Yes

2.3.5 Biostratigraphic datasets

Reports on two of the four wells (B-03 and B-04) analysed for their fossil contents by Mosunmolu Limited, Lagos, Nigeria and Global Geotechnical and Environmental Systems, Los Angeles, United States (Du Chene and Adegoke, 2006; Mosunmolu, 2008) were re-assessed and incorporated in this study. These are confidential reports submitted to the Department of Petroleum Resources (DPR) and were provided among other datasets for this study. Cuttings from these wells were analysed for palynomorphs (pollen, spores, and dinoflagellate cysts)

microfossils (foraminifera and ostracodes) and nannofossils (Tables 2.6 to 2.9; Du Chene and Adegoke, 2006; Mosunmolu, 2008).

Table 2.5: Well co-ordinates used for the plotting of the four wells provided into Kingdom suite.

<i>Parameters</i>	<i>Aje-01</i>	<i>Aje-02</i>	<i>Aje-03</i>	<i>Aje-04</i>
<i>Date Drilled</i>	<i>26 March 1996</i>	<i>23 Oct., 1996</i>	<i>21 August 2005</i>	<i>29 January 2008</i>
<i>Rig Name</i>	<i>Jack-Up</i>	<i>Adriatic IX</i>	<i>Sedco 709</i>	<i>Deepwater Pathfinder</i>
<i>Well Location</i>	<i>N680724.00 m E489809.00 m</i>	<i>N680723.4m E489809.1 m 06°09'30.5''N 002°54'28.4''E</i>	<i>N674326.00 m E488848.00 m 06°06'02.148''N 002°53'57.166''E</i>	<i>E 492,521.30 m N 678,710.50 m</i>
<i>WGS84 projection</i>	<i>UTM Zone 31</i>	<i>UTM Zone 31</i>	<i>UTM Zone 31</i>	<i>UTM Zone 31</i>
<i>Rig Floor Elevation (ft)</i>	<i>80 ft (24.4m)</i>	<i>80 ft (24.4m)</i>	<i>80 ft (24.4m)</i>	<i>79 ft (MSL) (24.1m)</i>
<i>Water Depth (ft)</i>	<i>320 ft (97.5m)</i>	<i>320 ft (97.5m)</i>	<i>3,018 ft (920m)</i>	<i>958 ft (292 m)</i>
<i>Well Total Depth (ft)</i>	<i>13,260 ft (4041.6m) MD, 7,862 ft (2396.3m) TVD</i>	<i>16,138 ft (4918.9m) MD/ 11,551 ft (3520.7m) TVD</i>	<i>8,482 ft (2585.3m) TVDBRT 8,482 ft (2585.3m)MDBR T</i>	<i>12,625 ft (3848.1m)MD/ 12,355 ft (3765.8m)TVD</i>
<i>Well Status</i>	<i>Exploratory/ Suspended</i>	<i>Exploratory</i>	<i>Exploratory/ Appraisal</i>	<i>Oil & Gas Appraisal</i>
<i>Well type</i>	<i>Directional</i>	<i>Directional</i>	<i>Vertical</i>	<i>Directional</i>

Some of the biozone data were uploaded into this project research and tied to the horizons identified on the seismic sections. The uploading of these biozones and formation tops into the Kingdom project forms the basis for the assignment of ages to all interpreted horizons (Figure 2.3). This was possible through the use of a synthetic seismogram for the reference well B-04 (Figure 2.4) and time-depth curves for all other wells (Tables 2.10 – 2.12). The time-depth data provide information on the time-depth correlations between the well data (depth in metre or feet) and the seismic data (depth in seconds TWT). The time-depth correlation allowed the tying of well data to seismic data (Figure 2.4).

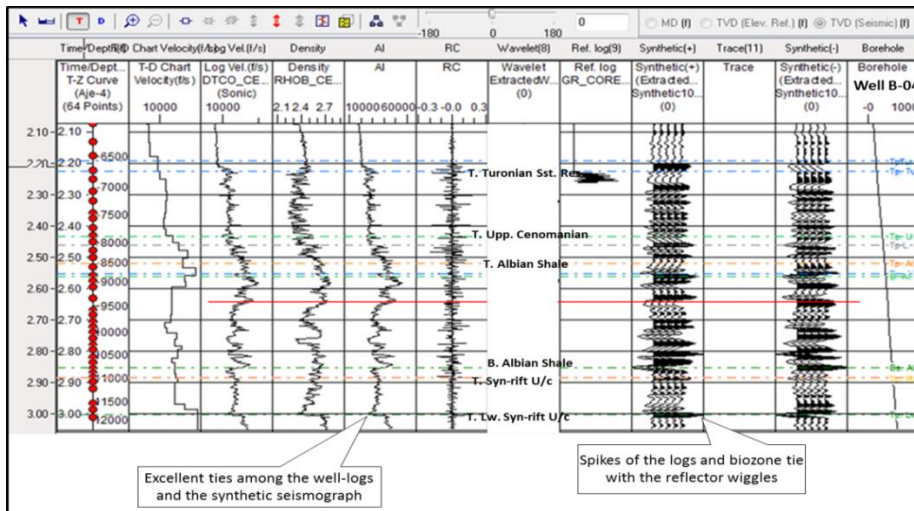


Figure 2.4: Different well-logs (Velocity, Sonic, and Density) of Well B-04 cross-plotted with the synthetic seismograph on Kingdom Workstation. Formation Tops that were provided correlate and tie with some spikes. Reflection terminations (onlap, downlap, toplap and erosional truncations) identified in this study correlate and tie with these Formation Tops.

2.3.6 Other datasets

Other datasets provided for this study include geophysical, geochemical, and technical reports on the drilled wells. The geophysical reports consist of details on how the seismic data were acquired and processed. Well data reports provide information on time-depth correlation, the drilling of the wells, including the date each well was spudded, well location, types of rig and drilling mud utilised. The geochemical reports present results of organic geochemical analyses carried out on ditch cuttings and cores. Some of the organic geochemical analyses include spore colour index (SCI), total organic carbon contents (TOC), and vitrinite reflectance (Ro %).

2.4 Explanation of the abbreviations and definitions of terminology used in this study

Below are definitions of terminology applied in this study:

Compression: An expression extensively used for compressional stresses e.g. Marrett and Peacock, 1999; Fossen, 2012).

Contraction: reduction in length. It is the same as ‘shortening’. These two ‘strain’ terms are regarded as interchangeable in this thesis (e.g. Marrett and Peacock, 1999; Fossen, 2012). Where appropriate the term ‘inversion structure’ has been applied where a process of reactivation of pre-existing structures has been interpreted. However, contractional deformation is widely accepted nomenclature for describing structures (folds and thrusts) and so this has been retained where most appropriate. According to Marrett and Peacock (1999), “it is preferable to use strain terms to describe and classify geological structures, as strains are more directly measurable than stresses. Tectonic events should not, therefore, be described as ‘compressional’ if what is being measured is a contractional strain in the horizontal plane. Stress terms are inappropriate for field descriptions ...” We would include interpretation of seismic data as effectively a “field description”.

Contractional structures: these are structures formed contraction or shortening.

Post-rift: after rifting, typically used about the sequence of sediments deposited during the phase of thermal subsidence after the cessation of rifting and related extensional faulting and stretching.

This study has adapted the terminology ‘megasequence’ which was introduced by Hubbard (1988) when he worked on the Jurassic and Cretaceous rifted continental margins of the South Atlantic, North Atlantic, and the Arctic Oceans. Hubbard

(1988) defined megasequence as “a stratigraphic unit deposited during one distinct phase of basin evolution separated by a major unconformity which often marks fundamental basin-controlling processes”. This unconformity often represents principal periods of change in basin geometry and polarity (Hubbard, 1988). This implies that the basis of this definition is the occurrence of a major angular unconformity that represents either onset or end of basin-controlled processes, such as rifting. The Hubbard (1988) definition was applied when the main subsidence mechanism changed (i.e. pre-rift, syn-rift, to post-rift). An episode of syn-rift phase may, therefore, represent a megasequence.

In this study, the post-rift unconformity (PRU) and the rift onset unconformity to represent an angular unconformity defined by reflection terminations and change in reflection patterns. The post-rift unconformity separates the overlying parallel reflection pattern of the post-rift phase from an underlying divergent reflection pattern for the syn-rift phase (Figure 2.6). The rift onset unconformity is made up of onlap surface that separates the divergent pattern of the syn-rift phase from a parallel pattern of the pre-rift phase below it (Figure 2.6).

Megasequences and megasequence boundaries have been numbered consecutively, with MS1 and MSB1 being the oldest and MSB6 the youngest. The MS number is defined by the MSB at its base, so MS1 has MSB1 at its base and MSB2 at its top. Where megasequences have been subdivided into sequences, the sequences are numbered after the megasequence they are within (e.g. S2A is within MS2). The sequences are differentiated by a letter, so S2A is the basal sequence of MS2, with S2B, 2C etc. above it. This is illustrated in Figure 2.5. These systems of numbering are used in all parts of this study.

Table 2.6: Formation tops, biozones and their relative ages as estimated from Cenozoic calcareous Nannofossils in well B-04 (after Mosunmolu, 2008).

Measured Depth (ft)	Epoch/Period	Age (Ma)	Zones (Martini, 1971)	Significant Microfossil Datums
2850	<i>U. Miocene</i>	>7.8	NN11	<i>Minylitha convalis</i>
3000	<i>U. Miocene</i>	8.6	NN11	Base <i>Discoaster quinqueramus</i>
3150	<i>U. Miocene</i>	9.1	NN10	Top <i>Discoaster bollii</i>
3210	<i>U. Miocene</i>	9.4	NN9	Top <i>Discoaster hamatus</i>
3300	<i>U. Miocene</i>	9.5	NN9	Base <i>Minylitha convalis</i>
3510	<i>U. Miocene</i>	10.7	NN9	Base <i>Discoaster hamatus</i>
3570	<i>U. Miocene</i>	10.9	NN8	Base <i>Catinaster coalitus</i>
3780	<i>M. Miocene</i>	11.8	NN7	?Base <i>Discoaster kugleri</i>
3990	<i>M. Miocene</i>	13.6	NN5	Top <i>Sphenolithus heteromorphus</i>
4080	<i>U. Oligocene</i>	-	?NP25	In: <i>Cyclicargolithus abisectus</i> , <i>Dictyo - coccites scrippsae</i> and <i>Ilseolithina fusa</i> .
4090	<i>M. Oligocene unconformity</i>	30	NN4 & MP23 missing	MP20-13; P670, 650,630,580, 560 & 540 missing
4110	<i>L. Eocene</i>	>50.6	NP 12	In: <i>Tribrachiatum orthostylus</i> , <i>Toweius callosus</i> , <i>Toweius spp</i> and <i>Discoaster kuepperi</i> .
4290	<i>L. Eocene</i>	53.64	NP11	Base <i>Tribrachiatum orthostylus</i>
4590-4950	<i>L. Eocene - U. Paleocene</i>	-	NP10- NP11	In: <i>Rhomboaster bitrifida</i> , <i>R. cuspis</i> , <i>R. claptrata</i> , <i>Ellipsolithus marcellus</i> , <i>Toweius eminens</i> , <i>Tribrachiatum bramlettei</i> , <i>Coccolithus formosus</i> and some species of <i>Cruciplacolithus</i> , <i>Neochiastozygus</i> and <i>Chiasmolithus</i> .
4950	<i>U. Paleocene</i>	-	NP9	Base <i>Discoaster multiradiatus</i>
5370	<i>M. Paleocene</i>	59.7	NP5	Base <i>Fasciculithus tympaniformis</i>
5460	<i>K/T Boundary</i>	-	NP1-CC25 missing	P470, 450,430, 420, 370, & 330 missing
5400-5550	? <i>E. Paleocene-U. Cretaceous</i>	-	Significant floral decline	

Table 2.7: Biozones and their relative ages as estimated from Cretaceous calcareous Nannofossils in well B-04 (Du Chene and Adegoke, 2006).

<i>Measured Depth (ft)</i>	<i>Epoch/Period</i>	<i>Age (Ma)</i>	<i>Zones (Sissingh, 1977)</i>	<i>Significant Nannofossil Datums</i>
5400-5550	<i>L. Paleocene –U. Cretaceous</i>	-	-	<i>Significant floral decline</i>
5460-5730	<i>?Maastrichtian</i>	-	-	
5490	<i>Topmost Maastrichtian</i>	66	<i>Maximum flooding surface (mfs)</i>	
5580	<i>U. Cretaceous (Campanian)</i>		CC19	<i>In: Cyclagelosphaera reinhardtii, Uniplanarius sissinghi, Micula decussata and Stauroolithites spp.</i>
5640	<i>Campanian</i>	~80.0	CC18	<i>Top Marthasterites furcatus</i>
5730-5970	<i>Campano-Maastrichtian</i>	-	-	<i>Thin sediments</i>
5790	<i>Mid-Senonian unconformity</i>	-	CC19-21 missing	<i>SB and erosional surface could be at 5760ft by log interpretation</i>
5640-6180	<i>Campanian-Santonian</i>	-	CC18-CC16	<i>In: Marthasterites furcatus, Eiffelithus eximius, Lucianorhabdus maleformis, Micula decussata, Micula concava and Micula staurophora.</i>
5970-6210	<i>(?) Santonian</i>	-		<i>At 6150' major condensed interval & probable mfs.</i>
6210	<i>L. Santonian</i>	-	CC15	<i>Top Lithastrinus septenarius</i>
6450	<i>U. Coniacian</i>	-	CC14	<i>Base Micula decussate</i>
6750	<i>L. Coniacian</i>	86.0	CC13	<i>Base Marthasterites furcatus</i>
6780-7830	<i>Turonian</i>	-	CC12-CC11	<i>Floral decline</i>
7860-7920	<i>Turonian-?Cenomanian</i>	-	CC11	<i>Upper Cretaceous assemblage without Eiffelithus eximius</i>
8250	<i>Cenomanian</i>	-	?CC10	<i>In: Eiffelithus monechiae</i>
8280-10410	<i>Cenomanian & Older (/Albian)</i>	-	-	<i>Significant floral decline</i>
10440-10560	<i>Albian</i>		?CC8 & older	<i>In: Eiffelithus turriseiffelii</i>
10560-11820	<i>Albian- ?Aptian</i>		?CC8 & older	<i>Floral decline</i>
11850	<i>Aptian</i>		CC7	<i>In: Nannoconus quadriangulus Quadriangulus</i>
11880-12625	<i>?Aptian & older</i>		-	<i>Significant floral decline</i>

Table 2.8: Formation tops, biozones and their ages extracted from the biostratigraphic reports for well B-03

Measured Depth (ft)	Epoch/Period	Age (Ma)	Zones	Significant Nannofossil Datums
5900- 6120	Upper Araromi	Early Paleocene	P1	<i>Globigerina daubjergensis</i>
6050	Top Lower Araromi			<i>Dinogymnium spp.</i>
6200	Top Awgu Shale	Santonian-Coniacian		<i>Cretacael portea spp., H. emellanovi</i>
6200	Senonian Unconformity			
6270	Santonian & Older		Base of <i>Dicarinella asymetrica</i> zone	FDO of <i>Heterohelix reussi</i>
6980	Top Eze Aku Shales		SB Tu 4	<i>H. emellanovi</i> abundant
7100	Top Abeokuta Sandstone		SB Ce 5	<i>Classopollis spp.</i>
7490	Abeokuta Sandstone		SB Ce 3	
8013	Top Albian Sandstone		mfs Al 10	<i>Cicaltricosporites polomacensis, C. beroluetetie</i>

Following Hubbard (1988), both rift onset and post-rift unconformities have been identified as megasequence boundaries tagged MSB2 and MSB3 respectively in this study (Figure 2.5). The term ‘megasequence’ was however used in this study when the overall genetic behaviour changed (e.g. from tectonic subsidence to thermal subsidence with inversion: Cretaceous post-rift megasequence, MS3; or when there was active gravity-driven slumping: transgressive megasequence, MS4; or from transgressive to regressive sequence sets: regressive megasequence, MS5; Figure 2.5).

2.5 Methodology

The methodology applied in this research project involved two methods, namely structural and well-log/seismic sequence stratigraphic analyses.

2.5.1 Seismic stratigraphic interpretation

Some of the concepts and principles that formed the basis of this research project include seismic stratigraphy and seismic sequence stratigraphy.

Table 2.9: Formation tops extracted from the well reports that accompanied the datasets in this study.

Tops	B-02 (MD in feet)	B-03 (MD in feet)	B-04 (MD in feet)
Water depth	320	3018	958
NN10			3150
Upper Miocene			3210
Middle Miocene			3780
Top Oligocene Sand			3984
Mid-Oligocene Unconformity			3992.6
Top Imo Shale		5530	
Top Araromi Shale		5830	
Top Awgu Formation			
Top Lower Tertiary			4922.5
Cretaceous-Tertiary Boundary			5460
Topmost Maastrichtian			5490
Top Upper Cretaceous			5637.3
Santonian Unconformity		6270	5790
Top Turonian Sandstone reservoir	6797.7	6933	6864.5
Top Upper Cenomanian	7881	7100	8083.6
Top Lower Cenomanian		7972	8284
Top Albian Carbonate	8324	8402	9019
Base Albian Carbonate			9096
Basal Albian Shale			11072
Top syn-rift			11285
Base post-rift			11288
Top rift unconformity			11312.8
CC7			11850
Top Lower Rift Unconformity			12174.
Total Depth (TD)	16138	8482	13260

Principles of seismic stratigraphic interpretation have been summarised in literature (e.g. Emery and Myers, 1996; Catuneanu et al., 2006; 2009) and the basic concepts of sequence stratigraphic interpretations can be ascribed to the early works published in AAPG Memoir 26 (Payton, 1977). The concepts of seismic stratigraphy were first introduced by Mitchum et al. (1977).

The seismic stratigraphic methodologies are those able to identify the three stages of tectonic evolution of a rifted basin/passive margin (Leeder and Gawthorpe,

1987; Prosser, 1993; Driscoll et al., 1995; Gawthorpe et al., 1994; 1998; Gawthorpe and Leeder, 2000; Kaki et al., 2012):

- ❖ Pre-rift stage
- ❖ Syn-rift stage and,
- ❖ Post-rift stage.

Table 2.10: Depth-time data uploaded into Kingdom software and used to tie the seismic to well data. Depth-time data for well B-02

Measured Depth (feet)	Time (Two-way time in seconds)
0.00	0.00
100.0	0.04
500.0	0.19
900.0	0.35
1461.2	0.55
1839.2	0.68
2385.1	0.86
3088.8	1.09
3455.0	1.22
4036.9	1.44
5074.4	1.78
5573.8	1.92
6039.4	2.06
6562.8	2.19
7089.9	2.31
7434.3	2.37
7709.6	2.41
8458.3	2.53
9038.8	2.61
9333.7	2.66
9925.8	2.74
10222.8	2.79
10819.2	2.88
11316.3	2.95
11515.1	2.98

These stages were identified on the seismic data on the basis of the distinct wedge-shape geometry of the syn-rift stage while the parallel to sub-parallel configurations directly underlying and overlying the wedge pattern were picked to represent the pre-rift and post-rift stages respectively (Figure 2.6; Falvey, 1974; Driscoll et al., 1995).

Table 2.11: Depth-time data uploaded into Kingdom software and used to tie the seismic to well data. Depth-time data for well B-03

Measured Depth (feet)	Time (Two-way time in seconds)
0.00	0.00
51.69	0.02
200.27	0.08
430.6	0.17
502.3	0.20
900.7	0.36
1051.7	0.43
1400.6	0.57
1900.8	0.77
2051.9	0.83
2190.5	0.88
2277.2	0.92
2400.9	0.97
2772.1	1.12
3022.5	1.22
3633.7	1.45
4010.9	1.59
4440.8	1.75
5040.9	1.96
5626.8	2.14
6025.4	2.26
6514	2.40
7248.5	2.58
7763.5	2.70
8203.7	2.80
8314.8	2.51
8357	2.82
8436.8	2.83

Seismic sequence analysis was also applied on each megasequence in order to establish the seismic sequences for it. The analysis was based on the identification of stratigraphic units composed of a relatively conformable succession of genetically-related strata, termed depositional sequence. Depositional sequences are often bounded on top and bottom by unconformities or their correlative conformities. These unconformities are marked by reflection terminations (Brown and Fisher, 1977; Mitchum et al., 1977; Vail et al., 1977; Vail, 1987; Galloway, 1998) on seismic reflection data.

Table 2.12: Depth-time data uploaded into Kingdom software and used to tie the seismic to well data. Depth-time data for well B-04

Measured Depth (feet)	Time (Two-way time in seconds)
0.00	0.00
2021.5	0.82
3013.4	1.13
3608.7	1.31
4005.4	1.43
4600.2	1.61
5045.2	1.75
5487.8	1.88
6018.4	2.02
6440.6	2.13
7001.3	2.25
7655.7	2.36
7936	2.40
8218.9	2.45
8604	2.50
8845.8	2.53
9087	2.56
9376	2.60
9955	2.68
10100	2.71
10196.3	2.72
10436.5	2.76
10677.2	2.79
10869.5	2.82
10966.4	2.84
11111	2.86
11207.4	2.87
11303.7	2.88
11400	2.90
11544.6	2.92
11881.9	2.97
12026.7	2.99
12267.9	3.01
12648.3	3.05

Reflection terminations include onlap, downlap, toplap, erosional truncation and their correlative conformities (Figure 2.7). This research project has adopted the seismic sequence stratigraphic methodology of Hubbard (1988), Christie-Blick et al. (1991), Prosser (1991), Catuneanu et al. (2009), Abreu et al. (2003; 2010); Neal and Abreu (2009).

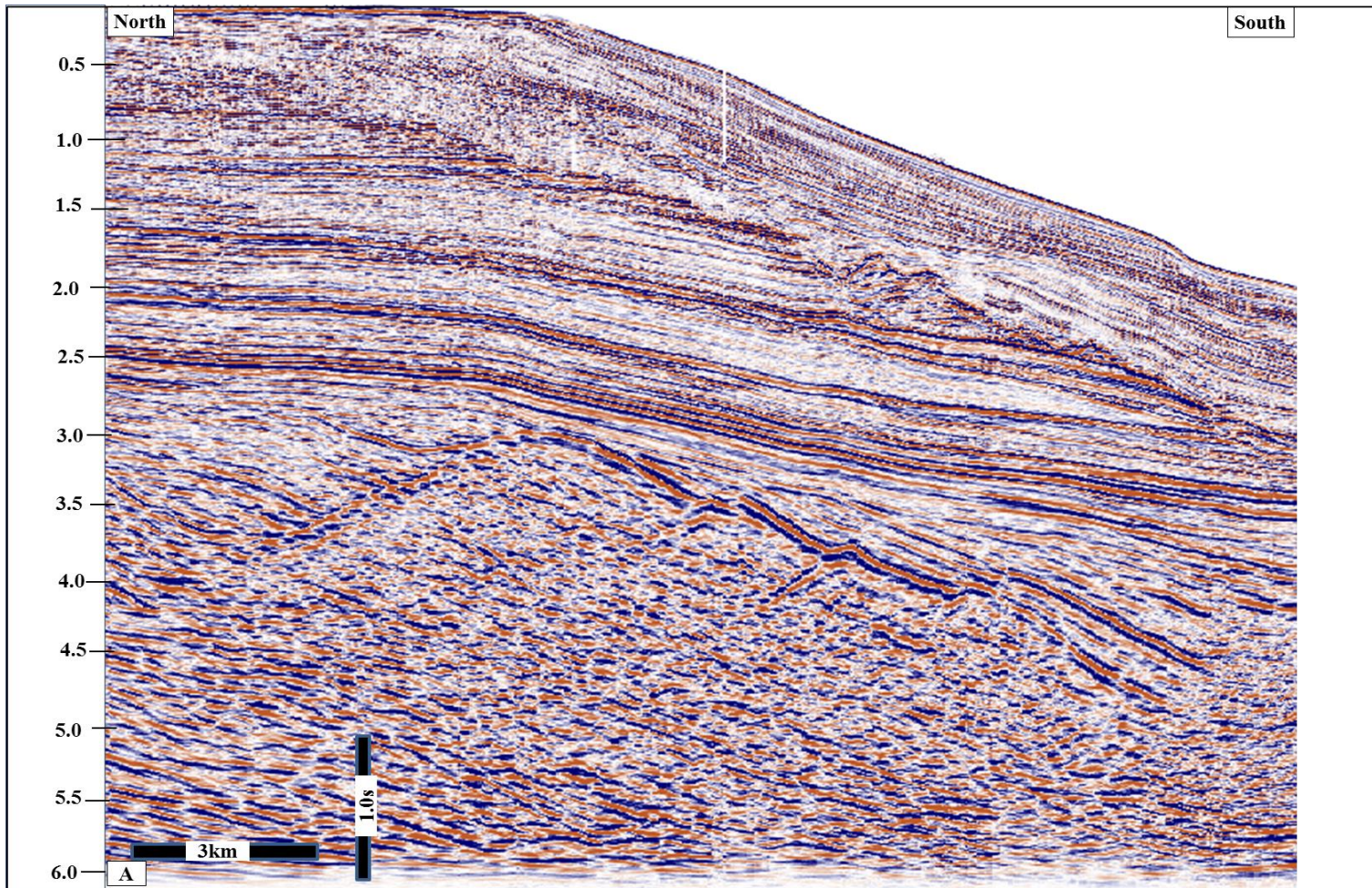


Figure 2.5A) Uninterpreted 3D seismic section (crossline 4342). See Figure 2.5B for the interpretation of the seismic section.

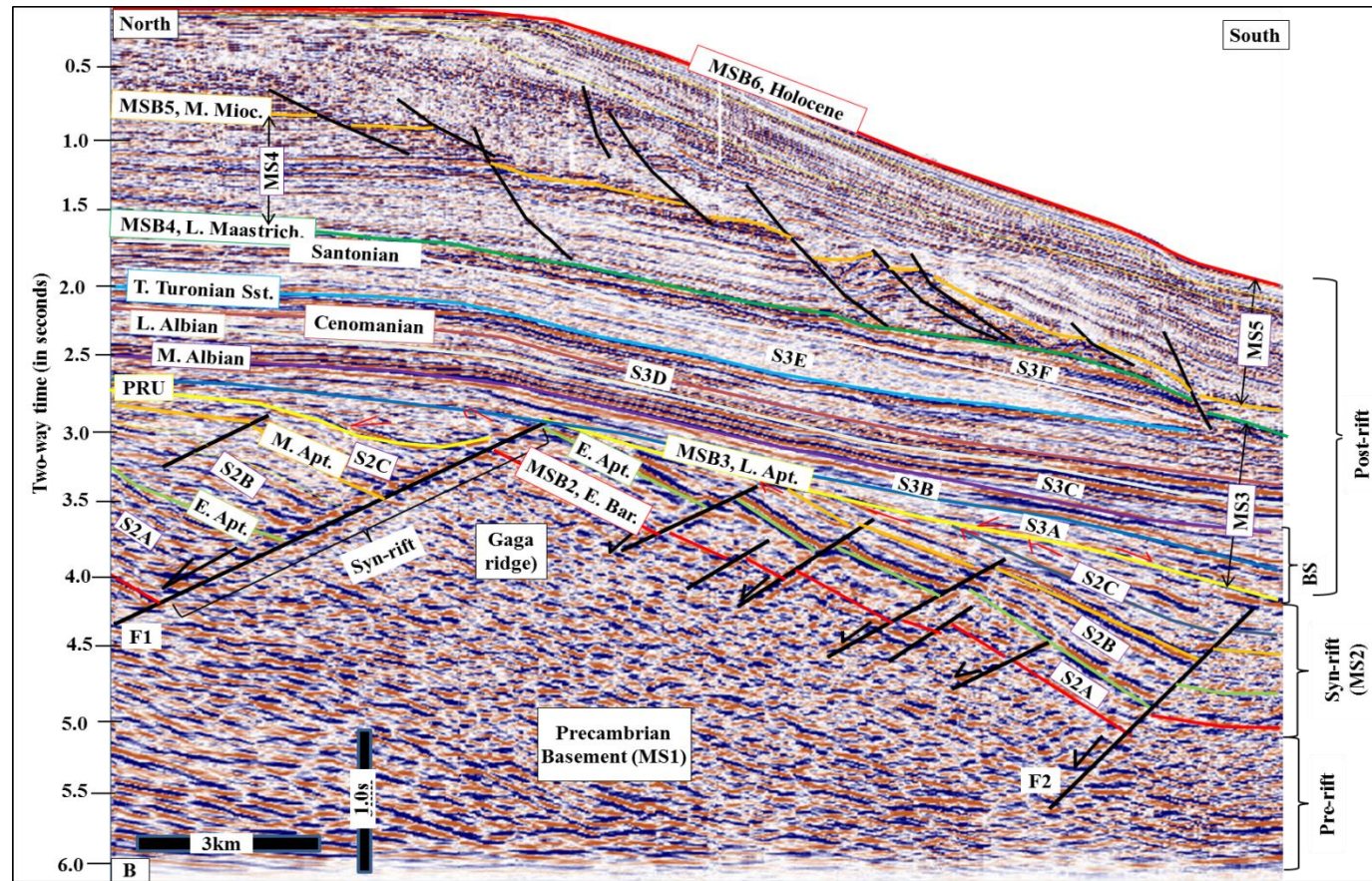


Figure 2.5 (..continued)B: Vertical profile showing the stratigraphic and structural framework established for the offshore Benin Basin in this study. Five megasequences (MS1-MS5) define for two half-grabens bounded by major faults (F1 and F2). The megasequence MS3 is deformed by at least two phases of contractional deformation. Where Apt. = Aptian; PRU = post-rift unconformity; L. = late; M. = middle; T. = Top. Others are as explained in the text. See Figure 2.1 for the location of the seismic section.

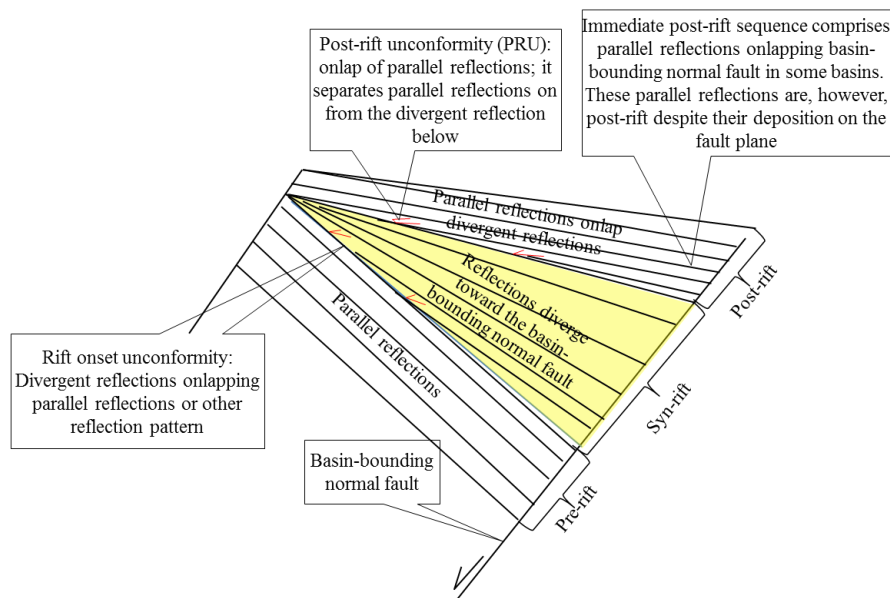


Figure 2.6: Line diagram showing a characteristic wedge-shaped geometry (yellow) of the syn-rift phase of basin development. The syn-rift phase consists of reflections diverging away from the main fault (the basin-bounding normal fault). The dips also increase downwards because of progressive rotation in the hanging-wall. Note that both pre-rift and post-rift phases comprise parallel reflections. However, the pre-rift may sometimes show chaotic reflections. Reflections of the wedge geometry progressively onlap the rift-onset unconformity, while the post-rift reflections onlap the post-rift unconformity. Red arrows point to stratal onlap (modified after Leeder and Gawthorpe, 1987; Prosser, 1993).

2.5.2 Seismic facies analysis

This is the analysis of a seismic sequence on the basis of its internal reflection character (Figure 2.8). The aim of seismic facies analysis is the prediction of facies types and gross depositional environments for the overall sequence (Mitchum et al., 1977; Sangree and Widmier, 1979; Hubbard et al., 1985; Sawyer, 2006). Some of the reflection characteristics include reflection configuration, reflection continuity, reflection frequency, reflection amplitude, interval velocities, reflection geometry and external form (Sangree and Widmier, 1977; Berg, 1982; Sawyer, 2006; Zeng, 2013).

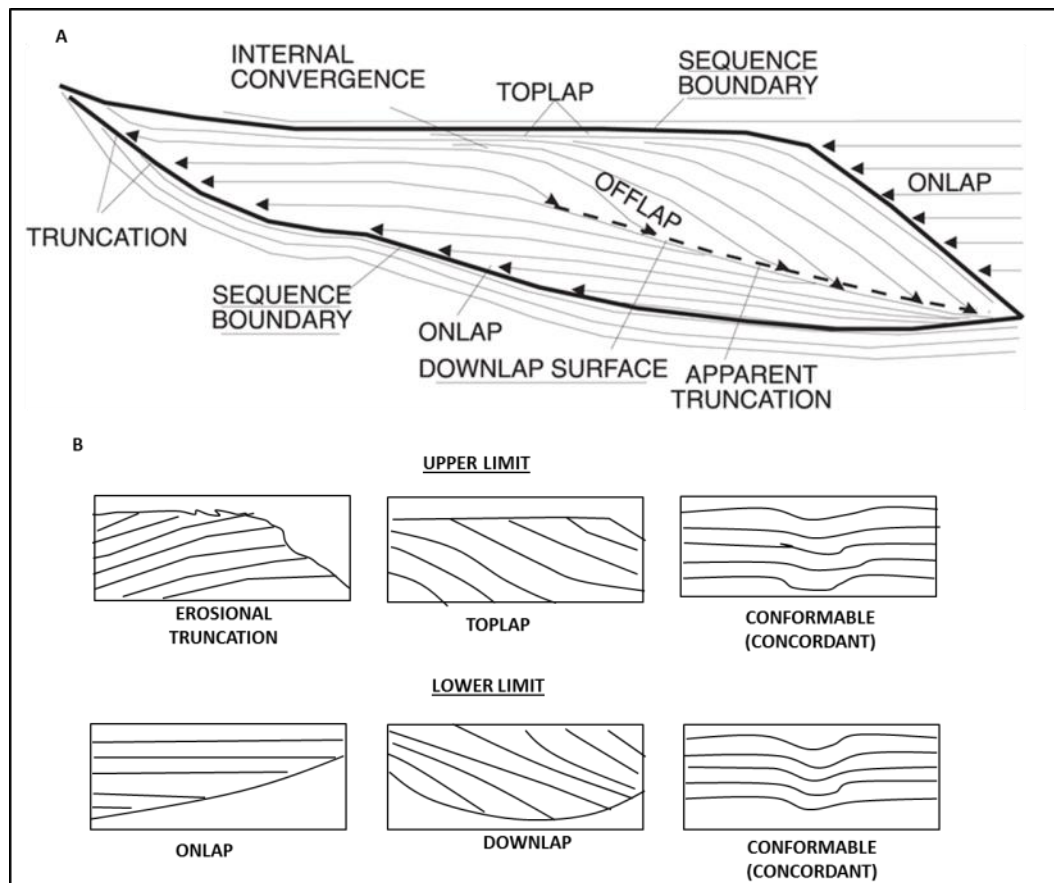


Figure 2.7: Reflection terminations used to define seismic sequence and megasequence boundaries (from Mitchum et al., 1977).

2.5.3 Well-log analysis

Well-logs were used to complement the interpretation of the seismic data. The well-log interpretation was carried out independently of the seismic data. The interpretations from both datasets were later tied and correlated together. The suites of well-logs provided for this research project were analysed for main lithologies and depositional environments. The well-logs that were used for these purposes include gamma-ray (GR), spontaneous potential (SP), resistivity, density and neutron logs.

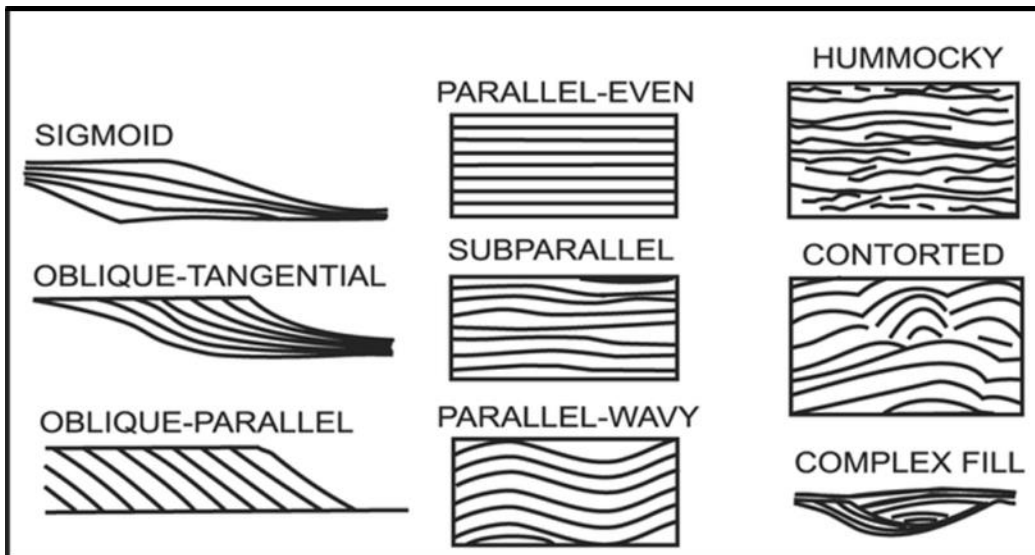


Figure 2.8: Some examples of reflection configurations used for the identification of seismic facies. They often describe the internal components of a seismic sequence (after Vail et al., 1977 and Mitchum et al., 1977).

The facies analysis was carried out using the well-logs on the basis of identifying the log patterns (Figure 2.9; Riders, 1990). Depositional environments were interpreted for the established sequences.

The basis of using GR logs for sequence stratigraphic is that they can measure formations' radioactivity in strata such as shales (i.e. shales comprising radioactive elements such as potassium (K), uranium (U), and thorium (Th)).

2.5.4 Structural analysis

The structural analysis was carried out before the stratigraphic interpretation, thereby allowing the identification of discontinuities and subtle deformation features in seismic reflections. Significant faults were identified on seismic data on the basis of the recognition of their offsets in a reflection horizon (Figure 2.10).

- GR +	Overall trend	Dominant environment
	Cleaning-up or funnel trend Prograding Gradual upward decrease in gamma, sharp top	Crevasse play, river mouth bar, delta front, shoreface, submarine fan lobe; change from clastic to carbonate; catch-up carbonates
	Dirtying-up or bell trend; Retrograding: gradual upward decrease in gamma	Fluvial point bar, tidal point bar, deep-tidal channel fill, tidal fill, transgressive shelf; Give-up carbonates
	Boxcar or cylindrical trend Aggrading: low gamma, sharp boundaries, no internal change	Eolian, braided fluvial, distributary channel fill, submarine canyon fill, carbonate shelf margin; evaporite fill; Keep-up carbonates
	Bow or symmetrical trend Prograding and retrograding: gradual decrease then increase in gamma	Reworked offshore bar, regressive to transgressive shoreface delta
	Irregular or serrated trend Aggrading	Fluvial floodplain, storm-dominated shelf and distal deep-margin slope

Figure 2.9: Log patterns for palaeoenvironmental reconstructions (after Nyantakyi et al., 2013).

One of the challenges of seismic data is the ambiguity surrounding estimation of true dips of structures. Most seismic data are presented in a form that distorts the true dips of structures to apparent dips. Most of the seismic sections in this study were initially presented with two way travel time (TWT) along the vertical axis which, given the assumed seismic velocities, most likely significantly reduce the vertical scale if converted to depth. Apparent dips of structures are, therefore, most likely to be significantly lower than the true dips in any seismic sections presented in this way. In order to estimate true dips (θ), key seismic sections were printed off the Kingdom project, having ensured that both vertical and horizontal scales were the same. The angle of dip of the structure (fault, fold axis) was manually measured with respect to the horizontal (Figure 2.11). The dip for the basin-bounding normal faults was measured only in seismic sections that are parallel to the dip direction (i.e. dip sections). The angle of the dip was similarly measured for other dipping structures.

Other structures such as folds that are associated with the faults were also identified as reflection deformation (flexure) (Figure 2.12).

Construction of two-way time (TWT) structural maps and isochrons

A time slice is the horizontal display of 3D seismic reflection data (Brown, 2004; Bacon et al., 2009). It displays strata with respect depth (or time) of structures, such as faults and salt, to ensure that the structural interpretation is correct. It also helps to know the extent of the structures in depth or time (Brown, 2004; Bacon et al., 2009). The seismic data interpretation was complemented by the construction of two-way time (TWT) structural and isochron maps. These form the basis for the structural, seismic–stratigraphic and basin analysis presented in this research project. In order to generate isochron maps, fault polygons were established as groups of faults cutting through a defined seismic surface of interest. In this study, isochron maps have been generated for the rift onset unconformity (MSB2), post-rift unconformity (MSB3), and the fold onset unconformity (e.g. the late Aptian/early Albian and the Santonian, SB3F deformation).

2.6 Seismic stratigraphic framework of the offshore Benin Basin

Following the seismic stratigraphic methodology described above, seismic data were analysed for similar geometrical arrangements that define the pre-rift, syn-rift and post-rift successions for the offshore Benin Basin (Figure 2.5). The offshore Benin Basin consists of five megasequences:

- ❖ Pre-rift megasequence (MS1), Precambrian - Barremian (MSB2)
- ❖ Syn-rift megasequence (MS2), Barremian (MSB2) – Aptian (MSB3)
- ❖ Cretaceous post-rift megasequence (MS3), late Aptian (MSB3) - latest Maastrichtian (MSB4)

- ❖ Transgressive megasequence (MS4), latest Maastrichtian (MSB4) - middle Miocene (MSB5)
- ❖ Regressive megasequence (MS5), middle Miocene (MSB5)–Holocene (MSB6; Figures 2.5 and 2.13; Table 2.13)

The seismic stratigraphy of this pre-rift, syn-rift and post-rift megasequences established are broadly analysed and described in this chapter, while their detailed interpretations and implications are discussed in the subsequent Chapters 3-5.

2.6.1 Pre-rift megasequence (MS1), Precambrian - Barremian

The pre-rift megasequence (MS1) is made up of transparent, chaotic reflections in both northern and southern half-grabens (Figures 2.5 and 2.14). The seismic reflections have been interpreted as crystalline basement rocks (Brownfield and Charpentier, 2006; Kaki et al., 2012). The crystalline basement rocks have been studied onshore by many authors (e.g. Ajibade and Fitches, 1988; Caby, 1989; Rahaman, 1989; Oyinloye, 2004; Ayodele, 2013). These crystalline basement rocks include both igneous (e.g. granite) and metamorphic (e.g. schist, metaconglomerate) rocks. These crystalline basement rocks are generally aged Precambrian and formed during the Pan-African orogeny (Grant, 1970; Ajibade and Fitches, 1988; Caby, 1989; Rahaman, 1989; Annor et al., 1997; Ayodele, 2013).

The pre-rift megasequence (MS1) consists of some structural fabrics (Figure 2.14) that generally strike in the same direction as the basin-bounding normal faults. Occasionally, seismic reflections are displaced and folded due to probable shortening (Figure 2.12). The basement occurs as basement high separating the northern and southern half-grabens. This basement high is referred to as the Gaga ridge in this study (Figure 2.5).

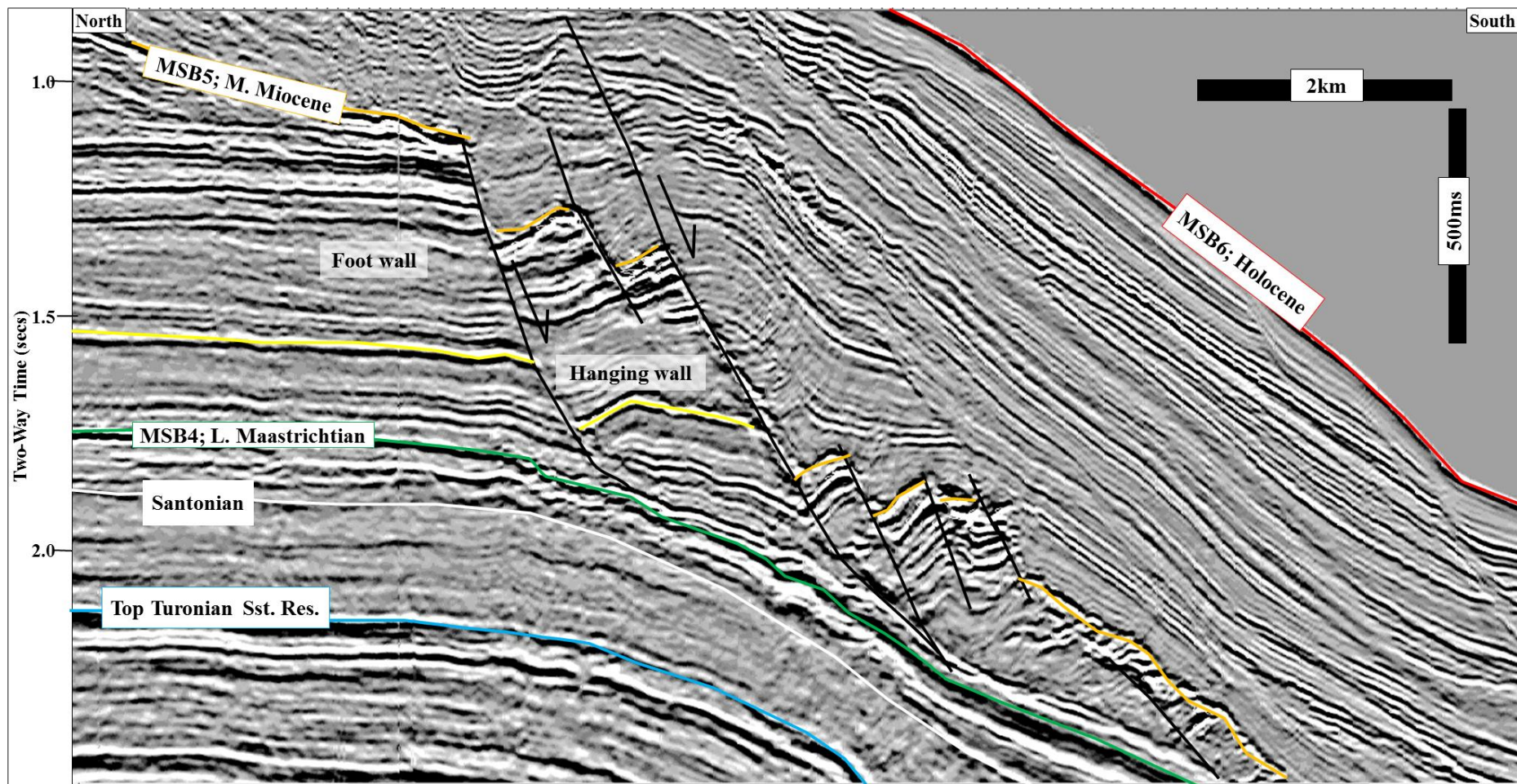


Figure 2.10: Fault interpretation on a seismic section (crossline 3828) based on the discontinuity and displacement of seismic reflections. See Figure 2.1 for the location of the seismic section.

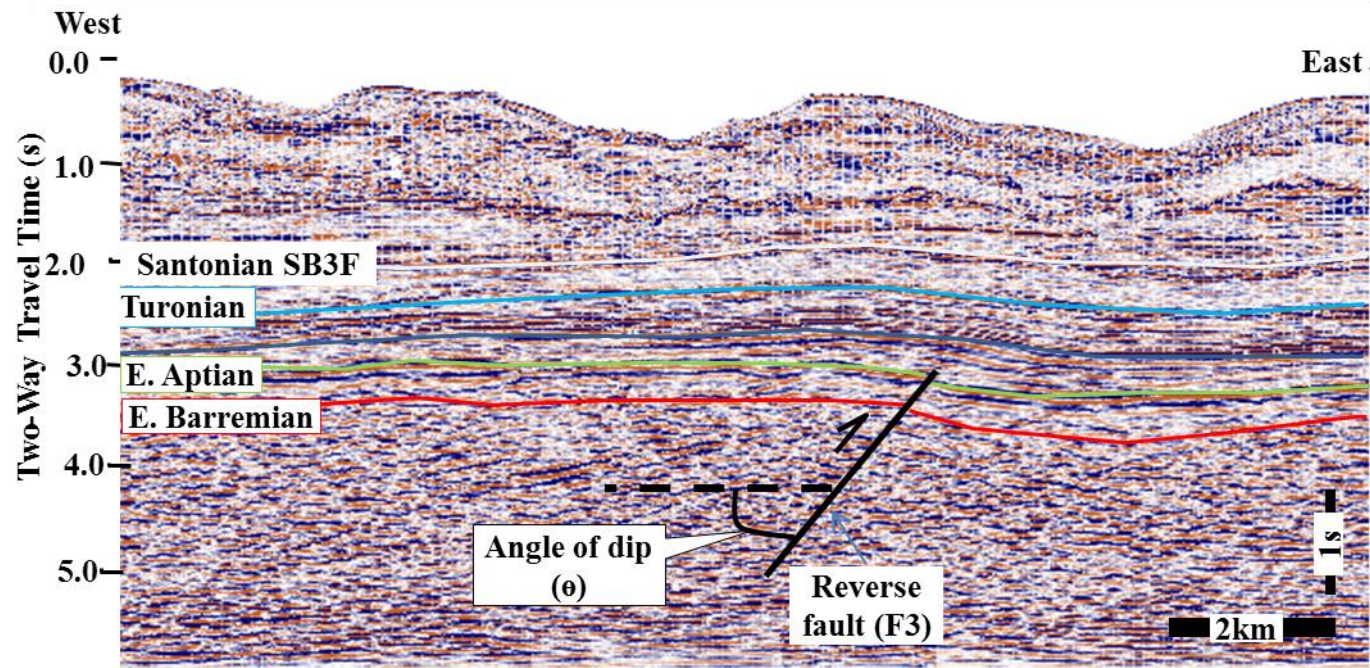


Figure 2.11: Measurement of fault dips (e.g. reverse fault, F3). The dip (θ) of the fault was taken using the horizontal line (black broken line) as reference. See Figure 2.1 for the location of the seismic section (Inline 1344).

The pre-rift megasequence (MS1) is overlain by a well-developed wedge pattern of reflections that defines the syn-rift phase of basin development (Figure 2.14). It is separated from the wedge pattern by an onlap surface (rift onset unconformity, early Barremian, MSB2).

2.6.2 Syn-rift megasequence (MS2), Barremian (MSB2) – Aptian (MSB3)

The syn-rift megasequence consists of low- to high-amplitude divergent reflections (Figure 2.14). Internally, the divergent reflections show different seismic characteristics from the base to top; three distinct sequences have therefore been established the syn-rift megasequence (MS2). The three sequences include early rift sequence (S2A), rift-climax sequence (S2B), and late rift sequence (S2C). The syn-rift megasequence (MS2) shows lateral thickness variations by thickening towards the basin-bounding normal faults (F1 and F2) in both half-grabens (Figures 2.14 and 2.15). There are, however, some subtle differences in their seismic reflections in both half-grabens; the seismic reflections in the northern half-graben are folded in spite of its divergent character, while the southern half-graben is not folded.

The base and top of the syn-rift megasequence (MS2) in both half-grabens are marked by overlapping surfaces (Figure 2.14). The basal onlap is mapped as the rift onset unconformity (MSB2) and dated as early Barremian, while its top corresponds to the post-rift unconformity (PRU) dated as late Aptian (MSB3; Figures 2.13 and 2.14). The implications of these unconformities (rift-onset and post-rift unconformities) for the onset and end of rifting in the offshore Benin Basin will be validated in Chapter 3.

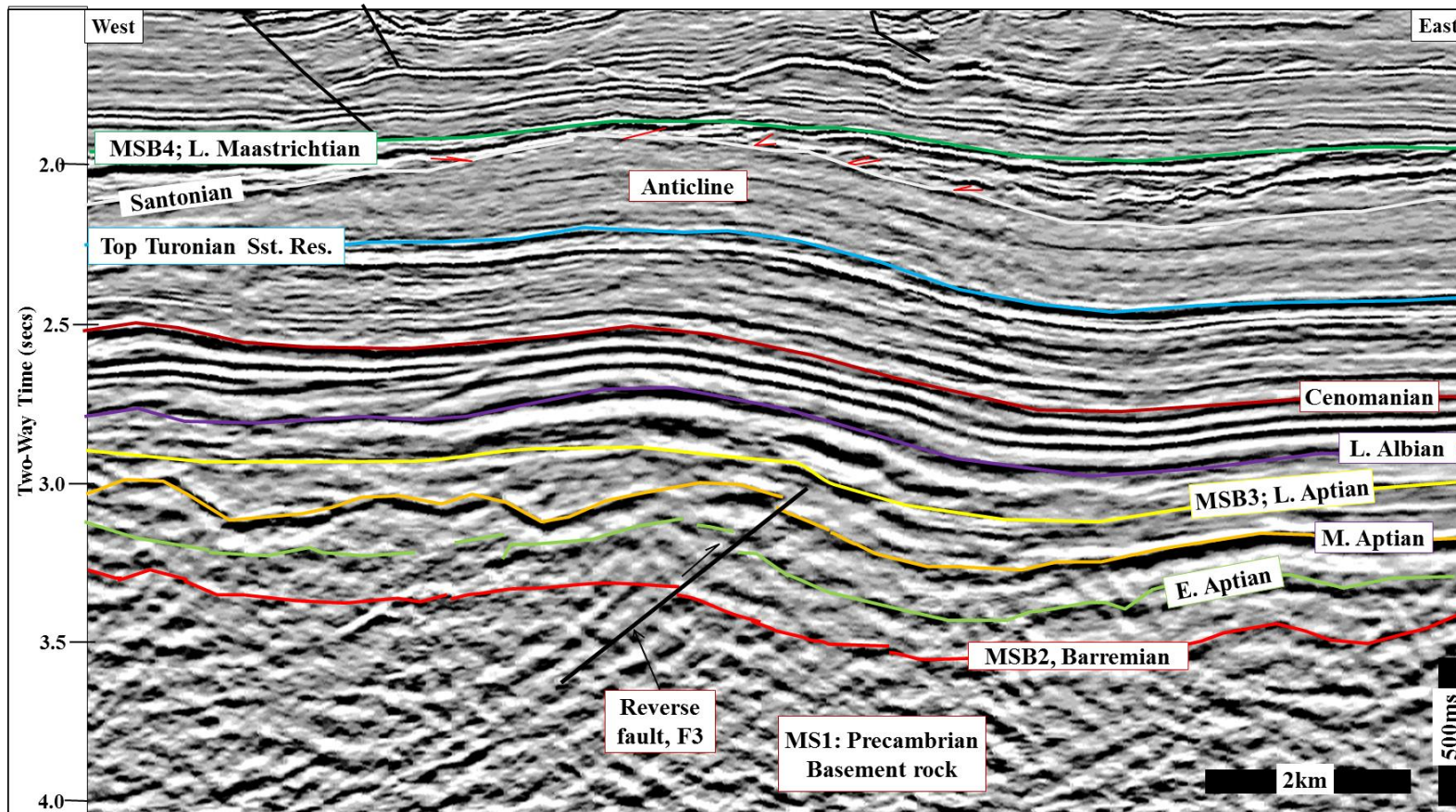


Figure 2.12: Interpretation of a fold on a seismic section (inline 1329); a flexure of a seismic horizon often indicates a fold. The pre-rift megasequence (MS1) has been displaced by the reverse fault (F3). Strata that were deposited before the Santonian are all folded, whereas younger strata above the Santonian unconformity appear to be nearly horizontal and sub-parallel. Reflections overlying the Santonian onlap these later strata (red arrows indicate onlap). See Figure 2.1 for the location of the seismic section.

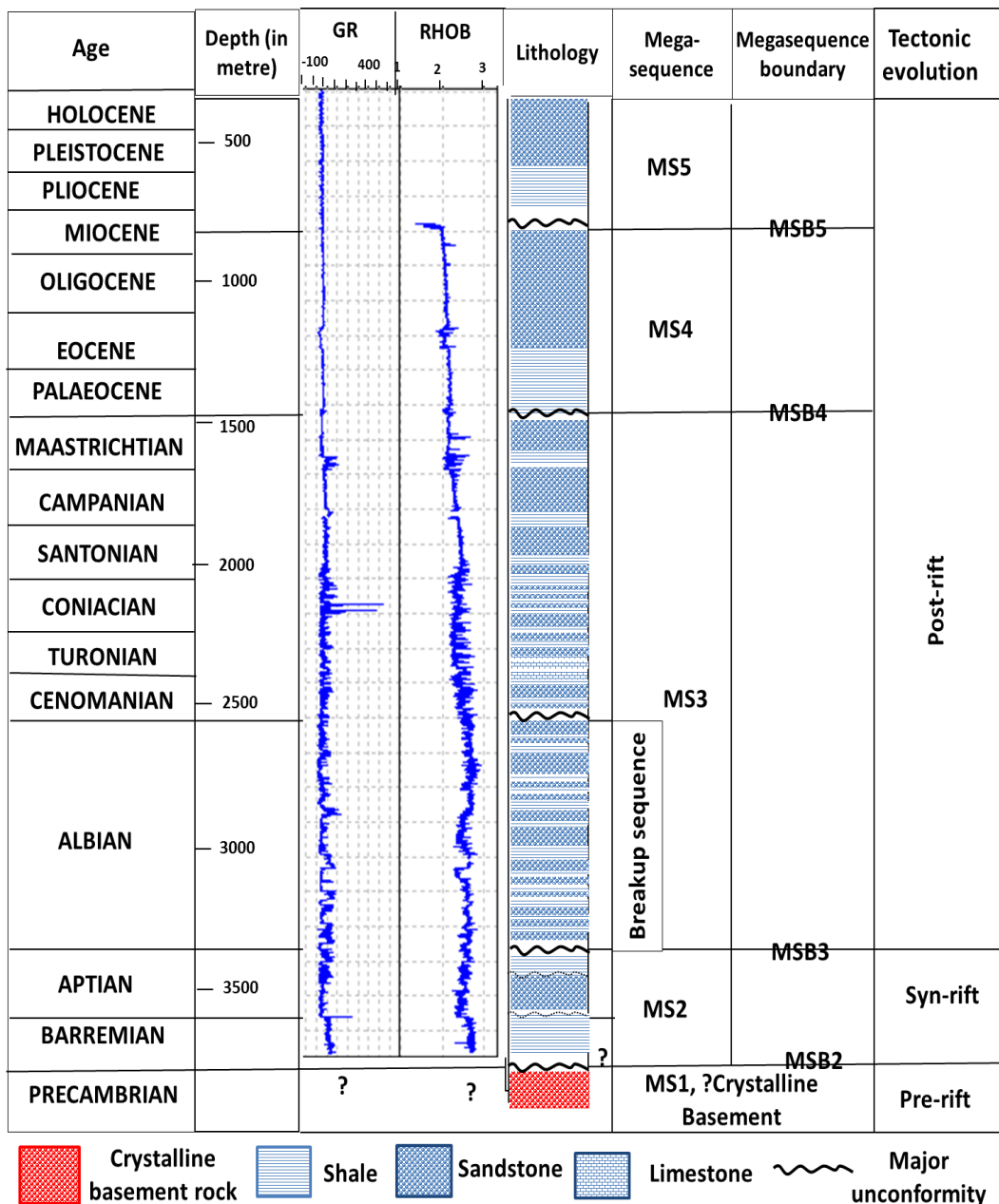


Figure 2.13: Megasequences (MS2-MS5) interpreted based on well-log data (GR and resistivity logs) from well B-04. The pre-rift megasequence (MS1) was interpreted as crystalline basement on the basis of its reflection character. The base (MSB2) of the syn-rift megasequence (MS2) was not penetrated by the well. The early-rift sequence (S2A) was partly penetrated.

2.6.3 Post-rift stratigraphy (MS3, MS4, and MS5)

The post-rift stratigraphy is made up of three megasequences (MS3 to MS5) that overlie the syn-rift megasequence (MS2) in the offshore Benin Basin.

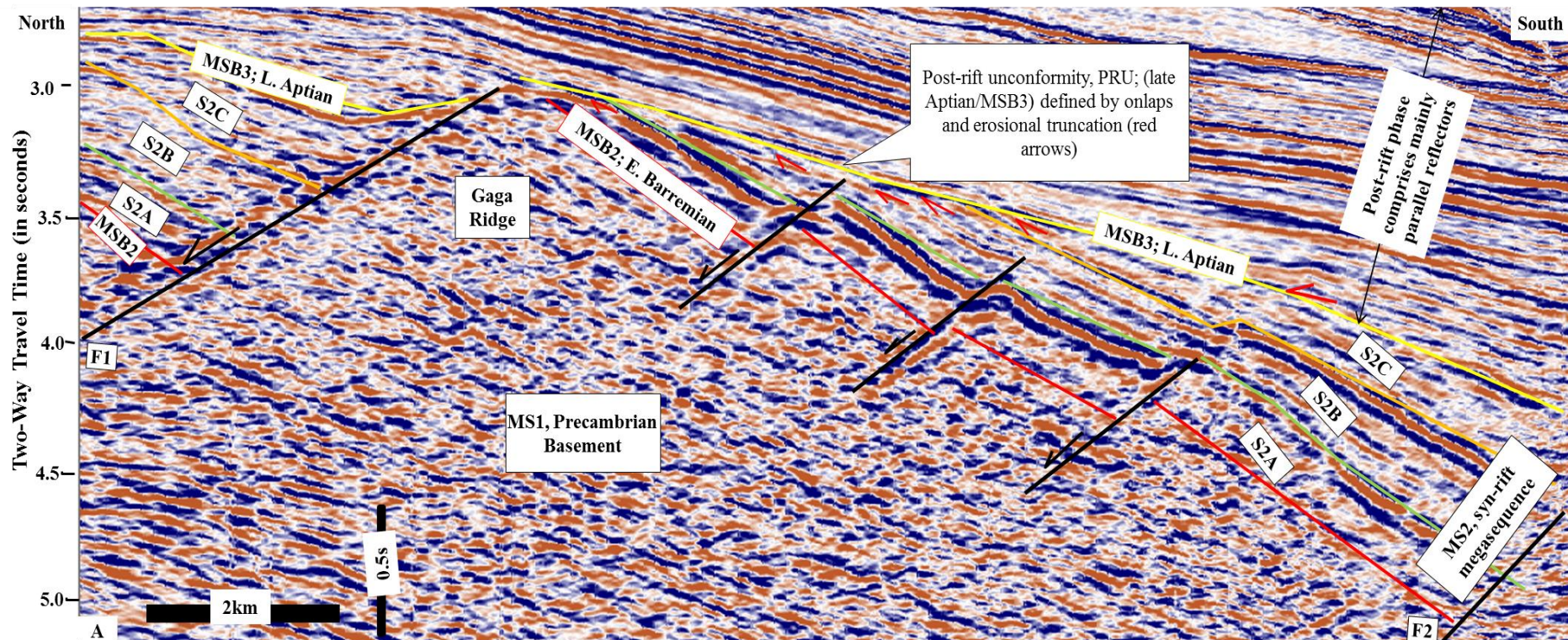


Figure 2.14: A) Crossline 4342 showing the two half-grabens referenced to in the text with their characteristic wedge geometries. The seismic reflections of the syn-rift megasequence (MS2) thicken toward the basin-bounding normal faults (F1 and F2) in both half-grabens. The syn-rift megasequence (MS2) is subdivided into three sequences early rift sequence (S2A), rift-climax sequence (S2B), and late rift sequence (S2C). See Figure 2.17 for the location of the seismic section.

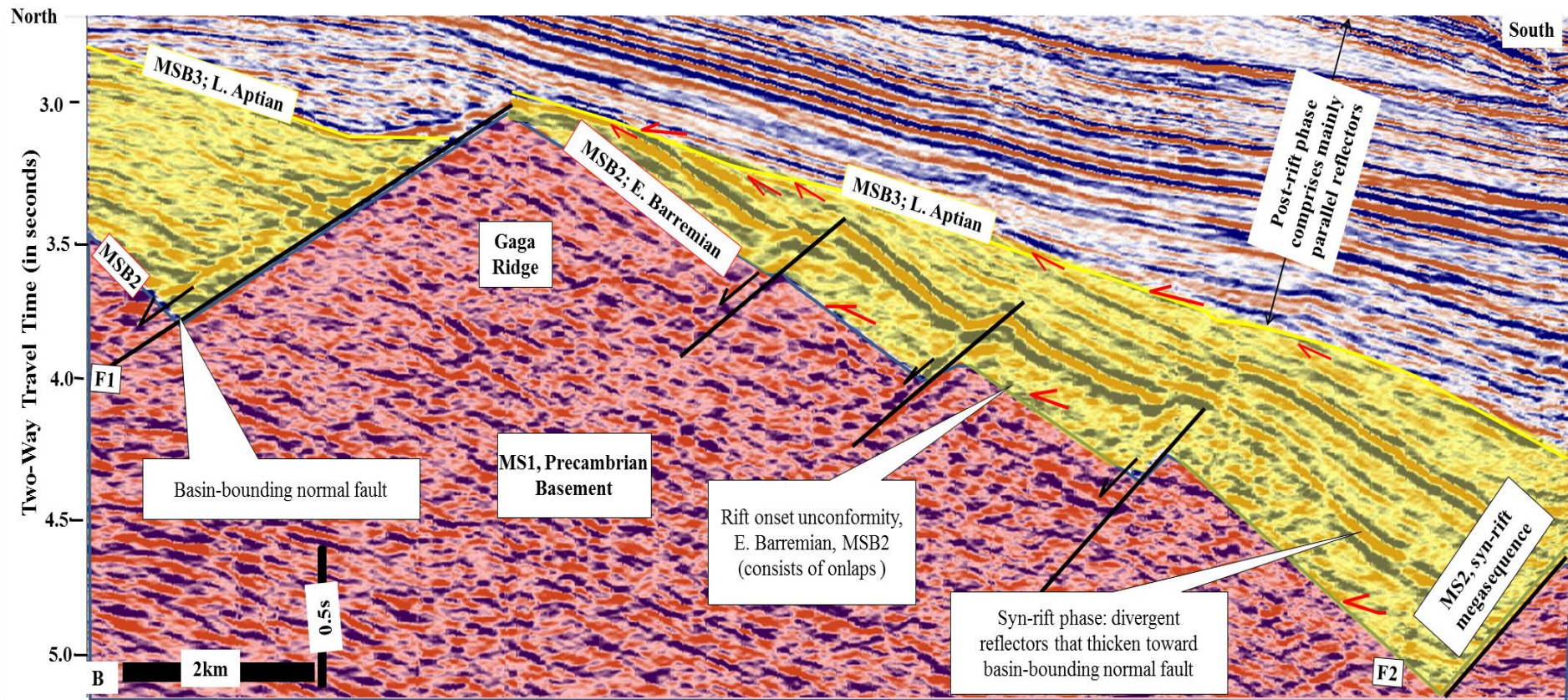


Figure 2.14B): The pre-rift, syn-rift and post-rift megasequences defined on the basis of the divergent reflections of the syn-rift megasequence, MS2 (yellow) overlain by parallel reflections of the post-rift phase. Syn-rift megasequence (MS2) is separated from the post-rift megasequence by a post-rift unconformity, late Aptian. The unconformity comprises of onlap and erosional truncation (red arrows). Same seismic section presented in Figure 2.14A.

Cretaceous post-rift megasequence (MS3), late Aptian (MSB3) - latest Maastrichtian (MSB4)

This is the oldest megasequence belonging to the post-rift phase in both the northern and southern half-grabens. It is characterised by mostly parallel to sub-parallel reflections, but occasionally may show transparent to chaotic reflections. MS3 consists of seven sequences namely: S3A, S3B, S3C, S3D, S3E, S3F, and S3G (Figure 2.18). This megasequence shows some evidence of an episode of tectonic shortening, represented by local folding (up to sequence S3E; Figure 2.18). The nature and cause of this deformation will be described fully in Chapter 4.

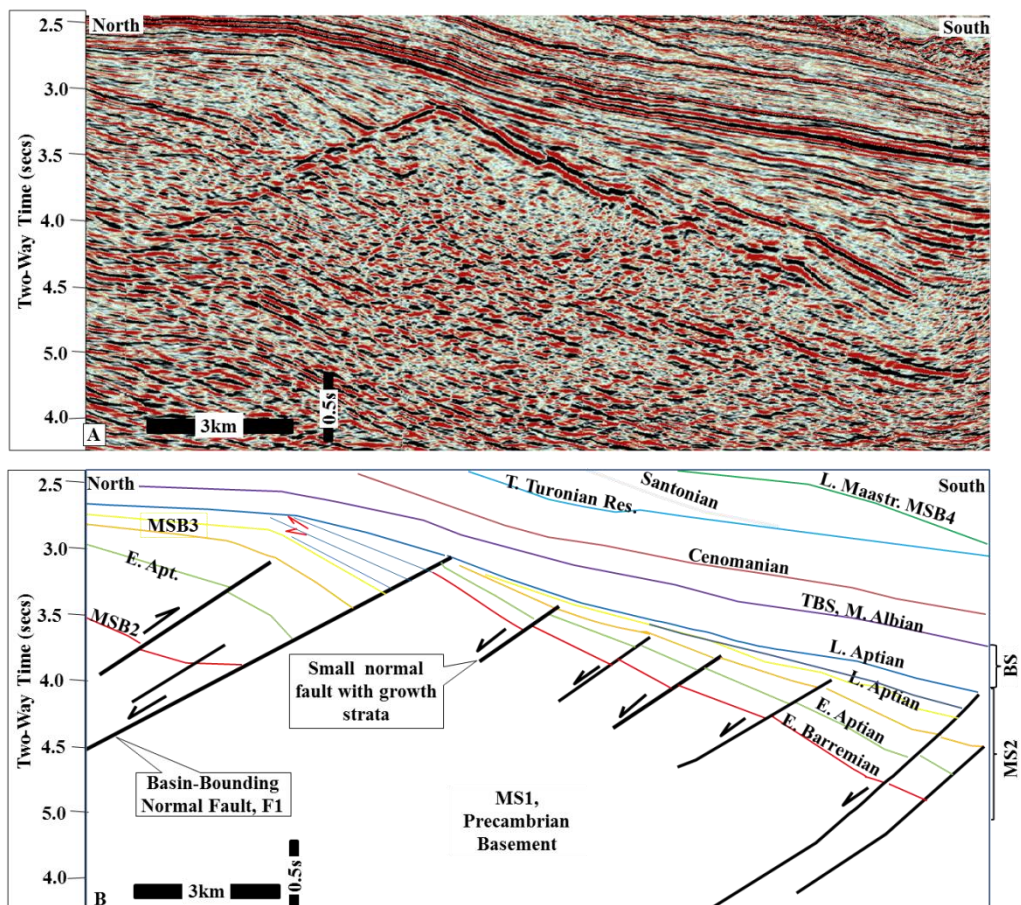


Figure 2.15: A) Uninterpreted seismic section (crossline 4608). B) Line interpretation of the pre-rift, syn-rift, and parts of the post-rift megasequences. The wedge geometry of the syn-rift megasequence (MS2) is overlain by parallel reflectors. TBS = Top of breakup sequence; BS = breakup sequence. See Figure 2.17 for the location of the seismic section.

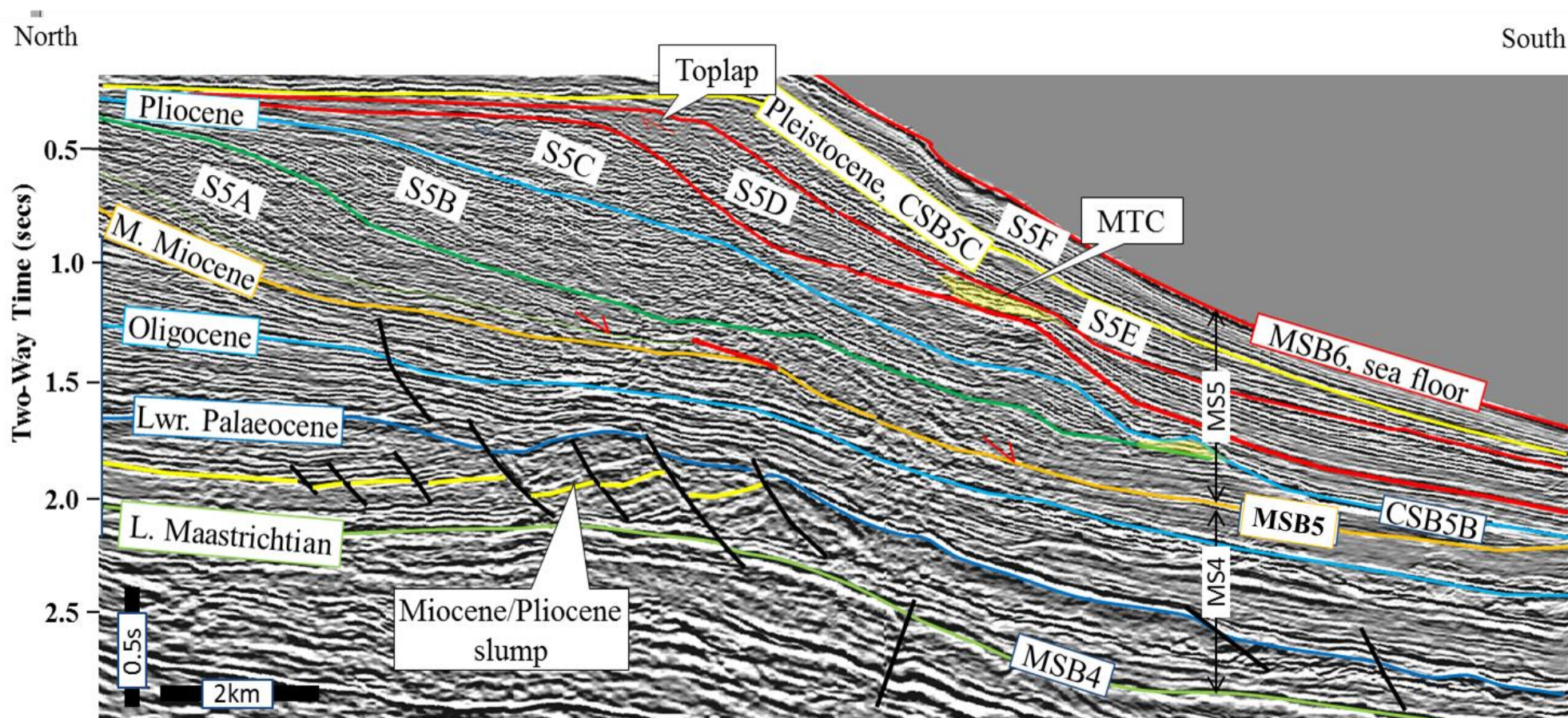


Figure 2.16: Crossline 2482 summarises the Cenozoic geology in the offshore Benin Basin. Cenozoic strata are grouped into two megasequences in this study: a transgressive megasequence (MS4) and a regressive megasequence (MS5). Gravity-induced faults and some other mass-transport complexes (MTCs) are associated with both megasequences. Red arrows indicate reflection terminations. CSB = composite sequence boundary. See Figure 2.17 for the location of the seismic section.

On the basis of their reflection characters and geometry, the first and second seismic sequences (i.e. S3A and S3B) of megasequence MS3 have been identified as the breakup sequence (Figure 2.5; Soares et al., 2012 and 2014). The remaining five seismic sequences (S3C to S3G) are consequently referred to as the post-breakup sequences in this basin (e.g. Soares et al., 2012 and 2014). The lower and upper boundaries of the MS3 are MSB3 (late Aptian) and MSB4 latest Maastrichtian based on the biostratigraphic data provided for this study (Tables 2.6-2.8).

Transgressive megasequence (MS4), latest Maastrichtian (MSB4) - middle Miocene (MSB5)

This unit consists of a succession of parallel to sub-parallel seismic reflections that have quite clear low amplitude in places, and are rarely chaotic (except in some slumps). It is also largely affected by gravitational tectonics (see Figure 2.16). It onlaps the underlying megasequence MS3. It seems to be a thick unit of mostly parallel, oceanward-dipping reflections affected by slumping to the south. It appears to represent a major phase of deepening. Its top is a highly erosive unconformity dated middle Miocene (MSB5). This sequence is, however, characterised by the development of large-scale slumps etc.

Regressive megasequence (MS5), middle Miocene (MSB5)–Holocene (MSB6)

The Neogene strata in offshore Nigeria have been studied by Pacht et al. (1994); Lang et al. (1995); Olabode and Adekoya (2008). Pacht et al. (1994) studied the sequence stratigraphy of the Neogene strata in offshore Nigeria when they covered both the Niger Delta Basin and the Nigerian sector of the Benin Basin.

Table 2.13: Reflection characteristics of the five megasequences studied in this thesis. Lithologic interpretation was based on both well-log interpretation and seismic character. However, megasequence MS1 and sequence S2A in megasequence MS2 were based on seismic character because they have not been drilled.

Seismic Facies unit	Age	Reflection Configuration	Reflection Amplitude	Reflection Continuity	External form of Facies unit	Lower Boundary	Upper Boundary	Predicted Depositional Environment	Lithology prediction
MS5	middle Miocene (MSB5) – Holocene (MSB6)	Parallel, sub-parallel, progradational clinofolds	Moderate to high	Continuous to discontinuous	Channel fills	Onlap, downlap	Onlap, offlap	Marine	Sandstone, mudstone
MS4	Latest Maastrichtian (MSB4) – middle Miocene (MSB5)	Parallel, sub-parallel	High	Discontinuous	Channel fills	Onlap, erosional truncation	Erosional truncation	Marine	Sandstone, mudstone
MS3	Late Aptian, (MSB3) - latest Maastrichtian, (MSB4)	Parallel, sub-parallel, progradational clinofolds,	Low to high	Continuous to discontinuous	Channel fills,	Onlap, downlap	Toplap, onlap	Marine	Sandstone, mudstone, ?limestone
S2C	Middle Aptian – late Aptian (MSB3)	Divergent	Moderate to high	Discontinuous	Wedge	Onlap, downlap	Offlap, onlap, downlap	Shallow marine	Sandstone, mudstone
S2B	Early Aptian – middle Aptian	Divergent	Moderate to high	Discontinuous	Wedge	Onlap	Onlap, downlap	Fluvial, lacustrine	Sandstone, mudstone
S2A	Barremian (MSB2)	Divergent	Low to moderate	Continuous to discontinuous	Parallel to wedge	Onlap	Onlap	Alluvial fan	Sand, mudstone
Basement (MS1)	Precambrian- early Barremian (MSB2)	Transparent/ Chaotic	High	Poor		Base not reached	Onlap	Continental	Crystalline rocks

They proposed that lowland, transgressive and highstand systems tracts are associated with these Neogene strata. The regressive megasequence (MS5) is the youngest megasequence in this basin. It is composed of parallel to sub-parallel reflections and, most characteristically, by progradational clinofolds (Figure 2.16). The reflections have moderate to high amplitude. The seismic reflections are continuous to non-continuous. It represents a major change from transgressive to progradational and through to a prolonged phase of basinward progradation of the shelf and slope. The reflection terminations include onlap, toplap, downlap, erosional truncations and their correlative conformities. The association of these reflection terminations suggests that sedimentation was controlled by a relative fall in sea level and sediment supply. Some of these reflection terminations have been used to define sequence boundaries (using the methodology of Mitchum et al., 1977; Neal and Abreu, 2009). The regressive megasequence (MS5) is made up of at least six sequences which include S5A, S5B, S5C, S5D, S5E, and S5F (Figure 2.16).

2.7 Structural framework in the offshore Benin Basin

Rift basins and passive margins are associated with different structural elements ranging from extensional to compressional structures (Doré et al., 2008). Some of these structures are formed during continental rifting while others evolved during the post-rift phase of the basin development.

The structural elements in the study area can generally be grouped into two:

- ❖ Tectonic-related structures
- ❖ Gravity-induced structures

2.8 Tectonic structures

Tectonic structures include those formed through both regional extension and compression. Larger tectonic structures typically involve basement. However, their vertical extent cannot be determined because of limited seismic data penetration. Tectonic structures in the area are sub-divided on the basis of their kinematics:

- 1 Extensional structures
- 2 Contractional structures

2.8.1 Northern and southern half-grabens and their basin-bounding normal faults (F1 and F2)

A half-graben is an asymmetrical basin with a single major basin-bounding normal fault. Half-grabens are complex tectono-sedimentary systems with three-dimensional rift-parallel, oblique structures that exert a strong control on sediment production, transport pathways, and the accumulation of both clastic and carbonate sediments (Gawthorpe and Hurst, 1993; Morley, 1995; Bosence et al., 1998; Levy and Jaupart, 2011). The half-graben is often characterised by a wedge pattern comprising divergent reflections.

The study area exhibits two regional half-graben structures, one to the north and the other in the south. They are characterised by two major basin-bounding normal faults that have been identified as main tectonic structures in this basin. The basin-bounding normal faults (F1 and F2) dip landwards (northwards) (Figure 2.5). Other minor normal faults exist as either synthetic or antithetic structures to the main bounding faults in both half-grabens; the antithetic faults are generally

subordinate in number. The geometry, kinematics, and mechanisms of the basin-bounding normal faults, and the associated minor synthetic normal faults, are discussed in Chapter 3.

2.8.2 Transfer structure (F5)

The transfer structure observed on seismic data occurs mainly in the northwestern part of the northern half-graben where it forms part of a major transfer zone (Figure 2.17). The transfer fault connects the basin-bounding normal fault (F1) with another sub-basin (F4) in the northern half-graben (Figure 2.17). Such faults also appear to have a significant component of normal displacement but are generally steeper than the main fault (F1). Other smaller normal faults also trend obliquely to the main fault (F1) but are parallel to sub-parallel to the major transfer fault (F5) (Figure 2.17). The role of the transfer fault for the basin evolution in the offshore Benin Basin will be validated in Chapter 4.

2.9 Tectonic contractional structures

Tectonic-related structures in the forms of thrusting and folding form in extensional, strike-slip and compressional settings. For example, strike-slip or thrust faults are generally known to be associated with compressional tectonic regimes but can also occur during regional extension, especially where significant slopes are being generated (Park, 1997). The structures include reverse and thrust faults, fault-related anticlines, and more extensive, but quite gentle, fold structures that form away from major faults.

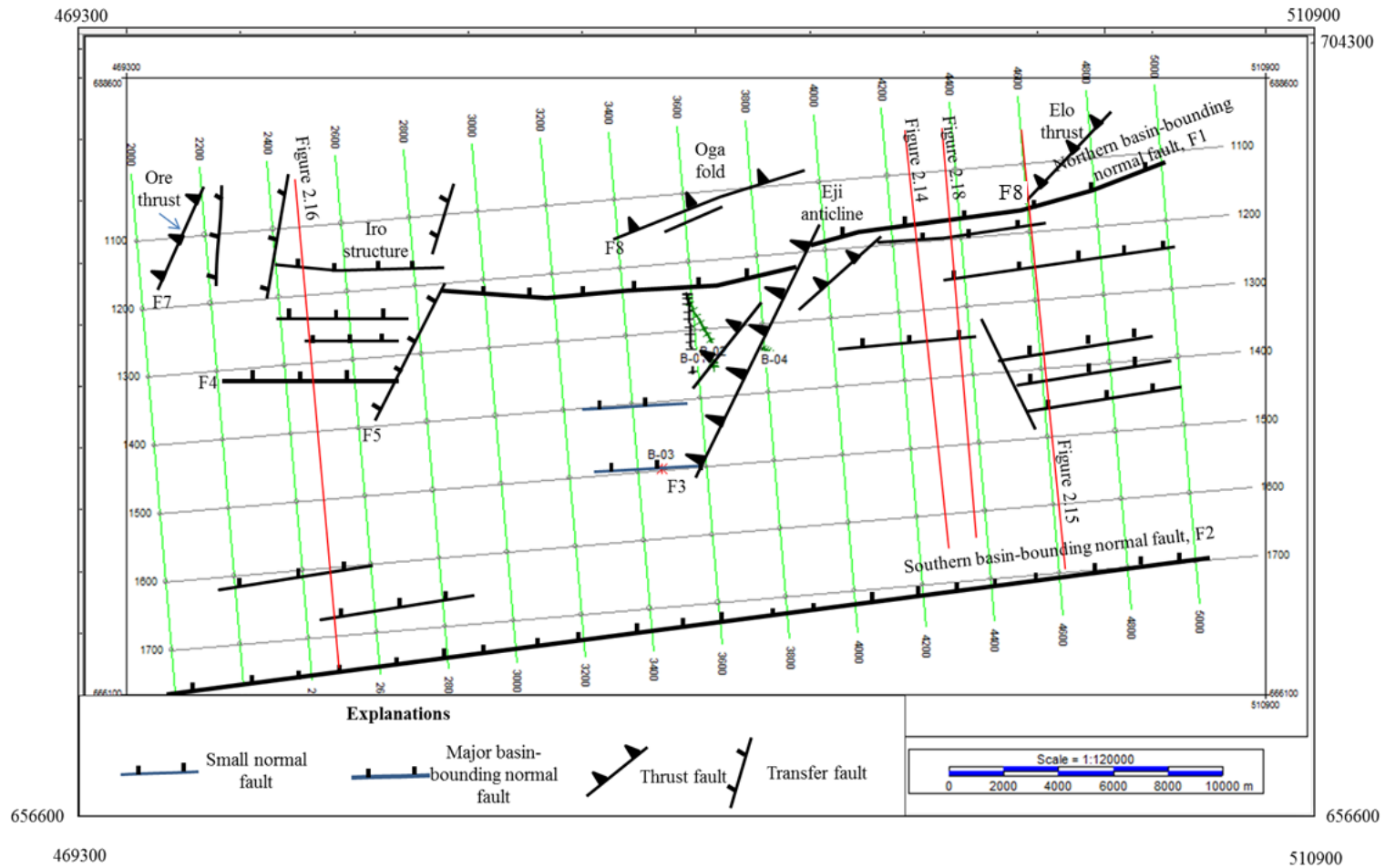


Figure 2.17: A composite structural element map showing the main tectonic structures (the main basin-bounding normal faults, F1 and F2; transfer fault, F5; thrust and reverse faults) in the study area. The location of some of the figures cited in this chapter are also indicated.

The fold structures recorded on the seismic data of the offshore Benin Basin will be analysed for their kinematics and mechanisms for their evolution. However, the spatial arrangement and relative timing of the contractional structures identified in this study suggest that they developed under regional compression, as discussed in Chapter 4.

2.9.1 Inverted structures

Inversion tectonics may occur when basin-bounding normal faults are reactivated in a reverse sense during later contractional tectonics (De Graciansky et al., 1989; Brun and Nalpas, 1996; Bernal and Hardy, 2002; Casas et al., 2002; Castelltort et al., 2004; Shaw et al., 2004; Turner and Williams, 2004; Casas-Sainz et al., 2005; Bigi, 2006; Zhang et al., 2006; Aschoff and Schmitt, 2008; Sun and Zhang, 2009; Nigro and Renda, 2014). This often leads to some (mild inversion) or all (total inversion) of the basin stratigraphy which can be lifted above the regional elevation (i.e. the basin becomes a positive feature) (Williams et al., 1989). Reactivated normal faults may retain net extension at depth but net compression (often associated with an anticline and a possible growth sequence) in the upper portion. The two segments of the reactivated fault are separated by the null point, where the fault has zero net displacement.

The northern half-graben shows evidence of mild basin inversion. This structure is referred to as the Oga fold (Figure 2.18). It occurs in the northwestern part of the northern half-graben. Chapter 4 gives a description of this structure.

2.9.2 Reverse and thrust faults

The reverse fault (F3) is one of the main structures observed in both northern and southern parts of the study area. The fault geometry shows that it is oblique to the

main basin-bounding normal faults (Figure 2.17). It is steeply-dipping reverse fault (Figure 2.12). The reverse fault is associated with an anticline, which is referred to as the Eji anticline for the remainder of this study (Figure 2.12).

Thrust faults, and their associated folds, also occur in two different locations within the northern half-graben. They have been named Elo thrust and Ore thrust structures in this study.

2.9.3 Anticlinal structures

Anticlines are common structures associated with both extensional and compressional forces. Fold geometries (Figure 2.11) on seismic data suggest that these anticlines are associated with reverse faults. The fold axis strikes in the NE-SW direction. The anticlinal structure associated with the reverse fault (F3) was further studied in Chapter 4.

The implications of all the structural elements (basin-bounding normal faults, transfer faults, relay structure, isolated normal faults, obliquely-dipping normal fault, and reverse/thrust fault) for the tectonic origin of the offshore Benin Basin will be tested in Chapter 4.

2.10 Gravity-induced structures

Gravity-induced structures are thought to form by gravity acting on a slope. A slump is defined as a rotational motion on a concave-upwards shear plane (Varnes, 1978; Woodcock, 1979; Watts and Stewart, 1998). A slide can be used to describe both rotational and non-rotational slope failures (Hesthammer and Fossen, 1999).

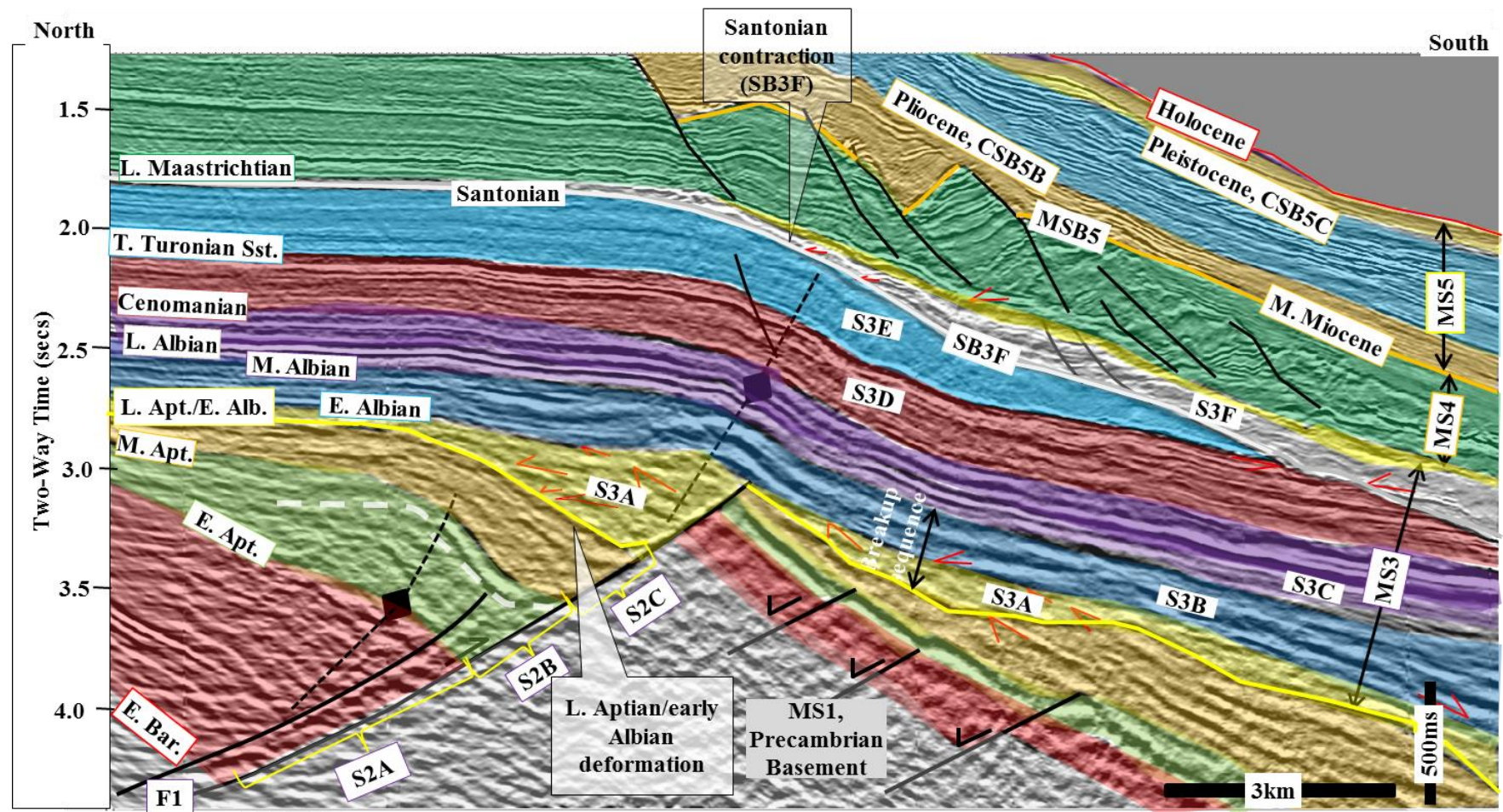


Figure 2.18: 3D seismic section (crossline 3940) displaying the two main contractional deformation phases analysed in this thesis (late Aptian/early Albian and Santonian). See Figure 2.17 for the location of the seismic section.

Gravitational collapse structures are observed in many settings around the world. They may range from a few centimetres to hundreds of kilometres in length. A good example of their importance in petroleum exploration is the adjacent Tertiary Niger Delta where growth faults and their associated roll-over anticlines serve as the main trapping structures (Evamy et al., 1978; Weber et al., 1978; Doust, 1990; Maloney et al., 2010; 2012).

The offshore Benin Basin is affected by at least two episodes of gravity-driven deformation as indicated by the presence of oceanward-dipping normal faults. Their angles of dip decrease with depth from nearly vertical to less than 30°. The first one is the 'Campanian' slump that deforms the Late Cretaceous sequences belonging to the megasequence MS3. The second is the late Miocene/Pliocene slump that affected both the Cenozoic comprising the transgressive megasequence (MS4) and the regressive megasequence (MS5; Figure 2.16).

The Campanian slump is localised because it deforms only the post-Santonian sequence, whereas the Miocene/Pliocene slump has a widespread occurrence. The geometry of the Miocene/Pliocene slump generally signifies rotational movement about an axis parallel to the slope. The main slump blocks broke into a series of secondary slumps and associated scarps to form a stair-step pattern of displaced blocks at places.

The Miocene/Pliocene slump shows some evidence of transport in the form of deposition of low to high chaotic reflections that onlap onto their normal fault plane. These chaotic reflections have been grouped as deposits of the mass-transport complexes (MTCs). The mass-transport complex appears to have a widespread occurrence in the regressive megasequence (MS5).

2.11 Problems of correlating across the northern and southern half-grabens

Correlating the onset of rift unconformity (MSB2) across the northern and southern half-grabens was problematic due to the presence of a footwall high (Gaga ridge) (Figure 2.14). This ridge is composed of chaotic reflections interpreted as crystalline basement rock. The problem was compounded because the syn-rift succession has not been completely drilled. The study area covers the Aje Field that contains the deepest well in the entire basin (Kaki et al., 2012) so correlating the syn-rift succession with the Seme Field (Figure 2.1) to the west of the study area was not possible. Another problem is the poor data resolution at depth in the southern half-graben. Correlation across the two half-grabens was, however, possible by tying seismic character across the study area.

2.12 Regional correlation of the megasequence boundaries (MSB2-MSB5)

Two of the megasequence boundaries (rift-onset unconformity, MSB2; and post-rift unconformity, MSB3) are interpreted to represent significant changes in subsidence mechanism during deposition as they are the rift onset and post-rift unconformities, respectively. The other two boundaries (MSB4 and MSB5) are unconformities whose correlative conformities represent significant changes in the genetic behaviour of the post-rift succession, or periods characterised by prolonged gravity-driven deformation (i.e. slumping; Chang, 1975; Sacchi et al., 1999; De Santis, 2013; Qu et al., 2014). These binaries separate sets of higher order sequences.

MSB2 (rift onset unconformity) is characterised by the onlapping of the divergent reflections of the syn-rift megasequence (MS2) onto the chaotic reflections of the pre-rift megasequence (MS1). This sequence boundary has been folded in the northern half-graben possibly due to localised shortening. MacGregor et al. (2003) and Brownfield and Charpentier (2006) ascertained that syn-rift strata have not yet been drilled in the offshore Benin Basin, and so the age of the syn-rift megasequence (MS2) is not known for certainty. This study that provides age up to the base of rift-climax sequence (S2B) (Figure 2.17) will, therefore, better our understanding on the evolution of the offshore Benin Basin. The rift onset unconformity (MSB2) is assigned an inferred early Barremian age following Moulin et al. (2010) and Fairhead et al. (2013) who postulated that rifting probably started in the Barremian in this region.

The dating of the rift-onset in the Equatorial Atlantic is generally connected with one of the following problems:

- ❖ Lack of magnetic anomalies during the Cretaceous magnetic quiet zone
- ❖ Lack of well data on the deeper syn-rift.

These problems have led some authors (e.g. Brownfield and Charpentier, 2006; Kaki et al., 2012) to assign the Late Jurassic as the rift-onset in the Equatorial Atlantic margin. These authors highlight the fact that the rifting started in the southern South Atlantic and propagated northwards. According to Moulin et al. (2010), as rifting continued to propagate northwards it is thought to have resumed in the Equatorial Atlantic during the Barremian. The megasequence boundaries interpreted in this study are thus correlated with those of the African intraplate rifting (Figure 2.19; Fairhead et al., 2013).

MSB3 (post-rift unconformity, PRU): It is a parallel to sub-parallel, mainly continuous, moderate to high amplitude reflection. It correlates across the northern and southern half-grabens. These reflection terminations and their geometries suggest that the sequence boundary is an angular unconformity (Figure 2.14). This angular unconformity exists between an underlying syn-rift megasequence (MS2) and the overlying post-rift successions. This unconformity is dated as late Aptian in this study. It correlates with the post-rift unconformity of many basins in the South Atlantic region (Moulin et al., 2010). The post-rift unconformity corresponds to the base of a fining-upward sequence (Figure 2.13).

MSB4 is present across the whole study area and is locally characterised by erosional truncation beneath it, and widespread onlap above. It is composed of parallel to sub-parallel, continuous, moderate to high amplitude reflections (Figure 2.16). It has been dated as latest Maastrichtian in this study. Although it does not show any tectonic significance in this study, it correlates regionally with the onset-of-rifting in Muglad Basin in Central Africa and in the Ténéré Basin in West Africa (Figures 2.19; Fairhead et al., 2013). It also correlates with the end-of-rifting in Bornu Basin, Upper Benue Trough (both in West Africa) and Kantem Basin in Central Africa (Figure 2.19) (Nwachukwu, 1971; Olade, 1975; Browne and Fairhead, 1983; Guiraud et al., 1992; Fairhead et al., 2013). All these basins in both West and Central Africa are thought to have undergone polyphased rifting (GETECH, 2002, Fairhead et al., 2013).

MSB5: this is an erosional truncation and sometimes it is composed of onlap. It runs through the continental shelf, continental slope into the abyssal plain. It crosscuts into the vast majority of the succession of normal regressive phase. It bounds a phase dominated by regression and expansion of the shelf into the

Atlantic during the Cenozoic, starting in Middle Miocene. MSB5 is dated as middle Miocene by biostratigraphy data in this study (Mosumolu, 2008). This unconformity does not show any significant tectonic implication in the offshore Benin Basin. However, it correlates with the continuation of rifting in a few basins such as Ténéré Basin (Figure 2.19) (Fairhead et al., 2013).

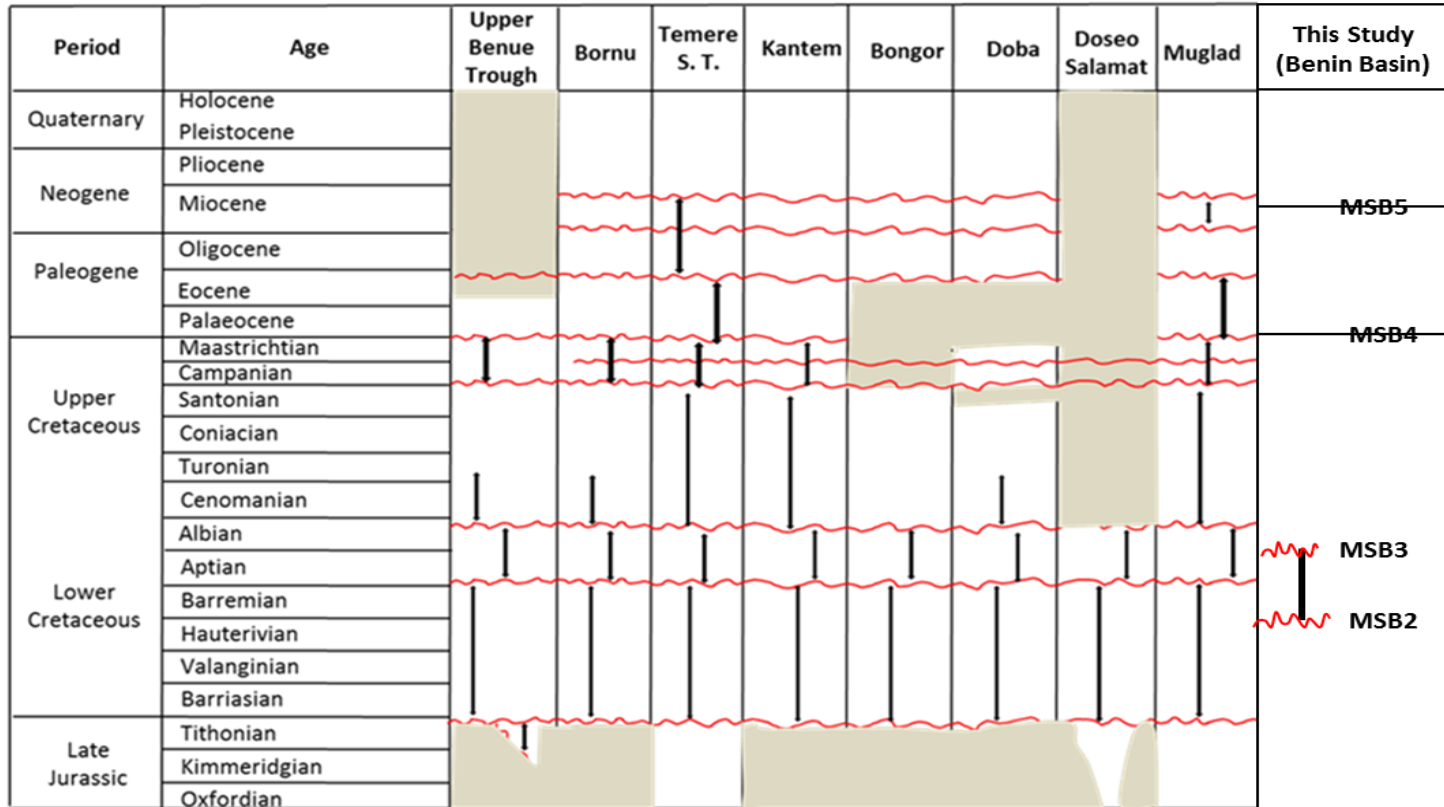


Figure 2.19: A regional correlation of the megasequence boundaries interpreted for the offshore Benin Basin (OBB), highlighting the continental rifting episodes in the intraplate basins of West and Central African rift system (WCARS). Note that the rift onset (MSB2) and post-rift (MSB3) unconformities in the offshore Benin Basin correlate with on-going rifting in the WCARS. Other megasequence boundaries (base of transgressive megasequence MSB4, and base of regressive megasequence MSB5), despite their non-tectonic origin, correlate respectively with end-of- and on-going-rifting in the WCARS. Vertical thick lines indicate rifting events whereas wavy red lines denote unconformities. Shaded areas show erosion or much-reduced sedimentation, i.e. condensed sections (modified after Fairhead et al., 2013).

Chapter Three

3.0 Tectono-stratigraphy and structure of the syn-rift megasequence MS2, offshore Benin Basin

This chapter presents a structural and stratigraphic analysis of the syn-rift megasequence (MS2), comparing it to other continental rift basins in the literature. It also focuses on the implications of this analysis to the timing and nature of rifting in the Equatorial Atlantic.

3.1 Introduction

The main aim of this chapter is to establish the tectonic evolution of the Benin Basin based on structural and tectono-stratigraphic arguments. The validity of interpretations will be evaluated against published tectonic models for the Equatorial Atlantic margin (e.g. Matos, 2000; Brownfield and Charpentier, 2006; Moulin et al., 2010; Fairhead et al., 2013, Heine and Brune, 2014; Basile, 2016). Most of the existing models view sedimentary basins along both margins of the Equatorial Atlantic as involving during what is referred to as ‘transform’ tectonism (e.g. Moulin et al., 2010; Heine and Brune, 2014; Basile et al., 2015). Others have proposed that continental rifting was by orthogonal extension (e.g. Fairhead et al., 2013). Orthogonal extension involves extension perpendicular to the direction of plate movement, whereas oblique extension involves extensional movement oblique to plate movement. Both orthogonal and oblique extension may develop low-angle normal faults during the movement.

Little published literature is available on the tectonic evolution of the offshore Benin Basin (e.g. Deitel et al., 1974; MacGregor et al., 2003; Brownfield and Charpentier 2006; Kaki et al., 2012). Significant questions remain concerning the validity of published models for the

evolution of the offshore Benin Basin in relation to oblique versus orthogonal extension. The timing of rifting of this basin is also controversial; is it Late Jurassic to Early Cretaceous (e.g. Brownfield and Charpentier, 2006; Kaki et al., 2012) or Barremian to Aptian (e.g. Moulin et al., 2010)? There is, however, a considerable overlap between these two age ranges, so they do not disagree completely. Rift propagation models for the opening of the South Atlantic may explain the time overlap (see section 1.9 for detail discussion).

The seismic and well datasets used for this study provide the opportunity to better understand the evolution of this part of the Equatorial Atlantic. The main focus of this chapter is the syn-rift megasequence (MS2) (identified in section 2.10) of the northern and southern half-grabens, their basin-bounding normal faults, F1 and F2 (see sub-section 2.7.1) and associated structural elements. Analysis of the 2D and 3D seismic datasets provide new insights into rift geometries and structural architecture, and contribute to our further understanding of the tectonic evolution of this basin.

3.2 Aims and objectives

The aims of this chapter include the following:

- ❖ To provide a description of the syn-rift stratigraphy and structural architecture of the offshore Benin Basin;
- ❖ To evaluate how the syn-rift stratigraphy and structural architecture of the offshore Benin Basin compare to existing models for rift basin evolution and the extent to which this can better understand the evolution of the Equatorial Atlantic.
- ❖ To provide a description of the structural architecture of the offshore Benin Basin and how this evolved through the rift phase.

In order to achieve the aims of this chapter, the following objectives were addressed;

- ❖ Undertake seismic facies analysis of the syn-rift megasequence (MS2) based on seismic reflection characteristics (Vail et al., 1977; Prosser, 1993; Driscoll et al., 1995).
- ❖ Describe the structural style of the syn-rift succession as extension evolved from continental rifting to the post-rift stage, and compare it to other studies which show the development of continental rift basins (e.g. Ravnas and Steel, 1998; Gawthorpe and Leeder, 2000; Alves et al., 2003; Cowie et al., 2005; Pereira and Alves, 2011).
- ❖ Analyse basement-involved normal faults (the basin-bounding normal faults, F1 and F2, and their associated small normal faults for how their fault-growth controlled sedimentation during rifting (e.g. Pollard and Aydin, 1988; Corfield and Sharp, 2000; Gawthorpe and Leeder, 2000; Crowell, 2003; Corti et al., 2005; Corti, 2012).
- ❖ Identify the main syn-rift episode in the study area and correlate this with those along the neighbouring margin (Guiraud et al., 1992; Brownfield and Charpentier, 2006; Moulin et al., 2010; Fairhead et al., 2013).

3.3 Review of rift models and rift stratigraphy

3.3.1 The models of lithospheric extension

Different plate tectonic models have been proposed to explain the processes, geometries or rheological behaviour of the lithosphere during continental extension (McKenzie, 1978; Wernicke, 1981; Lister et al., 1986; Buck, 1991; Corti et al., 2003; Karner et al., 2007; Rosenbaum et al., 2008; Merle, 2011). Such models depend largely on the variations of distinct components such as thermal structure, strength, rheology heterogeneities, strain rates,

thickness and the nature and composition of the lithosphere (Corti et al., 2003; Rosenbaum et al., 2008).

Buck (1991) postulated three main types of geometries and modes of extension on the basis of identifying distinct architectures on rifted margins:

- ❖ The narrow rift mode
- ❖ The wide rift mode and,
- ❖ The core complex mode (Buck, 1991).

Narrow rifts are commonly a few hundreds of kilometres in width (Figure 3.1B). They are often formed where the lithospheric extension is intense and generally possess horst-graben geometry. Examples include the Rhine Graben, the Gulf of Suez, the East African Rift and the Sergipe-Alagoas Basin (Brazil) (Buck, 1991). The narrow rifts may show large lateral gradients in thickness of the crust and in topography.

Sedimentary basins complying with the wide rift mode (Figure 3.1A), for example, the North American Basin and Range, the São Paulo Basin in SE Brazil, are characterised by extension accommodated by normal faults in the order of 600 to 800 km in width (Buck, 1991). The wide rifts are typified by small lateral gradients in crustal thickness (Buck, 1991).

Rifts of the core complex model are characterised by high-grade metamorphic rocks and the presence of a lower crust low-angle detachment (Figure 3.1C; Wernicke, 1981; 1985; Buck, 1991). This type of rift model has been considered as a type of wide rift model (Merle, 2011).

Other models reviewed in this study include McKenzie (1978); Wernicke (1981) and later Coward (1986) and Lister et al., 1986). McKenzie (1978) postulated a “pure-shear” model for the Basin and Range Province (continental United States of America) in order to predict

crustal thickness, subsidence histories and gravity profiles in extended terranes. The model assumes homogeneous thinning of the lithosphere. It does not however fully explain the differences in the architecture of continental crust of asymmetric rifted margins (Figure 3.2A; Lister et al., 1986).

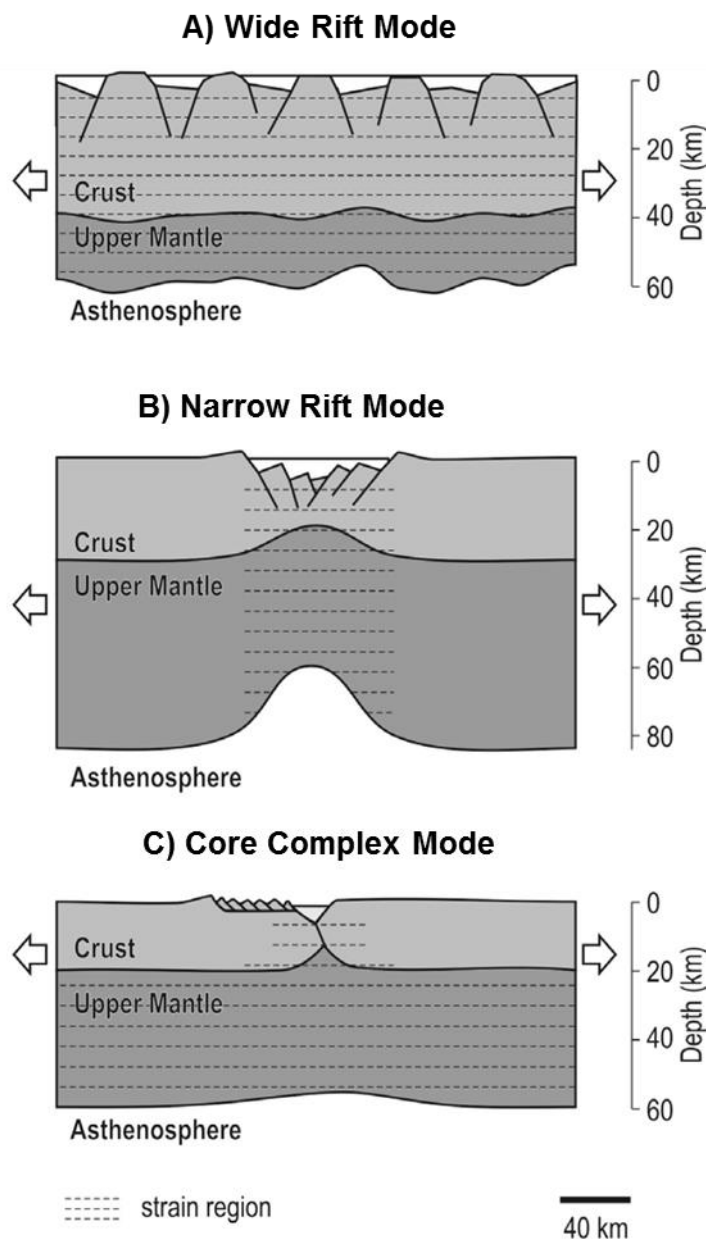


Figure 3.1: Schematic representation of the principal modes of lithospheric extension, A) Wide rift mode B) narrow rift mode, C) core complex mode (after Buck, 1991; Rosenbaum et al., 2008).

This, consequently, led Wernicke (1981) and later Coward (1986) to postulate the existence of a deep lower crust detachment that may explain the variations in crustal thinning and the geometry of rift-related normal faults (i.e. the “simple shear model”). They also noted that multiple detachments often control the evolution of rifted margins which are characterised by the marginal highs, ribbons, and plateaus (Lister et al., 1986).

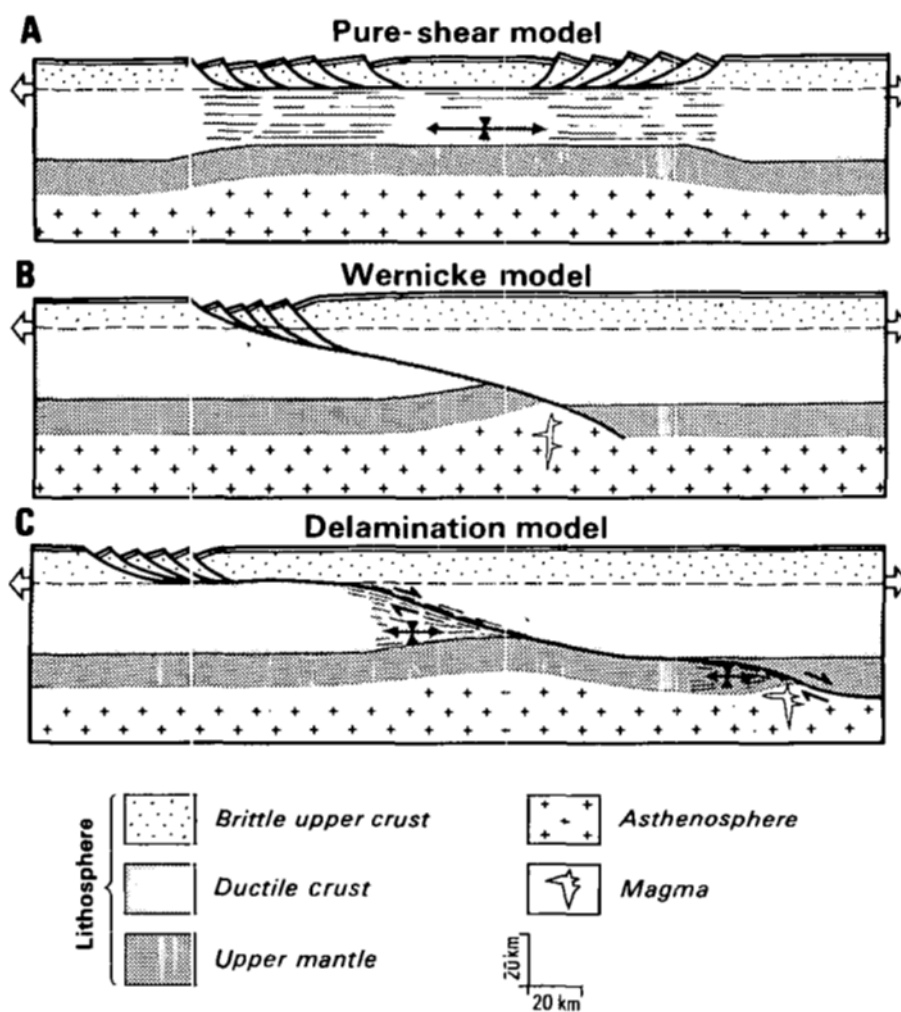


Figure 3.2: Schematic models of continental lithospheric extension: A) McKenzie pure shear model, B) Wernicke simple shear model, C) delamination model (after Lister et al., 1986).

The terminologies “narrow” and “wide” rifts are considered by some authors (e.g. Davison, 1997) as descriptive and do not have any mechanical, kinematic or major geodynamic significance. Lister et al. (1986) attempted to explain the evolution of shallow-dipping detachment faults during lithospheric extension. These authors invoked the presence of a deep crustal detachment to explain the symmetry and asymmetry of passive rifted margins. In their explanation, the concepts of ‘simple shear’ and ‘pure shear’ were used in addition to the ‘delamination model’ (Figure 3.2).

Lister et al. (1986) postulated the “delamination model” as an alternative explanation for thinned continental margins that show steepening lower crust detachments (Figure 3.2C). The assumptions of Wernicke (1981) that the rifted margins can be asymmetric and that extension is largely controlled by deep detachment faults led Lister et al. (1986) to suggest “upper-plate” and “lower-plate” geometries for passive continental margins, each with characteristic subsidence/uplift signatures and distinct distribution of a so-called continent-ocean boundary (COB) along the margin (Figure 3.3).

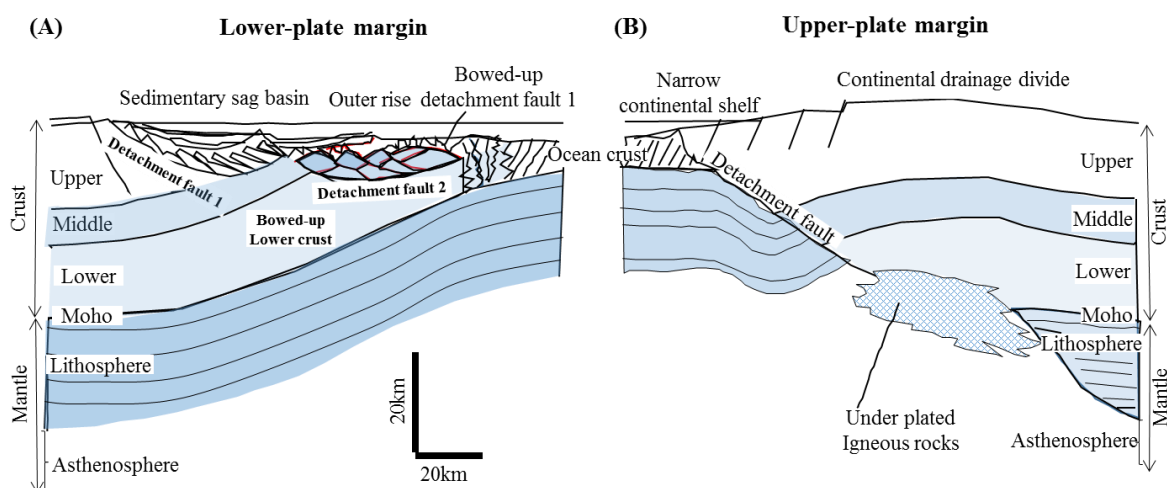


Figure 3.3: Detachment-fault model for passive continental margins with A) lower-plate or upper-plate characteristics. The lower-plate margin has complex structure; tilt blocks are remnants from the upper plate, above bowed-up detachment faults. B) The upper-plate margin is relatively unstructured. Uplift of the adjacent continent is caused by underplating of igneous rocks. Multiple detachments have led to two generations of tilt blocks in the diagram shown. Opposing passive margin pairs exhibit marked but complementary asymmetry (after Lister, 1986).

Lister et al. (1986) consider the upper-plate margins as consisting of rocks that were originally above the detachment faults while the lower-plate margins comprise the deeper crystalline rocks of the lower plate. The lower plate margins are usually overlain by highly faulted remnants of the upper plate (Figure 3.3). Both the upper-plate and lower-plate margins differ principally in their rift-stage structure as well as in their uplift/subsidence characteristics. Other differences may arise from variation in the location of the continent-ocean boundary, complex detachment-fault geometries, and movement of the master detachment faults on transfer faults (Lister et al., 1986).

3.3.2 Basin development and geometry

Extensional basins and passive margin basins are generally characterised by arrays of half-grabens separated by transfer zones or accommodation structures (Jackson et al. 1982; 2005; Gibbs, 1984; Milani and Davison, 1988; Gawthorpe and Hurst, 1993; Gawthorpe et al., 1994; McClay and Khalil, 1998; Young et al., 2000; Smith et al., 2001; Kornsawan and Morley, 2002; Withjack et al., 2002; Younes and McClay, 2002; Acocella et al., 2005; Fossen and Rotevatn, 2016). Major active normal faults in areas such as the Basin and Range, Aegean Sea and East Africa have shown that they are segmented along strike (Jackson, 1987; dePolo et al., 1991; Machette et al., 1991; Gawthorpe and Leeder, 2000; Cowie et al., 2005). The length of recent basin-bounding normal faults is commonly 35-60 km; with individual fault strands at the surface of about 15-20 km (Ravnas and Steel, 1998). Fault segments are commonly 15-20 km long or more (Jackson and White, 1989; Jackson and Blenkinsop, 1997). The width of classic linear rift valleys varies from about 50 to 100 km. The width may be up to 1000 km or more in regionally extended rift provinces (Ravnas and Steel, 1998).

Segment boundaries are often characterised by an increased density of small-displacement faults (e.g. Peacock and Sanderson, 1991; Trudgill and Cartwright, 1994; Jackson and

Leeder, 1994; Anders and Schlische, 1994; Cartwright et al., 1996; Dawers et al., 2000; Gawthorpe and Leeder, 2000; Peacock et al., 2000; Peacock, 2002). Jackson et al. (2005) demonstrated that the evolution of normal fault segments is an important control on syn-rift depositional patterns and sequence stratigraphy (Figure 3.4). Gawthorpe and Leeder (2000) provided a review of the role of fault growth on rift basin evolution and stratigraphic evolution. They identified three stages: fault initiation, fault interaction and linkage and a through-going fault zone stage. Fault initiation stage involves the formation of small faults that grow as extension continues. The fault interaction and linkage stage comprises the phase in which faults interact and are linked to develop a large fault with large displacement (Schlische and Anders, 1996). The through-going fault zone records the final linkage of the existing closely spaced smaller faults to form a rift zone. The quality of seismic data usually available on continental margins means that identification of these stages in the syn-rift has proven quite difficult. An attempt was however made and the interpretation is presented in the subsequent section.

Most rift basin geometry is dependent on whether the extension is orthogonal or oblique to the rift axis. Many studies have been carried out on the geometries of rift basins (Figures 3.4 and 3.5) by different authors including Leeder and Gawthorpe (1987), Frostick and Steel (1993), Lambiase and Bosworth (1995), Nottvedt et al. (1995), Ravnås and Steel (1998), Matos (2000), DeVault and Jeremiah (2002).

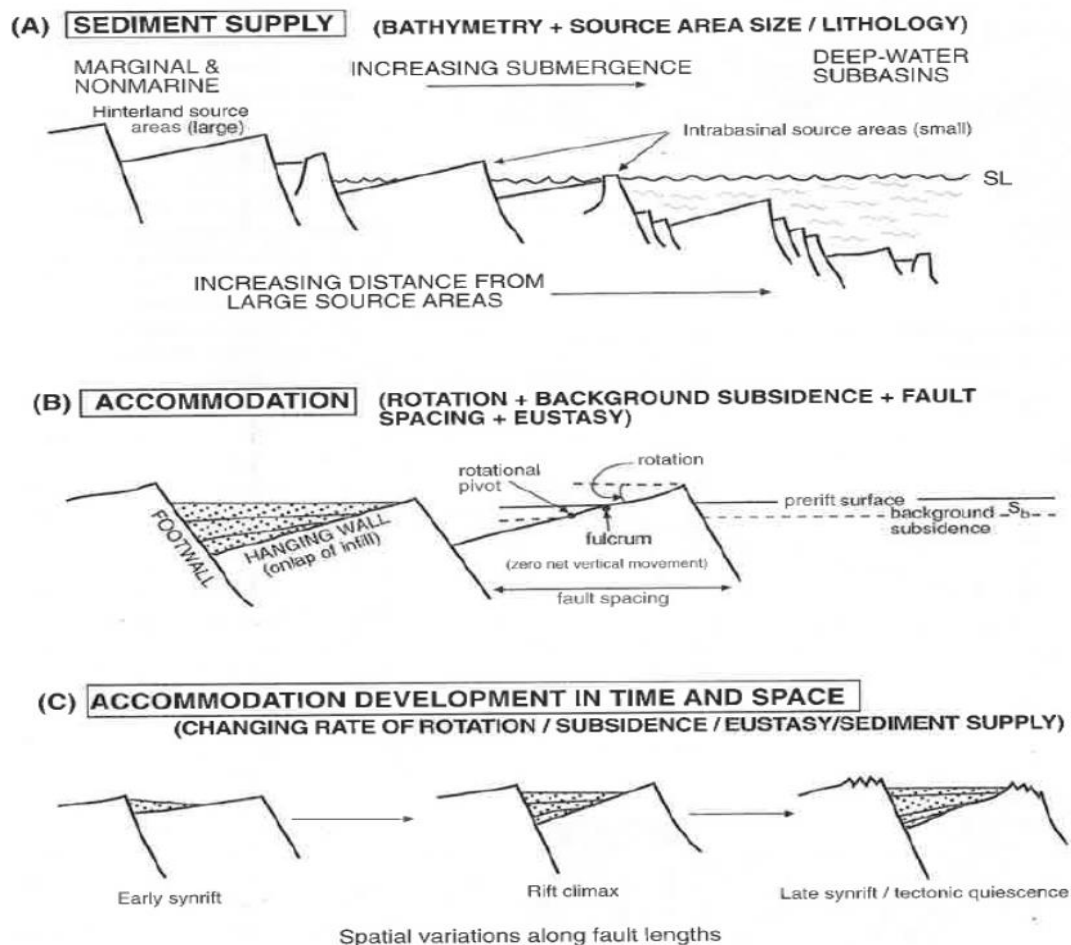


Figure 3.4: Basin development and characteristic geometry of rift basins (after Ravnas and Steel, 1998).

The structural style of rifts is chiefly dependent on the following:

- ❖ The rheological structure of the lithosphere
- ❖ The availability of crustal discontinuities that can be tensionally reactivated
- ❖ The mode (orthogonal or oblique) and amount of extension
- ❖ The lithological composition of pre- and syn-rift sediments (Ziegler and Cloetingh, 2004).

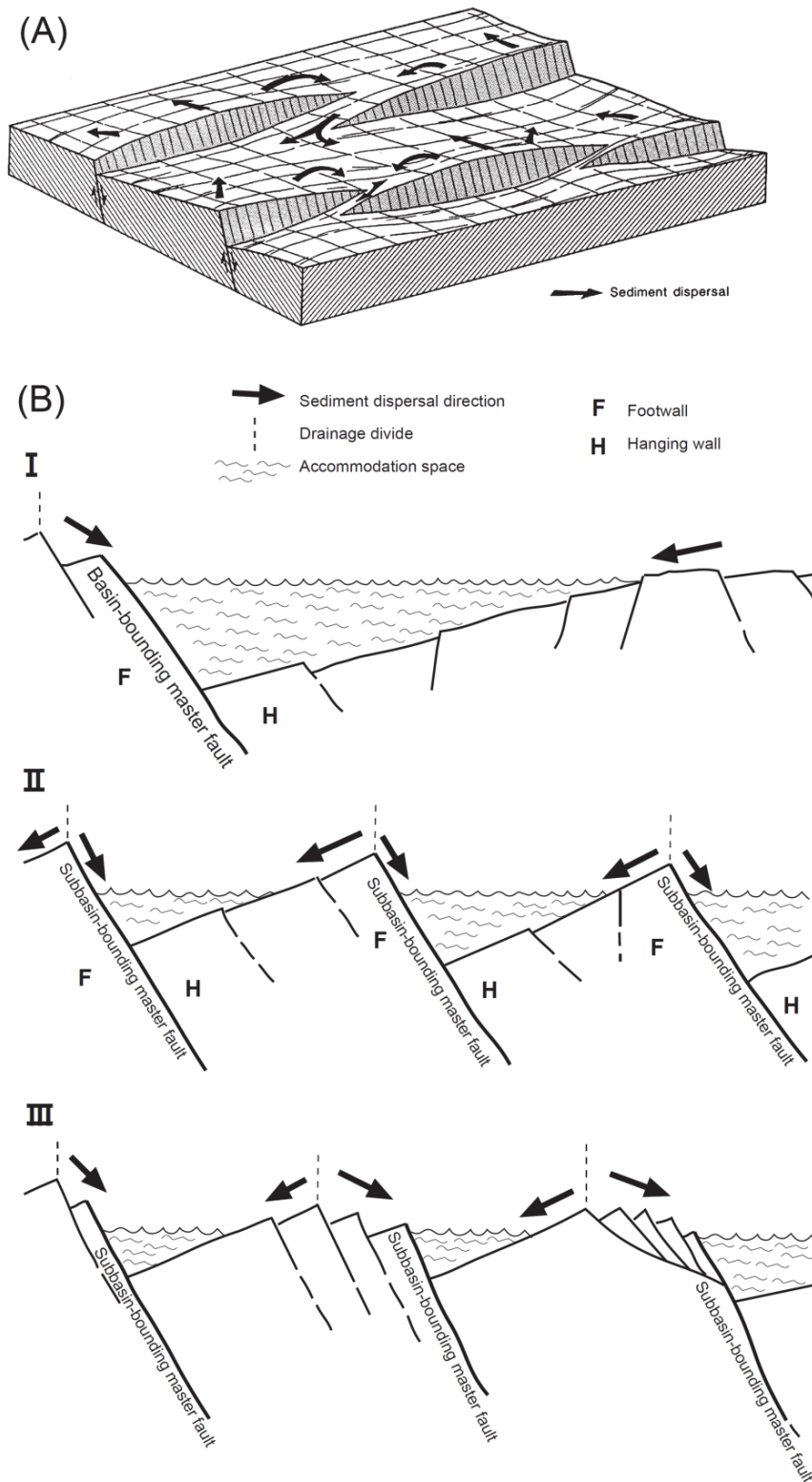


Figure 3.5: A) Half-graben morphology and rift-interior sediment dispersal pattern. B) Dip section through rifted terrains showing accommodation, intrabasinal drainage, and sediment dispersal direction in: (I) a solitary half-graben, (II) a series of half-grabens with simple basin-bounding master faults, and (III) a series of half-grabens with segmented fault-complex or collapsed footwall as basin-bounding structures (after Ravnâs and Steel, 1998).

3.4 Rift tectono-stratigraphy

Tectono-stratigraphy is the stratigraphy related to the timing of tectonic events (Hinz, 1981; Mutler, 1985; White et al., 1986; Prosser, 1993; Ravnas and Bondevik, 1997; Hinz et al., 1999; Manga et al., 2001; Trudgill and Underhill, 2002; Withjack et al., 2002). It has been reported that sequences/megasequences that represent these tectonic events are sometimes separated by major unconformities (Shelton, 1984; Nottvedt et al., 1985; DeVault and Jeremiah, 2002; Kyrkjebo et al., 2004). The seismic signatures of syn-rift sedimentary sequences have been used to suggest possible linkage of specific signatures to tectonic events, or to date and quantify motion on extensional faults (Withjack and Drick-Pollock, 1984; Prosser, 1993; Lambiase and Bosworth, 1995; Nottvedt et al., 1995; Ravnas and Bondevik, 1997; Gawthorpe and Leeder, 2000; Withjack et al., 2002; Cowie et al., 2005; Jackson et al., 2005; Burton and Wood, 2010). Many workers have based the timing of continental rifting mainly on growth strata within the rifted basin (e.g. Withjack et al., 1998; Schlische and Withjack, 2009; Pereira and Alves, 2011).

Since Vail et al. (1977) pioneering work on seismic stratigraphy, many studies have been carried out on the recognition of architectural signature that is diagnostic of syn-rift basin-fills (Surlyk, 1978, 1989; Alexander and Leeder, 1986; Frostick and Reid, 1987; Leeder and Gawthorpe, 1987; Hamblin and Rust, 1989; Morley, 1989; Gabrielsen et al., 1990; Mack and Seager, 1990; Schlische and Olsen, 1990; Lambiase, 1990; Prosser, 1993; Nottvedt et al., 1995; Ravnås and Steel, 1998; Ravnås et al., 2000; Paton and Underhill, 2004; Pèron-Pinvidic et al., 2007; Davison and Underhill, 2012). Variations in syn-rift basin-fill depend largely on the interplay between creation of accommodation space for the syn-rift deposit, climate, type and volume of sediment supply, and relative base- or sea level stand and their changes (Leeder and Gawthorpe, 1987; Surlyk, 1989; Prosser, 1993; Leeder, 1995; Ravnås

and Steel, 1997; 1998; Ravnås et al., 2000; Gawthorpe and Leeder, 2000). Syn-rift architecture of the extensional basins or passive rifted margins of continental, marine or transitional settings have been carried out by many authors (Prosser, 1993; Ravnås and Bondevik, 1997; Scholz and Contreras, 1998; Scholz et al., 1998; Matos, 2000; Ravnås et al., 2000; Larsen et al., 2010; Duff et al., 2015; Roy et al., 2015).

3.5 Methodology

Studies of basin architecture using seismic data have been developed by many workers in different areas (Remus et al., 1993; Nottvedt et al., 1995; Milia and Torrente, 1999; Mohriak et al., 2000; Ravnås et al., 2000; Wilson et al., 2003; Rohais et al., 2007; Jammes et al., 2010; Nemcok et al., 2013a; Moustafa, 2014; Selim, 2016). These workers applied basin architectural concepts to characterise their tectono-stratigraphy (Nottvedt et al., 1995; DeVault and Jeremiah, 2002), to predict when rifting started and ended (rift basin evolution) (Prosser, 1993; Nottvedt et al., 1995; DeVault and Jeremiah, 2002). Others have used basin architecture to infer the extent and nature of extension (Jackson et al., 1982; Jackson et al., 2005; 2006; Duffy et al., 2015).

The analytical and interpretive approach outlined in section 2.4 have been focussed towards the syn-rift megasequence (MS2), identified from divergent reflections in both half-grabens (Figure 3.6; Jackson et al., 1982; Gibbs, 1984; 1990; Leeder and Gawthorpe, 1987; Hubbard, 1985; 1988; Christie-Blick et al., 1991; Prosser, 1993). For a detailed analysis of the syn-rift megasequence MS2, the criteria of Williams (1993) and Driscoll et al. (1995) were followed when positioning of the post-rift unconformity.

- ❖ Strata below the post-rift unconformity often diverge towards the basin-bounding normal faults due to differential subsidence resulting from block rotation during

rifting. The overlying post-rift sedimentary succession typically has greater spatial persistence and more constant thickness reflecting regional thermal subsidence (Falvey, 1974; Meador and Austin, 1988; Meador et al., 1988; Embry and Dixon, 1990).

- ❖ The basin-bounding normal fault on the hanging-wall block is usually below the post-rift unconformity. However, the basin-bounding normal may sometimes prolong above the post-rift unconformity (Figure 3.6). The seismic character above this unconformity is often parallel to sub-parallel.
- ❖ Faulting and offset should diminish markedly across the post-rift unconformity.
- ❖ Subsidence rate often decreases across the post-rift unconformity.
- ❖ Igneous activity tends to be preferentially associated with the sedimentary succession below the post-rift unconformity (Falvey, 1974; Enachescu, 1987; 1988; Chang, 1975; Embry and Dixon, 1990).

The base of the wedge geometry of the syn-rift megasequence is marked by onlap of the divergent reflections on to parallel or chaotic reflections below the wedge geometry; this onlapping surface often defines the rift onset unconformity (e.g. Falvey 1974; Williams et al., 1993; Driscoll et al., 1995). The syn-rift megasequence was also analysed internally for reflection configurations that help define lower order seismic sequences and their bounding unconformities. The identification of seismic sequences in the syn-rift megasequence (MS2) followed the methodology of Vail et al. (1977); Prosser et al. (1993); and Gawthorpe and Leeder (2000).

Data limitation is emphasised on applying Prosser (1993) because of the relatively low resolution that characterised the syn-rift megasequence (MS2) offshore Benin Basin.

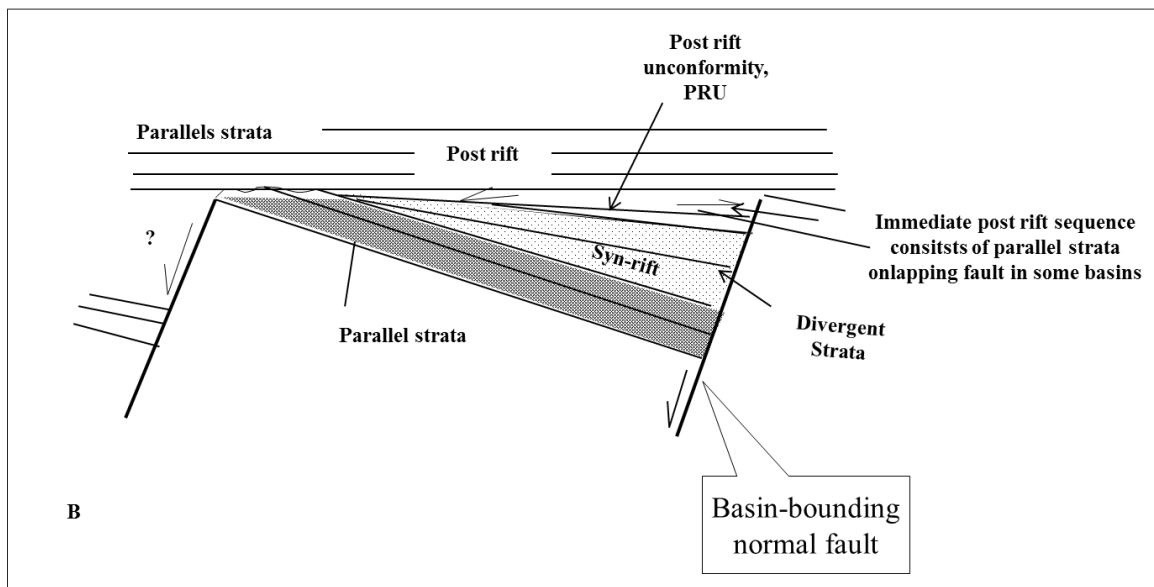
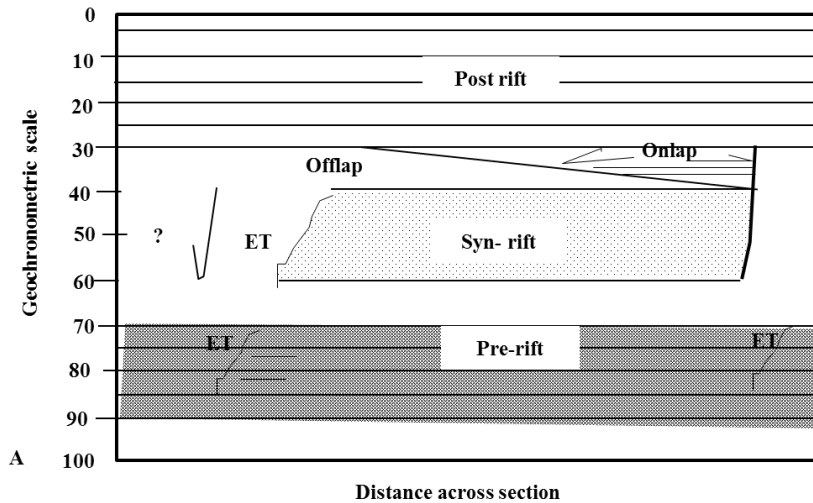


Figure 3.6: Line diagram showing the different configurations of pre-rift, syn-rift and post-rift strata in both lateral (A) and cross-section (B) views. ET = erosional truncation; PRU: post-rift unconformity. Modified after Williams (1993).

3.5.1 Structural analysis

Because of the correlation problems outlined in section 2.11, structures in both the northern and the southern half-grabens were independently analysed and later correlated to establish if they were equivalent or linked. The basin-bounding normal faults of the two half-grabens were analysed for their fault patterns to predict the mode of extension (orthogonal or oblique) for the offshore Benin Basin. The structural analysis also included measuring the apparent

dips and directions of dips for basin-bounding normal faults; this will be used to complement the mode of the extension. The structural styles of the basin will be determined using both major (basin-bounding normal) and minor (small normal) basement faults. These will be used to predict the direction of rift propagation for the two half-grabens. Following Gawthorpe and Leeder (2000), fault growth analysis was also carried out in order to predict how the basin-bounding normal faults evolved through fault interaction and linkage of many small normal faults (e.g. Ferrill et al., 2012; Watterson, 1986; Davidson, 1987; Gawthorpe and Leeder, 2000; Claringbould et al., 2015). Two-way time (TWT) isochron maps were plotted for both the rift-onset unconformity and rift-climax.

The analysis of fault orientations is an important in structural geology because it often leads to prediction of the movement direction of causative faults (Spencer, 1969; Reches, 1978; Aydin and Reches, 1982; Dewey, 1982; 1989; 1998; Park, 1997). The study includes dynamic analysis which is concerned with the reconstruction of the orientation of the stress field that generated tectonic faults in the study area. By convention, three principal stresses are known: maximum (σ_1), intermediate (σ_2), and minimum (σ_3) principal stresses (Figure 3.7A). Three principal stresses often define stress ellipsoid (Figure 3.7B). All the principal stresses may be compressive especially when the crust is being extended, such as in rift valleys (Park, 1997; Rowland et al., 2007). The assumption of Anderson (1942) that one of the principal stresses must be vertical explains the three classes of faults: normal faults σ_1 is vertical; strike-slip σ_2 is vertical; and thrust fault σ_3 is vertical (Figure 3.8).

3.6 Detailed syn-rift stratigraphy and structure of the offshore Benin Basin

The stratigraphic framework established for the offshore Benin Basin (section 2.6.2) shows that the syn-rift phase consists of three superimposed successions, characterised by divergent reflection packages (from the base to the top, Figure 3.9):

- ❖ An early rift sequence S2A (Early Barremian, MSB2 - late Barremian/early Aptian, SB2B).
- ❖ A rift-climax sequence S2B (late Barremian/early Aptian, SB2B - middle Aptian, SB2C).
- ❖ A late rift sequence S2C (middle Aptian, SB2C – late Aptian, MSB3).

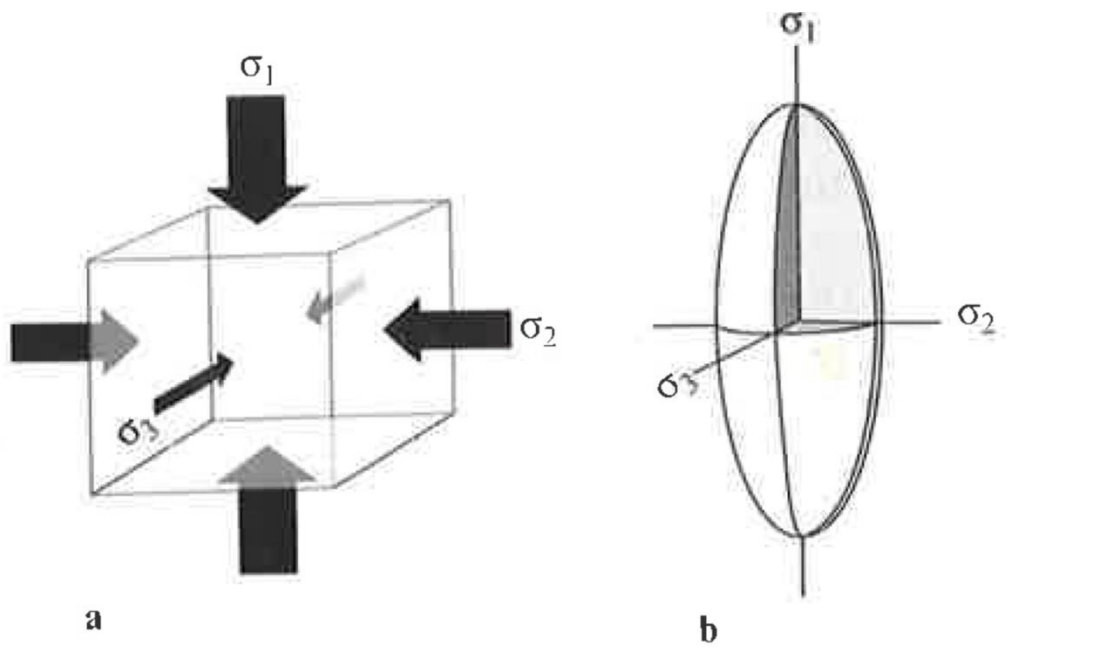


Figure 3.7: a) The three principal stresses and the three planes of zero shear stress on which they act. B) The three stress ellipsoid, defined by the three principal stresses (after Rowland et al., 2007).

The degree of divergence in seismic reflections generally increases from the early rift sequence to the late rift sequence. The implication of these variations will be tested to validate their control by block rotation during basin development in section 3.9.1 of this study.

3.6.1 Early rift sequence S2A (Early Barremian, MSB2 - late Barremian/early Aptian, SB2B)

This sequence is the basal unit of the syn-rift megasequence (MS2) comprising divergent, high amplitude reflectors. Its seismic reflections are continuous to non-continuous. An overall thickness of about 260 ms TWT to 750 ms TWT was deposited during early rift (Table 3.1) stage. In the northern half-graben, these seismic reflections are folded probably due to the contractional deformation that locally affected it (see Chapter 4 for post-rift contractional deformation). The early syn-rift sequence (S2A) overlies chaotic to transparent reflectors interpreted as the Precambrian basement (MS1) in both half-grabens (Figure 3.9).

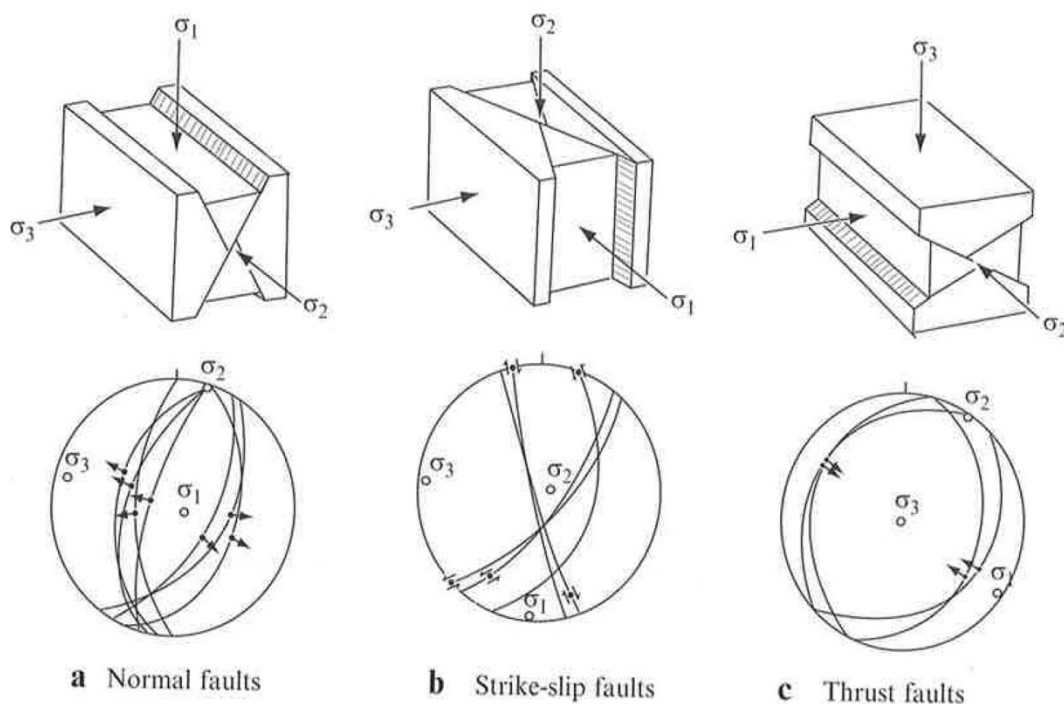


Figure 3.8: Block diagram and equal area plots of the three classes of faults predicted by Anderson (1942). The equal area stereograms show typical fault and slickenside orientation data for each set of faults within each of Anderson's (1942) classes. For normal faults (a) and thrust faults (c), the arrows on the great circles of the stereograms point in the direction of the hanging-wall motion. For strike-slip faults, the arrows on the great circles indicate the sense of shear (after Rowland et al., 2007).

Table 3.1: Thickness of the syn-rift megasequence MS2, and its sequences S2A, S2B, and S2C, in both the northern and the southern half-grabens

Northern half-graben					Southern half-graben			
Seismic line no	S2A (ms TWT)	S2B (ms TWT)	S2C (ms TWT)	MS2 (ms TWT)	S2A (ms TWT)	S2B (ms TWT)	S2C (ms TWT)	MS2 (ms TWT)
N07	750	430	440	1620	630	508	430	1568
4394	590	545	530	1665	346	290	365	1001
4420	718	371	265	1354	260	130	210	600

Divergence of seismic reflectors is better developed in the overlying sequences (S2B and S2C) than in this sequence (S2A). The early rift sequence (S2A) shows minor thickening of the seismic reflections towards basin-bounding normal faults (F1 and F2) in both the northern and southern half-grabens (Figures 3.9 and 3.11). This, according to Prosser (1993), Råvnas et al. (1997), Gawthorpe and Leeder (2000), Withjack et al. (2002); Schlische and Withjack et al. (2009), and Pereira and Alves (2011), this character suggests that less significant and widespread subsidence possibly occurred during its deposition (early Barremian, MSB2 to late Barremian/early Aptian, SB2B).

The early rift sequence (S2A) is also characterised by an array of small-displacement normal faults in both the northern and southern half-grabens (Figure 3.11). These small normal faults are closely-linked. They are spaced 2 to 4 km; occasionally, they are less than 2 km apart in both northern and southern half-grabens. The length of these small normal faults varies between 2 and 5 km (Figures 3.10 and 3.11).

The limited divergence of seismic reflections in the early rift sequence (S2A) may imply:

- ❖ Either very rapid deposition so the degree of fault rotation between each phase of deposition was very moderate;
- ❖ It may also mean that there was less differential subsidence in the early syn-rift stage because the main basin-bounding faults were not taking up all the displacement. Hence sedimentation is deposited in the associated small normal faults.
- ❖ Both conditions may also lead to the moderate divergence in seismic reflections.

The base of the early rift sequence was not drilled but its top has been dated as early Aptian (Figure 3.11). It comprises a fining upward sequence of siltstone, fine sand and mudstone (Figure 3.12). The early syn-rift sequence (S2A) correlates with continental deposits grouped as part of the Ise Formation by Brownfield and Charpentier (2006), and Kaki et al. (2012) (Figure 1.11). Brownfield and Charpentier (2006) reported the age of the Ise Formation as ranging from Upper Jurassic to Neocomian. The age assigned to the syn-rift phase by Brownfield and Charpentier (2006) implies that rifting probably started relatively early in this basin. The Upper Jurassic to Neocomian age is difficult to justify. Despite these uncertainties, an early Barremian age will be used in this dissertation because continental rifting is thought to have propagated northwards from the southern South Atlantic toward the Equatorial Atlantic in the Barremian (e.g. Moulin et al., 2010).

This correlates with the continued continental rifting in the Pontiguar Basin (NE Brazil), as well as in parts of the intraplate basins in West and Central Africa (Binks and Fairhead, 1992; Guiraud and Maurin, 1992; Guiraud et al., 1992; Moulin et al., 2010; Fairhead et al., 2013). Its top sequence boundary (Late Barremian/Early Aptian) correlates with the end and onset of syn-rift phases in most of the West and Central African intracontinental basins (e.g. Guiraud et al., 1992; Moulin et al., 2010; Fairhead et al., 2013).

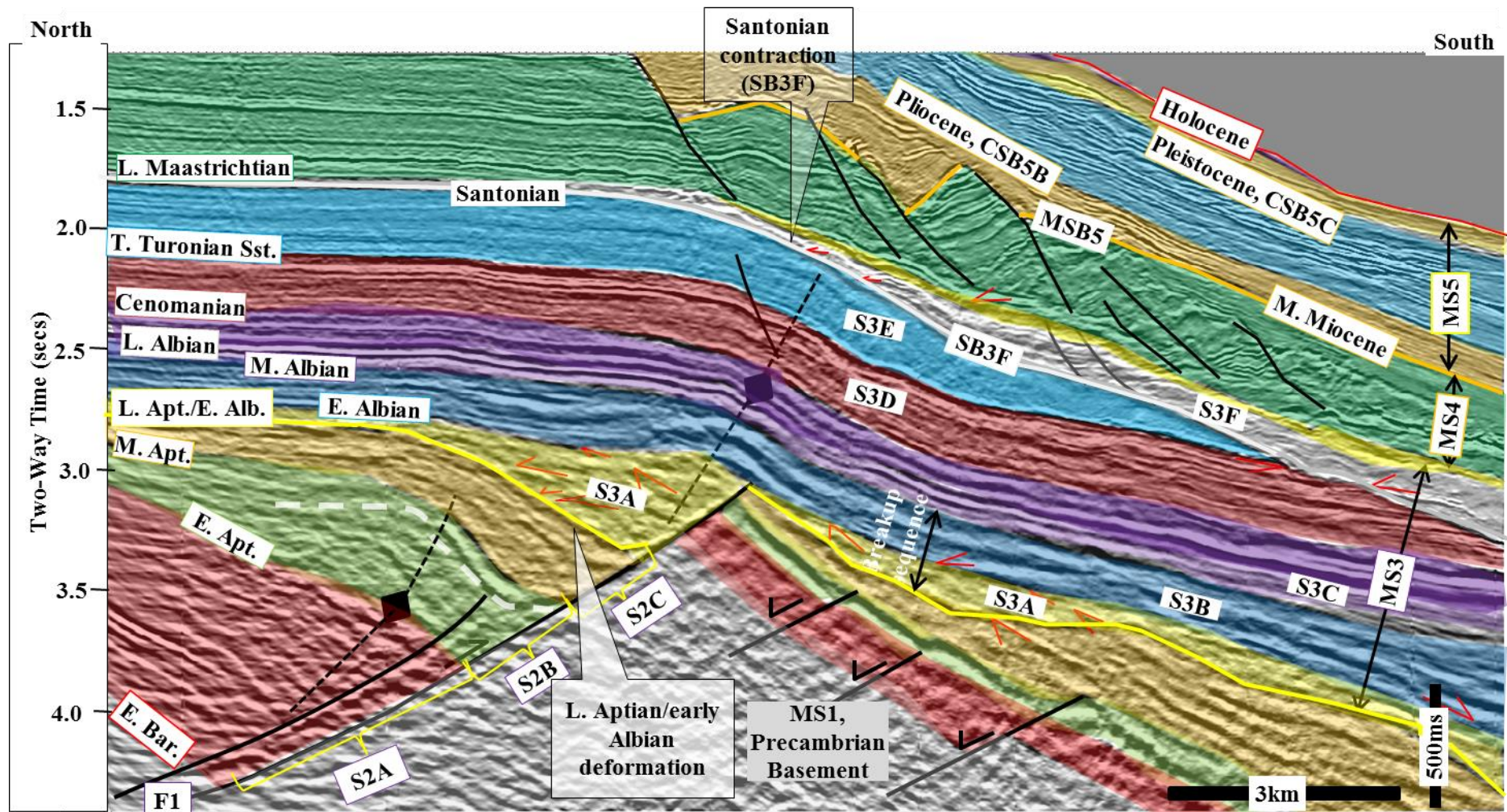


Figure 3.9: 3D seismic section (crossline 3940) showing syn-rift megasequence MS2 (S2A, S2B, and S2C) comprising thickening of strata towards the main basin-bounding normal fault (F1) in spite of the late Aptian/early deformation in the northern half-graben. See Figure 2.17 for the location of the seismic section.

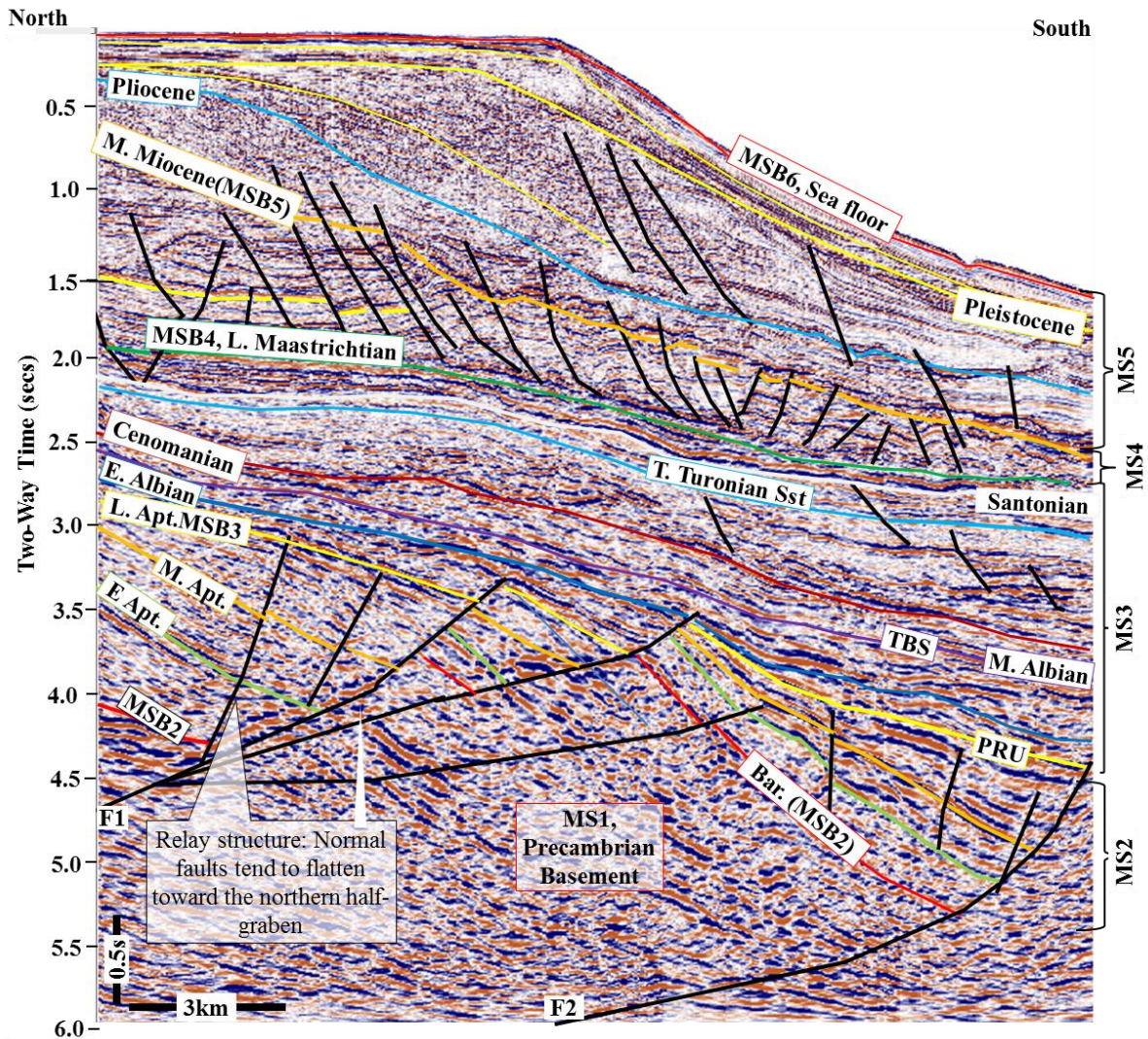


Figure 3.10: Relay structure with synthetic normal faults and its stratigraphy. See Figure 3.14 for the seismic section location.

3.6.2 Rift-climax sequence S2B (late Barremian/early Aptian - middle Aptian)

The rift-climax sequence (S2B) has an overall wedge pattern comprising divergent reflections which onlapping onto the early rift sequence (S2A) (Figure 3.13). It has moderate amplitude, continuous to non-continuous, divergent seismic reflections. An overall thickness of about 1.2 to 1.4 seconds TWT was deposited during the sequence (S2B). The thick sediment infilling of the half-grabens during the rift-climax stage does only suggest more accommodation generation but it also implies deposition in deeper environments than the early rift stage (Figure 3.13).

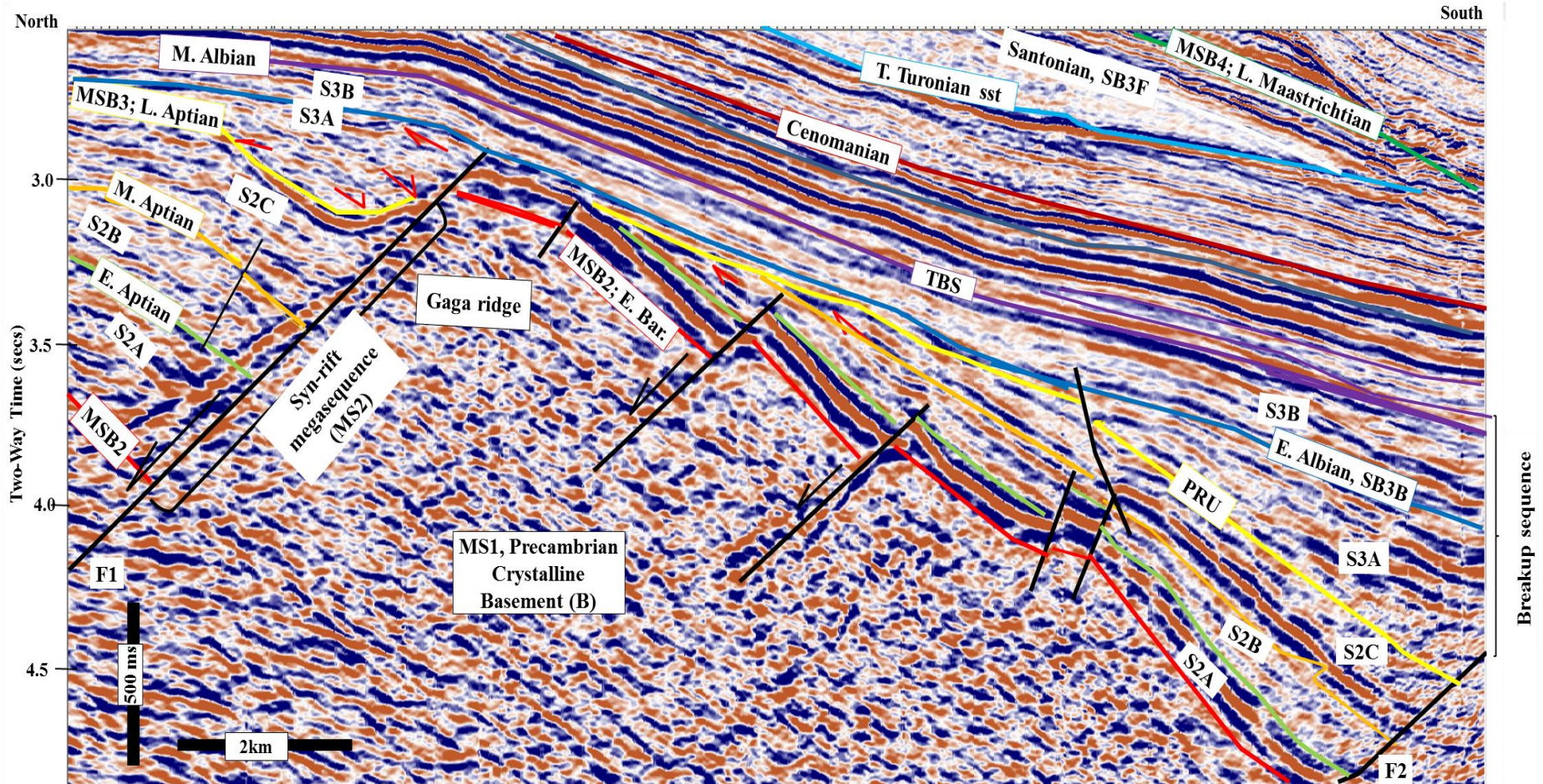


Figure 3.11: Crossline 4328 showing a syn-rift megasequence (MS2) comprising the three sequences S2A, S2B, and S2C. Note the reflection divergence that characterises the syn-rift megasequence. The post-rift unconformity (PRU), MSB3, shows onlap, erosional truncation, and offlap (red arrows). TBS = Top of breakup sequence. See Figure 3.14 for the location of the seismic section.

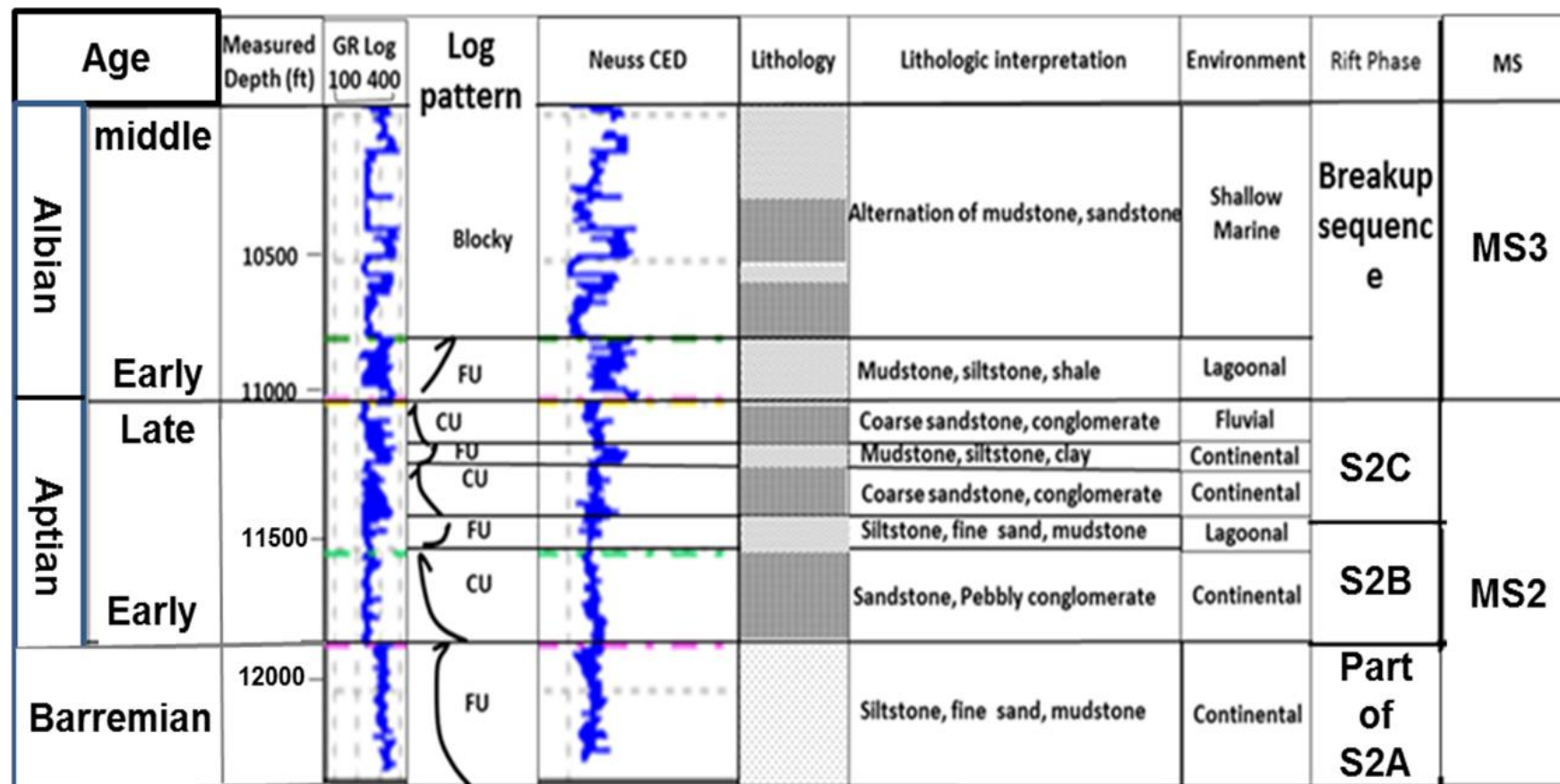


Figure 3.12: Lithologic interpretation of the syn-rift megasequence, MS2 (S2A+S2B+S2C) Barremian to late Aptian and the overlying breakup sequence (early to middle Albian, part of the Cretaceous post-rift megasequence, MS3). The syn-rift megasequence is composed of both fining- (FU) and coarsening-upward (CU) patterns. Whereas the breakup sequence is made up of the cylindrical pattern.

The relay and transfer structures were already active in the northern half-graben during the rift-climax stage (Figures 3.10 and 3.14). See section 4.7.3 for their discussion. The seismic reflections onlap one another such that they aggrade upward; that is, they show increasing aggradation (e.g. Prosser, 1993). This aggrading unit is the bottom-most unit of this sequence. These divergent reflections also show increasing lateral thickness towards the basin-bounding normal fault (e.g. F2). They, however, thin out towards the fault tip (Figure 3.13). The rift-climax sequence (S2B) is made up of fewer small normal faults. The main basin-bounding normal faults in both half-grabens have greater lengths than during the early rift sequence (S2A). This may probably be due to fault interaction and linkage among small normal faults and the main basin-bounding normal fault (Gawthorpe and Leeder, 2000).

3.6.3 Late rift sequence, S2C, (middle Aptian, SB2C – late Aptian, MSB3)

The late rift sequence (S2C) consists of continuous to non-continuous, moderate to high amplitude divergent reflections. The late rift sequence (S2C) may account for about 210 ms TWT to 530 ms TWT of strata in the study area (Table 3.1). Its reflections also thicken toward the basin-bounding normal fault. These reflections onlap the basin-bounding normal fault and the underlying rift-climax sequence (Figure 3.13). Its seismic reflections also aggrade as they progressively onlap one another. Seismic reflections in this sequence thicken towards the basin-bounding normal fault. Rift-related strata of middle Aptian to Late Aptian age (S2C) are represented in well B-04. The strata interpreted on GR logs include shale and sandstone (Figure 3.12) with coarsening- to fining-upwards facies (Figure 3.12). These suggest a gradation from fluvial to lagoon environments. Sequence S2C generally comprises the minimal or absence of small normal faults. However, the available accommodation space is being provided by the basin-bounding normal faults in both half-grabens (Figure 3.13).

Table 3.2: Summary of the principal features of syn-rift megasequence MS2 in the offshore Benin Basin

Sequence	Probable Age	Internal character	Lithology
S2C (late rift sequence)	Middle Aptian – late Aptian	Divergent reflections that show growth towards the basin-bounding normal fault. These reflections were truncated by the post-rift unconformity (PRU) (late Aptian).	Sandstone, siltstone, clay, mudstone, coarsening-, fining-upward; fluvial.
S2B (rift-climax sequence)	Early Aptian – middle Aptian	Divergent reflections that thicken towards the basin-bounding normal fault. widespread growth	Sandstone, siltstone, mudstone, pebbly conglomerate; coarsening-upward; lagoon.
S2A (early-rift sequence)	Barremian	Divergent reflections that thicken towards the basin-bounding normal fault; less widespread. Reflections onlap the crystalline basement rock and forms the rift-onset unconformity (early Barremian; MSB2)	Mudstone, fine sands, siltstone; fining-upward sequence; though base not reach by well.

The syn-rift megasequence MS2 is truncated by a prominent unconformity referred to as the post-rift unconformity (PRU) in this study. All the sequences of the syn-rift megasequence (MS2) are folded in the northern half-graben. Chapter 4 of this study describes this event and another later shortening phase that possibly affected the study area.

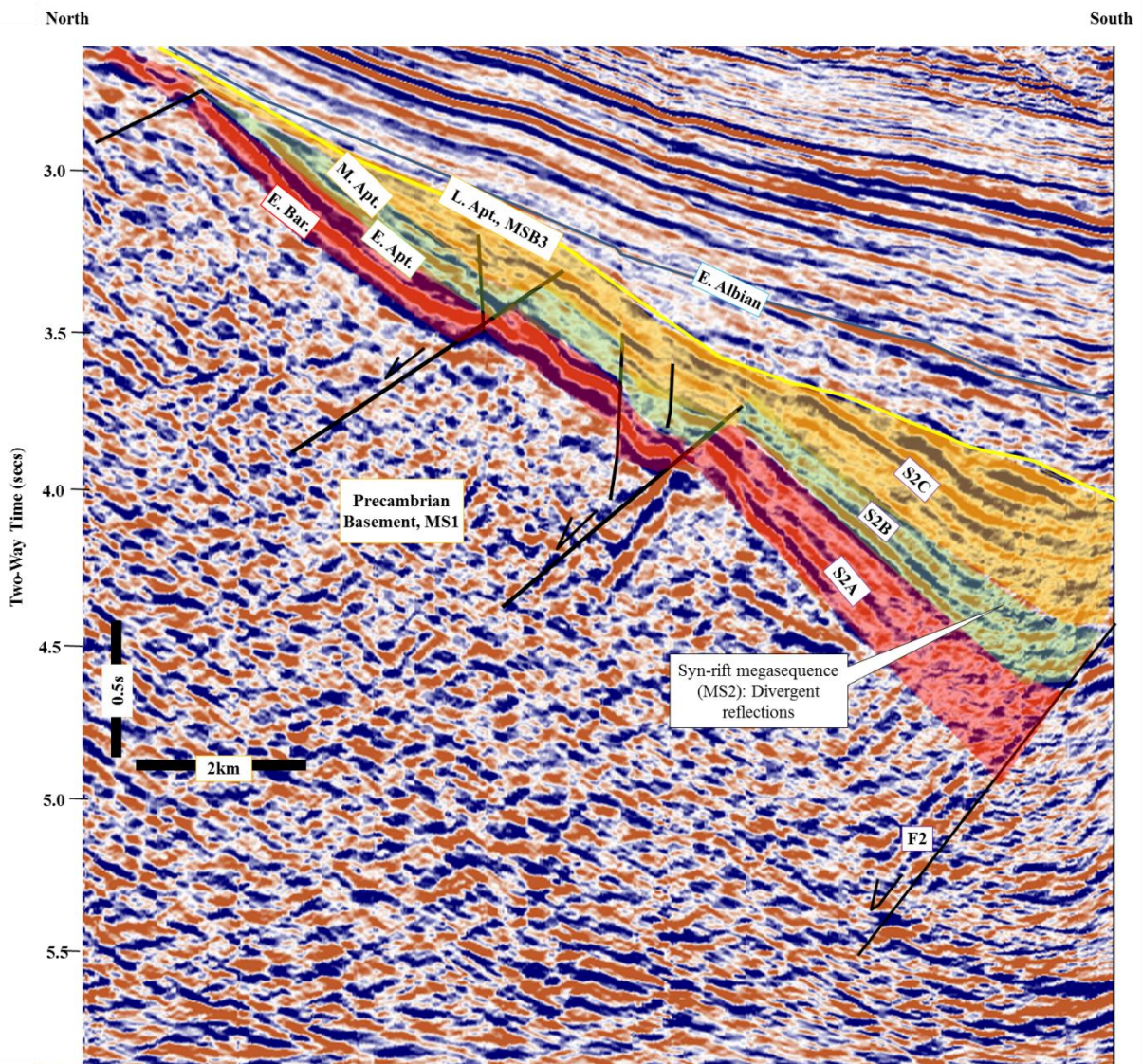


Figure 3.13: Vertical profile (crossline 4640) showing the southern half-graben and its characteristic wedge geometry consisting of three sequences (S2A, S2B, and S2C) which have been classified as the syn-rift megasequence (MS2). S2A = early rift sequence; S2B = rift-climax sequence, and S2C = late rift sequence. Red arrows indicate the reflection terminations. Figure 3.14 shows the location of seismic section.

3.7 Analysis of the basin-bounding normal faults (F1 and F2) and their orientations

The interpretation of seismic data has been applied by many authors in the determination of the strike of tectonic structures (e.g. faults, and folds). Faults and folds can be mapped on seismic data to determine their orientation, and time slices and coherency cubes can be imaged on 3D data to help determining the orientation of key structural features. The vertical seismic sections show that these faults are basement-involved normal faults as their hanging-wall blocks appear to have moved downwards relatively to the footwall blocks. The fault geometry of the two main normal faults was observed mainly on the dip sections of the 2D profiles, and crosslines of the 3D seismic data, suggesting that the basin-bounding normal faults are dip-slip faults. The fault geometry of the basin-bounding normal faults (F1 and F2) may have been formed with σ_1 acting vertically downwards while the intermediate and minimum stresses are horizontal (Figure 3.8A). This arrangement probably led to the resulted deformation that was accommodated as horizontal extension (Figure 3.8A). Cross-sections obtained perpendicular to the passive margin in the study area (e.g. Figures 2.3 and 3.2) demonstrate that the deformation was extensional as they have generated large displacements that have been filled by syn-tectonic sediments in the Barremian-Aptian. It can be suggested that the forces that caused the relative motion between African and South American Plates might have been directed such that the two plates were moving away from each other. This would result in crustal extension and subsequent creation of a new oceanic crust at their common spreading centre (e.g. Park, 1997).

The structural analysis of the seismic data indicates that both major and minor normal faults prevailed during the Barremian-Aptian rifting episode. The two-way time (TWT) isochron map of the rift-onset unconformity (early Barremian, MSB2; Figure 3.10) records a

combination of both basin-bounding normal faults (F1 and F2) and some small, synthetic normal faults (Figure 3.8). These basin-bounding normal faults (F1 and F2) controlled subsidence in the early Barremian to late Aptian because they are the only major normal faults that remained active throughout the rifting episode (Figure 3.8). Detailed fault analysis suggests that both the displacement and length of these small normal faults increase with depth.

The basin-bounding normal faults indicate a displacement of as much as 2540 ms TWT (Table 3.1), and bound half-graben basins containing divergent reflections characteristic of the syn-rift megasequence MS2 (Figure 3.8; see section 3.7 for detail of the syn-rift megasequence, MS2). The fault geometry of the northern and southern half-grabens shows that basin-bounding faults generate subsidence in their hanging-walls (i.e. the half-graben basin) which provides accommodation space where sediments accumulated. The accumulated sediment is often proportional to the displacement of the hanging-wall (Table 3.2). The lengths of the basin-bounding normal faults range from 20 to about 24 km, while the maximum displacement varies from 1800 ms TWT to 2540 ms TWT (Table 3.2).

The basin-bounding normal faults (F1 and F2) are generally low-angle dip faults (30-50°). The low-angle dips of these basin-bounding normal faults do not, however, imply that they evolved as low-angle normal detachment faults. The relatively high fault displacements associated with these low-angle normal faults may suggest that these basin-bounding normal faults could have started as more steeply-dipping angle normal faults. The tectonic evolution of the basin-bounding normal faults of the northern and southern half-grabens may not be related to fault detachment hence the fault detachment mechanism may be applicable to the offshore Benin Basin.

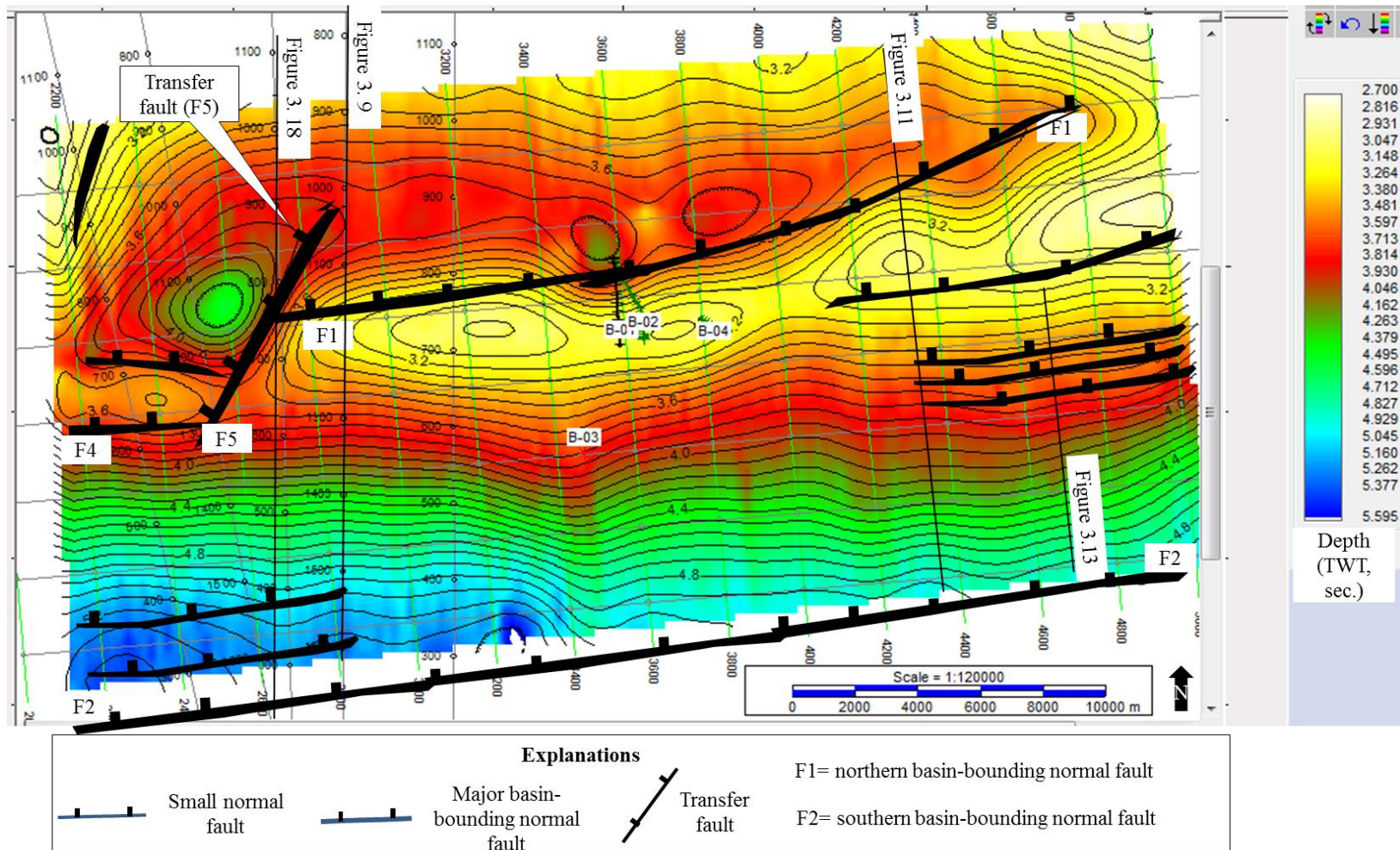


Figure 3.14: TWT structural map of the base of the rift-climax stage (early Aptian) showing the strike of the main structures (fault and anticline) as E-W to ENE-WSW. The basin-bounding normal fault (F2) of the southern half-graben was not fully covered by the 3D survey. The southern half-graben, however, maintains a similar strike to the northern half-graben.

Table 3.3: Measurements of the maximum displacements of basin-bounding normal faults (F1 and F2) and their corresponding lengths, in both the northern and southern half-grabens.

Seismic line no	Northern half-graben: maximum displacement on F1 (ms TWT)	Northern half-graben: length of fault, F1 (in km)	Southern half-graben: maximum displacement on F2 (ms TWT)	Southern half-graben: length of fault, F2 (in km)
N06	2200	20.00	2000	15.50
N07	2120	20.60	2150	18.20
N08	2100	19.50	1950/	15.20
N09	2540	24.60	1800	14.70
N10	2200	19.70	2300	18.60

The shallowness of these faults must be due to rotation of the fault blocks during the syn-rift and post-rift phases of basin development. For example, when flattening the seismic data on the top of the breakup sequence (TBS), the original fault geometries of the two half-grabens were restored (Figure 3.15).

The strike of the synthetic small normal faults are similar to those of the basin-bounding normal faults, suggesting that they are compatible and therefore could have experienced similar deformational events during their evolution.

Although the basin-bounding normal fault (F2) of the southern half-graben appears listric (i.e. having a characteristic steeper angle at shallow depth and flattens out at depth; Figure 3.13), it is thought that this is a seismic artefact resulting from viewing the fault in time sections. The difference in the fault planes of the northern and southern half-graben may probably be

due to differences in their rate of rotation since rate of extension was constant (Spencer, 1969; Park, 1997; Gawthorpe and Leeder, 2000). The fault geometry depicts that both basin-bounding normal faults (F1 and F2) in the two half-grabens are planar faults. It, therefore, implies that the basin-bounding normal fault (F2) of the southern half-graben might have rotated more than the basin-bounding normal fault (F1) of the northern half-graben (Figure 3.13).

3.8 Structural styles in the offshore Benin Basin

The basin-bounding normal faults (F1 and F2) in both half-grabens are basement-involved suggesting a tectonic origin. Both faults dip at about 30° - 50° i.e. they are relatively low-angle faults compared with the average dip of normal faults, which falls in the range 65° - 70° (Fossen, 2012). The angle of dip of rift basins is often thought to undergo flattening during extension because the fault blocks are always rotating in response to increasing rates of mechanical subsidence. The angles of dip of the basin-bounding normal faults of rift basins are thus decreased after extension ceased. Flattening to the top of the breakup sequence (TBS) (Figure 3.15) show that these basin-bounding normal faults in both the northern and the southern half-grabens dip steeper than when unflattening them (Figure 3.11). The low-angle that characterised the basin-bounding normal faults (F1 and F2) in these half-grabens, therefore, suggests that they probably did not only rotate during the syn-rift phase but they probably underwent further rotation during the post-rift phase. The E-W to ENE-WSW striking offshore Benin Basin (Figure 3.14) depicts a probable evolution where the maximum principal stress is directed N-S to NNE-SSW. Rift location was most probably controlled by a lithospheric scale Precambrian weakness during the early Barremian (MSB2) (Guiraud et al., 1992).

In assessing the regional tectonic significance of the basin-bounding normal faults (F1 and F2) of the two half-grabens, their strikes are therefore critical. Their strikes may be related to their kinematic extensional directions (Park, 1997; Khalil and McClay, 2002; Condie et al., 2003; Kinabo et al., 2007). The E-W to ENE-WSW strike of the basin-bounding normal faults (F1 and F2) suggests that the offshore Benin Basin might have formed due to orthogonal extension. The directions of the strikes and dips of these basin-bounding normal faults (F1 and F2) are typical of dip-slip normal faults.

The E-W to ENE - WSW strike of the two basin-bounding normal faults (F1 and F2) is consistent throughout the Barremian to Aptian rifting episode (Figure 3.14). This suggests that the maximum principal stress had probably remained in a vertical direction (Figure 3.8A) in the Barremian-Aptian time. The implication is that the stress field direction did not change throughout the Barremian-Aptian rifting episode in the offshore Benin Basin.

The northward dipping of these basin-bounding normal faults (F1 and F2) in both half-grabens also suggests that the maximum principal stress is vertical and deformation was accommodated as horizontal extension (i.e. perpendicular to the E-W or ENE-WSW strike of the offshore Benin Basin). The validity of the basement reactivation for the tectonic evolution of the offshore Benin Basin will be tested when the geodynamics of the study area will be discussed in Chapter 6.

3.9 Benin Basin: an extensional or a transform basin?

The fault geometry associated with the basin-bounding normal faults (F1 and F2) favour continental rifting by orthogonal extension over those of the transform faulting that characterises the Equatorial Atlantic margin at present, and after syn-rift (e.g. Moulin et al., 2010; Heine and Brune, 2014; Basile, 2016). The following reasons can be presented for the orthogonal extension:

- ❖ The basin-bounding normal faults (F1 and F2) are basement-involved faults that are characterised by large displacements (Figure 3.9).
- ❖ The basin-bounding normal faults affected most parts of the study area, implying that they may have a regional extent.
- ❖ The basin-bounding normal faults (F1 and F2) propagate above the post-rift unconformity (late Aptian, MSB3). However, these major basin-bounding normal faults still preserve their net extension suggesting that the half-grabens are similar to the ‘Atlantic-type’ margin which is typified by orthogonal extension (e.g. Falvey, 1974; Driscoll et al., 1995; Ravsnas and Steel, 1998).
- ❖ The orientation of the two basin-bounding normal faults and associated structures follows E-W to ENE-WSW directions in the Barremian-Aptian rifting episode (Figure 3.14).
- ❖ In spite of the low-angle of the basin-bounding normal faults (F1 and F2), they are characterised by well-developed wedge geometry in adjacent strata.
- ❖ The two half-grabens in the study area do not record any evidence of transform tectonism during their evolution. Strike-slip faulting is often typified by a high-angle normal fault and associated contractional and extensional structures (Park, 1997; Janecke et al., 1998; Condie et al., 2003; Fossen, 2012). The seismic data show apparent lack of flower structures or other structures associated with strike-slip faulting (Matos, 2000). The tectonic evolution of the offshore Benin Basin may not, therefore, be related to transpression.
- ❖ The seismic data record well-preserved wedge geometry comprising divergent reflections interpreted as a syn-tectonic sequence of Barremian-Aptian age. On the

contrary, the wedge geometry that represents the continental rifting prior to syn-transform phase is often masked by transform faulting (e.g. Matos, 2000). This often leads to difficulty in its identification, or to its total absence. This study, however, reveals a wedge geometry that overlies the Precambrian crystalline basement rock and is truncated by the post-rift unconformity (Figure 3.13).

3.10 Discussion

3.10.1 Evolution of the offshore Benin Basin

Rift-initiation stage (Barremian)

The creation of accommodation space for syn-tectonic sedimentation in rift basins is largely dependent on the displacement history of associated normal faults (Leeder and Gawthorpe, 1987; Schlische, 1991; Gawthorpe et al., 1994; Dawers et al., 2000). Arrays of small isolated normal faults associated with the early rift sequence (S2A) are thought to form during the rift-initiation stage (Leeder and Gawthorpe, 1987; De Polo et al., 1991; Prosser, 1993; Gawthorpe et al. 1997; Cowie, 1998; Gawthorpe and Leeder, 2000; Cowie et al., 2005). The small faults probably started as fractures at the inception of rifting (Figure 3.16A).

The early rift sequence (S2A) is characterised by limited deposition, probably due to the small faults with less accommodation space (Figure 3.17B). From the fault geometry registered on the seismic data, the early rift sequence (S2A) is thought to be deposited as a product of the rift-initiation stage in the Barremian (Figures 3.16A and 3.17B). The early rift sequence (S2A) may, therefore, be thought to represent the onset of continental rifting, where normal fault-controlled depocentres accommodate deposits resulting possibly from the erosion of the Precambrian basement rocks (Brownfield and Charpentier, 2006; Kaki et al., 2012).

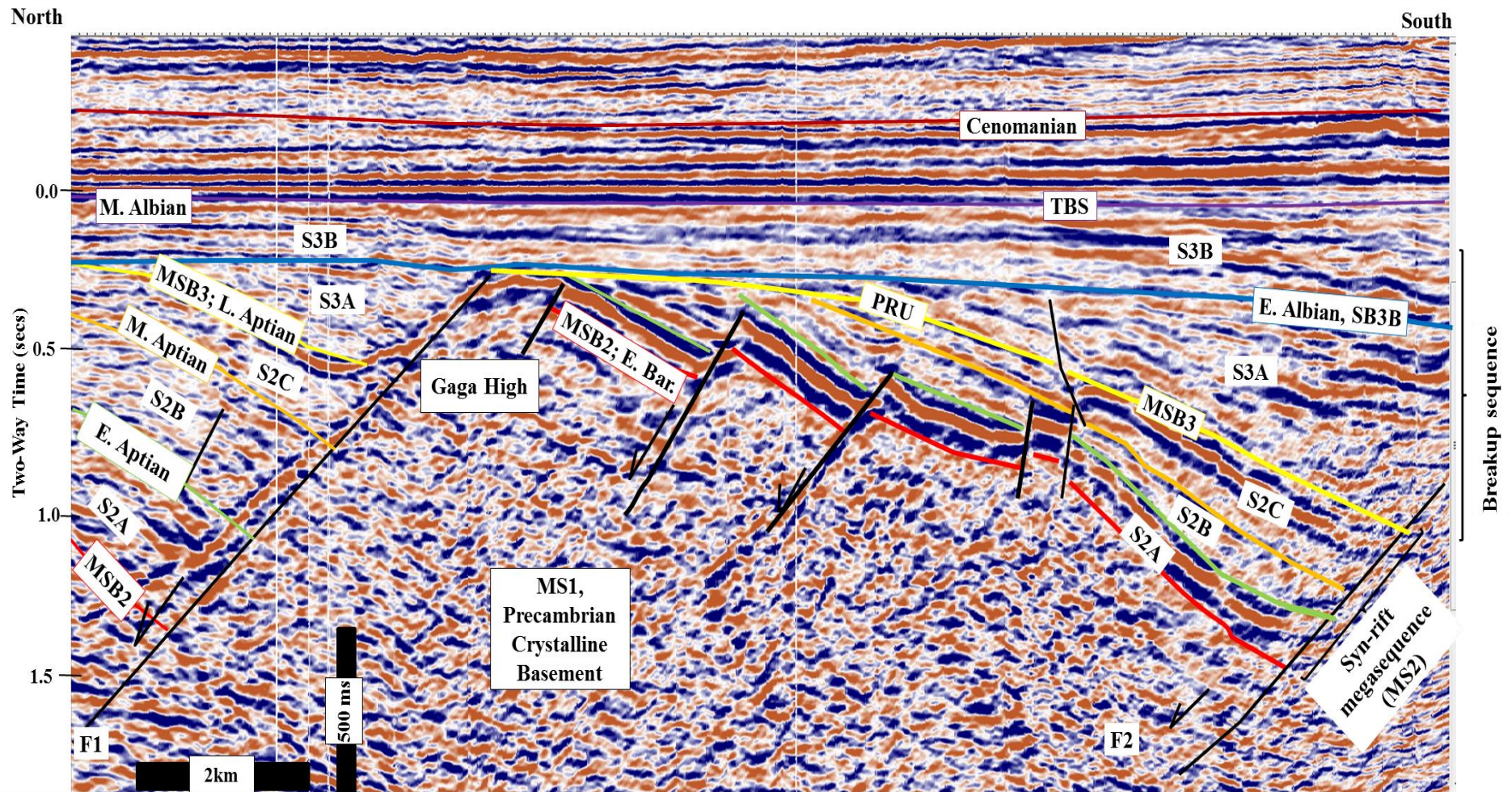


Figure 3.15: Seismic section (crossline 4328) interpreted and flattened along the top of the breakup sequence (TSB). Note that the two half-grabens retained their wedge geometries below MSB3 (i.e. the post-rift unconformity, PRU). The basin-bounding normal faults (F1 and F2 appear steeper after the flattening is applied, see also on Figure 3.11. MSB2= rift onset. See Figure 3.14 for the location of the seismic section.

The onlapping of the divergent reflections of the early rift sequence on the Precambrian basement rocks suggests an onset of rifting in the offshore Benin Basin in the early Barremian (MSB2).

Rift-climax stage (Early Aptian to middle Aptian)

Widespread growth associated with the rift-climax sequence (S2B) suggests its deposition may be related to when continental rifting was at its peak. The widespread subsidence associated with the rift-climax sequence (S2B) can be explained using two models:

- ❖ Fault-linkage and interaction model (e.g. Gawthorpe and Leeder, 2000)
- ❖ Block rotation model (e.g. Ravnås and Steel, 1998)

Fault-linkage and interaction model (e.g. Gawthorpe and Leeder, 2000)

The main consequence of the fault linkage is the creation of a large-displacement normal fault (Figure 3.16B and 3.17D). Such fault linkage may be due to stress feedback between the fault segments of the small faults that influence growth and deformation in the fault array, leading to localisation of deformation along the major basin-bounding normal fault zone (Gawthorpe and Leeder, 2000). The other sequences (S2B and S2C) are deposited during the rift climax stage (Figures 3.17C and D). According to Gawthorpe and Leeder (2000), the late rift sequence (S2C) was probably deposited due to possible interaction/linkage of the remaining (small) normal faults that were active during the sedimentation of the immediate underlying sequence S2B. (Figure 3.17D). Fault often grows at its fault tip and may interact with an adjacent one to form bigger fault (McLeod et al., 2000). Stress feedback between the segments (e.g. Fii, Fiii, and Fiv in the south) influences growth and deformation in the fault array begins to become localised along major fault zone (Fi, Fii, Fiii, Fiv). Similar fault linkage also occurred synchronously in the north (Figure 3.16B).

The death and/or the linkage of these small normal faults may lead to deformation becoming localised along the major basin-bounding normal fault zones (F1 and F2; Figure 3.16C). The increase in the fault displacement of the basin-bounding normal fault in the Aptian suggests that the basin-bounding normal faults (e.g. F2 of the southern half-graben) probably grew, while small normal faults ceased to grow (Figures 3.16 and 3.17). This probably gave rise to the two main half-graben depocentres in the northern and southern parts of the study area. These depocentres are named northern and southern half-grabens in this study. The fault interaction/linkage of the arrays of small-displacement normal faults characteristic of the early rift sequence (S2A), leading to through fault zone stage in the S2C (e.g. Leeder, 1995; Gawthorpe and Leeder, 2000), may account for the large displacement and length of the basin-bounding normal faults (F1 and F2) of the study area (Table 3.2).

Block rotation model (e.g. Ravnås and Steel, 1998)

The rift-climax sequence (S2B) shows greater variations in lateral thicknesses than in the early rift sequence (S2A). These variations suggest a probable greater widespread subsidence than it is in the early rift phase (Figure 3.9). The divergent reflections of sequence S2B suggest that significant block rotation may be involved (e.g. Ravnås and Steel, 1998). This implies that subsidence rate in the study area may have probably increased more than at the S2A sequence. The block rotation involved in the sedimentation of the syn-rift megasequence (MS2) may account for the general thick syn-rift sequences (e.g. sequences S2B and S2C) associated with it. These depict a change from the rift-initiation phase to the fault interaction and linkage zone of Gawthorpe and Leeder (2000) (Figure 3.16).

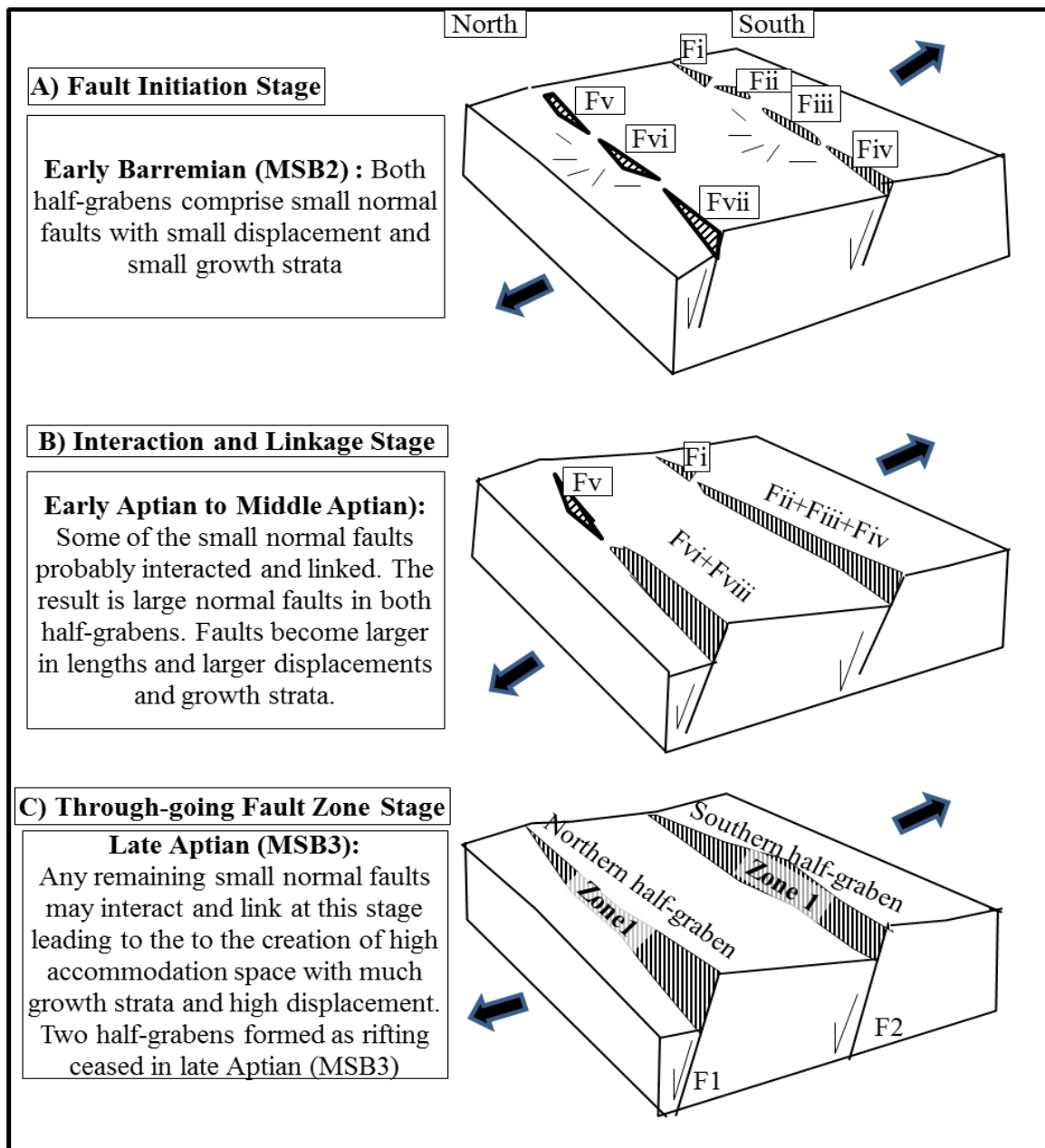


Figure 3.16: Gawthorpe and Leeder (2000) models modified for the study area. Schematic diagram showing that the 3D evolution of normal fault arrays can enhance the formation of a major basin-bounding normal fault. A) Fault initiation stage in the study area was characterised by a large number of small-displacement normal fault segments (Fi-Fvii) in the Barremian. B) Fault interaction and linkage stage; at this stage small-displacement normal faults (Fii, Fiii, and Fiv) were linked together C) Through-going fault zone stage, where deformation is localised along major border fault zone 1; a final linkage to the remaining small faults give rise to the evolution of two basin-bounding normal faults (F1 and F2).

The syn-rift wedge reflections overlying the transparent reflections of the pre-rift megasequence (MS1), interpreted as crystalline basement rock, shows that the study area possibly underwent rifting in the Barremian-Aptian.

The increasing dip of the divergent reflections with depth depicts that continental extension progressively propagated from early rift through rift-climax stages (Figures 3.17B and 3.17C). The thickening of the seismic reflections towards basin-bounding normal faults is best developed during the rift-climax stage (Figure 3.9). It was initially thought that such thickening may be due to increasing extension rates (e.g. Prosser, 1993) but subsequent studies (Gawthorpe et al., 1997; Gupta et al., 1998; 1999; Gawthorpe and Leader, 2000) suggest that extension rates are constant. These later authors thought that faults become linked so subsidence rates and rotation around basin-bounding faults increase (Figure 3.18).

On the basis of the northward dipping of both basin-bounding normal faults (F1 and F2), their fault geometry and styles, the two synchronous northern and southern half-grabens suggest that sedimentation was probably accumulating in a landward direction (i.e. northwards) during continental extension in the study area. The fault geometry of both the small faults and major normal faults depict a northward propagation of rifting (Figure 3.18). Each of these half-grabens may, therefore, be regarded as discrete sub-basins implying that the offshore Benin Basin developed as a series of sub-basins northwards. Delteil et al. (1974) postulated that the offshore Benin Basin is probably made up of series of sub-basins.

Chapter 6 discusses the control of pre-existing basement grain for the development of orthogonal extension and its implication for geodynamics of the Equatorial Atlantic margin in the Barremian-Aptian.

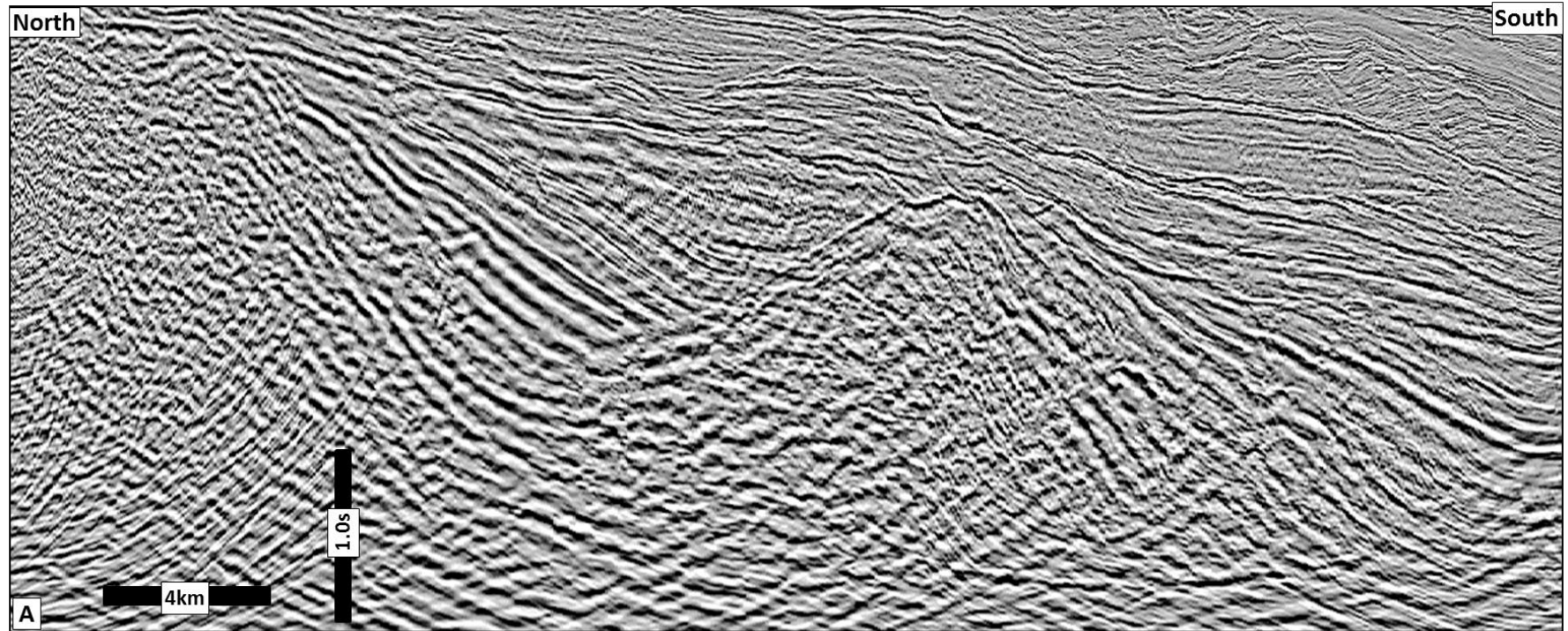
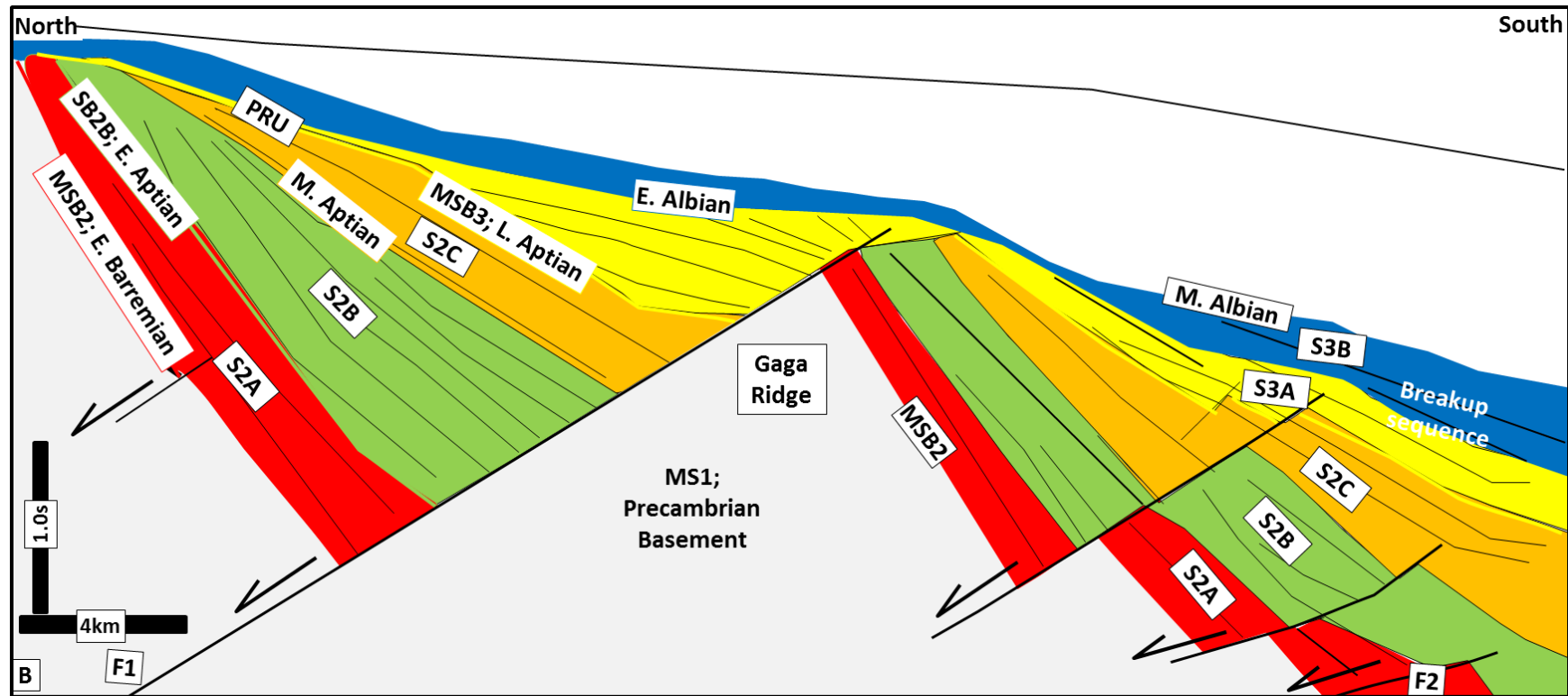


Figure: 3.18 A) Uninterpreted 2D seismic section (N08). See Figure 3.14 for the location of the seismic section.



Transition to seafloor spreading:
marked block rotation; syn-rift
patterns represented by rift-climax
phase (S2C)

Advanced rifting is characterised by
block rotation that resulted in the
development of syn-rift patterns
represented by S2B and S2C

Early rifting geometry is
characterised by limited subsidence
represented by S2A

Figure 3.18 A): Uninterpreted seismic section (on preceding page). **B):** Schematic representation of the tectonic evolution of the offshore Benin Basin in the Barremian-Aptian. A localised inversion post-dated continental rifting in the northern half-graben in the late Aptian/early Albian.

3.11 Conclusions

The structural elemental map of the extensional structures (e.g. basin-bounding normal faults, small normal faults) shows that the offshore Benin Basin trends E-W to ENE-WSW (Figure 2.17). This basin has the following characteristics:

1. The offshore Benin Basin is probably made up of a series of asymmetric half-grabens, the study area reveals two synchronous half-grabens of northward-dipping of the basin-bounding normal faults (F1 and F2; Figure 3.9).
2. The basin-bounding normal faults (F1 and F2) propagated above the post-rift unconformity (late Aptian, MSB3). They, however, remain in net extension. These basin-bounding normal faults (F1 and F2) have, thus, been interpreted as rift-related (Barremian-Aptian).
3. The northern and southern half-grabens are separated by a basement high, the Gaga Ridge, thereby making correlations between them difficult.
4. Well-developed wedge geometry of divergent reflections thickening towards the basin-bounding normal faults in both half-grabens, which are interpreted to depict syn-rift stratigraphy (Figure 3.8). The syn-rift megasequence (MS2) internally consists of three superimposed sequences: early rift sequence, S2A (early – late Barremian), rift-climax sequence, S2B (late Barremian/early Aptian – middle Aptian), and late rift sequence, S2C (middle - late Aptian). These sequences show an increase in the degree of strata divergence from bottom to top.
5. The syn-rift megasequence (MS2) overlies the transparent and chaotic reflections (MS1) interpreted as crystalline basement rock of possibly Precambrian age. Onlap terminations exist between the overlying syn-rift megasequence (MS2) and the pre-rift megasequence (MS1). The onlap surface is interpreted as the rift-onset

unconformity (MSB2) and a Barremian age is assigned to it as the entire syn-rift megasequence (MS2) has not been drilled. The well data for this study has provided dating up to the base of the rift-climax sequence (S2B). Age assignment of the early rift sequence (S2A) was based on stratigraphic correlations with other basins within the intracontinental African Plate.

6. The syn-rift megasequence (MS2) is truncated by the most prominent unconformity, as the post-rift unconformity (MSB3, late Aptian), which is defined by onlap, downlap, offlap, and erosional truncation surfaces (Figure 3.9). This unconformity marks the initiation of continental breakup in the study area. The unconformity ties with late Aptian (Qu et al., 2014).
7. Transfer structures with normal offsets and some relay faults represent later deformation affecting the syn-rift megasequence (Chapter 4).
8. The syn-rift megasequence (MS2) was deformed by an early phase of deformation in the late Aptian/early Albian and a later Santonian deformation event (see Chapter 4).

The rift architecture and the syn-rift stratigraphy suggest that the offshore Benin Basin was probably formed by rifting through orthogonal extension. The models of Gawthorpe and Leeder (2000), and Ravnâs and Steel (1998) have been invoked to explain its evolution. The basin is thought to have developed by fault-propagation, which started as numerous small-displacement normal faults that tend to grow through their fault-tips. The fault linkage and interaction continues as much as the continental stretching permits. However, it ceased in late Aptian (MSB3) when mechanical subsidence stopped and thermal subsidence began to control sedimentation in the Benin Basin.

The rifting of the E-W to ENE-WSW striking offshore Benin Basin is therefore not consistent with basins of the Equatorial Atlantic transform margin that are characterised by strike-slip

movement. The transpressional rift models for the evolution of the Equatorial Atlantic margin (see Chapter 1) do not fit the evolution of the offshore Benin Basin.

Chapter Four

4.0 Cretaceous post-rift megasequence MS3 (late Aptian – latest Maastrichtian)

This chapter concerns the analysis of Cretaceous post-rift megasequence MS3 (late Aptian, MSB3 to latest Maastrichtian, MSB4) so to evaluate post-rift deformation in the Benin Basin. The breakup sequence will also be analysed and interpreted in relation to the timing and plate configuration during continental breakup of the African-South American Plate. The Cretaceous post-rift megasequence of the offshore Benin Basin is characterised by several fault-related folds which, as argued here, are related to regional shortening. This chapter describes and dates these structures, and interprets their significance.

4.1 Introduction

Accommodation space for sedimentation during the post-rift phase of basin evolution is often controlled by thermal subsidence and uplift (e.g. Ravnas and Steel, 1998). The post-rift phase starts with a post-rift unconformity as a result of erosion that often follows tectonic uplift (Doré et al., 2008). Deposition later resumes as accommodation space is created by thermal subsidence. As plates move apart during drifting, the directions of plate movement may vary as a result of changes in the stress field. Changes in stress field often lead to formation of new structures, reactivation of older structures, or the generation of inverted structures. Extensional basins and passive margins are thus characterised by different types of structures: extensional structures (e.g. basin-normal faults and roll-over anticlines) and contractional structures (e.g. thrusts and folds, inverted structures).

The post-rift phase in a rift basin (or passive margin) may occasionally be interrupted by compressional deformation (e.g. Doré et al., 2008; Martinez et al., 2012). In such cases, contractional structures may relate to regional compression and wholesale basin inversion, or to local reactivation of existing structures within the basin, often producing zones of localised transpression and uplift (Zalan et al., 1985; Cooper et al., 1989; Hayward and Graham, 1989; Williams et al., 1989; Guiraud et al., 1992; Moores and Twiss, 1995; Schlische, 1995; Doré et al., 2008; Warren, 2009; Cooper and Warren, 2010; Zalan, 2011; Sengör and Bozkurt, 2013; Delvaux et al., 2016). Alternatively, compression may reflect gravity-driven deformation on continental slopes, for example, when involving the contractional toes of slumps (e.g. Hesthammer and Fossen, 1999; Apotria et al., 2004; Bilotti and Shaw, 2005; Bilotti et al., 2005; Corredor et al., 2005; Frey-Martinez et al., 2005; Briggs et al., 2006; 2009; Cobbold et al., 2001; 2009).

This chapter documents the seismic sequence stratigraphy of the sequences of the megasequence MS3. It includes an analysis of the megasequence MS3 and the distribution of contractional structures in the study area. These structures are examined for their styles and timings in order to evaluate the likely causes of compression in the offshore Benin Basin.

4.2 Aims and objectives

- ❖ To analyse and evaluate post-rift megasequences (MS3 and younger) in terms of their seismic character so to determine the depositional history of post-rift strata;
- ❖ To analyse the nature and timing of the sequence boundary at the base of the post-rift strata (MS3) in order to ascertain if it corresponds with the onset of ocean spreading in this part of the Equatorial Atlantic.
- ❖ A critical evaluation of the nature, distribution, timing, and causes of folds and thrusts in the study area.

4.3 Methodology

The seismic and sequence stratigraphic (seismic sequence and seismic facies) methods described in Chapter 2 were also applied to the Cretaceous post-rift megasequence (MS3) in order to analyse and interpret possible depositional environments. Contractional structures were identified by analysing the megasequence for faults and associated folds using the structural methods also described in Chapter 2. Seismic sequence stratigraphic analysis was applied in order to identify pre-, syn- and post-folding sequences recording the deformation identified.

4.4 Post-rift stratigraphy

4.4.1 Breakup unconformity and breakup sequence concepts

Concept of breakup unconformity

Continental extension often leads to a breakup of the continental plate (i.e. lithospheric breakup event), with subsequent accretion of oceanic lithosphere and the formation of conjugate passive margins (Wilson, 1965; Rosendahl, 1987; Busby and Ingersoll, 1995; Buck, 2007; Soares et al., 2012; Allen and Allen, 2013). In other cases, extension ceases before the development of the conjugate margin, leading to the generation of failed rifts (Moulin et al., 2010; Fairhead et al., 2013; Heine and Brune, 2014). The formation of a breakup unconformity results from thermal expansion resulting from the upwelling of asthenospheric mantle during the breakup (Falvey, 1974). The thermal expansion will lead to a brief period of crustal uplift and erosion, followed by post-rift subsidence due to thermal contraction (Figure 4.1).

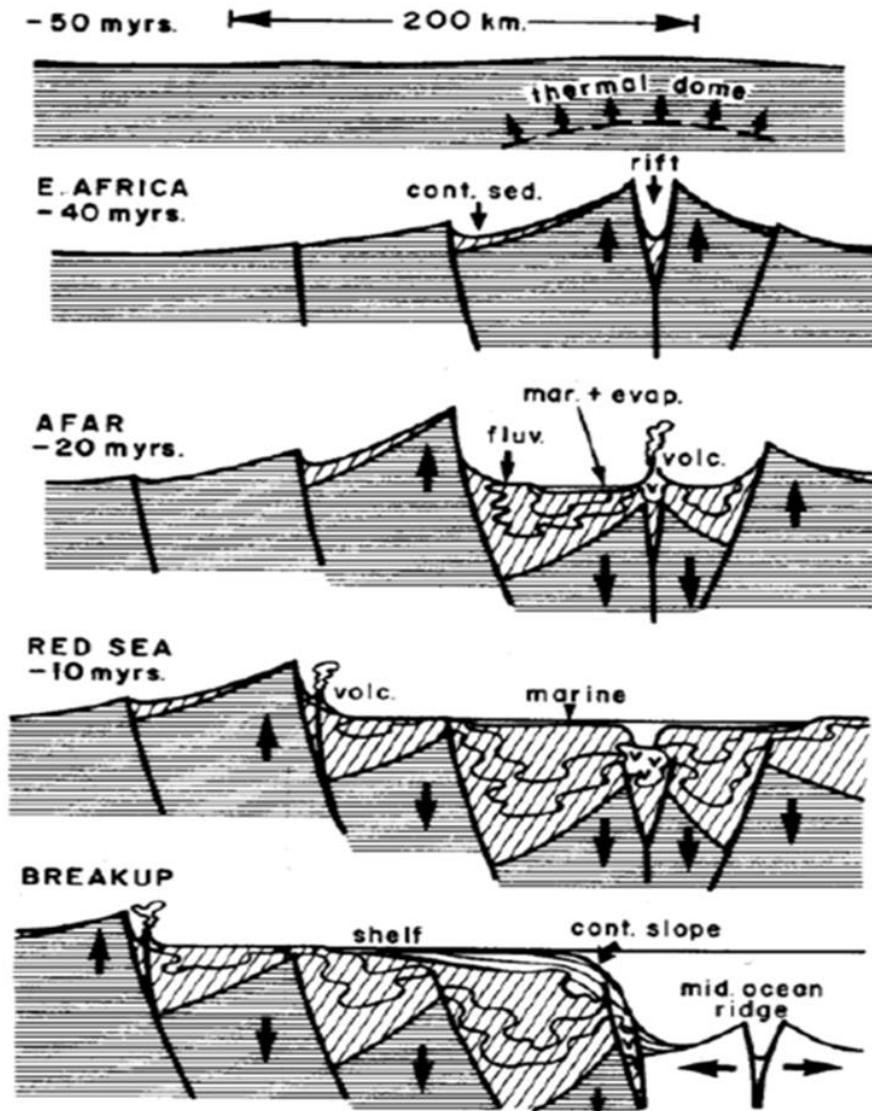


Figure 4.1: Development of Atlantic-type or rifted continental margins from their initial doming' to an incipient rift, widening rift valley and continental breakup. Seafloor spreading and subsidence of the new continental margin occur after continental breakup (after Falvey, 1974).

Some rift basins are thought to possess a transitional developmental stage that documents the change from syn-rift to post-rift, although the transitional sequence is not recognised in all rift basins (Moore, 1992; Cainelli and Mohriak, 1999; Beglinger et al., 2012; Soares et al., 2012). Transition sequences are therefore considered to be restricted to specific rift basins rather than a general characteristic (Embry and Dixon, 1990; Withjack et al., 1998; 2012; Jungslager, 1999; Whitmarsh and Wallace, 2001; Kyrkjebø et al., 2004; Dupré et al., 2007;

Huismans and Beaumont, 2011). Despite the importance of the breakup unconformity in understanding rift basin processes, geological interpretations vary and remain controversial. Such controversy may be as a result of the localised transition sequence. The transitional sequence is also referred to as the breakup sequence (Soares et al., 2012).

Some of the questions posed by the breakup unconformity include:

- ❖ Does the breakup unconformity really mark the end of rifting and the onset of drifting?
- ❖ What process(es) generated the breakup unconformity?

Some of the mechanisms proposed for the breakup unconformity include:

- ❖ Thermal uplift
- ❖ Cessation or decrease of extensional in-plane stresses acting on continental plates resulting in flexural rebound (Falvey, 1974; Coward, 1986; Braun and Beaumont, 1989).

The most prominent unconformity in the study area has been mapped as the post-rift unconformity (PRU) (Falvey, 1974; Hubbard, 1988). This unconformity represents the initiation of crustal lithosphere separation. This study has shown that the post-rift unconformity (PRU) occurred in the late Aptian (MSB3). However, previous authors (e.g. Greenroyd et al., 2008 Greenhalgh et al., 2011) have suggested that the final lithospheric separation in the Equatorial Atlantic occurred in the middle Albian.

Following Soares et al. (2012), this chapter analyses megasequence MS3 for any possible seismic sequence(s) deposited between the late Aptian, MSB3 (post-rift unconformity) and middle Albian (final breakup; Greenoyd et al., 2008; Greenhalgh et al., 2011) as the breakup sequence (BS) in the offshore Benin Basin.

4.5 Seismic Stratigraphy of the Cretaceous post-rift megasequence MS3 (late Aptian, MSB3 - latest Maastrichtian, MSB4)

4.5.1 Immediate post-rift sequence, S3A (late Aptian - early Albian)

This is the first sequence deposited during the post-rift phase, thereby corresponding to strata belonging to the immediate post-rift (Figure 4.2). It is made up of discontinuous, parallel to sub-parallel seismic reflections, occasionally hummocky to oblique reflection patterns (Figure 4.3). These are of moderate to high amplitude. On dip sections, these reflections show a wedge geometry similar to the underlying syn-rift megasequence (MS2; Figure 4.3), but the individual reflectors do not diverge towards the basin-bounding normal fault. These parallel reflections are interpreted as post-rift deposits representing an infilling of remnant syn-rift topography (Figure 4.3; Moore, 1992; Prosser, 1993). Such remnant syn-rift topography is interpreted (e.g. Moore, 1992; Prosser, 1993) to result from unfilled half-graben accommodation space due to subsidence rate outpacing sedimentation rate during rift-climax. This seismic reflection geometry is similar to those described as characterising breakup sequence by Soares et al. (2012) and (2014). It is bounded by a basal post-rift unconformity (MSB3) and at its top by an onlap surface that correlates with the early Albian.

4.5.2 Parallel reflection sequence S3B (middle Albian)

Sequence S3B is the second unit in megasequence MS3. It is composed of parallel to sub-parallel, high amplitude, high frequency, continuous to discontinuous seismic reflections. It shows progradational strata (mainly sigmoidal but occasionally oblique clinoforms) at places. These clinoforms, which are well-recorded on strike sections (Figure 4.4), indicate westward progradation from Nigeria.

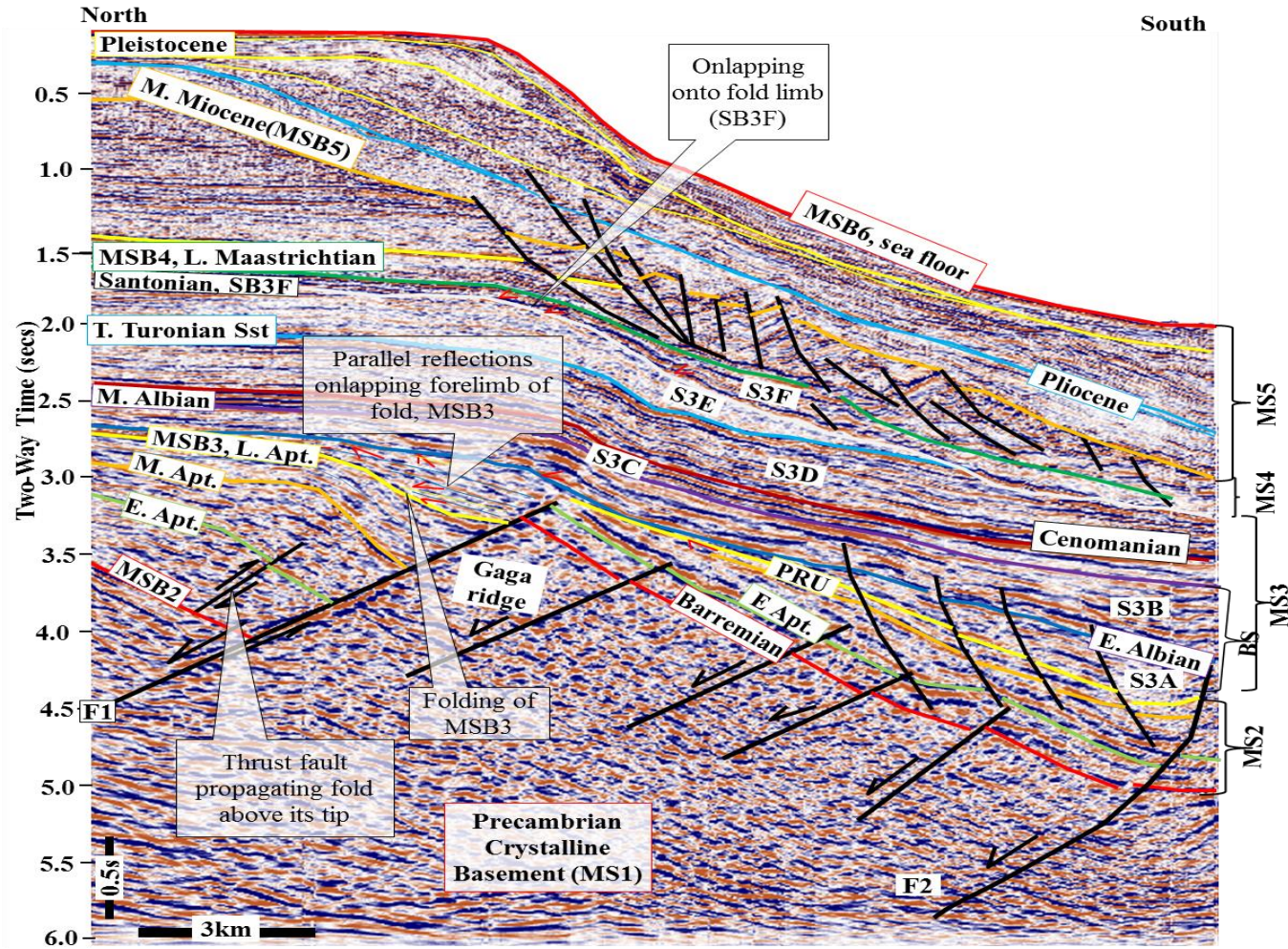


Figure 4.2: Crossline 3968 showing main seismic sequences and at least two phases of deformation events in the late Aptian/early Albian, and Santonian (SB3F). Red arrows show onlap onto fold limb in both phases. Apt. = Aptian, Alb. = Albian, E. = early, M. = middle, L. = late, PRU = post-rift unconformity. See Figure 4.8 for the location of the seismic section.

The oblique clinoforms suggest forced regression. This implies a period of sediment transport into the deeper margin. The total thickness of the breakup sequence (S2A and S2B) varies from about 250 ms TWT to 360 ms TWT (Figure 4.3). Its top boundary is marked by an erosional truncation surface, and is dated middle Albian. The parallel to sub-parallel reflections suggest transgression. These imply that during the Albian, a marine setting became prevalent in the Equatorial Atlantic region (Moulin et al., 2010).

It can, therefore, be suggested that the offshore Benin Basin consists of a breakup sequence comprising S3A and S3B because these sequences immediately post-date the syn-rift megasequence (MS2) and were deposited between the onset of lithospheric separation that occurred in late Aptian and the final lithospheric mantle separation of middle Albian. The top of the sequence S3B, therefore, represents the top of the breakup sequence (TBS) in the Benin Basin. The significance and implication of the breakup sequence for the continental separation of the African-South American Plate will be discussed in Chapter 6.

4.5.3 High amplitude parallel reflections, S3C (late Albian - Cenomanian)

This sequence overlies the breakup sequence, and it can be referred to as the first unit of the post-breakup phase. Sequence S3C is composed of moderate to high amplitude, high frequency, continuous seismic reflections. Well reports show that it consists of carbonate sediments. The well-logs (GR and resistivity logs) reveal high GR and resistivity, suggesting that a proportion of the carbonate sediment is shaley. Its thickness on the GR-log is about 285 m. Its basal boundary shows onlap while its top is marked by onlap and occasionally downlap. It is sometimes truncated by an erosional surface on its top (Figures 4.5 and 4.6). This erosional surface is dated as Cenomanian, while its basal surface is middle Albian. Its age suggests that it was deposited after crustal separation. The parallel reflections suggest aggradation (i.e. deposition under relative rise in sea level) suggesting deepening.

Table 4.1: Reflection characteristics and interpretations for discrete seismic sequences in megasequence MS3

Seismic Facies unit (MS3)	Age	Reflection Configuration	Reflection Amplitude	Reflection Continuity	External form of Facies unit	Lower Boundary	Upper Boundary	Predicted Depositional Environment	Lithology prediction
S3G (High amplitude reflection)	Late Maastrichtian	Parallel, sub-parallel	Moderate to high	Continuous to discontinuous		Onlap, downlap	Onlap, offlap	Marine	Sandstone
S3F (Divergent reflection)	late Santonian	Divergent	High	Continuous to discontinuous		Onlap, erosional truncation	Erosional truncation	Marine	Sandstone, mudstone
S3E (Transparent reflection)	Turonian - Santonian	Parallel to sub-parallel, transparent reflections,	Low	Continuous to discontinuous		Onlap, downlap	Toplap, onlap	Marine	Sandstone, mudstone,
S3D (Parallel reflection)	Cenomanian – late Turonian	Divergent	Moderate to high	Continuous to discontinuous		Onlap, downlap	Offlap, onlap, downlap	Shallow marine	Sandstone, mudstone, ?limestone
S3C (High amplitude parallel reflections)	Late Albian-Cenomanian	Parallel to sub-parallel, oblique	Moderate to high	continuous		Onlap	Onlap, downlap	Shallow marine	Sandstone, mudstone
S3B (parallel)	Middle Albian	Parallel to sub-parallel	High	Continuous to discontinuous		Onlap	Onlap	Shallow marine	Sandstone, mudstone, ?limestone
S3A (Immediate post-rift)	Early Albian	Parallel to sub-parallel, oblique reflections	Moderate to high	Continuous to discontinuous		onlap	Onlap	Shallow marine	Sandstone, mudstone

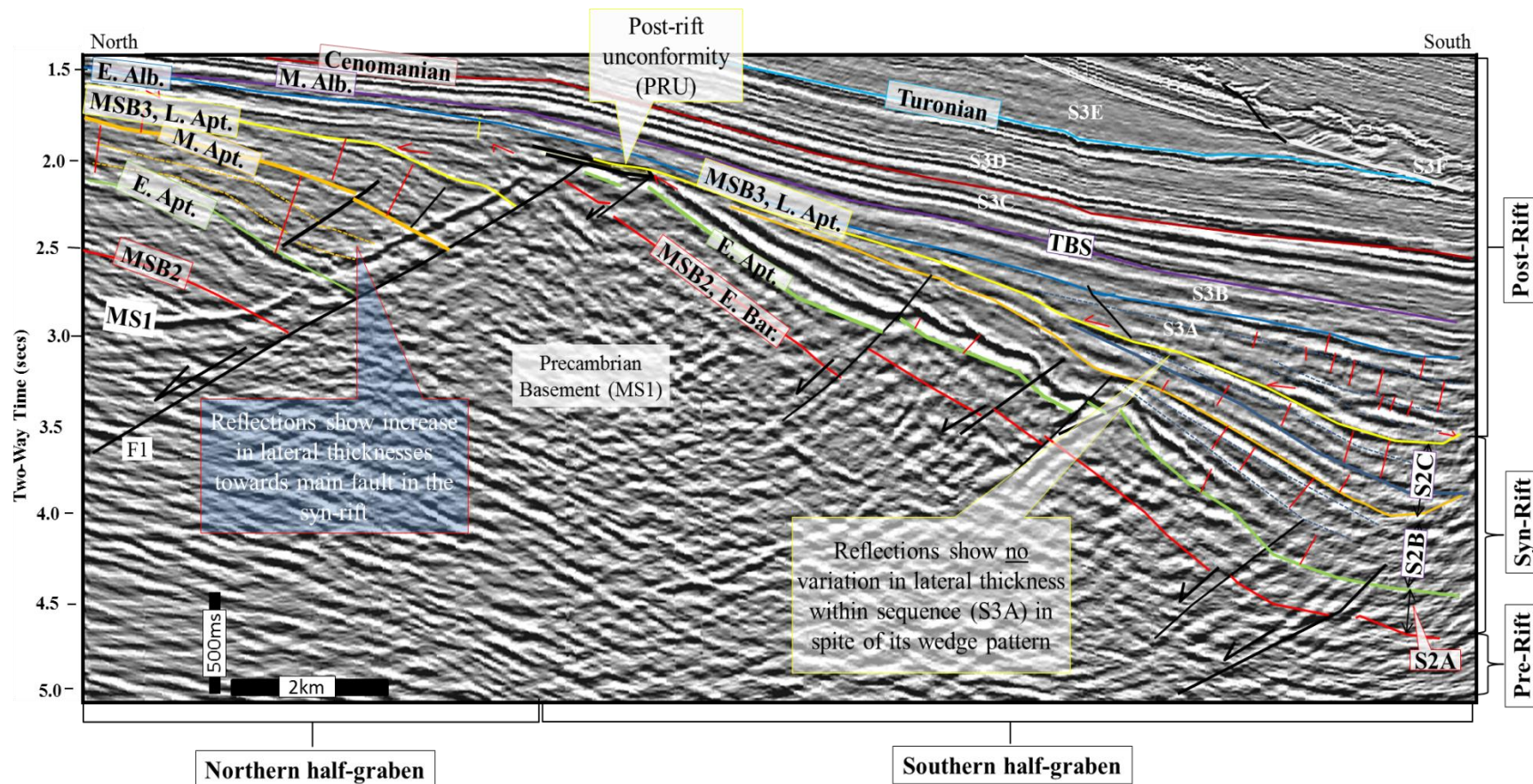


Figure 4.3: Crossline 4646 showing the seismic sequences in the syn-rift megasequence with a characteristic wedge pattern. The post-rift phase developed a parallel to sub-parallel reflection geometry. Note the propagation of the basin-bounding normal fault (F1) above the post-rift unconformity (PRU) in the northern half-graben. Sequence S3A comprising parallel reflections passively filled an inherited ‘wedge geometry’ in both half-grabens. See Figure 4.8 for the location of the seismic section.

4.5.4 Parallel reflection sequence (S3D) (Cenomanian - late Turonian)

This sequence consists of continuous to discontinuous, parallel to sub-parallel reflections (Figures 4.3). Some high amplitude chaotic seismic reflections may occur internally (Figure 4.3). The reflections have moderate to high amplitude. Internally, it consists of oblique clinoforms ranging between 40-60 ms TWT thick (Figure 4.3). The total thickness of this sequence is about 300 ms TWT. The sequence shows evidence of incision by submarine canyons (Figure 4.7). The sequence consists of high-frequency reflections suggesting the presence of heterolithic and relatively thinly bedded sediments. Sandstone with a few intercalations of mudstone has been interpreted for this sequence (Brownfield and Charpentier, 2006).

The base of the unit is composed of onlapping and/or downlapping surfaces (Figure 4.5) and an erosional surface at its top. This sequence corresponds to what Brownfield and Charpentier (2006) identified as the 'Turonian Sandstone', or the Abeokuta Sandstone (see section 1.12.3; Kaki et al., 2012). Olabode (2006) interpreted clays, sandstones, and conglomerates in this unit. Its age ranges from Cenomanian to late Turonian (Kaki et al., 2012) and it is a source interval in parts of the Equatorial margin of Brazil.

4.5.5 Transparent reflections sequence (S3E) (Turonian - Santonian)

This seismic sequence is composed of continuous to non-continuous, low amplitude to transparent reflections (Figures 4.5 and 4.7); it is sometimes reflection-free. Internally, it is made up of thin units of oblique clinoforms with thickness ranging from 70-90 ms TWT. Its total thickness is about 270 ms TWT.

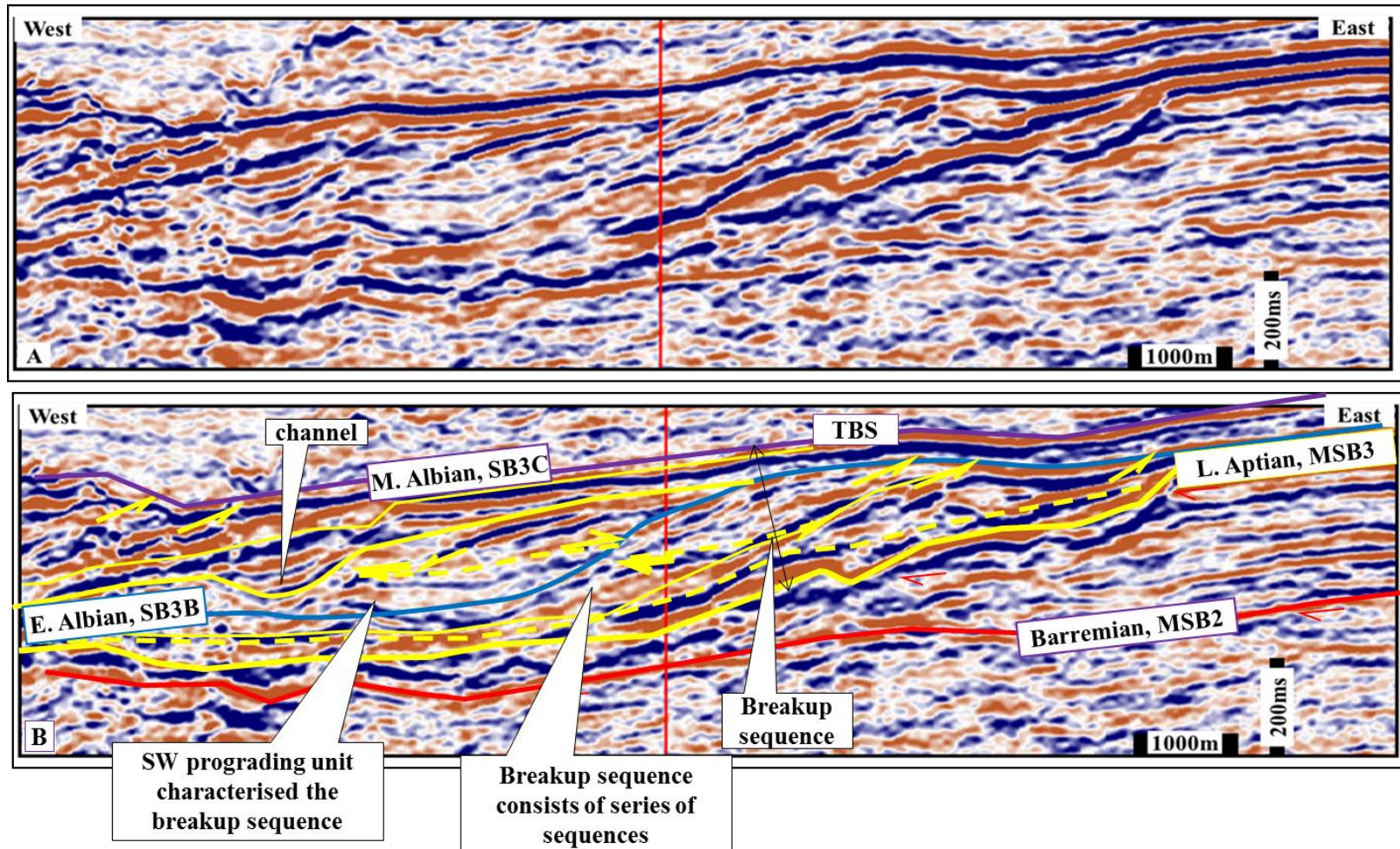


Figure 4.4: Uninterpreted (A). Interpreted inline 1100 (B) showing erosional features (forced regression) at MSB3 forming an erosional ‘canyon’ into MS2). This has been draped by a series of sequences that correlate to the breakup sequence (S3A and S3B). See Figure 4.8 for location of the seismic section.

The sequence is locally affected by erosion related to slumping and submarine canyon/incision (Figure 4.7). It is interpreted as a sandy shale. It is bounded by erosional truncation and onlap surfaces along both its base and top. It correlates with the Agwu Shale of Brownfield and Charpentier (2006) (Figure 1.11). Its base marks an important unconformity surface dated as Turonian, while its top is characterised by an erosional surface dated as late Santonian (Brownfield and Charpentier, 2006; Kaki et al., 2012).

4.5.6 Parallel reflection sequence (S3F) (late Santonian)

This sequence consists of high amplitude parallel reflections (Figure 4.7). It has a wedge-shape geometry and shows parallel reflections that onlap the limbs of locally-developed monoclinical folds (Figure 4.7). Seismic reflections locally onlap the erosional top to the low amplitude sequence S3E (Santonian). The parallel reflection sequence (S3F) is, therefore, identified in this study as the sequence that immediate post-dates a phase of Santonian folding but observed in parts of the basin (section 4.6). The sequence S3F has also been deformed by younger gravitational sliding (Figure 4.7; see section 4.9). Its top is marked by onlapping reflections (SB3G).

4.5.7 High amplitude reflection sequence (S3G) (Maastrichtian)

This is the youngest sequence of the post-rift megasequence (MS3). It is composed of parallel to sub-parallel, high amplitude reflections, and progradational clinoforms. It is overlain by Cenozoic strata and, therefore, marks the end of the Late Cretaceous depositional phase. Its top is MSB4 which is correlated with the top-Maastrichtian unconformity (Figure 4.7; and Table 4.1).

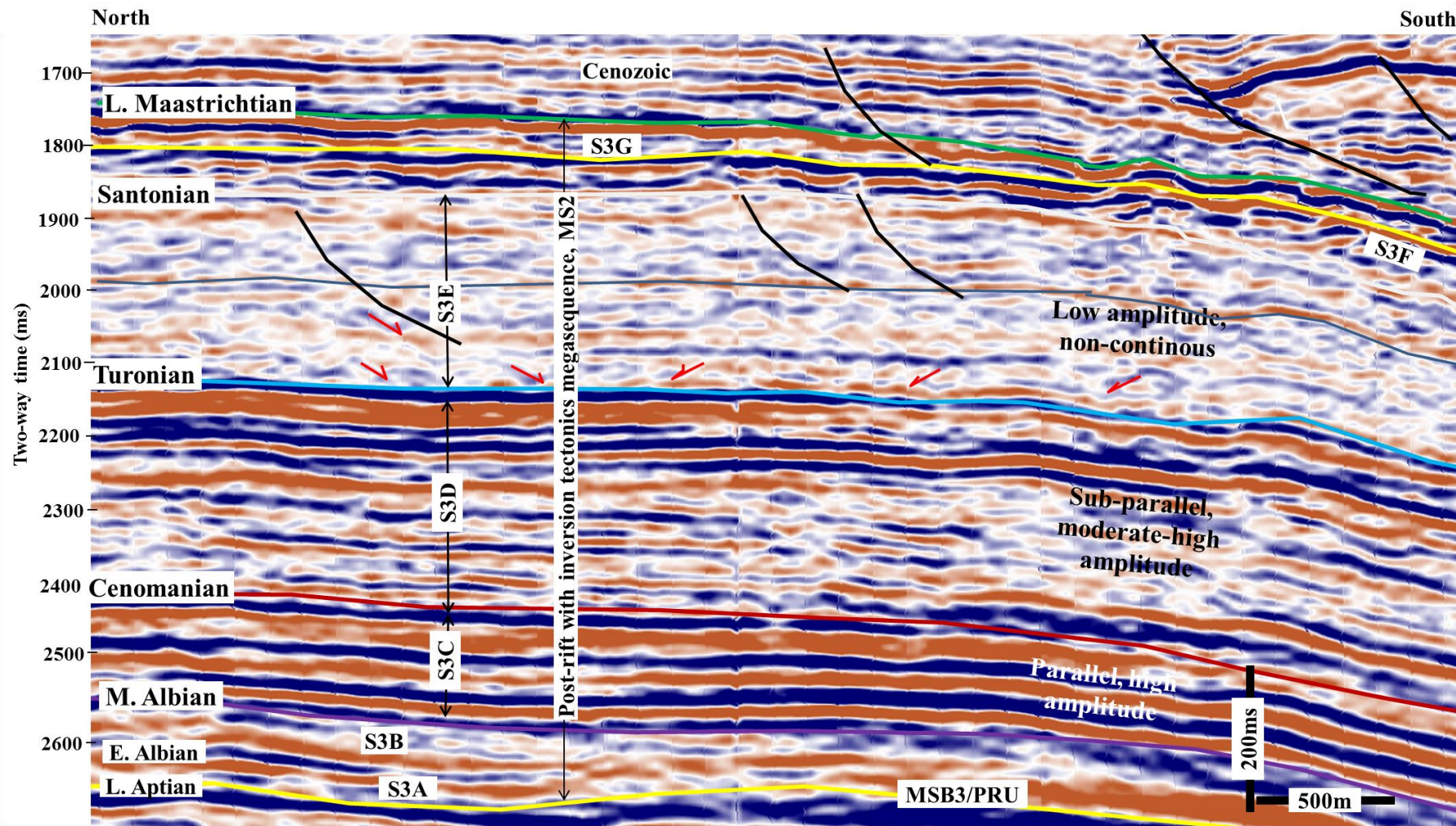


Figure 4.5: Vertical profile (crossline 3808) highlighting the upper part of the post-rift succession within a folded megasequence MS3. See Figure 4.8 for the location of the seismic section.

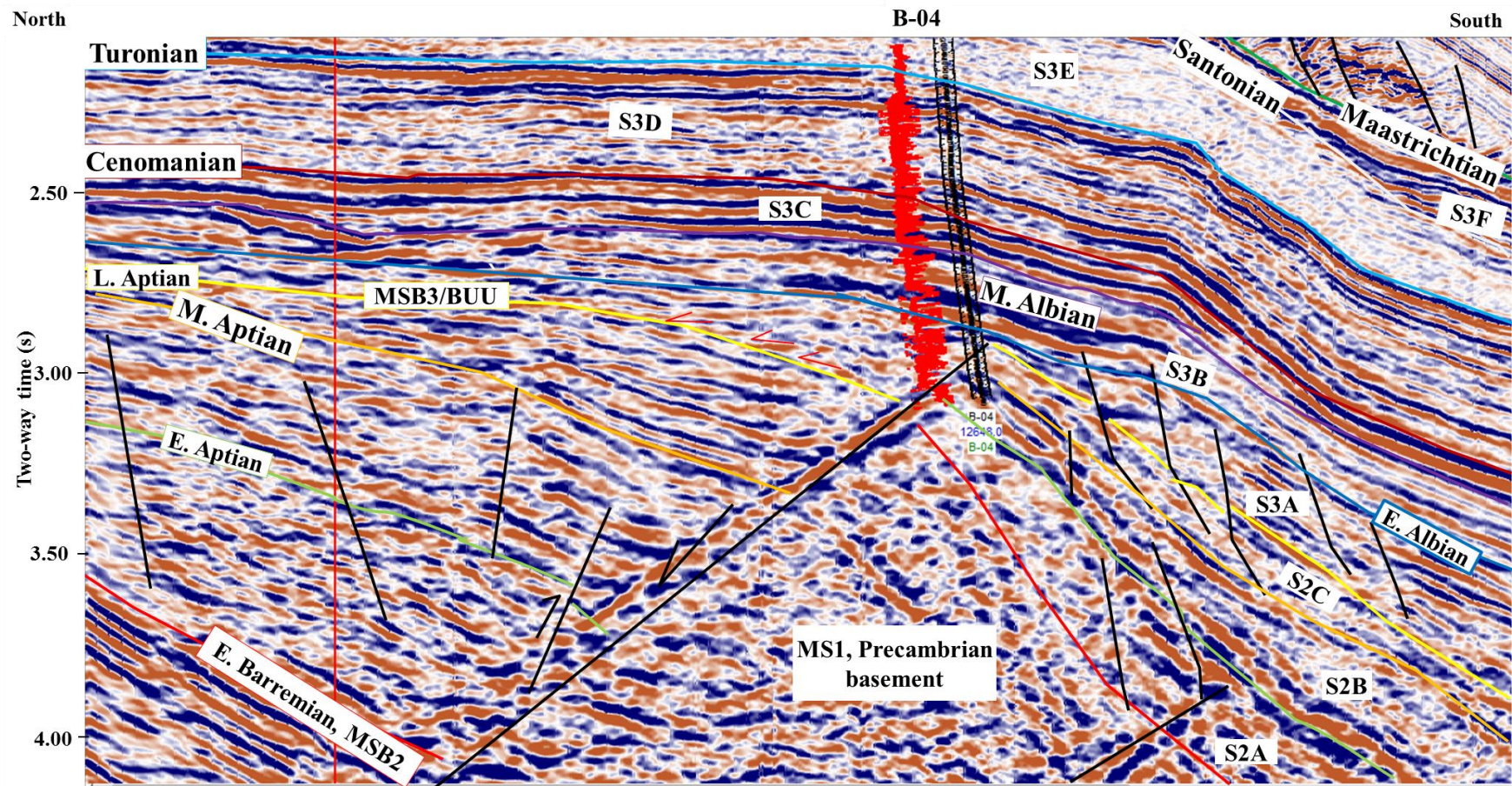


Figure 4.6: Crossline 3762 showing the internal seismic characters of sequences of megasequences M2 and MS3. Well signatures of the megasequence MS3 are also shown. See Figure 4.8 for the location of the seismic section.

4.6 Post-rift contractional deformation in offshore Benin Basin

Multiphase contractional deformation is a common feature in the post-rift evolution of passive margins and extensional basins (Dorè et al., 1997; 2008; Cloetingh et al., 2008). The styles of the structures that deformed the megasequence MS3 are analysed and described (see sections 4.7 and 4.8).

Seismic stratigraphic and structural analysis indicates that there were two main phases of deformation events (thrust-related folding) in the study area. The first occurred in the northern part of the basin at around the time of formation of megasequence MS3. The second focused around the structural high between the northern and southern half-grabens (Eji anticline), occurred around the time of formation of sequence S3F. Both of these phases of deformation indicate small amounts of NW-SE shortening.

4.7 Late Aptian/early Albian deformation

The initial phase of deformation occurred during the deposition of post-rift megasequence (MS3) and it is limited in the northern half-graben. Four main structural elements have been identified as representative of this phase of deformation:

- ❖ Elo thrust
- ❖ Oga fold
- ❖ Iro transfer zone
- ❖ Ore thrust (Figure 4.10).

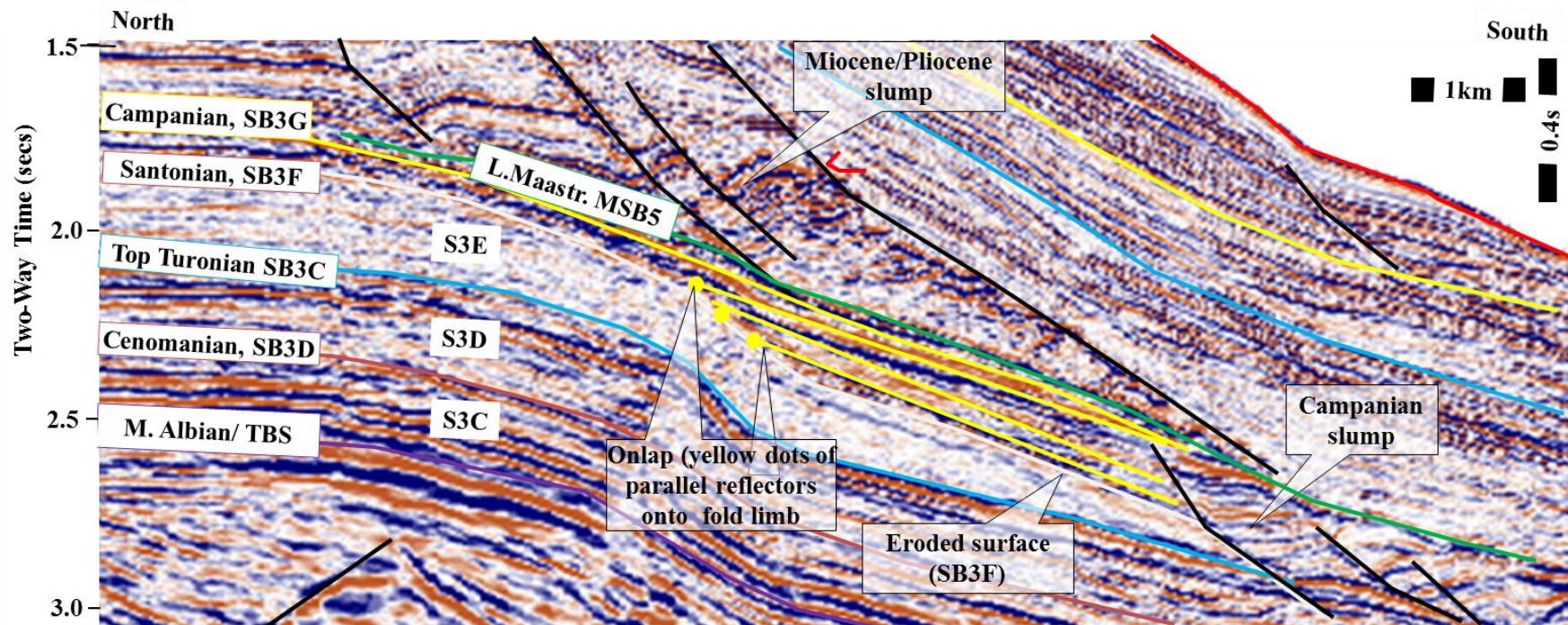


Figure 4.7: Crossline 3884 highlighting the relationship between the Santonian (SB3F) contractional deformation, Campanian slumping and the Miocene/Pliocene slumping observed in the study area. SB3F cuts down through sequences S3E and S3D. The erosion of these sequences is not related to slumping because they are not translated downslope. Red arrows and yellow dots show onlapping reflections. See Figure 4.8 for the location of crossline 3884.

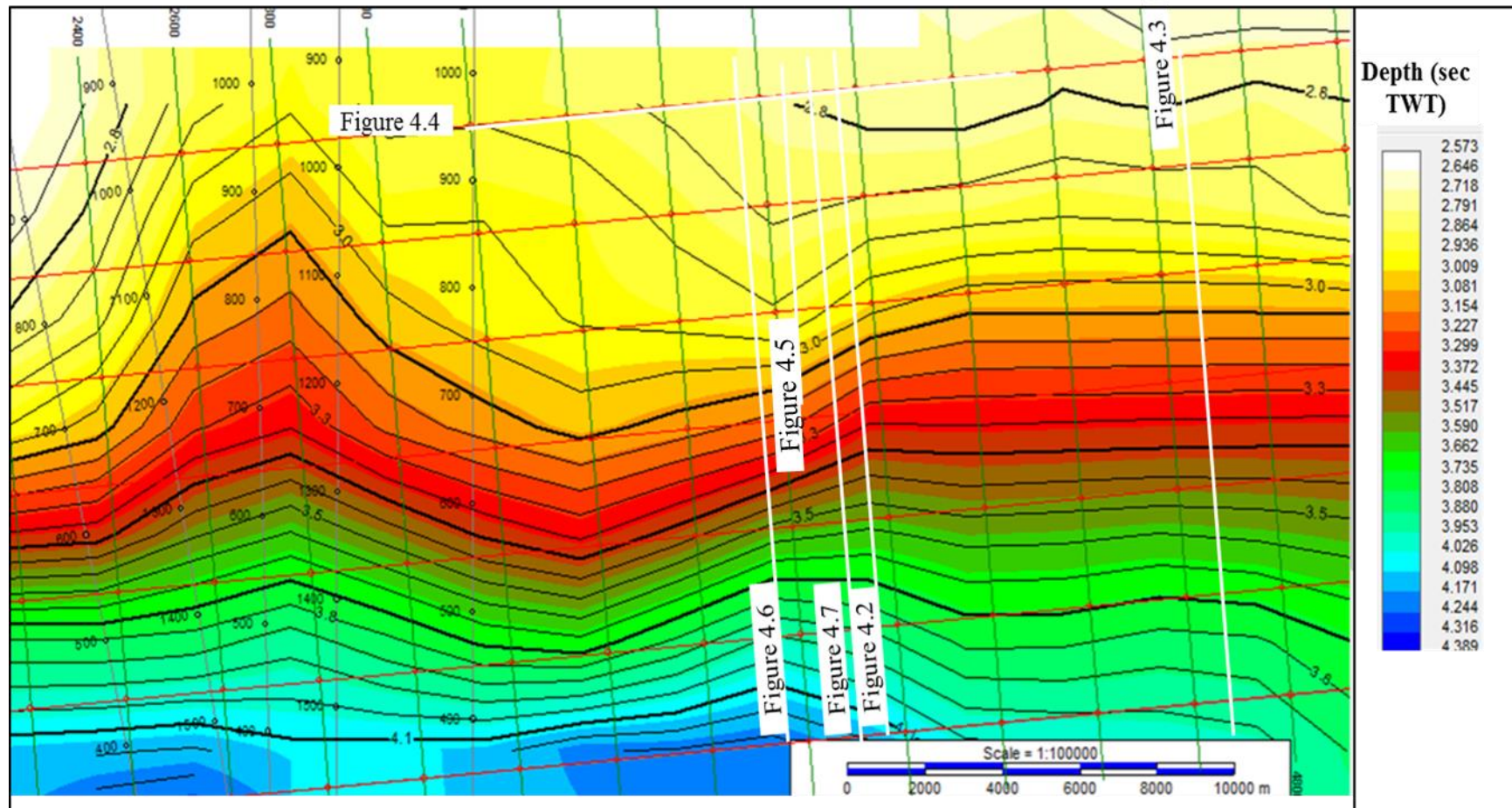


Figure 4.8: TWT isochron map of the top of breakup sequence, S3A (early Albian). Some of the figures cited in this chapter are indicated in this figure.

4.7.1 Elo thrust (late Aptian/early Albian)

Description of the Elo thrust

The Elo thrust has been identified in the northeastern part of the northern half-graben (Figure 4.10). This fault has an apparent angle of dip of less than 45°, and a characteristic reverse sense of motion (Figure 4.9). In seismic sections, the fault dips northwest and strikes NE-SW in map view (Figure 4.10). The main thrust surface has several sub-ordinate, synthetic imbricate thrusts in its hanging-wall. These involve stratigraphic sequences as young as middle Aptian and include basement units, as does the main thrust (Figure 4.9). A SE-vergent antiformal fold was identified in the hanging-wall of the Elo thrust system, suggesting a SE-directed transport on the main thrust itself. The displacement on imbricate thrusts appears to tip-out within late Aptian (MSB3) strata, with folding located ahead of the fault tips, indicating fold-propagation folding. Seismic sequences representing pre-, syn- and post-folding can be identified. The pre-fold phase of the Elo thrust structure is composed of parallel to sub-parallel, continuous to non-continuous reflections in syn-rift megasequence (MS2). The Elo thrust occurs close to the basin-bounding normal fault, F1 (Figure 4.9).

Origin of Elo thrust

Most folds related to thrusting sit on the hanging-wall of these same thrusts. The fact that thrusts appear to tip out immediately below the folds is most suggestive of a fault-propagation fold (Figure 4.9). This type of structure has been described by multiple authors (e.g. Jamison, 1978; McClay, 1989; Williams et al., 1989; Suppé et al., 1992; López-Blanco et al., 2002; Vergés et al., 2002; Nemčok et al., 2005; Tavani et al., 2007; Poblet and Lisle, 2011).

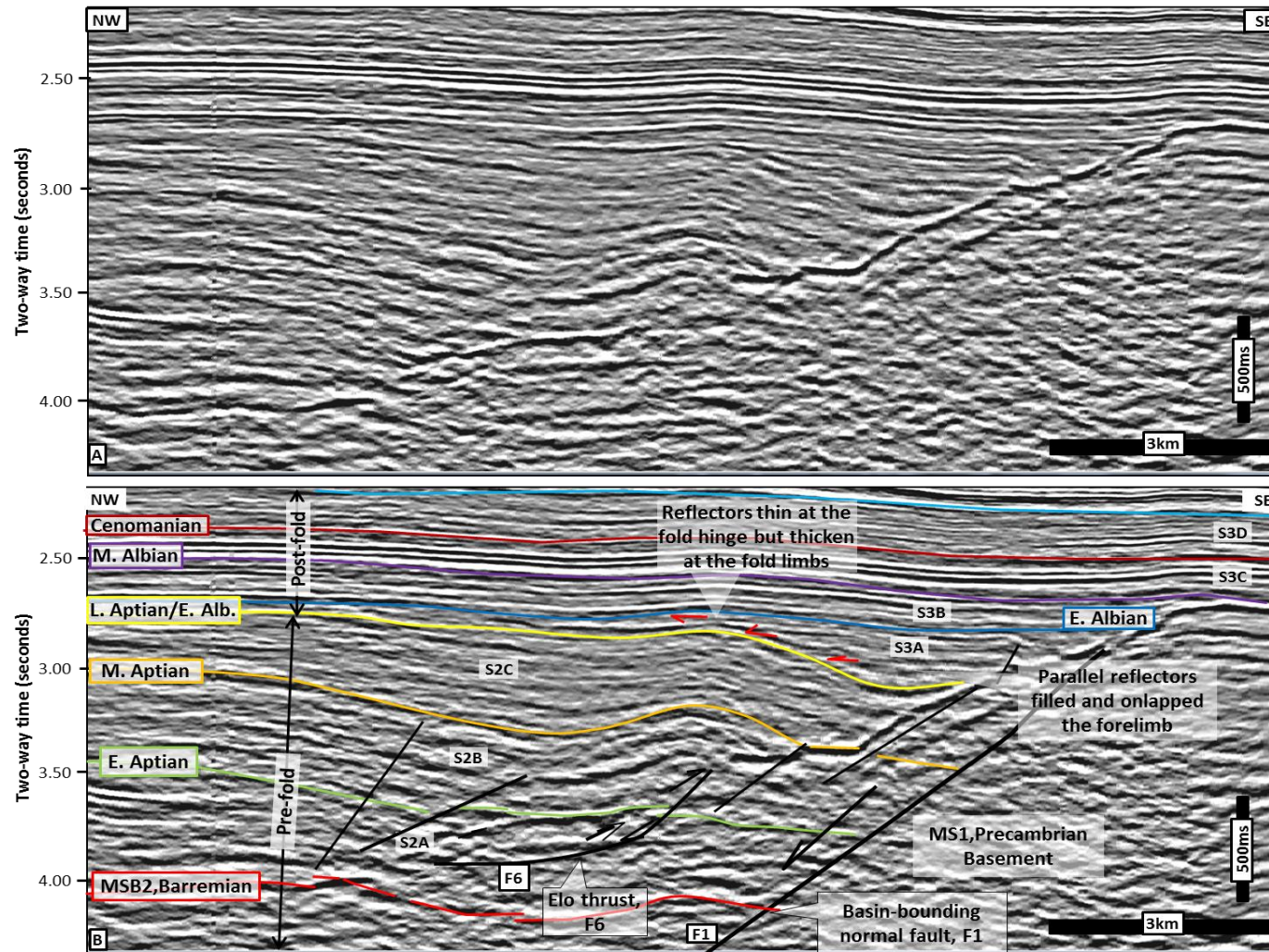


Figure 4.9: Arbitrary line (NW-SE) seismic section uninterpreted (A) and interpreted section (B). Elo thrust (F6) is located close to the main basin-bounding normal fault (F1). The roll-over structure of the main fault (F1) and the wedge pattern associated with F1 are still preserved. Fault F1 is still in net extension, suggesting it was not inverted. The thrust fault (F6) offsets the early Aptian. Onlap of parallel reflections onto the fold limb of fold (late Aptian/early Albian. See Figure 4.10 for the location of the seismic section.

The fact that the Elo thrust only seems to occur close to the original rift-shoulder fault (F1) suggests that this large, basement-involved normal fault (F1) was the only structure reactivated during mild “basin inversion”.

4.7.2 Oga fold (late Aptian/early Albian)

Description of Oga anticline

The Oga fold structure is located in the northeastern part of the northern half-graben. It lies to the western part of the Elo structure (Figure 4.10). The anticline has an ENE-WSW trending axis, is monoclinical and verges SSE (Figure 4.11). It sits in the immediate hanging-wall of a significant normal fault, although its hanging-wall is also cut by a smaller thrust fault (F8) appearing to be spatially linked to the Oga fold (Figure 4.11). The thrust fault dips at a low-angle ($15-22^{\circ}$) to the NNW and strikes ENE-WSW, parallel to the axial trace of the Oga anticline (Figure 4.11). The thrust fault does not obviously cut basement rocks in the hanging-wall of the basin-bounding normal fault (F), suggesting that its deformation style is thin-skinned (Coward, 1983; Nemcok et al., 2005). Basement rocks across the adjacent normal fault remain in net-extension, as does the basin-fill, up to at least the middle-late Aptian/early Albian (Figure 4.11).

A null point within the syn-rift megasequence (MS2) could not be identified along the basin-bounding normal fault. A minor component of reverse reactivation cannot be discounted, but the late Aptian post-rift succession (MSB3) does not appear to be offset. The horizontal shortening accommodated by folding and thrusting in the hanging-wall is very small (Sengor and Bozkurt, 2013).

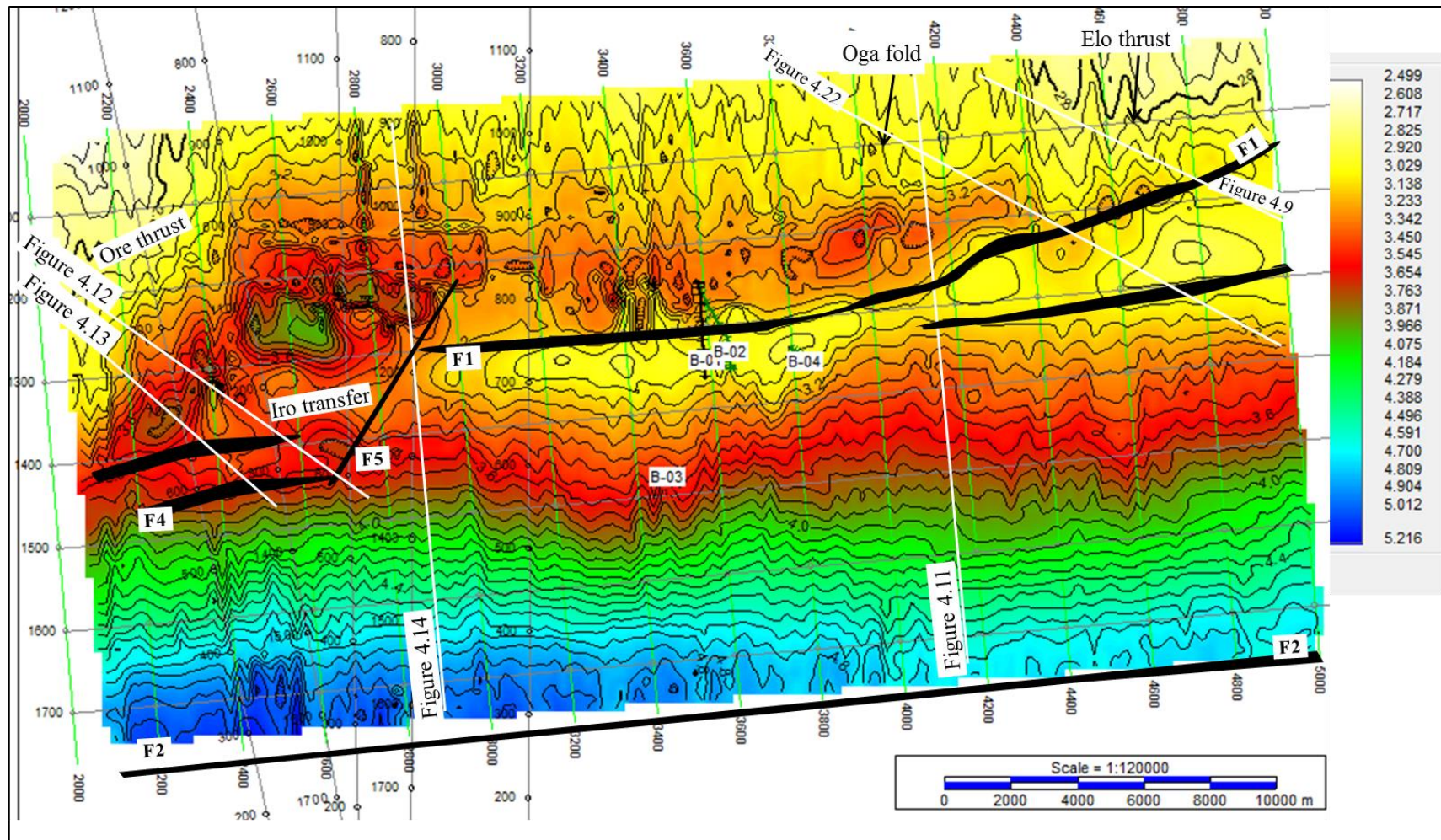


Figure 4.10: Isochron map of the top of the late Aptian/early Albian fold onset unconformity. Location of seismic sections shown in this chapter indicated in this figure.

Both pre-fold and post-fold successions have been identified in association with the Oga Fold. The pre-fold phase consists of the syn-rift megasequence (MS2). The pre-fold succession is made up of folded, parallel to sub-parallel, continuous to non-continuous seismic reflections. The pre-fold sequences still preserve their characteristic syn-rift (wedge) patterns on seismic data (Figure 4.11). The syn-fold phase is absent. The post-fold phase is made up of parallel to sub-parallel reflections that onlap the post-rift unconformity (MSB3, late Aptian). This unconformity separates the underlying pre-fold successions from the overlying post-fold successions. The immediate post-fold sequence of this deformation phase correlates to the immediate post-rift sequence (S3A) in the southern half-graben (Figure 4.11).

Origin of Oga fold

The Oga fold shows a roll-over structure in the hanging-wall of the basin-bounding normal fault (F1), in the northern half-graben. The roll-over structure appears to have been shortened during later deformation, and a thrust fault (F8) was developed. The basin-bounding normal fault (F1) is still in net extension but the fault plane shows evidence of reverse reactivation.

The presence of the thrust fault (F8) on the hanging-wall of an early basin-bounding normal fault suggests that a mild inversion may have locally affected the northern half-graben in the late Aptian/early Albian.

The fault geometry of the basin-bounding normal fault (F1) shows a normal drag in the syn-rift megasequence (MS2) on the hanging-wall of the basin-bounding normal fault (F1). The preserved syn-rift pattern still shows strata thickening towards the basin-bounding normal fault (F1) i.e. its growth can still be used to predict a tectonic evolution for the offshore Benin Basin (see Chapter 3). Since the basin-bounding normal fault (F1) is in net extension, it was not affected by this deformation, but it was rather the intense buckling of the roll-over

anticline associated with basin-bounding normal fault (F1) that formed the Oga fold. A similar mechanism is invoked for the Elo thrust.

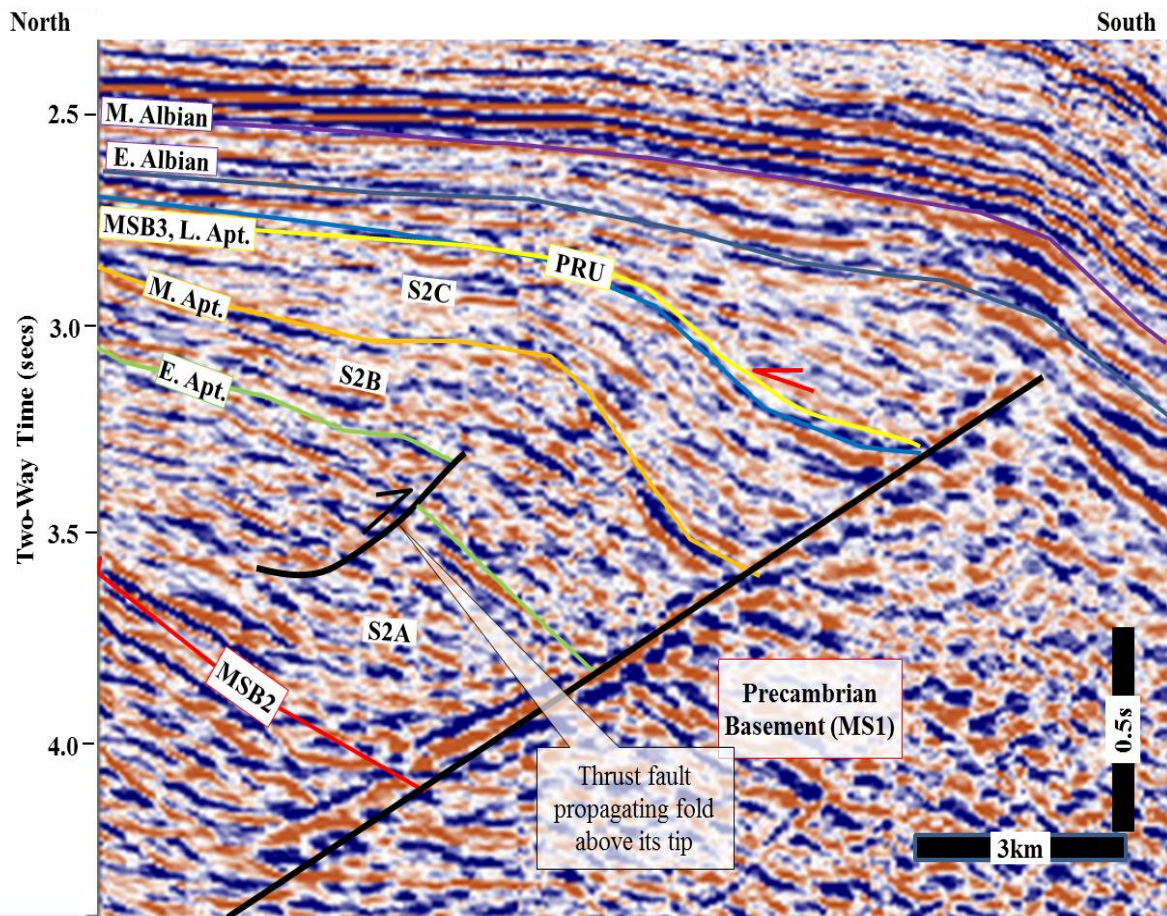


Figure 4.11: Dip line (crossline 3968) depicting the Oga fold in the northern half-graben. Note the onlapping seismic reflections on the forelimb of the fold. Seismic reflections were truncated by the post-rift unconformity (MSB3, Late Aptian). See Figure 4.10 for the location of the seismic section.

4.7.3 Ore thrust (late Aptian/early Albian)

Description of the Ore thrust

The Ore thrust occurs in the northwestern part of the northern half-graben (Figure 4.10). The seismic data indicate that the fault strikes NE-SW and dips 28-35° to the NW (Figure 4.13). A SE verging hanging-wall anticline is identified above this fault (Figure 4.13). Its seismic geometry also indicates that the structure is a fault-propagation fold. It is made up of the

asymmetrical anticline. It is also a thin-skinned structure because the basement is not folded, but only the overlying sedimentary successions show evidence of vertical movement along the fault plane (Figure 4.12).

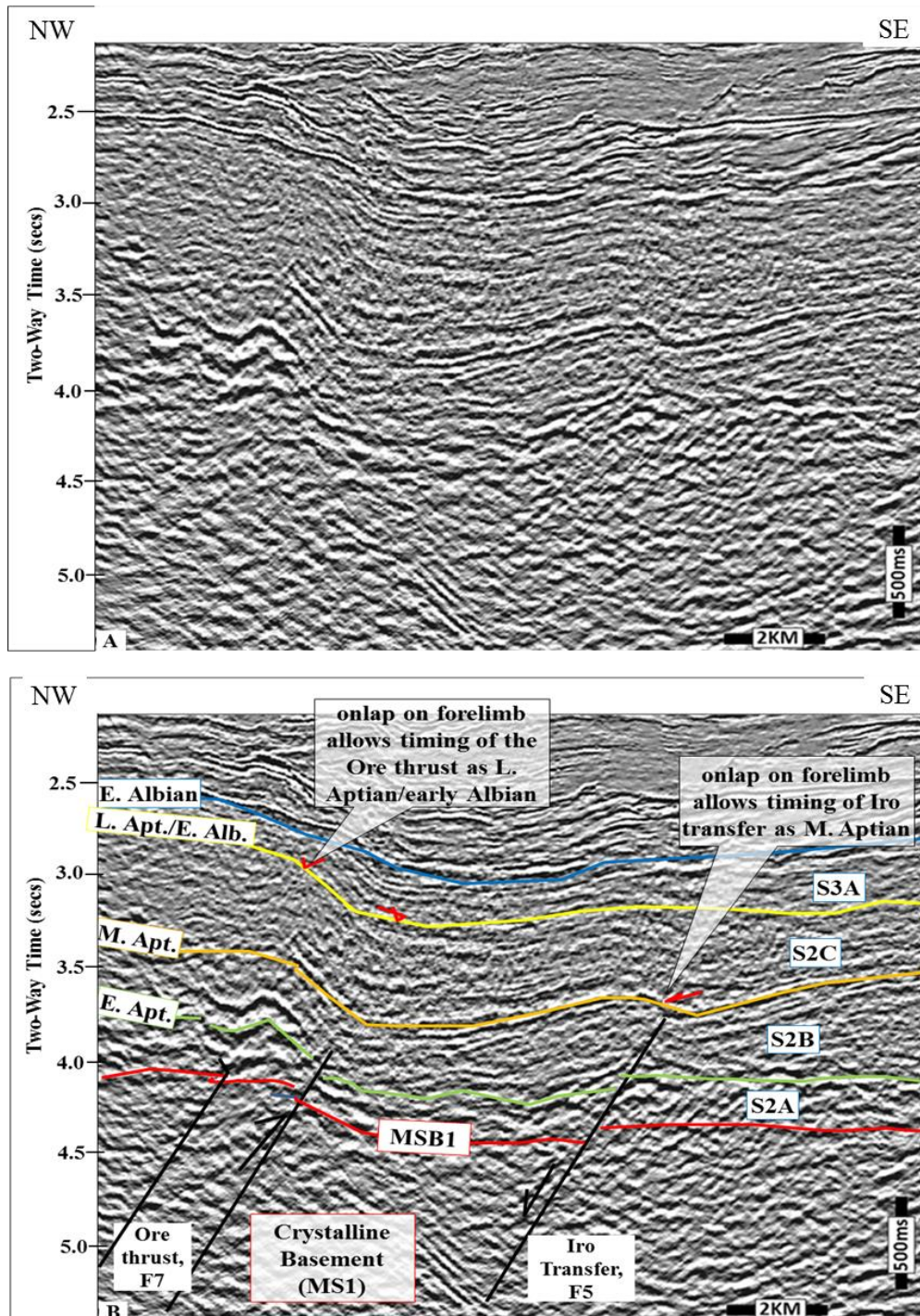


Figure 4.12: Arbitrary line (NW-SE) displaying the relationship between the Ore thrust and the Iro transfer in time of formation. See Figure 4.10 for the location of the seismic section.

The pre-fold succession is made up of folded parallel to sub-parallel reflections under the late Aptian (MSB3) onlap surface (Figure 4.13). The pre-fold succession consists of megasequences MS1 and MS2. No clear growth sequence is present around this fold structure. The Ore thrust is most-likely short-lived. Its forelimb consists of a syncline that is filled with post-fold strata comprising parallel to sub-parallel reflections (S3A) that onlap the forelimb (Figure 4.13).

Origin of Ore thrust

The seismic geometry indicates that the Ore thrust was formed by buckling against a pre-existing normal fault i.e. the basin-bounding normal fault (F1).

Timing of the late Aptian/early Albian deformation

The first phase of the deformation in megasequence MS3 (Elo thrust, Oga fold and Ore thrust) is dated using the onlapping relationship between parallel reflections in sequence S3A onto the fold limb of the associated fold (Figures 4.9 and 4.11). By definition, these parallel reflections post-dated the fold (MSB3) because a divergent reflection pattern is generally absent in sequence S3A.

The deformation in megasequence MS3 is interpreted to be short-lived. The onlapping surface (MSB3) is chosen to estimate the timing of this event because it is the first main onlap to the fold limb. The onlapping surface (MSB3) ties well to the post-rift unconformity (MSB3, late Aptian), while sequence S3A representing the oldest passive infill has been mapped as the immediate post-rift sequence and dated early Albian (Figure 4.11). The age of the phase of deformation that deformed megasequence MS3 is probably younger than the late Aptian, but older than the oldest deposits of the sequence S3A (early Albian). Therefore, it is interpreted that this phase of deformation in megasequence MS3 in the northern half-graben is late Aptian/early Albian in age.

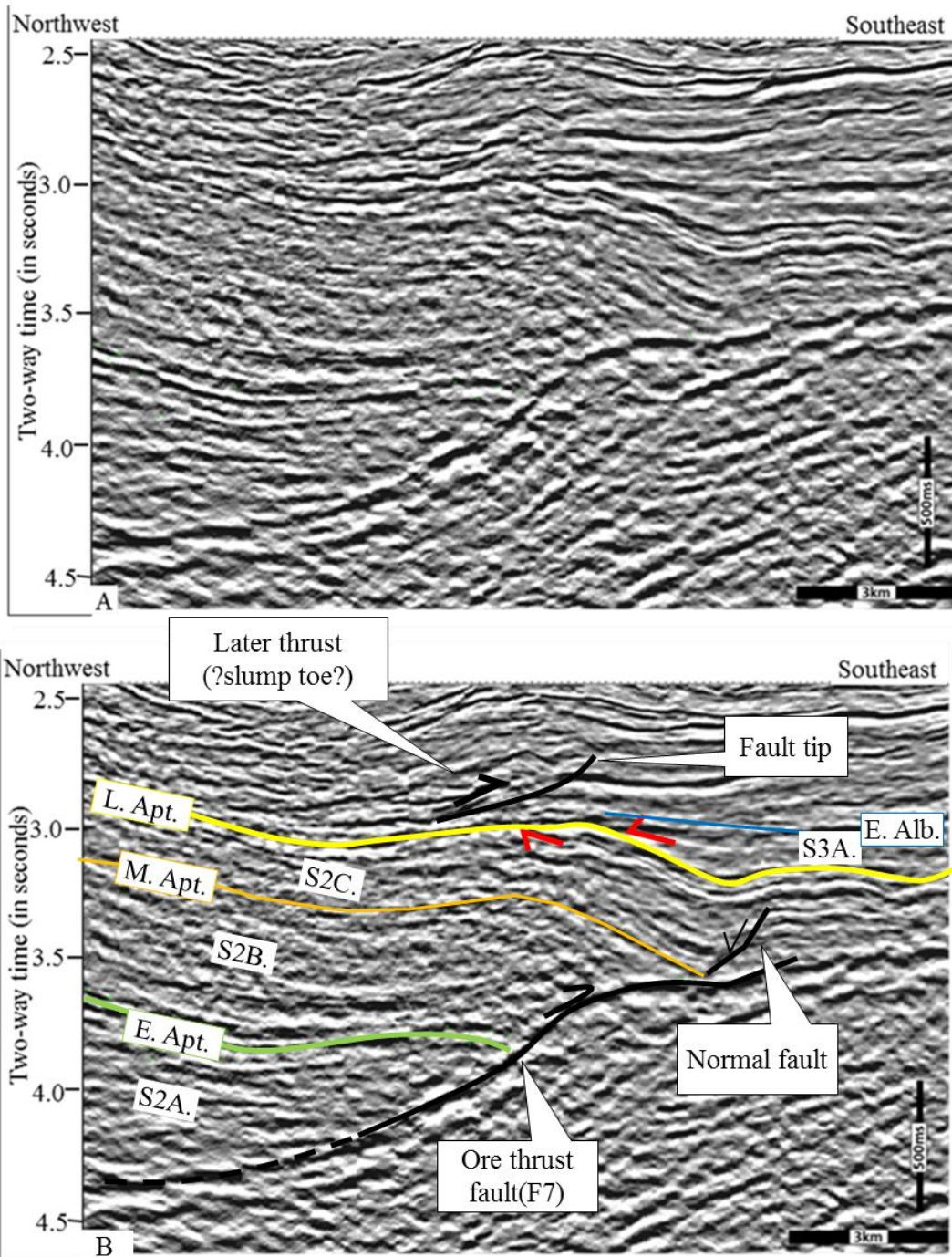


Figure 4.13: An arbitrary line (NW-SE) showing the Iro relay structure. See Figure 4.10 for the location of the seismic section.

4.7.4 Iro transfer zone (middle Aptian)

Description of Iro transfer

A transfer zone consisting of an association of transfer fault, relay, and basin-bounding normal fault exists in northwestern part of the study area (Figure 4.22). The transfer zone,

consisting of a NE-striking transfer fault, comprising a low-angle normal fault that connects two sub-basins (F1 and F4) in the northern half-graben (Figures 4.21 and 4.22). The relay structure is made up of a normal fault obliquely to the basin-bounding normal fault (F1). It dips northwesterly (Figure 4.12). The transfer structure is a basement-involved structure. Apart from these sub-basins, other smaller normal faults (Figure 4.14) also occur in the vicinity of these sub-basins. These normal faults are E- to ENE-striking, (i.e. parallel to the main basin-bounding normal fault (F1)).

Origin of the Iro transfer zone

The pre-fold succession includes both the sequence S2A, and sequence S2B while the syn-fold sequence is absent. The post-fold succession are the sequence S2C and younger. The fault geometry suggests a transfer of strain between the sub-basins (F1 and F4; Figure 4.21) as rifting in the northern half-graben reached the rift-climax stage in the middle Aptian. The small normal faults have similar mechanisms as the basin-bounding normal fault (F1) because of their orientations.

Timing of the Iro transfer zone

The seismic data show that the Iro transfer structure is relatively older than the Ore thrust (Figure 4.12). The seismic data suggest that the Iro transfer zone was not active until the middle Aptian. This implies that the transfer structure was probably active when continental rifting (Barremian – Aptian) was still on-going in the offshore Benin Basin. The Ore thrust, however, became active in the late Aptian/early Albian, i.e. after the cessation of continental rifting in the late Aptian.

4.8 Santonian deformation (SB3F)

This deformation is also associated with the post-rift megasequence (MS3) but considered to be significantly younger. The main structure associated with this deformation has been named the Eji anticline (Figure 4.15). The structure correlates to the major anticlinal trap structure in the Aje Field (e.g. Brownfield and Charpentier, 2006; Kaki et al., 2012).

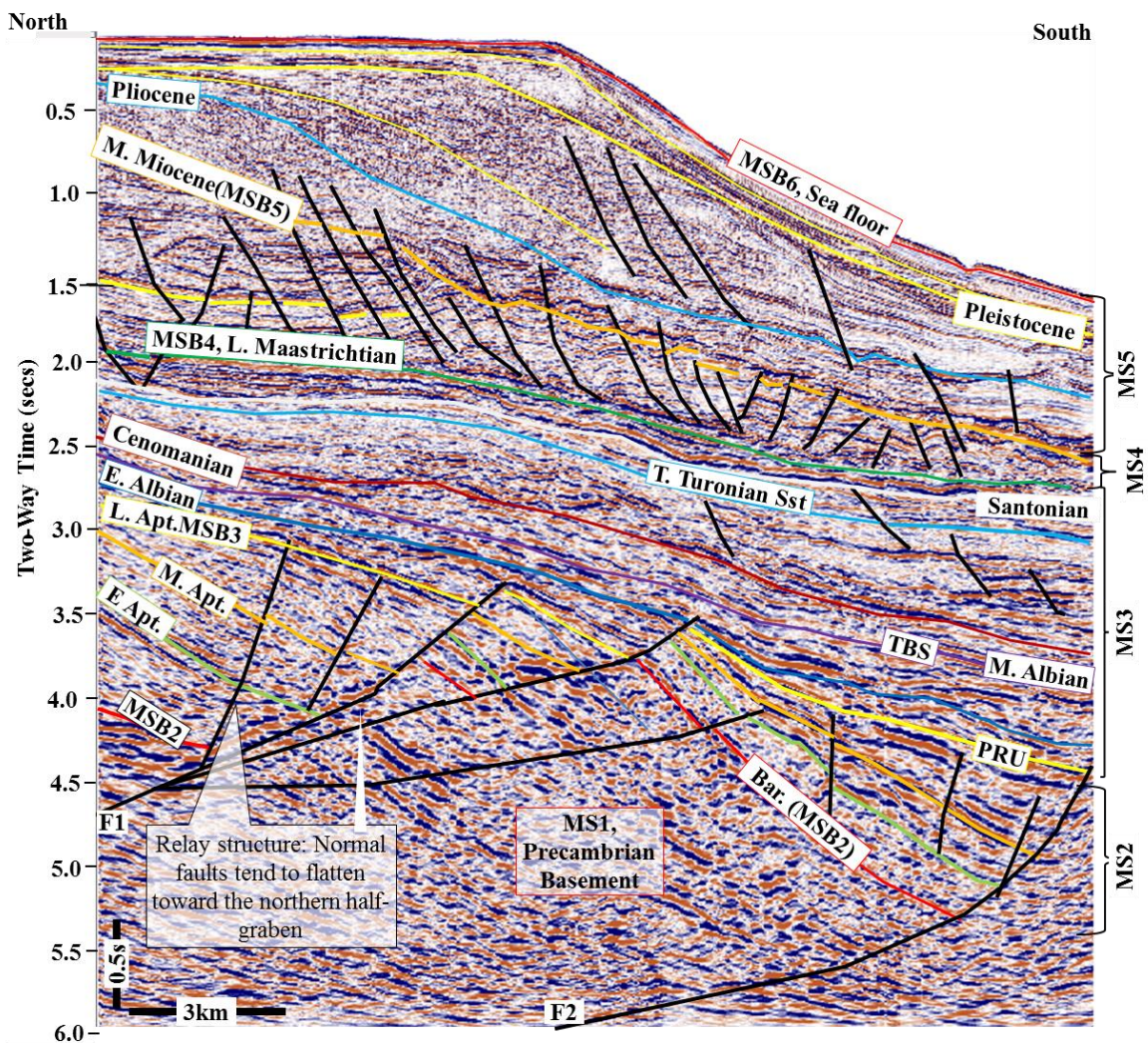


Figure 4.14: Association of some small faults (relay) and the basin-bounding normal fault (F1) in the northern half-graben, compared to the less deformed southern half-graben (see Figure 4.10 for the location of crossline 2698 shown in this figure).

4.8.1 Location of the Eji anticline (Santonian, SB3F) in megasequence MS3

The Eji anticline is mainly located in the southeastern part but is not in the half-graben – it is in the youngest strata above the basement highs separating the northern and southern half-grabens. However, it extends to the northeastern part of the northern half-graben (Figure 4.16). It is more regional in extent than other deformation events in the study area.

Description of the Eji anticline

The Eji structure is associated with a NE-striking (Figure 4.16), basement-involved thrust fault (F3) which dips 27-35° to the NW (Figure 4.15). The anticline is asymmetric, SE-verging, and plunges to the SW (Figure 4.15). It is interpreted to form only in the hanging-wall of the underlying basement-involved thrust fault, suggesting a genetic link between the two structures.

The geometry of the main thrust fault (F3) is relatively low in the basement but steepens upwards through the sedimentary cover (Figure 4.15). This fold, therefore, most likely comprises fault-propagation fold as there is no evidence of a pre-existing roll-over anticline. The fault disappears as it proceeds into the sediment cover. The basement has probably been offset by several thrust faults thereby make it look as a folded basement (Figure 4.15). At places, it behaves like a rigid block as folding is rarely observed. As a result of its basement-involvement, its style of deformation can be described as thick-skinned (Coward, 1983; Narr and Suppé, 1994; Nemçok et al., 2005).

The Eji anticline comprises the pre-fold, and post-fold successions (Figures 4.15 and 4.17). The pre-fold succession consists of high amplitude, chaotic and parallel to sub-parallel reflections comprising megasequence MS2, and in many sequences of MS3 (up to sequence S3E). Many of these sequences were affected by this phase of deformation probably because

the fault is steeper, longer and propagates from the basement. It also suggests that this phase of deformation post-dated sequence S3E (Santonian).

The fold does not show any clear evidence of growth. However, sequence S3F, a post-fold sequence of parallel reflections, thins onto the high, thickens to NW and SE and has small syn-sedimentary slump faults that dip away downslope from the anticline generated by faulting. The post-fold succession is composed of parallel reflections comprising sequences S3F and S3G, all sequences of MS4 and MS5.

A two-way time (TWT) structural map of the top of the fold onset unconformity (Santonian; SB3F) shows that there is a hinge line (which may mark the site of the palaeoshelf-edge) of Santonian age roughly along the blue line drawn in Figure 4.15. This is not exactly coincident with the anticline at all. The anticline does, however, mark a change in strike (trend) of the hinge line, and in the area to the NE, there is a major late Cretaceous embayment (or scallop) cutting back to the North. This canyon is clearly also seen on the seismic in Figure 4.16 (marked with the red and blue arrows), where it affects Cenomanian to Coniacian strata (S3C and S3E respectively) which seem to pre-date the Eji anticline.

Origin of the Eji anticline (Santonian, SB3F)

Basement reactivation during this phase of deformation appears not to involve the main basin-bounding normal faults (F1 and F2). This is because the ENE-WSW and E-W strike of the basin-bounding normal faults (F1 and F2) is not compatible with that of the NE-SW striking basement-induced reverse fault (F3).

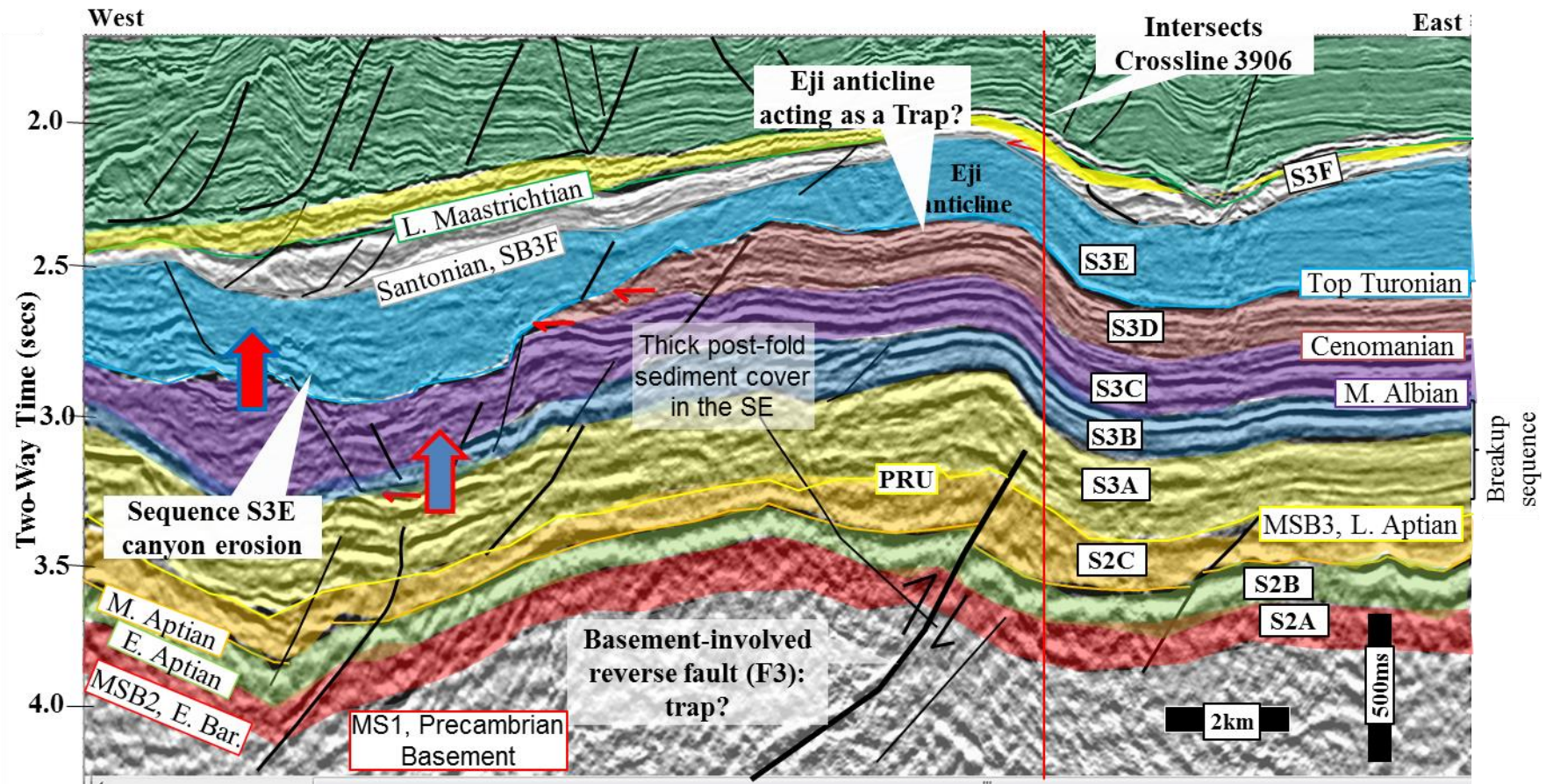


Figure 4.15: Inline 1398 showing the Eji anticline and the characteristic thinning of the sequence (S3F) at the fold hinge. In contrast, sequence S3F thickens at the backlimb and forelimb of the fold. Red arrows indicate where the canyon cuts to the north. Note the thick sediment to the SE as a result of Santonian deformation. See Figure 4.16 for the location of the seismic section.

Another evidence is that the reverse fault (F3) cross-cuts the basin-bounding normal fault (F1) in the northeastern part of the study (Figure 4.22). These observations suggest that the Santonian deformation is a much younger event affecting the Benin Basin than the continental rifting event. The basement structure separating these two half-grabens seems to have been reactivated. However, in this case, the deformation offsets the basement and did not reactivate the basin-bounding normal faults (F1 and F2) or uplift the syn-rift megasequence (MS2). A fault-propagation mechanism is suggested for this event, which accommodated deformation by folding at its fault tip (Figure 4.15).

4.9 Relationship in timing between the Santonian deformation and slumping

The timing of the Santonian deformation cannot be directly constrained because it also lacks an unequivocal growth sequence. The structures associated with this deformation, however, reflect no dip or thickness variations of the pre-fold sequences across the fold (Figure 4.18). Sequence S3F thins onto the anticlinal crest. Although there is little clear evidence that the sequence (S3F) was deposited during folding, it is more likely the folding event was short-lived. However, it generated a steeper slope to the SE and a gentler fold to the NW, leading to the slumping of post-fold sequence (e.g. sequence S3G; Figure 4.19). The older sequences S3C, S3D, and S3E were eroded by submarine canyon. The effect of the submarine canyon was to generate the erosive surface of the fold limb (i.e. SB3F) leading to its characteristic ‘S’ shape (Figure 4.19B). This may suggest that the folding caused increase in the slope gradient. Such sudden change in the slope gradient may lead to an emergence of submarine erosion and/or slumping. It can be suggested that the submarine erosion probably started at the same time as the Santonian deformation. The evidence supporting is the erosion of older sequences (S3C, S3D, and S3E; Figure 4.19C) prior to its deposition.

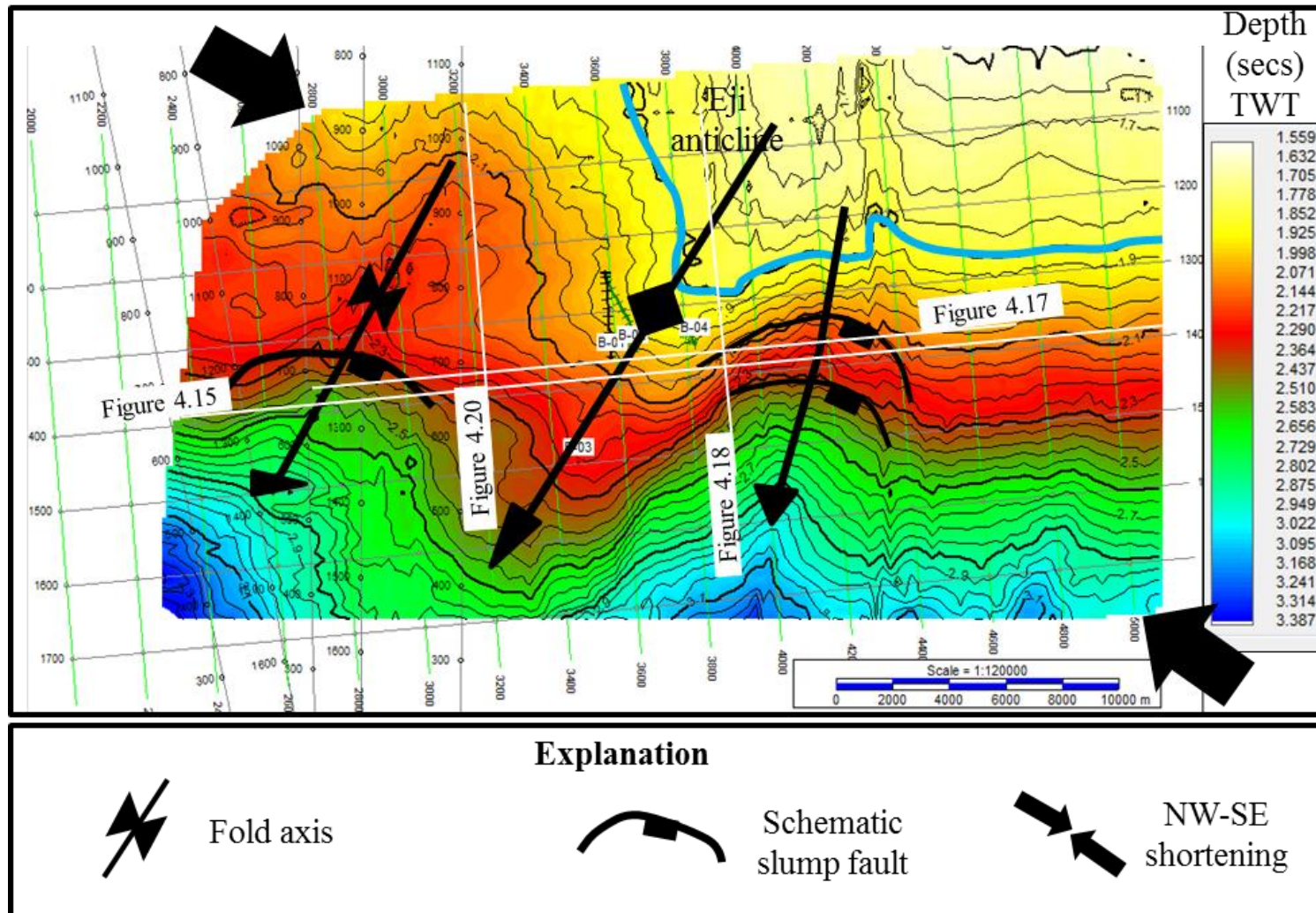


Figure 4.16: Time-structural map of the top Santonian (SB3F) in the study area. Note the high relief in the northeastern part of the map marking the position of the Eji anticline. A hinge line that may mark the Santonian palaeo-shelf edge occurs roughly along the thick blue line. Black arrows point to a NW-SE shortening direction. The locations of some of the seismic sections cited in the main text are indicated in this figure.

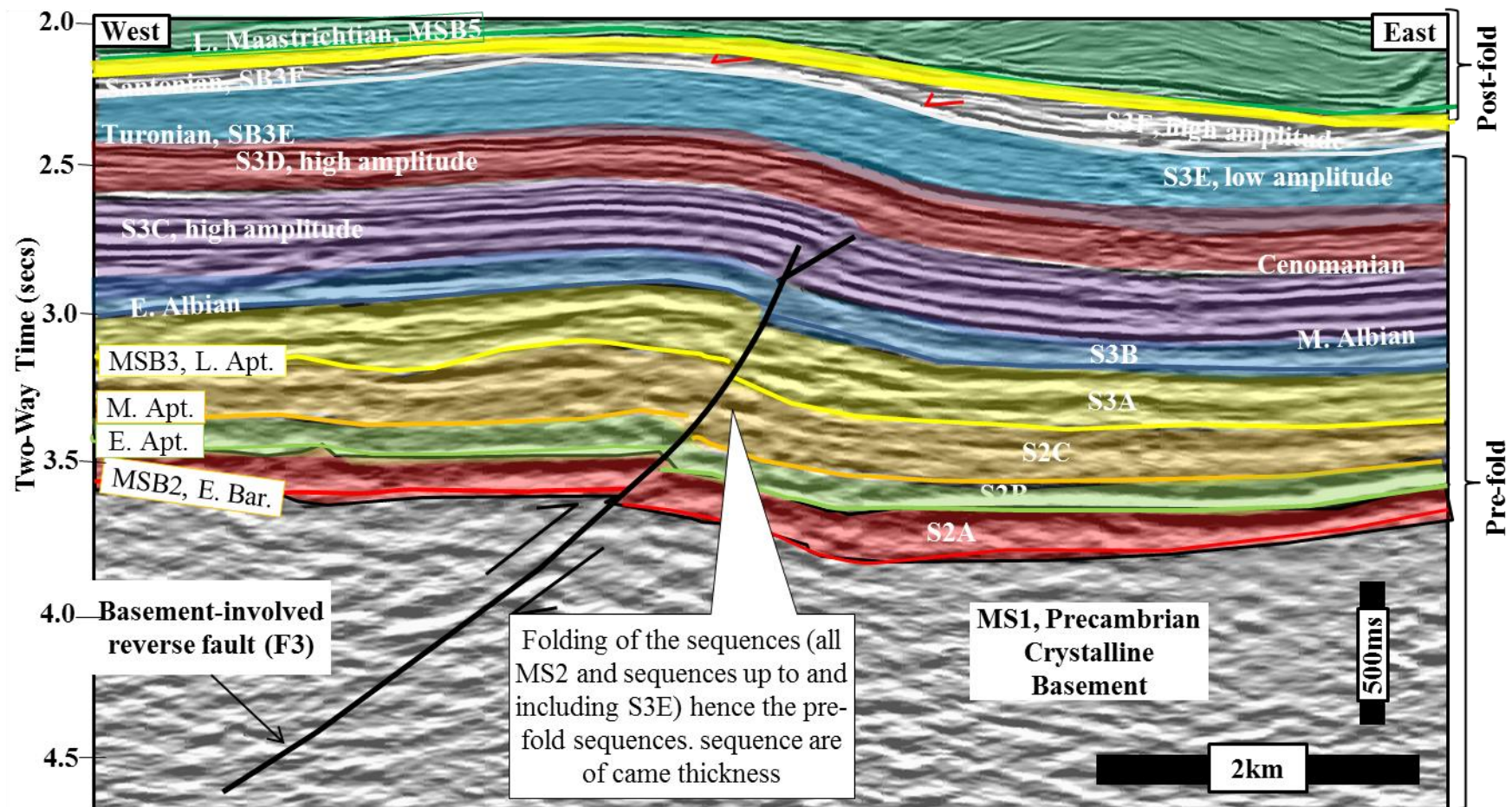


Figure 4.17: Coast-parallel line (inline 1380) showing the Eji anticline as formed by a basement-involved reverse fault (F3). Note the onlapping of parallel reflections on top of the forelimb of the anticline in SB3F (Santonian). Red arrows indicate the onlap of parallel reflections onto the forelimb of the anticline. The basement appears deformed by other subordinate small faults. See Figure 4.16 for the location of the seismic section.

Forced regression affecting these sequences is enhanced by the slope gradient. This was followed by the deposition of the post-fold sequence (S3F) that onlap the fold limb, in an event coeval with the downslope slumping (Figure 4.19D).

4.10 Young deformation event (?Miocene)

The main evidence for the possible occurrence of other deformation event is the folding of the seismic sequences after the Santonian (SB3F) (Figures 4.17 and 4.19). One of such inferred deformation events is associated with the transgressive megasequence (MS5) (Figure 4.20). The pre-fold succession of this deformation is made up of all sequences prior the Miocene. Growth sequences are not observed around these structures so it can be regarded as short-lived. The post-fold succession comprises parallel to sub-parallel reflections. This deformation may be dated ?Miocene. None of the possible contractional deformation events has been studied in detail in this thesis because these later structures were probably masked by Cenozoic erosion and canyon incision (Figure 4.20).

4.11 Mechanisms/causes of the contractional deformation in the offshore

Benin Basin

The geometry of folds and their internal features often reflect the mechanisms that formed them. The folding mechanism can be used to infer the general deformation conditions which persisted at the time.

Authors such as Suppé (1983), Schröder (1987), Williams et al. (1989), Mitria, 1990; 1993; Suppé et al. (1992), (1997), Ford et al. (1997), Smith and Hatton (1998), Finch et al. (2002) Vergés et al. (2002), Le Gall et al. (2005), Robert-Charrue and Burkhard (2008), Fossen (2012), Jabbour et al. (2012) and Masini et al. (2012) have studied the mechanisms of contractional structures.

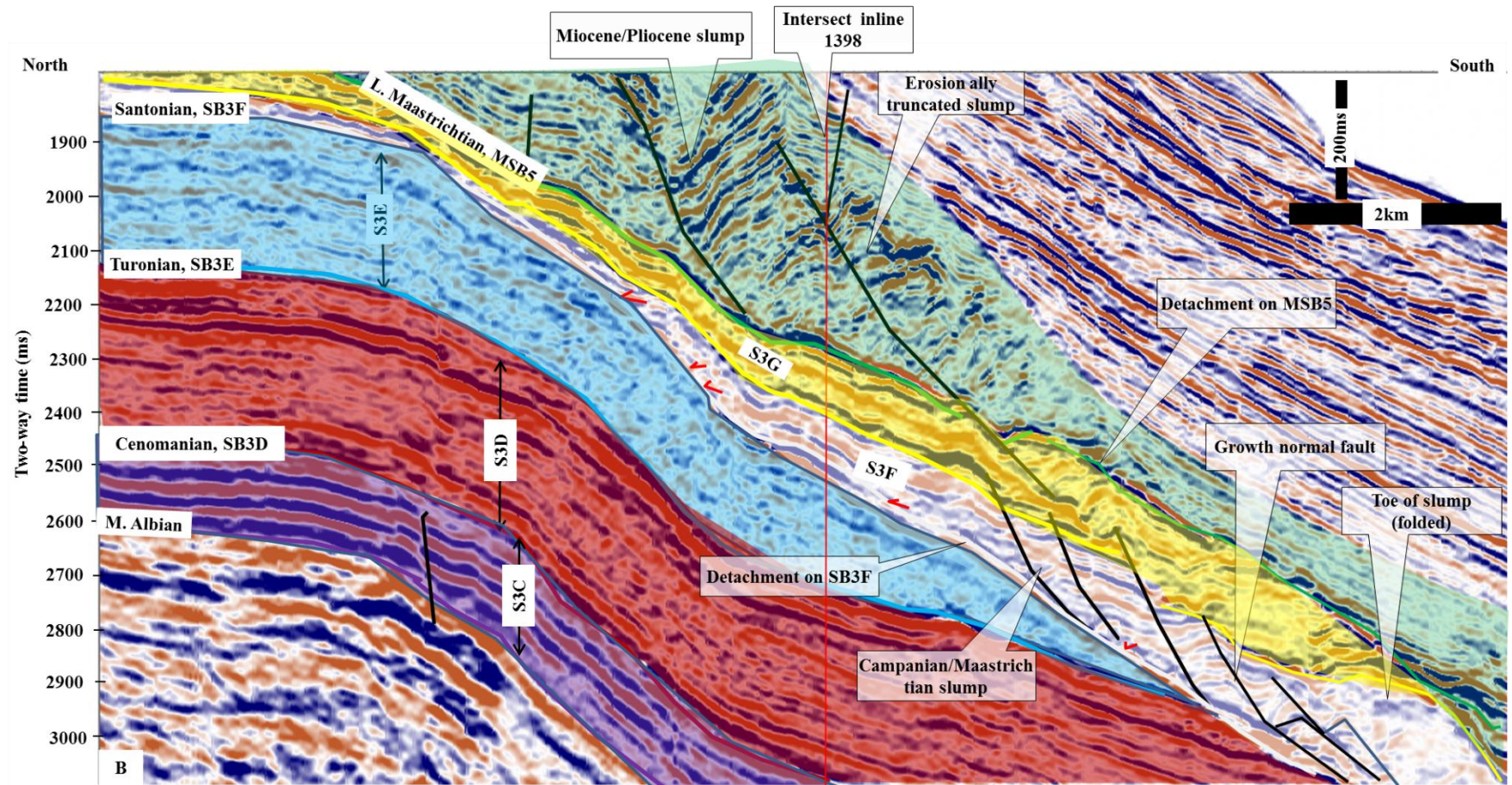


Figure 4.18: Crossline 3906 shows the relationship between the Santonian deformation, submarine erosion and slumping. See Figure 4.16 for the location of the seismic section.

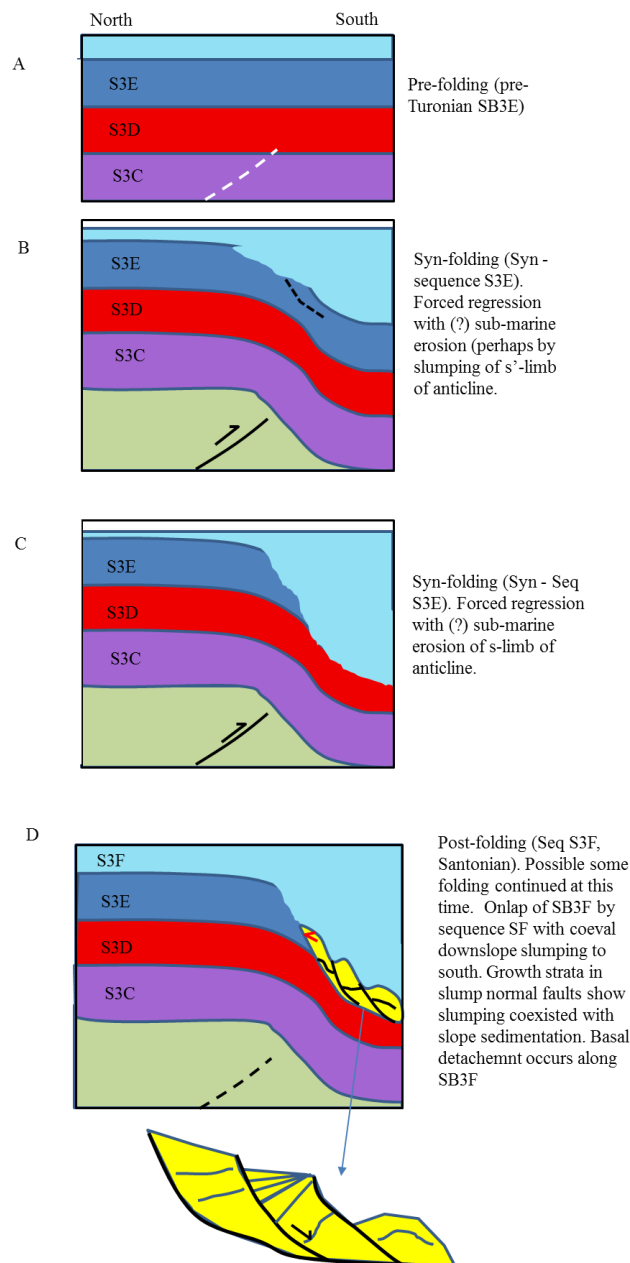


Figure 4.19: Schematic diagrams of the development of the Santonian deformation, submarine erosion and slumping.

It is important to establish the mechanisms of folding for these contractional structures because of the following:

- ❖ The folding mechanism may have a profound effect on fold geometry;
- ❖ The distribution of strain, and the types of structures that develop, all of which may serve to explore ore deposits and/or create structural traps for hydrocarbon reservoirs (Gutierrez-Alonso and Gross, 1999).

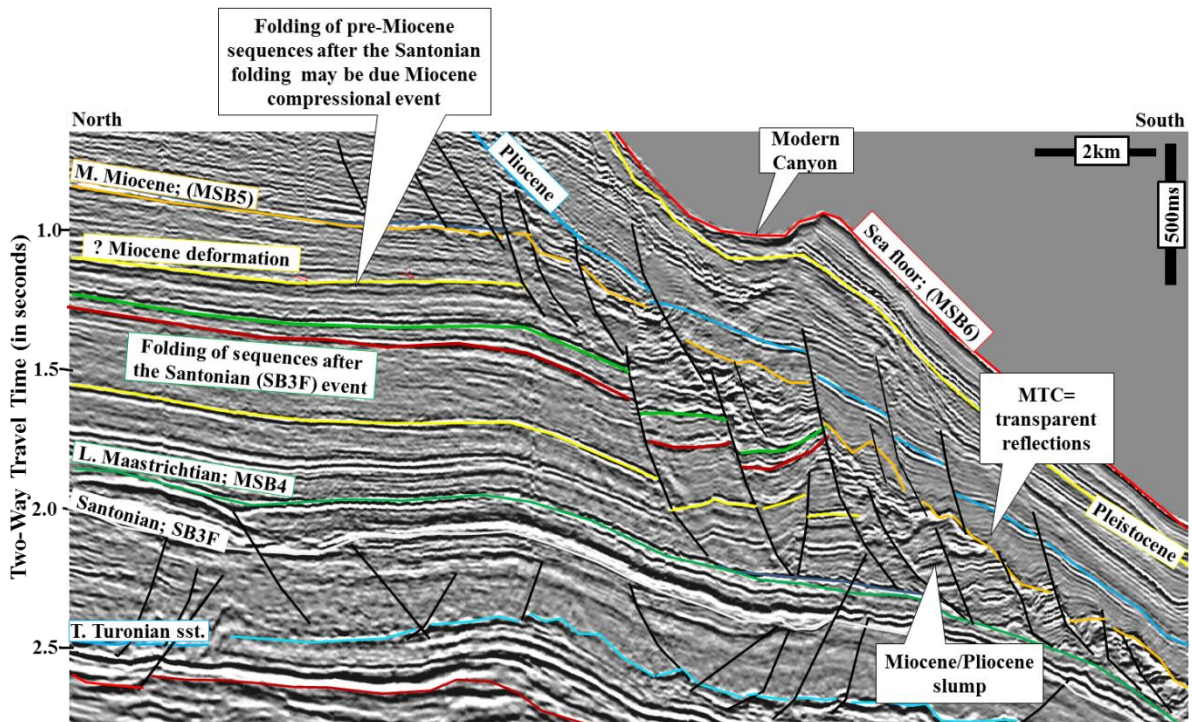


Figure 4.20: Crossline 3208 highlighting the folding of post-Santonian sequences. A possible ?Miocene folding event indicated by strata (red arrows) onlap, is proposed for this deformation. See Figure 4.16 for the location of the seismic section.

The different phases of deformation events that affected the offshore Benin Basin have some similarities in their geometries and orientations; for example, they both strike NE-SW (Figure 4.22). They are, however, incompatible in their ages. These imply that both late Aptian/early Albian and Santonian deformation evolved by different mechanisms. They are, however, deformed by similar NW-SE contraction. They are also different from those of the main basin-bounding normal faults (F1 and F2), which are the extensional faults that controlled sedimentation in the Barremian-Aptian rift episode in the Benin Basin (see Chapter 3). Therefore, this thesis suggests at least three major tectonic events in the offshore Benin Basin:

- ❖ Barremian-Aptian rifting (N-S extension; see chapter 3);
- ❖ Late Aptian/early Albian contractional deformation (giving rise to NE-striking structures) and;
- ❖ Santonian contractional deformation (also giving rise to NE-striking structures).

From the geometric analysis of the structures associated with late Aptian/early Albian deformation, there is no much direct evidence of reactivation in basin-bounding normal faults (F1 and F2) in the offshore Benin Basin. Folding of the Benin Basin was developed locally, typically in the vicinity of the basin-bounding normal faults. However, indirect evidence is the intensive buckling of the basin-bounding normal faults (F1 and F2), thereafter leading to deformation that was probably accommodated by thrusting and folding on the hanging-wall of the northern half-graben. Most folds appear to have developed as fault-propagation folds ahead of the tips of thrust faults. In many examples, the thrusts appear associated with reactivation of pre-existing normal faults, although new thrusts develop in areas of intense buckling (for example, during shortening of pre-existing roll-over anticlines). The ‘mild inversion’ of the NE-striking transfer fault is another probable mechanism for the late Aptian/early Albian deformation.

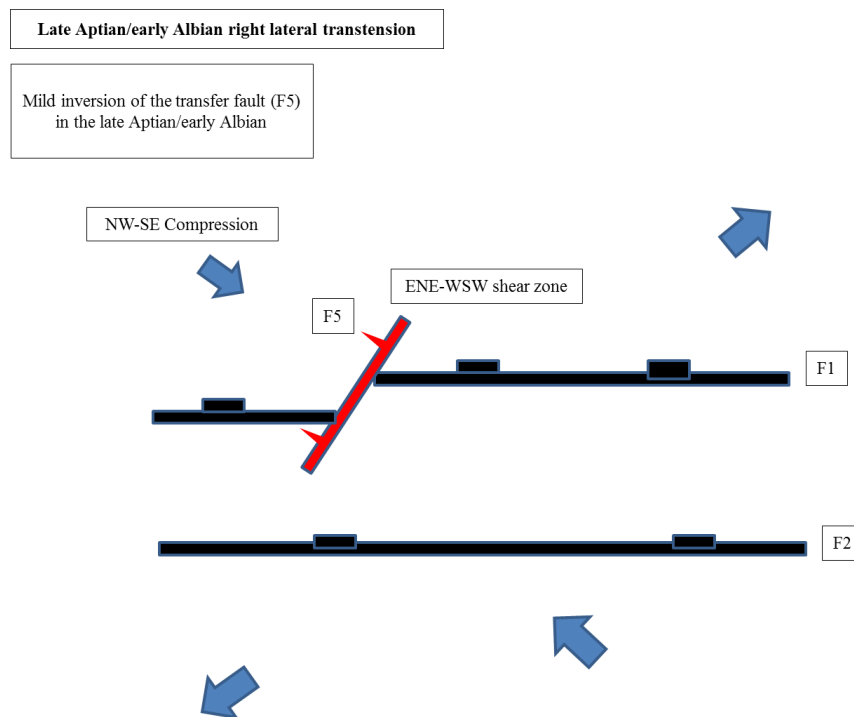


Figure 4.21: During the late Aptian/early Albian, a NW-SE oriented stress probably caused the mild inversion of the transfer fault F5.

The Santonian deformation is related to fault-propagation mechanisms where deformation is accommodated by thrusting and folding. It may be related to the reactivation that led to the development of a new NE-SW striking thrust and its associated fold. The discussion of the regional implications of these tectonic events is presented in Chapter 6.

4.12 Influence of the deformation events on stratigraphy and depositional systems in the offshore Benin Basin

The sequence stratigraphy of megasequence MS3, affected by the contractional deformation analysed in this dissertation shows that both the late Aptian/early Albian and Santonian (SB3F) deformation control the stratigraphy and depositional systems in the offshore Benin Basin. The late Aptian/early Albian deformation suggests passive infilling of the accommodation space. This is evidenced from the infilling of parallel reflections in the immediate post-rift sequence (S3A) that onlaps onto the fold limb. Such an infilling of parallel reflections is interpreted to have occurred after the folding ceased in the study area. The deformation event enhances erosion of the sequence because the deformation may have led to uplift and later erosion. The geometric analysis of structures associated with the Santonian deformation also suggests that it actively exerted an influence on the stratigraphy and depositional systems. The fault-related fold developed above a thrust fault that propagated from the basement into the Early Cretaceous units and stopped at Turonian level (i.e. sequence S3D). However, it accommodated further deformation by the folding of seismic sequences S3D and S3E (Figure 4.19). See Section 4.9 for the relationship between Santonian deformation and slumping. Well-log analysis of the sequence S3F shows that it consists of sands and mud (Figure 4.23).

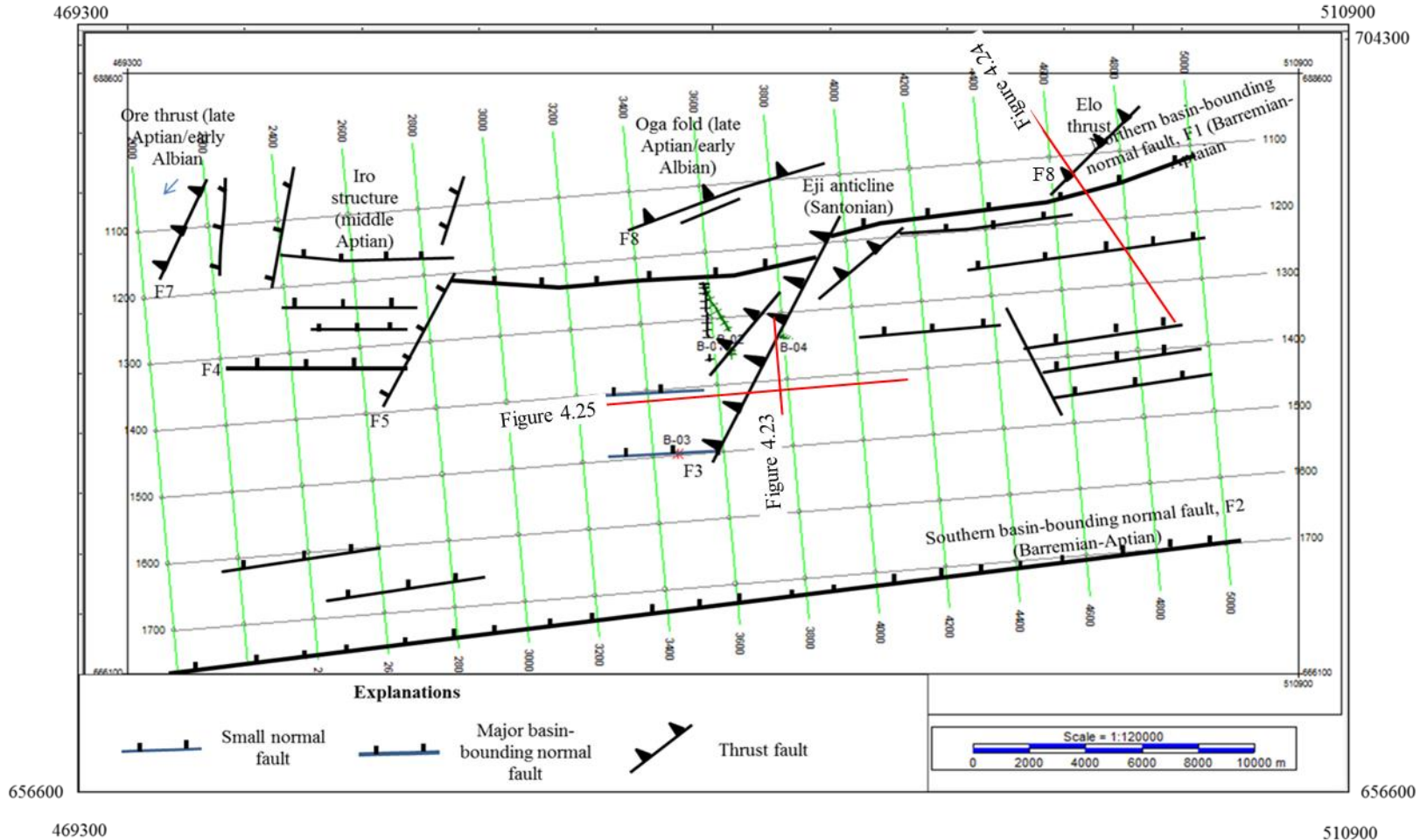


Figure 4.22: Structural elemental map showing the major tectonic features in the offshore Benin Basin. The major features are the E-W to ENE-WSW striking basin-bounding normal faults (F1 and F2) of Barremian-Aptian age. The later ones include NE-SW transfer structure (F5) (middle Aptian); the late Aptian/early Albian deformation (Elo thrust, Oga fold and Ore thrust). The last tectonic event recorded in the study area was in the Santonian (Eji anticline). Note how the later tectonic events (e.g. transfer fault F5; the reverse fault F3) offset the main basin-bounding normal fault F1 in the north. The locations of some of the seismic sections cited in the main text are indicated in this figure.

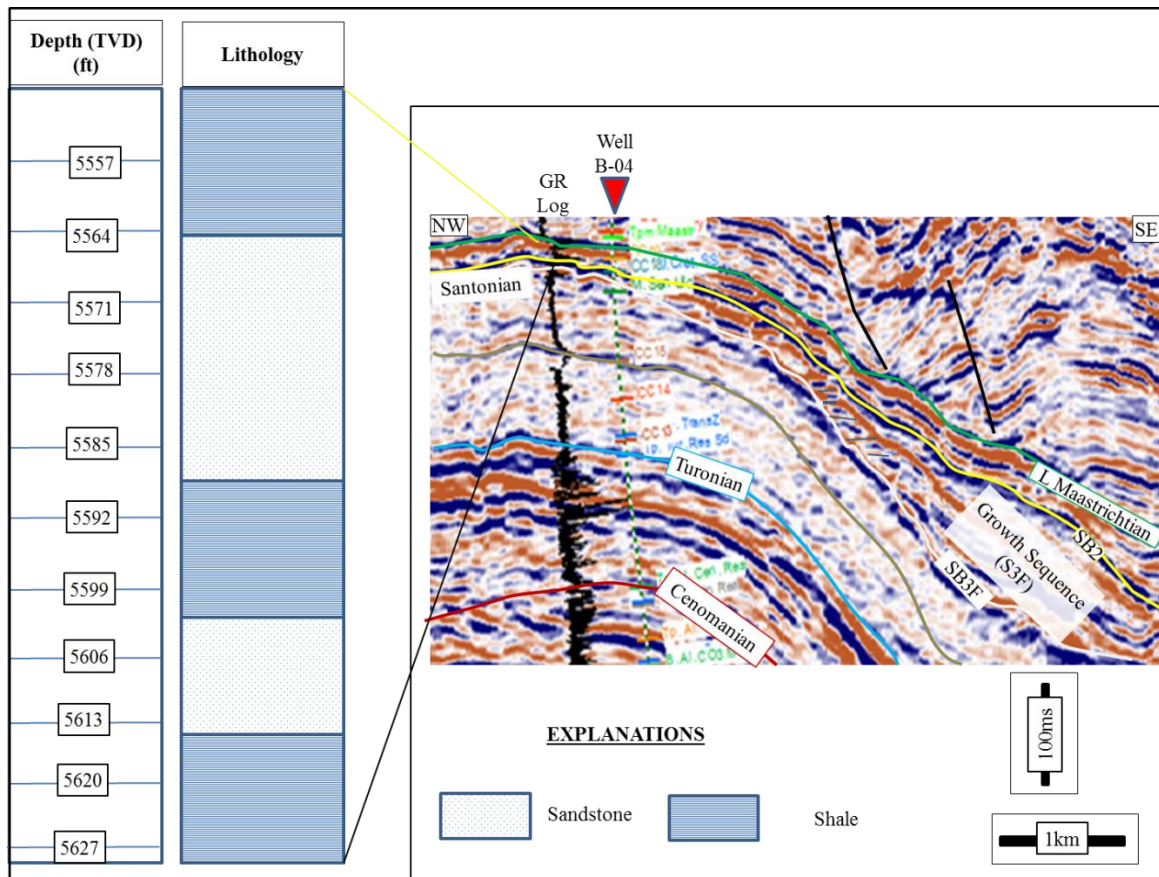


Figure 4.23: Lithologic analysis of sequence S3F based on the GR log of B-04. Sequence S3F consists of sandstone and shale. See Figure 4.22 for the location of the seismic section (crossline 3786).

4.13 Discussion

4.13.1 Significance of the breakup sequence in the offshore Benin Basin

The complete lithospheric breakup often occurred in two phases (e.g. Soares et al., 2012; 2014):

- ❖ The first stage of rifting and separation of the continental crust (i.e. this often involves continental crust breakup). This initial breakup of the African and South American Plates has been mapped and correlated in this study as the post-rift unconformity of late Aptian (MSB3).
- ❖ The second stage involves the upper mantle exhumation, extension and lithospheric breakup with accretion of normal oceanic crust (e.g. Whitmarsh et al., 2001; Tucholke

et al., 2007; Soares et al., 2012). Some authors have suggested that continental breakup is not quickly associated with normal oceanic crust on the distal margin (e.g. Whitmarsh et al., 2001; Tucholke et al., 2007; Soares et al., 2012). As a consequent of this, Soares et al., (2012) introduced a new terminology ‘lithospheric breakup surface (LBS)’ to replace the older breakup unconformity so to reflect the two stages.

Following Whitmarsh et al. (2001), Tucholke et al. (2007) and Soares et al. (2012), the breakup sequence (BS) has been established for the offshore Benin Basin on the basis of the regional correlations of two main seismic stratigraphic unconformities that mark these two stages of full continental breakup of the African and South American Plates in the Equatorial Atlantic segment.

- ❖ The late Aptian (MSB3) post-rift unconformity (this study)
- ❖ The middle Albian unconformity represents the final breakup of Africa and South America Plates in the Equatorial Atlantic margin (Greenoyd et al., 2008; Greenhalgh et al., 2011).

This study has shown that sequences S3A (early Albian) and S3B (middle Albian), belonging to the megasequence MS3, can be grouped as the breakup sequence (Figure 4.3). The two sequences (S3A and S3B) pre-date the middle Albian unconformity, which represents the final breakup of the African and South American Plates (Greenoyd et al., 2008; Greenhalgh et al., 2011). The top of the sequence S3B corresponds to the top of the breakup sequence (TBS; Figure 4.3). The identified TBS (middle Albian) comprises an onlapping surface and, therefore, correlates with the middle Albian unconformity of Greenoyd et al. (2008) and Greenhalgh et al. (2011).

The breakup sequence (sequences S3A and S3B) identified in this study correlates with the Albian Sandstone of Brownfield and Charpentier (2006) (Figure 1.15). Brownfield and Charpentier (2006) grouped the Albian Sandstone as belonging to the syn-transform

phase. The syn-transform grouping is in principle because the syn-transform phase often refers to post-rift phase of an extensional basin. This study has, however, demonstrated that the offshore Benin Basin is an extensional basin (section 3.7). The breakup sequence (sequences S3A and S3B, late Aptian-middle Albian) is a transitional phase that registers the change from syn-rift to post-rift condition in the offshore Benin Basin. Such a transitional phase has been identified on many divergent margins (e.g. Moore, 1992; Cainelli and Mohriak, 1999; Berglinger et al., 2012; Soares et al., 2012).

The seismic stratigraphic character of the breakup sequence (sequences S3A and S3B) presented in sections 4.5.1 and 4.5.2) suggests that these sequences were deposited under shallow marine conditions. This implies that the southwestern Nigerian margin, where the offshore Benin Basin is located, was already oceanic in the middle Albian whereas the Equatorial Atlantic margin was still evolving through prolonged transform tectonism (e.g. Heine and Brune, 2014).

The occurrence of the breakup sequence (S3A and S3B) in the offshore Benin Basin suggests that continental breakup process gradually took place in this region of the Equatorial Atlantic. It has been proposed by some authors (e.g. Sibuet et al., 2007) that extension on exhumed upper mantle, and normal oceanic crust emplacement, could have taken place contemporaneously until the later becomes predominant.

The breakup sequence (sequences S3A and S3B) overlying the post-rift unconformity (late Aptian, MSB3) does not only imply a change in sedimentation by mechanical subsidence to thermal subsidence but it also depicts that an abrupt change in stratigraphic architecture (and in the erosion locus) that often follows the continental breakup process. The breakup sequence (sequences S3A and S3B) marks the end of lithospheric thinning and the onset of erosion and uplift. This study has also shown that the offshore Benin

Basin was locally deformed during the deposition of the breakup sequence (sequence S3A, early Albian; see section 4.7).

4.13.2 Post-rift deformation and petroleum systems in the offshore Benin Basin

Tectonic deformation can enhance the accumulation of hydrocarbons on many passive rift basins of World (Harding et al., 1979). The tectonic inversion of hydrocarbon-bearing rifts can result in the remigration and redistribution of hydrocarbons into structures generated by the reactivation of pre-existing faults (Beauchamp et al., 1996; Cloetingh et al., 2008; Ziesch et al., 2017). Basin inversion can also form hydrocarbon traps for newly generated hydrocarbons. For such a migration of the generated hydrocarbon, it is required that the inverted structure is formed before hydrocarbon generation (North, 1985). It is, therefore, necessary to understand the deformation history of the rift basin before intensifying exploration, in order to reduce exploration risks. Examples of hydrocarbon-bearing inverted rift basins include the North Sea, Morocco (Beauchamp et al., 1996).

The structural style interpreted on the seismic data allows both the basin-bounding normal faults (F1 and F2) and other later faults such as the thrust/reverse faults (F3), and relay faults, to serve as hydrocarbon traps (Figures 4.24 and 4.25). These faults tend to act as migration pathways for hydrocarbons to move from the source rock into the reservoir rock. In Figure 4.24, the basin-bounding normal fault (F1) is a migration pathway for the hydrocarbon generated from potential source rocks (SR) in syn-rift strata (S2A). The other connecting faults, such as the late Aptian/early Albian thrust and associated faults, may also act as conduits for the hydrocarbon migration. Such hydrocarbons may then accumulate in the anticline associated with these later structures (Figure 4.24). The convex shape of the anticline prevents further upward migration of hydrocarbons. The hydrocarbons may then

accumulate in the associated folded structures (anticlines; Figure 4.24). The entrapment of the hydrocarbons was, therefore, enhanced by the late Aptian/early Albian basin inversion.

Other entrapment may be enhanced by Santonian (SB3F) deformation. For the examples in Figure 4.25, the hydrocarbons in other potential traps and reservoirs (e.g. the Albian, Cenomanian and Turonian reservoirs) are probably enhanced by the Santonian (SB3F) event. The structural styles registered on the seismic data reveal that the Santonian (SB3F) deformation event appears a more viable hydrocarbon trap than those traps formed by the late Aptian/early Albian deformation. The reason is probably because its reverse fault (F3) connects most of the pre-Santonian sedimentary strata and the crystalline basement rock (Figure 4.25). The reverse fault (F3), therefore, does not only allow the migration of hydrocarbons within the syn-rift megasequences (MS2) but also permits migration from potential sources in the syn-rift megasequence (MS2) to the potential reservoir rocks in the megasequence MS3 (Figure 4.25).

The migration of hydrocarbons through the reverse fault (F3) may probably lead to the accumulation of oil and gas in the Eji anticline. The Eji anticline may serve as the potential fold trap where its hydrocarbons accumulate. The Eji anticline is effective due to the presence of shale-dominated strata in sequence S3E acting as the potential seal preventing further vertical migration (Figure 4.25). The sealing competence of this shale unit, in addition to the trapping geometry of the anticline, increases the potential and viability of the Eji anticline. The hydrocarbons will eventually accumulate in the high-amplitude sequence S3D and interpreted as sandstone on well-logs. The sandstone reservoir is Turonian in age. This sandstone reservoir correlates with one of the proven reservoir rocks, i.e. the Cenomanian to Turonian sandstone reservoirs of Kaki et al. (2012). On the contrary, the structures formed during late Aptian/early Albian deformation tend to offer little potential for the accumulation

of hydrocarbons because they are generally small. The fault (F8) associated with these structures only connects sequences S2B and S2C (Figure 4.24B).

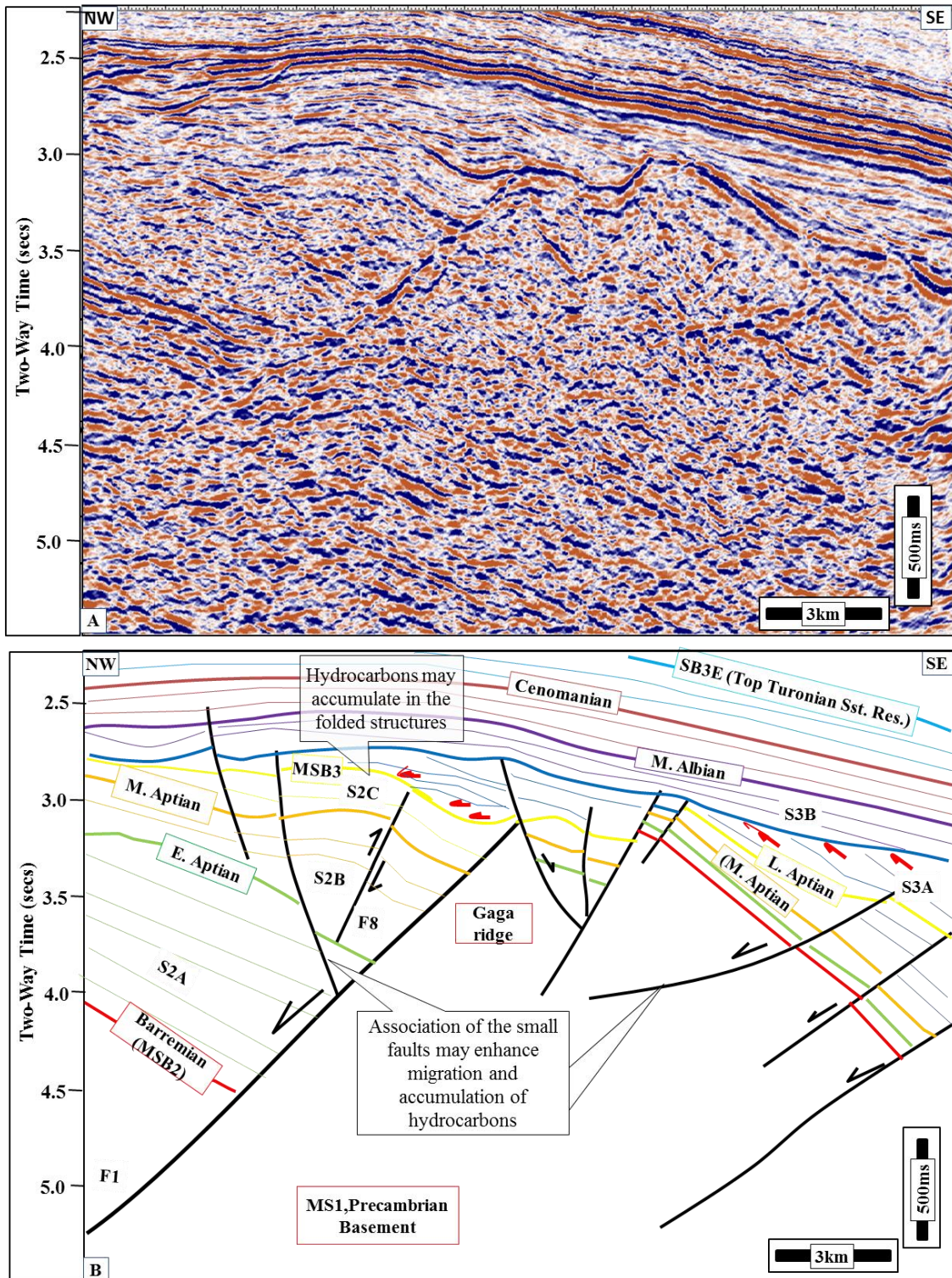


Figure 4.24: A) Uninterpreted NW-SE arbitrary seismic section. B) Interpreted section showing how contractional structures (folds and faults) may enhance accumulation of hydrocarbons in the offshore Benin Basin. See Figure 4.22 for the location of the seismic section.

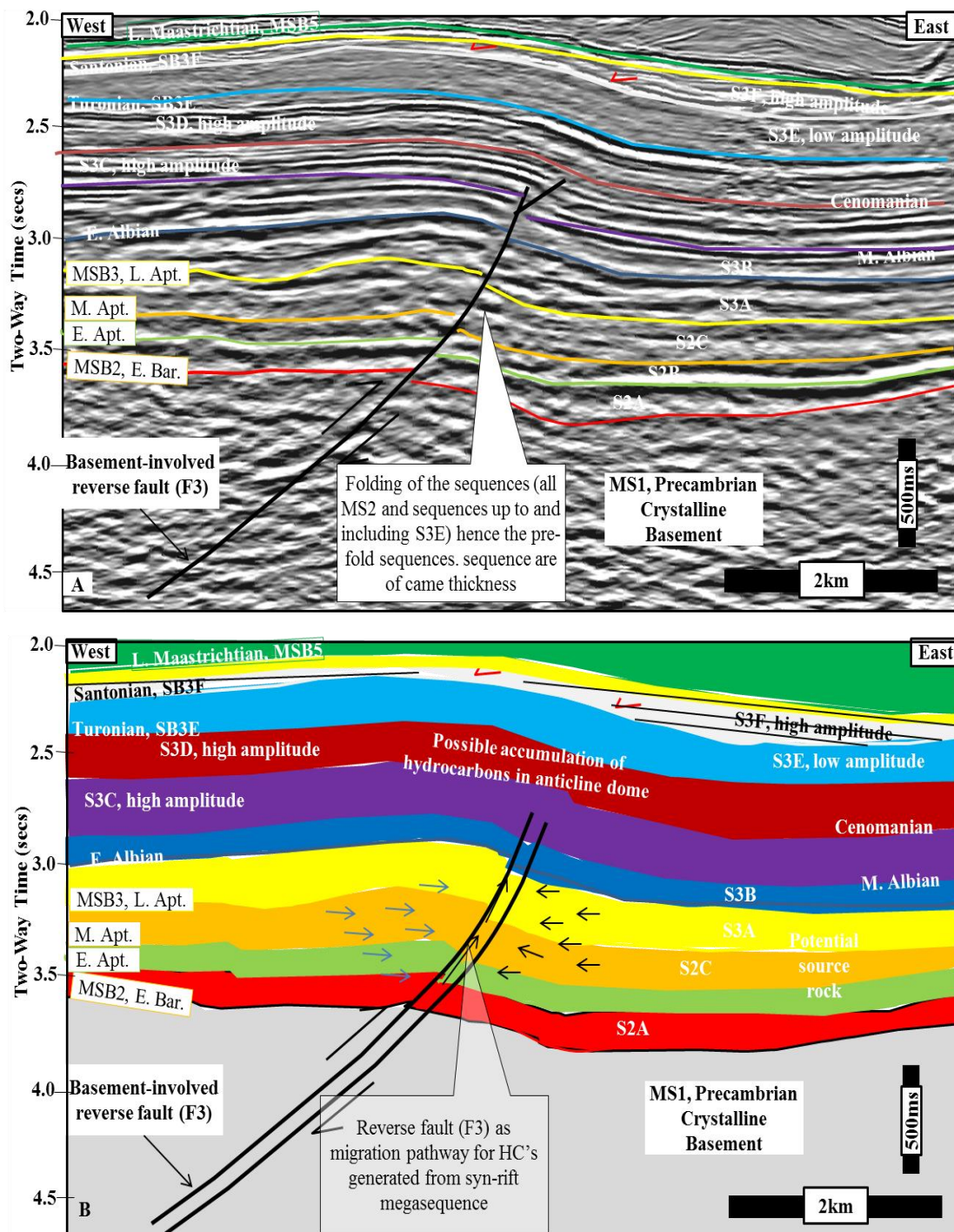


Figure 4.25: Summarised implications of the Santonian deformation for petroleum systems in the offshore Benin Basin. A) Interpreted seismic section (inline 1407) showing the seismic character of potential source rocks, reservoir rocks, petroleum seal and a possible migration pathway (F3) for the offshore Benin Basin. B) Petroleum systems of the basin as interpreted from seismic data. Note that the major reverse fault (F3) serves as migration pathway for hydrocarbons. See Figure 4.16 for the location of the seismic section. See Figure 4.22 for the location of the seismic section.

4.14 Conclusions

The megasequence MS3 reveals a seismic character that suggests thermal subsidence control sedimentation in the offshore Benin Basin since the late Aptian (MSB3). The seismic stratigraphy of the megasequence MS3 is generally characterised by parallel to sub-parallel, continuous to non-continuous, low to high amplitude reflectors that overly the divergent reflectors of the syn-rift megasequence (MS2). Seven sequences have been established for the megasequence MS3: sequences S3A, S3B, S3C, S3D, S3E, S3E, S3F, and S3G (Table 4.1). The megasequence MS3 is also comprises the breakup sequence (sequences S3A and S3B). The breakup sequence represents the transitional phase between onset of separation and final continental separation.

The sequences in megasequence MS3 have been deformed as their seismic reflectors are folded. Two of the contractional episodes that affected the basin have been studied:

- ❖ Late Aptian/early Albian deformation.
- ❖ Santonian (SB3F) deformation.

The two events created NE-SW striking structures. These strike directions differently from the E-W to ENE-WSW strike of the basin-bounding normal faults (F1 and F2), and suggest different mechanisms responsible for both extensional and contractional structures studied in the thesis.

The late Aptian/early Albian deformation is localised in the northern half-graben. The mechanism proposed for this deformation is intensive buckling of the roll-over anticline occurring in association with the basin-bounding normal fault (F1). This subsequently led to deformation of the basin by thrusting and ‘mild inversion of an initial NE-SW striking transfer fault in the study area.

The Santonian deformation was caused by a fault-propagation mechanism. Basement reactivation led to development of a new thrust (F3). Both deformation episodes are however related to structures formed by NW-SE directed compressional stress resulting in transpressional movements in the NE-SW direction. These imply that from the late Aptian/early Albian, the Nigerian and Brazilian margin had probably been separating from each other (see Sections 6.3 and 6.4 for their implication for geodynamics).

The study also shows that the Santonian deformation exerted a control on sedimentation between Santonian and Campanian. Structures developed during this deformation episode form structural traps for petroleum in this basin. The Santonian structures look more promising (e.g. Figure 4.25).

Chapter Five

5.0 Cenozoic Geology of the offshore Benin Basin

This chapter describes the two youngest megasequences (transgressive megasequence, MS4; and regressive megasequence, MS5) of Cenozoic age. These megasequences are located below the present day continental shelf to the continental slope. It considers the influence of the non-tectonic factors (relative sea level changes, sediment supply, and basin morphology) on sedimentation during the post-rift phase of the offshore Benin Basin.

5.1 Introduction

The understanding of deep-water depositional systems has progressively increased in recent years. In the past, much understanding of deep-water sedimentation was from studies of outcrops, recent fan systems, and seismic reflection data (Normark, 1978; Howell and Normark, 1982; Twichell and Roberts, 1982; Posamentier et al., 1991; Weimer, 1991; Mutti and Normark, 1991; Twichell, et al., 1992; Posamentier and Kolla, 2003; Masson et al., 2006). In recent years, 3D seismic data has provided more detailed understanding of the architecture of the mass-transport complexes (Frey-Martinez et al., 2005, 2006; Moscardelli et al., 2006; Bull et al., 2009).

The Cenozoic deposits of the offshore Benin Basin have not been studied in detail because of the lack of subsurface data. The few works that cover them include Billman (1992); Pacht et al. (1994); MacGregor et al. (2003); Nton et al. (2006); (2009); Brownfield and Charpentier (2006); Olabode and Adekoya (2008); Kaki et al. (2012); and D'Almeida et al. (2016). Most of these studies were done on a regional scale and not limited to the Cenozoic. In their

studies, Olabode and Adekoya (2008) discussed the seismic stratigraphy of the Avon Canyon, which is Cenozoic in age. Their study was based on 2D seismic data.

This chapter considers the seismic sequence stratigraphy of the Cenozoic strata in the offshore Benin Basin. It involves describing, interpreting and evaluating seismic geometries to infer the stacking patterns of sediments. The Cenozoic was evaluated for any possible occurrences of mass-transport complexes (MTCs) and their associated deposits. The seismic data were analysed for growth sequence to estimate when the MTCs were formed. The Cenozoic was tested for the control of relative sea level changes on sedimentation.

5.2 Aims and objectives

The aims of this chapter include:

- ❖ To describe, interpret and evaluate stratigraphic changes and gravity-driven deformation in Cenozoic strata of the study area.
- ❖ To produce a more detailed sequence stratigraphic interpretation for the prograding clastic successions of the regressive megasequence (MS5), and to interpret this in terms of changes in relative sea level and sediment supply.

In order to achieve these aims, the following objectives are addressed:

- ❖ The Cenozoic intervals will be analysed for possible gravity-driven structures in order predict a distribution style and possible cause of the slope failures in the study area.
- ❖ The growth sequences will be used to estimate the timing of when slumping possibly started and ended in the study area.
- ❖ The sequence stratigraphic models such Vail et al. (1977) and Neal and Abreu (2009) will be applied to the regressive megasequence (MS5) to test the validity of these models.

The Vail et al. (1977) model is based on the identification of reflection terminations that defined the sequence boundaries and subsequently the seismic sequences that these sequence boundaries bound. The Neal and Abreu (2009) model is based on shoreline trajectory of the depositional sequences.

5.3 Terminology applied in this chapter

Many terminologies have applied to describe deposits of MTCs in literature such as submarine slides, slumps, debris flow, turbidites, gravitational collapse structures, submarine landslides, slope failures (Almagor and Garfunkel, 1979; Hesthammer and Fossen, 1999; Canals et al., 2004). The deposits of the MTCs have also been referred to as mass-transport deposits (MTDs). In this study, MTCs will be used to cover the mass movement deposits that are strictly gravity-driven (Moscardelli and Wood, 2008). The MTCs, therefore, include the submarine slides, submarine slumps, and debris flows. Turbidites are not included because they are supported by fluid turbulence (fine particles such as muddy sediments flowing at high current velocity under the influence of gravity). MTCs are however consequences of slope instability events (Moscardelli and Wood, 2008; Alves, 2015).

According to Weimer and Shipp (2004), MTC is a seismic stratigraphic term that can only be applied to features at a scale that can be fully imaged on volumetrically large seismic surveys. They range in size and shape, from an infilling Intra slope basin to several 1000s square km in unconfined settings; their thicknesses vary from 5-100s metres (Weimer and Shipp, 2004). Weimer (1989, 1990) defined the term mass-transport complex as sediments occurring at the base of sequences and are overlain by channel and levee sediments. In some settings, about 70% of the entire slope and deep water environments are made up of MTCs and their associated deposits (Beauboeuf and Friedman, 2000; Maslin et al., 2004).

Sequence stratigraphy has also evolved so that different techniques and approaches, each with their own set of terminology, have developed (Posamentier and Vail, 1988; Posamentier et al., 1988; Hunt and Tucker, 1992; Posamentier and Allen, 1993; 1999). These have recently been reviewed by Catuneanu et al. (2009) and Embry (2009).

5.3.1 Mass-transport complexes (MTCs)

Mass-transport complexes are known to occur in rift basins and continental margins (Kenyon, 1987; Kenyon and Millington, 1995; Newton et al., 2004; Moscardelli et al., 2006; Moscardelli and Wood, 2008; Bull et al., 2009; Alves, 2015; Gamboa and Alves, 2015a and 2015b). MTCs have become the focus of research in the last two decades because they constitute a major part of the siliciclastic systems (Posamentier et al., 2000; Canals et al., 2004; Moscardelli et al., 2006; Posamentier and Walker, 2006; Gong et al., 2011). They may act as both lateral and top seals for petroleum accumulation in an underlying reservoir rock (Moscardelli et al., 2006; Weimer and Slatt, 2007; Gong et al., 2014). They generally have poor reservoir quality because of a high proportion of fine particles such as muddy sediments (Shepard, 1934; 1981; Shipp et al., 2004; Moscardelli et al., 2006; Weimer and Slatt, 2007; Zhu et al., 2011). Few have been recognised as reservoir rocks (Weimer and Slatt, 2007; Zhu et al., 2011).

MTCs have been documented in deep-water areas of most continental margins around the World such as in the Mid-Eocene/Oligocene Espirito Santo Basin (Gamboa et al., 2010; Omosanya and Alves, 2014; Gamboa and Alves, 2015b); the Miocene-Holocene Qiongdongnan Basin in China (Li et al., 2015); the Miocene Angola Slides, the Quaternary Israel Slump Complexes (Frey-Martinez et al., 2005) the Plio-Pleistocene Trinidad (Moscardelli et al., 2006; Moscardelli and Wood, 2008); the Holocene Gaviota MTC, California (Lee et al., 2004); the Pleistocene Amazon Fan MTCs (Piper et al., 1997); the

Holocene Storegga Slide (Bouriak et al. 2000; Haflidason et al., 2004, 2005; Bryn et al., 2005); Plio-Pleistocene Gulf of Mexico (Weimer, 1989; 1990; 1991). Their deposits have attracted interest from many workers because of their importance in sediment distribution and deposition between the continental shelf, continental slope, rise and deep-water environments (Lastras et al., 2004; Li et al., 2015). Many authors have documented their architectures which have been used to infer their kinematics (Bull et al., 2009; Gong et al., 2014).

Classifications of mass-transport complexes (MTCs) have been carried out by many authors (Nardin et al., 1979; Moscardelli et al., 2006; Moscardelli and Wood, 2008). Moscardelli and Wood (2008) classified mass-transport complexes (MTCs) on the basis of their causal mechanisms and pre-failure conditions (Figure 5.1). This scheme of Moscardelli and Wood (2008) emphasises the relationship between mass-failures and the geomorphology of their sources. Moscardelli and Wood (2008) grouped mass-transport complexes into three:

- ❖ shelf-attached systems: formed as shelf-edge deltas supplied sediments under the influences of changes in sea level and rates of sedimentation (Figure 5.1b);
- ❖ slope-attached systems: these are formed when upper slope sediments catastrophically fail due to gas-hydrate disruptions and/or earthquakes and (Figure 5.1a);
- ❖ Locally detached systems: these are formed due to local instabilities in the seafloor that trigger relatively small collapses (Figure 5.1c-e).

5.4 Methodology

5.4.1 Sequence stratigraphic analysis

The sequence stratigraphic analysis described in section 2.5.2 is applied to the Cenozoic megasequences (MS4 and MS5). The models of Vail et al. (1977) and Neal and Abreu (2009) are applied to middle Miocene - Holocene sequences of the regressive megasequence (MS5)

in order to establish the stacking patterns with respect to a relative change in sea level. Both time slices and two-way travel time (TWT) structural maps of the basal surfaces of the documented MTC of the transgressive megasequence (MS4) were made to understand the topographic controls on the overlying MTCs.

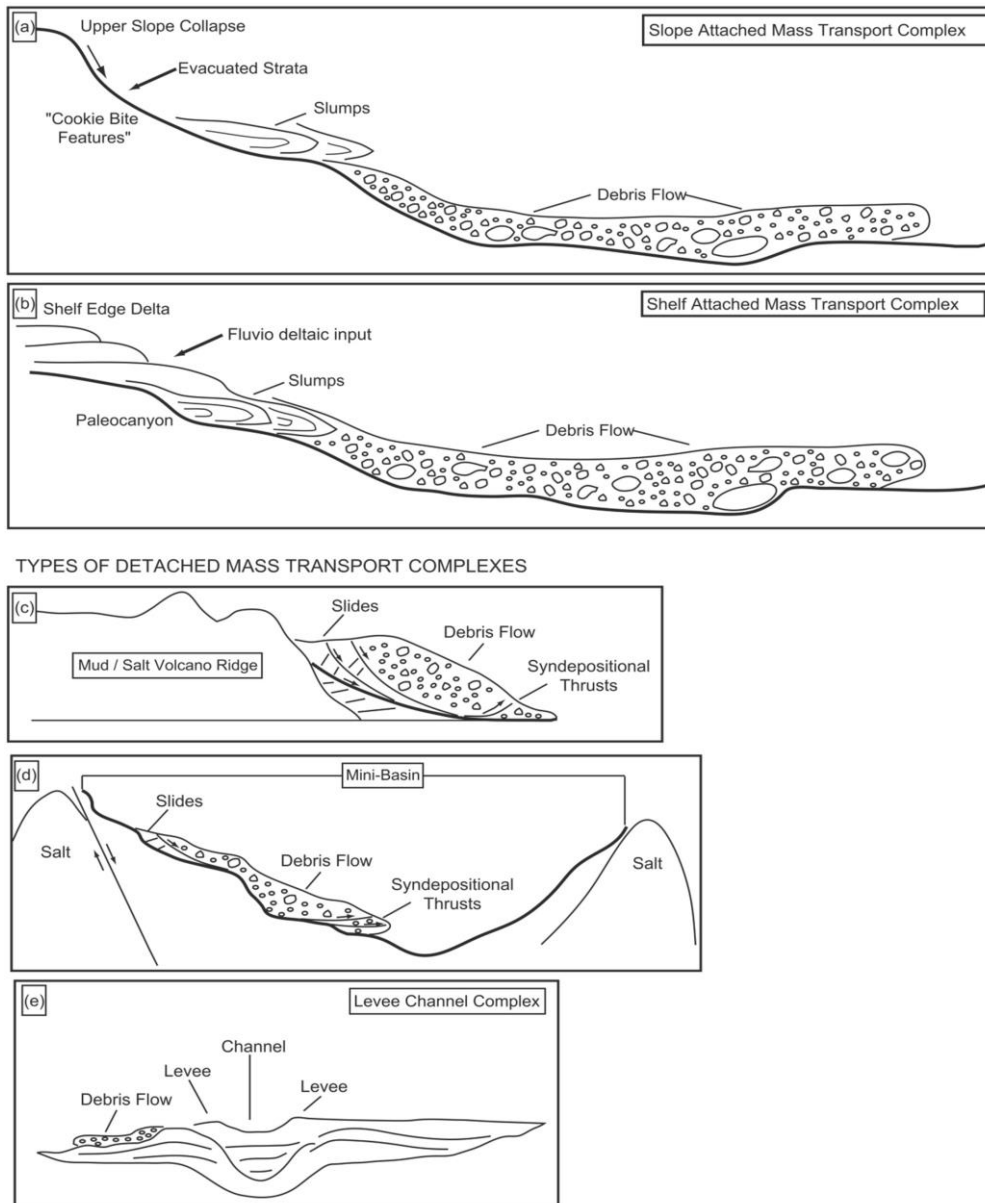


Figure 5.1: Schematic classification of MTCs based on causal mechanisms and pre-failure conditions. (a) Slope attached mass-transport complex. (b) Shelf-attached mass-transport complex. (c) Detached mass-transport from collapsing flank of a mud-volcano ridge. (d) Detached mass-transport complex formed through oversteepening of one of the margin. (e) Detached mass-transport complex derived from a levee-channel complex (from Moscardelli and Wood, 2008).

The shoreline trajectory analysis involves assigning traditional systems tracts on the basis of the assumption that rock strata are products of continuous spectrum of deposition during rising and falling relative sea level (Helland-Hansen and Gjelberg, 1994; Helland-Hansen and Martinsen, 1996; Mellere et al., 2002; Steel and Olsen, 2002; Helle and Helland-Hansen, 2009; Henriksen et al., 2009). It involves the identification of the offlap breaks on the seismic sections. Offlap breaks were identified at the points where changes in slope gradients were observed (Figure 5.2). Offlap breaks between two successive sequence boundaries were joined to establish the stacking pattern motifs (progradation-aggradation, retrogradation, and aggradation-progradation-degradation). Sequence boundaries were identified on the basis of recognition of coastal onlaps (Figure 5.2B). Coastal onlaps may imply availability of coastal accommodation that is thought to be filled with sediment through the interaction of eustatic changes relative to an inherited depositional profile (Jersey, 1988; Song et al., 2014).

5.4.2 Structural analysis

The structural analysis described in section 2.5.1. Structural analysis was applied to the Cenozoic strata in order to analyse and interpret the structures for the prediction of the mechanism for their formation. The associated slump in both transgressive and regressive megasequences were structurally analysed for their faults (extensional, contractional or both).

5.5 Sequence stratigraphy of the Cenozoic offshore Benin Basin

5.5.1 The transgressive megasequence (MS4)

The transgressive megasequence (MS4) is generally made up of parallel to sub-parallel reflections (Figure 5.3) that signify a relative rise in sea level leading to a subsequent landward encroachment of sediments. These can, therefore, be interpreted as aggrading strata deposited during the transgressive and highstand episodes (i.e. the transgressive

megasequence, MS4). Prior to the late Miocene/Pliocene slump event, the transgressive megasequence was deposited on the continental shelf through the continental slope to deep-water environments. Due to the slope-failure associated with the late Miocene/Pliocene slump, the transgressive megasequence (MS4) on the continental slope and beyond has been deformed (Braathen et al., 2004).

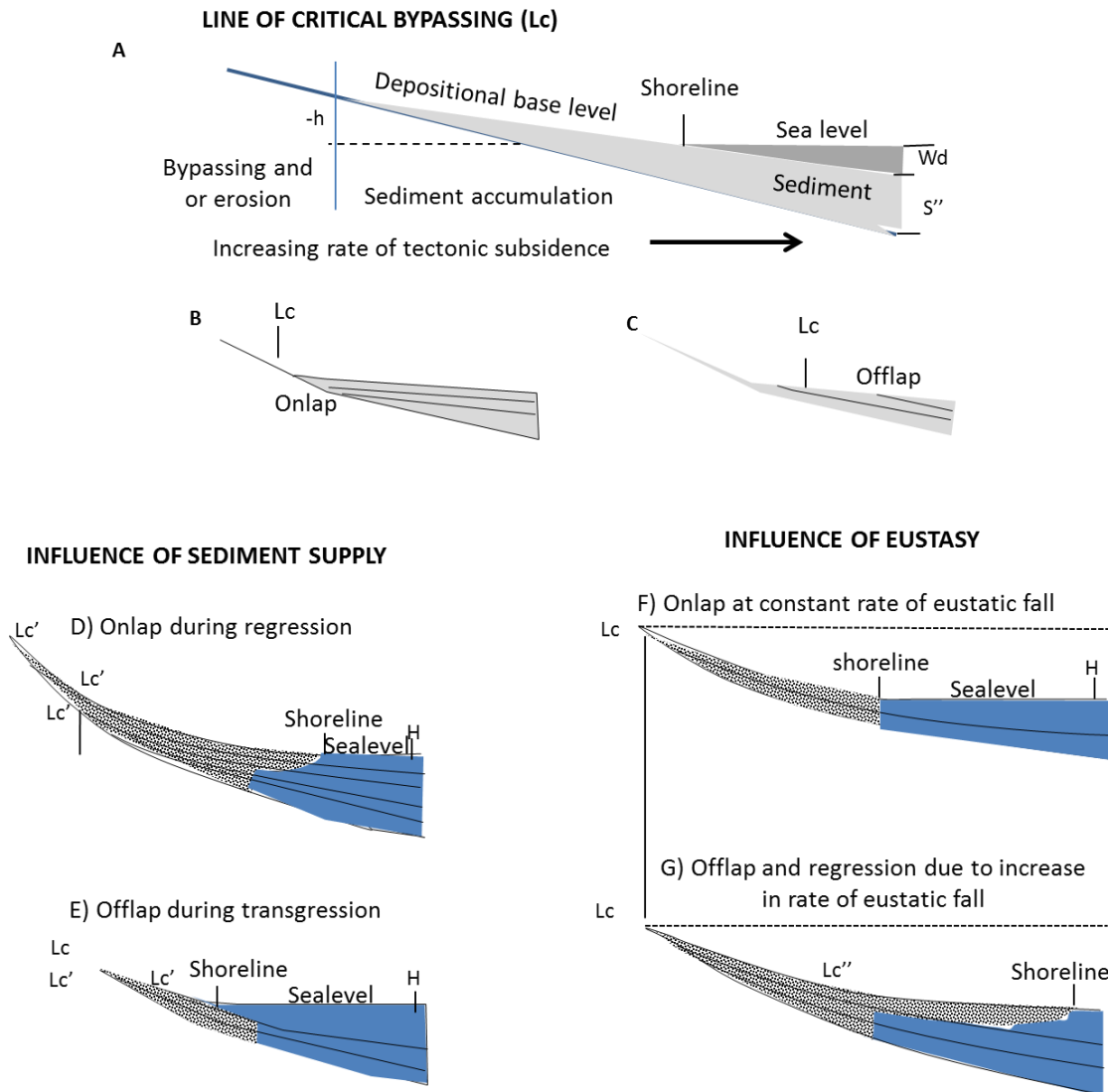


Figure 5.2: Interpretation procedure of shoreline trajectories (after Christie-Blicke, 1991).

The transgressive megasequence (MS4) has been grouped into three on the basis of the reflection characters (Figures 5.3 and 5.4):

- ❖ Low amplitude reflection facies (S4A) (latest Maastrichtian - Eocene).
- ❖ Low amplitude parallel reflection facies (S4B; Eocene - Oligocene).
- ❖ High amplitude reflection facies (S4C; Oligocene - middle Miocene).

Low amplitude reflection sequence (S4A; latest Maastrichtian - Eocene)

The sequence (S4A) is essentially deposited as sub-parallel to parallel, transparent, moderate to high amplitude, continuous, and high-frequency reflections. Its thickness may vary from about 200 ms TWT (Figure 5.4). It is deformed by Miocene-Pliocene slump on the continental slope (Figure 5.4; Vanneste et al., 2006).

The sub-parallel to parallel reflection configuration is suggestive of a uniform rate of sediment deposition on the continental shelf. The stacking pattern of the parallel reflections also implies a relative rise in sea level and the sediments aggraded upward. The relative sea level rise is suggestive of an increase in the rate of accommodation creation. The low amplitude exhibited by the seismic reflection is indicative of deposition of a finer fraction of sediments such as mudstone (Sangree and Widmier, 1977; 1978). The reflection continuity of this sequence probably suggests a widespread deposition of the strata.

Low amplitude parallel reflection sequence (S4B; Eocene - Oligocene)

The sequence S4B is made up of parallel to sub-parallel, continuous to non-continuous, low amplitude and transparent reflectors (Figure 5.4). Its thickness may be up to 300 ms TWT on the continental shelf but reduces with depth because of the erosional effects. Its seismic reflectors aggrade as a result of the vertical stacking of the reflectors. It is also affected by the gravity-induced normal faults on the continental slope.

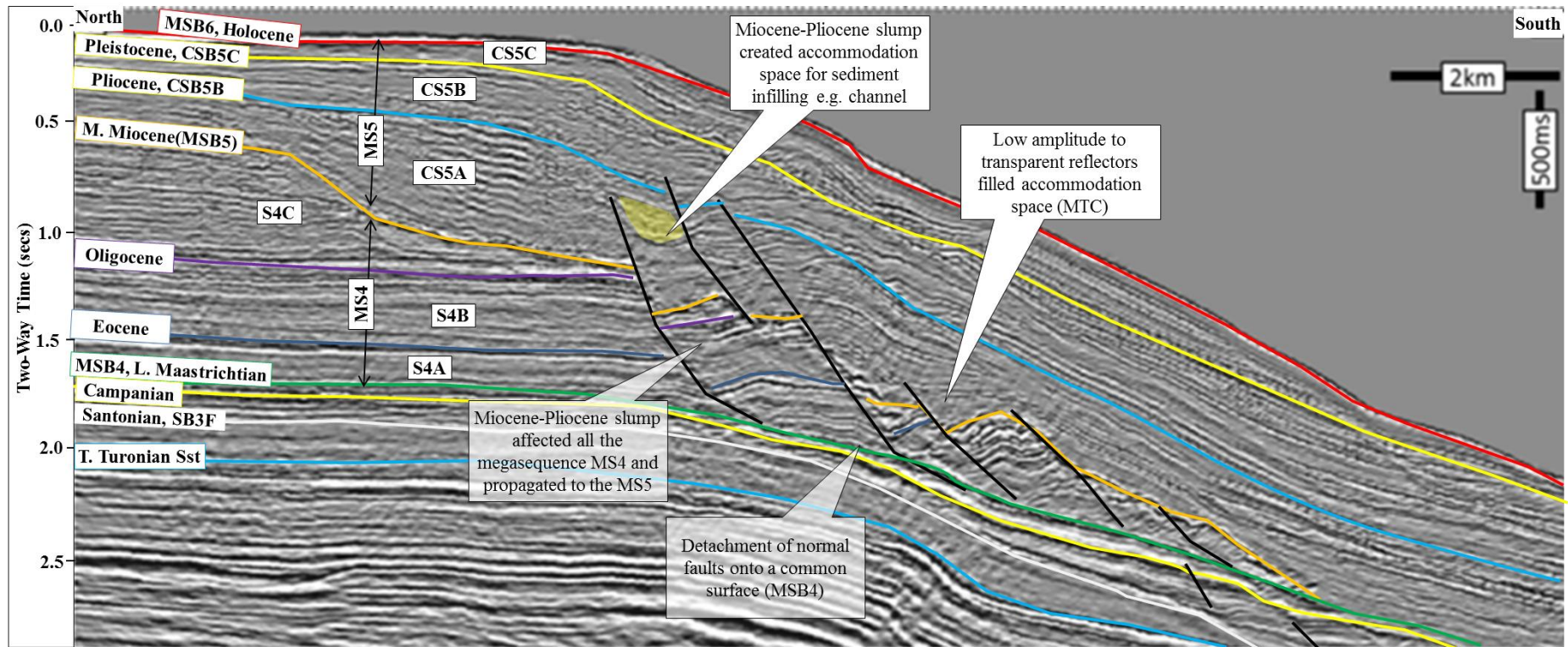


Figure 5.3: Crossline 3858 displaying slumping in megasequence MS4. The deformed MS4 mainly comprises extensional faults; reverse/thrust faults were probably eroded by canyon. See Figure 5.11 for the location of the seismic section.

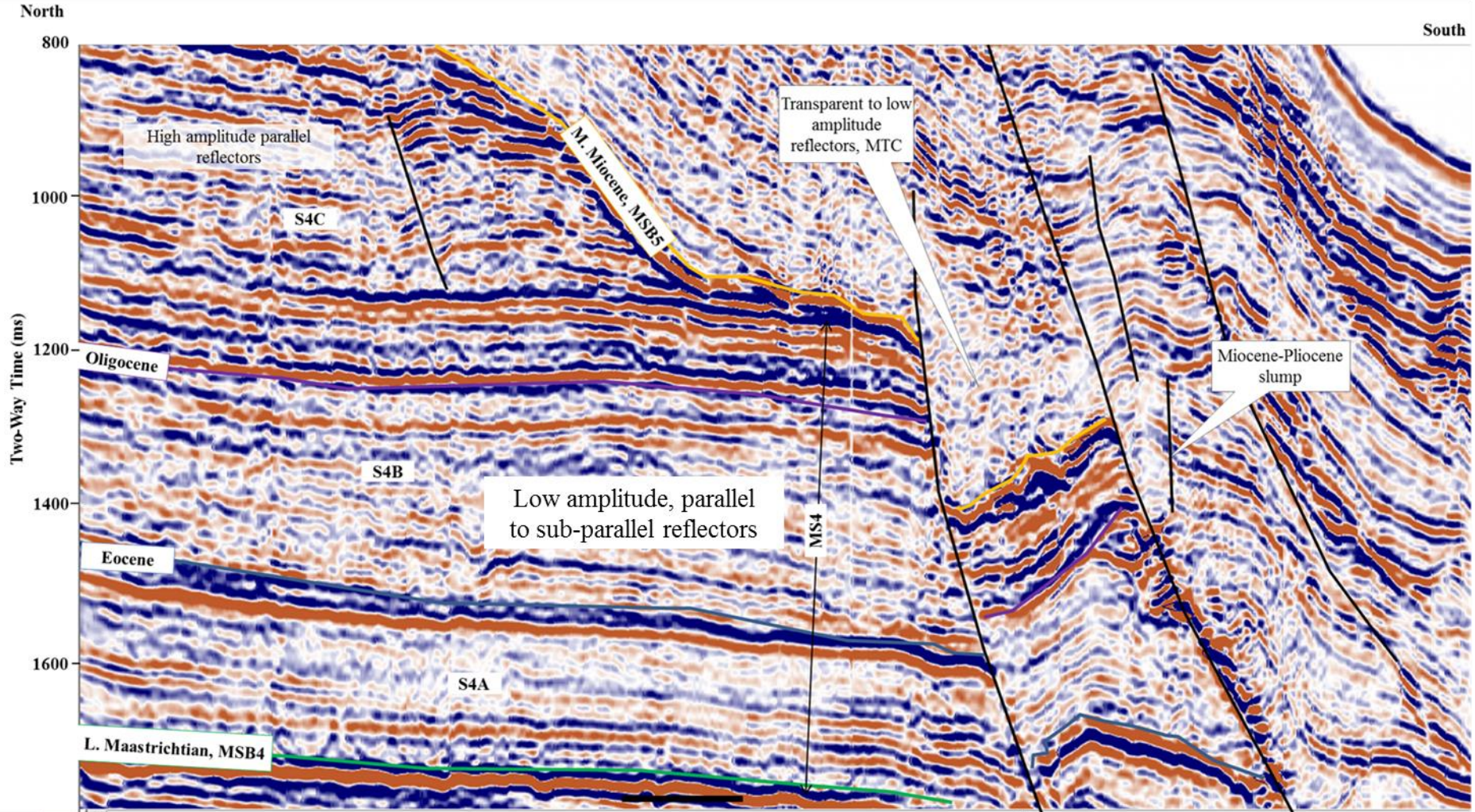


Figure 5.4 Crossline 3836 showing the internal character of transgressive megasequence MS4. See Figure 5.11 for the location of the seismic section.

High amplitude reflection sequence (S4C; Oligocene - middle Miocene)

The sequence S4C comprises parallel to sub-parallel, continuous to non-continuous, high amplitude reflectors (Figure 5.4). Its thickness may be up to 500 ms TWT on the continental shelf but reduces with depth because of the erosional effects. It is affected by gravity-induced normal faults. Its deposits may occur in form of remnant blocks or sometimes as rafted blocks at depth. These blocks occur as mounded reflection characteristics. Their sizes tend to decrease downslope. They have variable sizes. The high amplitude of this unit is suggestive of deposition of coarser sediments such as sand and pebbles (Sangree and Widmier, 1977). This conforms to the general thought that the continental shelf being the nearest to the non-marine environment, coupled with the generally low energy level in shelf area, it would receive a coarser fraction of the transporting medium load (Pirmez et al., 1998; 2000). Its basal boundary is made up of onlaps while its top comprises a major erosional surface that has been mapped as a megasequence boundary (i.e. MSB5) that separates the megasequence MS4 from megasequence MS5 (Figure 5.4). Its age ranges from Oligocene to middle Miocene.

5.5.2 The regressive megasequence (MS5) (MSB5, middle Miocene to MSB6, Holocene)

The regressive megasequence (MS5) consists of continuous to non-continuous, moderate to high amplitude parallel to sub-parallel reflections on the continental shelf. The megasequence MS5 consists of clinofolds stacking patterns on the continental slope (Figure 5.5). It often grades to prograding strata representing regressive episodes and associated submarine canyon incisions in the continental slope environment. On the continental slope the megasequence MS5 may consist of mass-transport complexes (MTCs) as result of the submarine incisions.

Such incisions are later filled by sediments transported from the continental shelf. See section 5.9 for discussion on the MTCs.

As a result of the clinoform stacking patterns, and reflection terminations (onlap, downlap, toplap, and erosional truncation) two sequence stratigraphic models are validated to predict how sedimentation is controlled by sea level changes (Vail, 1987). The two sequence stratigraphic models include namely:

- ❖ The Vail et al. (1977) model, and
- ❖ The Neal and Abreu (2009) model.

The Vail et al. (1977) sequence stratigraphic model

All types of reflection terminations (Figure 5.5) exist in the regressive megasequence. Therefore, it permits the application of sequence stratigraphic models (Vail et al., 1977; Mitchum et al., 1977; Mitchum and Vail, 1977; Plint and Nummedal, 2000; Neal and Abreu, 2009). Vail et al. (1977) studied depositional sequences on well controlled 2D seismic data. They were able to demonstrate that sedimentation may be controlled by eustatic sea level change. The methodology described in section 2.5 is applied on the regressive megasequence (MS5). The analysis of the seismic data shows that the six seismic sequences in megasequence MS5 are cyclic (i.e. repetitive), suggesting that their sedimentation was probably controlled by similar factors. These sequences will be discussed with respect to the models that are being applied.

The facies analysis of the seismic sequences of the regressive megasequence (MS5) show that the megasequence is composed of the following seismic reflection characters: parallel to sub-parallel, and prograding reflection patterns.

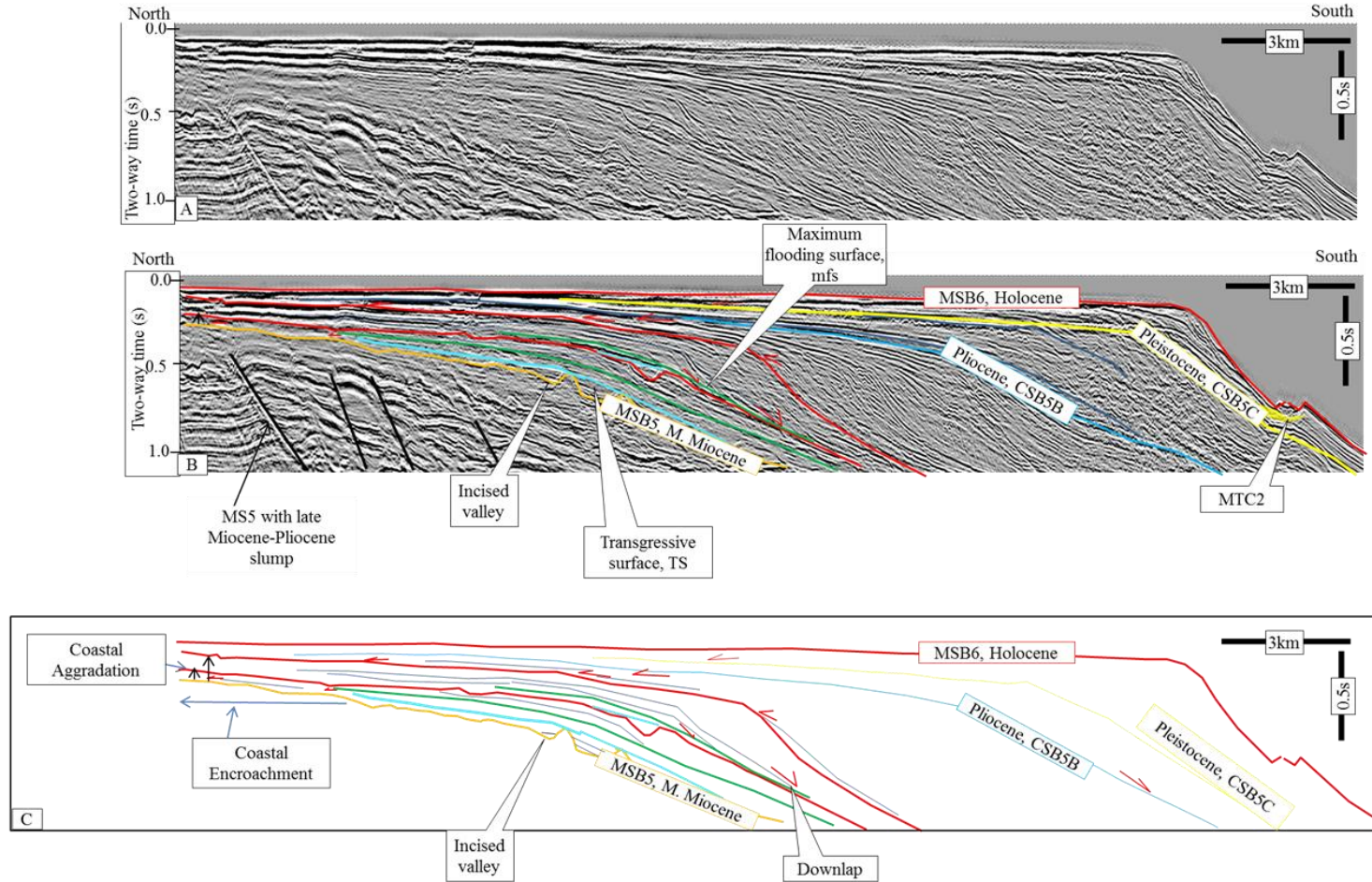


Figure 5.5: 2D line (N06) highlighting some of the stratigraphic features of the regressive megasequence MS5. A) Uninterpreted seismic profile. B) Regressive megasequence MS5 showing some of the diagnostic features for the recognition of seismic sequence. C) Line interpretation of the regressive megasequence MS5. Coastal onlaps define for the sequences. Red arrows indicate seismic reflection terminations. See Figure 5.11 for the location of the seismic section.

Parallel facies

This reflection configuration pattern is widespread (Figure 5.5B) occurring as sheets or fills where they fill incised valleys in most of the seismic sequences of the regressive megasequence MS5 (Figures 5.5B and C). This parallel facies comprises low to high amplitude, continuous and high-frequency configuration. The parallel reflection facies occurs mainly on the continental shelf of the offshore Benin Basin (Figure 5.5B). This parallel reflection pattern suggests constant rates of deposition on a uniformly subsiding shelf or stable basin plain (Mitchum et al., 1977; Sangree and Wildier, 1977). The parallel reflections of the sequence S5A show progressive onlapping of the coastal region. These coastal onlaps generally suggest that the continental shelf encroached.

The stacking of the parallel reflections implies aggradation. These, therefore, imply that their deposition was probably as a result of a relative rise in sea level. The parallel configuration may also suggest coastal aggradation (Mitchum and van Wagoner, 1977; Vail et al., 1977; van Wagoner et al., 1988; 1990; Christie-Blicle, 1991).

Prograding reflection facies

This facies is also widespread in all seismic sequences of the regressive megasequence (MS5), where it occurs as sigmoid, oblique and sometimes hummocky progradational pattern. The progradational pattern consists of progressive lateral development of gently sloping depositional surfaces referred to as clinofolds. The clinofold often signifies that variations in the rate of deposition and water depth. The upper part of the clinofold denotes deposition in shallow water while the lower part refers to deeper waters (Vail et al., 1977; Steel and Olsen, 2002).

The parallel reflection of the upper part of the sigmoid progradational pattern can be interpreted as a degree of up-building (i.e. aggradation) that is coincident with the

progradation of the middle segments. It depicts relatively low sediment supply, relatively rapid basin subsidence, and/or rapid rise in sea level such that it permits the preservation of the upper unit. It indicates a low energy of deposition (Vail et al., 1977).

The oblique progradational pattern depicts strata that build out from a relatively constant upper surface typified by absence of the topset units and by pronounced toplap termination of the foreset units (Figure 5.6; Vail et al., 1977).

5.6 Analysis of relative changes in sea level

Following Vail et al. (1977), a relative sea level curve was plotted for the Cenozoic megasequences in the offshore Benin Basin. The sea level curve was based on the analysis of the seismic data for coastal onlaps and toplaps within the seismic sequences established for both transgressive (MS4) and regressive (MS5) megasequences.

The seismic data, however, reveals that the regressive megasequence (MS5) permits the easy application of the seismic data for sea level curve. The reason is that of the associated progradation pattern that allows the preservation of coastal onlap and toplap. It has been suggested that the progressive onlapping of reflections on an initial surface implies a relative rise in sea level. A downward shift in coastal onlap indicates a rapid fall. A fall in sea level was also predicted by considering if there is a downward shift in clinoform patterns (Vail et al., 1977).

The regressive megasequence (MS5) that ranges from middle Miocene (MSB5) to Holocene (MSB6) is composed of an initial depositional surface tagged MSB5 in this study. The sea level curve obtained for the regressive megasequence (MS5; Figure 5.7) suggests that the sea level probably started rising in the middle Miocene after it had experienced a fall during that time in the offshore Benin Basin (Embry, 1993; 1995; 2002; 2009).

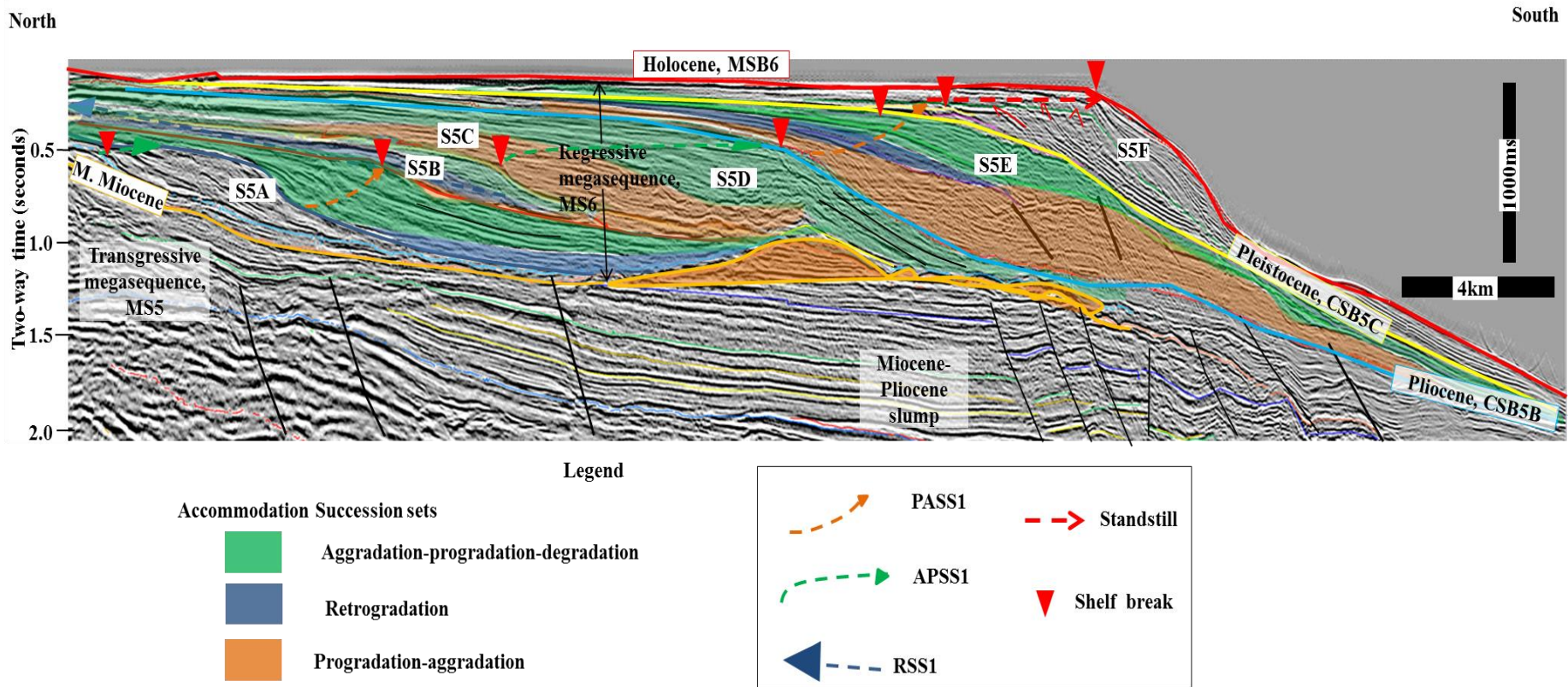


Figure 5.6: 2D line (N08) showing discrete sequences within the regressive megasequence MS5. See Figure 5.11 for the location of the seismic section.

Evidence of the previous fall in sea level occur such as incised valleys were formed (Figure 5.5B). Other evidence of the fall in sea level occur as canyon eroded sediment in the continental slope. The relative fall in the sea level in middle Miocene is important because it locally control sedimentation in the offshore Benin Basin (Garrison and Bergh, 2006). The erosional surface that represents this event is preserved in the offshore Benin Basin and it has been mapped in this study.

5.6.1 Neal and Abreu (2009) model

Within the regressive megasequence (MS5), coastal onlaps were identified in order to define the first sequence boundary. The seismic data comprising both sigmoidal and oblique clinoforms (Figure 5.6) whose offlap breaks were marked out. The offlap breaks between successive sequence boundaries were joined together to establish the stratal motifs (Figure 5.6) (Neal and Abreu, 2009).

The first sequence boundary identified within this megasequence is the composite sequence boundary defined by coastal onlaps at the shelf area, downlap of the bottomset of the clinoforms and toplap of their topsets. Altogether three sequence boundaries (MSB5, CSB5A, and CSB5B) were identified for the regressive megasequence (MS5; Figure 5.6).

On the basis of accommodation successions proposed by Neal and Abreu (2009), the regressive megasequence (MS5) is grouped into three sequence sets namely the progradation-aggradation sequences set (PASS), aggradation-progradation-degradation sequence set (APDSS) and retrogradation sequence set (RSS) (Figure 5.6).

Progradation-aggradation sequence set (PASS)

According to Neal and Abreu (2009), this sequence set represents lowstand consisting successions of sequences deposited during a relative fall in sea level. The stratal motif

suggests a rise in level sea whereby all coastal accommodation is filled with sediment leading to rapid progradation of clinoforms followed by aggradation of their topsets as they onlap the inherited depositional profile (Neal and Abreu, 2009). This succession is therefore typical of progradation-aggradation stacking pattern (Figure 5.6). The succession is considered to reflect changing rates of coastal accommodation (dA) and sediment fill (dS) (Neal and Abreu, 2009). For this type of stacking pattern, Neal and Abreu (2009) define the accommodation space to be increasing, $(dA)/(dS) < 1$.

Its basal surface is made up of a sequence boundary (MSB5) where the reflections onlap to give rise to coastal onlaps while the reflections downlap the sequence boundary on the slope environment (Figure 5.6). It represents an erosional truncation in parts of the slope and deep-water environments and it is evidenced by canyon incision (Figures 5.9 and 5.11).

Aggradation-progradation-degradation sequence set (APDSS)

This is the second sequence set of the regressive megasequence MS5. The stratal motif consists of reflections that aggrade on one another and overlapping an inherited depositional fill; this is followed by sigmoidal clinoforms that prograde basinward and oblique clinoforms that also prograde basinward (Figure 5.6). This is referred to as aggradation-progradation-degradation stacking pattern. This represents the stratal geometry of highstand systems tract. The APD systems tract suggests a decrease in accommodation on the shelf through time (Neal and Abreu, 2009). The accommodation space is, at this time, decreasing $(dA)/(dS) < 1$. The basal surface is defined by a sequence boundary referred to as a composite sequence boundary (CSB5A). It is defined by an onlap surface while its top surface is defined by toplap surface (CSB5B).

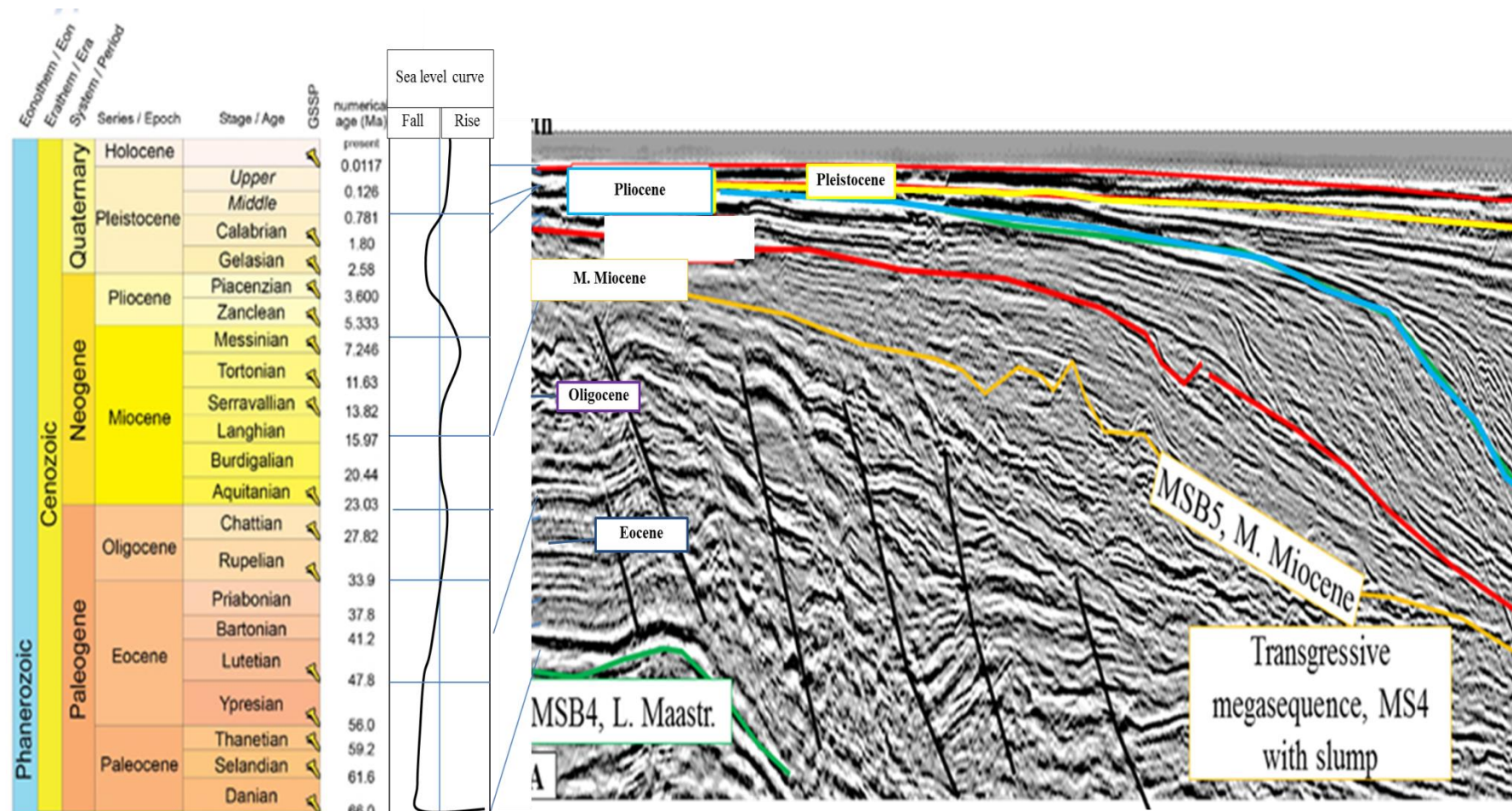


Figure 5.7: Sea level curve obtained for the Cenozoic Benin Basin (offshore) on the basis of the mapping of coastal onlaps. It shows a relative rise in sea level for the transgressive megasequence (MS4, Latest Maastrichtian to middle Miocene), and a relative fall in sea level for the regressive megasequence (MS5, middle Miocene to Holocene). See Figure 5.11 for the location of the seismic section. Modified after Vail et al. (1977) and Christie-Blick (1991). Geological time scale obtained from International Chronostratigraphic Chart, 2017.

Retrogradation sequence set (RSS)

This sequence set is generally well-represented on the seismic data partly because of data resolution. When present, it indicates a transgressive systems tract (TST). This systems tract is often said to be thin in most high-resolution seismic data. It is barely represented by parallel reflections suggestive of a rise in relative sea level leading to deposition on the shelf (Figure 5.6).

The identified sequence sets of the regressive megasequence on the continental shelf correlate with the mass-transport complexes (MTCs) in the upper slope area.

5.7 Structural setting of the Cenozoic offshore Benin Basin

The classical models of slump structures show that slumps are always characterised by structures that grade from extensional, through transitional to compressional zones as one moves from the upslope (head) to the downslope (toe) region (Damuth, 1994; Frey-Martinez et al., 2005; Bull et al., 2009).

The observed discontinuity of the seismic reflections of the Cenozoic strata in the offshore Benin Basin can be associated with bedding discontinuity that may be due to gravitational deformation (Figure 5.9). This is because their faults occur dominantly in the continental slope realm, where they deform the strata through gravitational forces acting on the slope. The faults tend to detach on a common surface known as decollement (Figure 5.8).

The seismic data show that Miocene-Pliocene slump is characterised by extensional faults (Figure 5.4) with little evidence of contractional deformation towards the toe of the slump. The extensional faults occur as normal faults, while evidence for contractional deformation includes a few thrust faults. The crests of the associated anticlines of the thrust faults have, however, been eroded by a later submarine canyon (Figure 5.6; Popescu et al., 2006). The

normal faults dip seaward, suggesting a downslope movement to the south. Most of these normal faults are synthetic. However, a few of them are antithetic (Figure 5.4). A similar observation was made in the Norwegian continental slope which is also characterised by slumps of mainly extensional geometries (Bull et al., 2009).

The normal faults are planar in both cross-section (Figure 5.4) and plan view (Figure 5.5). The displacement caused by the normal faulting varies from about 20 - 400 ms TWT on the hanging-wall. In map view, most of these normal faults in the southwestern part of the study area strike NW-SE direction while others in the southeast trend E-W (Figure 5.5). These normal faults are essentially related to gravitational collapse.

5.7.1 Late Miocene-Pliocene slump event

This slump event affects all the sequences of the transgressive megasequence (MS4). It propagates upward to the regressive megasequence (MS5) (Figure 5.4). In plan view, it covers a surface area of about 400 km² (Figure 5.5) occupying more than 30% of the 3D volume's area. In seismic cross-sections, it generally has a variable thickness that generally ranges from 500 to 1200 ms TWT (Figure 5.6). It varies from about 12 to 35 km in width. Due to the slope gradient of the continental slope environment, the MTC has evidently moved downslope in a basinward direction, that is, southerly (Figure 5.6). The Miocene-Pliocene slump event is a major event in the offshore Benin Basin as it caused deepening in the environment due to the normal faulting of the environment.

Timing of the Miocene-Pliocene slump event

This slump event consists of a growth sequence (Figure 5.8) that was used for its dating. The pre-slump succession consists of moderate to high amplitude, continuous to non-continuous, parallel reflections. The syn-slump succession is made up of moderate to high amplitude, divergent reflections. The syn-slump succession is separated from the pre-slump succession

by a slump onset unconformity. The slump onset unconformity is composed of onlap of the divergent reflections. The post-slump succession comprises parallel reflections (Figure 5.8). These parallel reflections suggest that they were probably deposited as post-slump strata. The Miocene-Pliocene slump appears to have controlled sedimentation in the offshore Benin Basin. Their activities have enhanced sedimentation by creating accommodation space for sediment deposition in form of mass-transport complexes (MTCs). The middle Miocene unconformity (MSB5) is a major erosional event in the offshore Benin Basin as it incised deep into older strata such as the Maastrichtian (Figure 5.8; Rossetti, 2011). It has also eroded most parts of the thrust and fold of the Miocene/Pliocene slump on the continental slope.

5.8 Mass-transport complexes (MTCs) of the offshore Benin Basin

Evidence of mass-transport complexes occurs as channel infills, low amplitude reflection patterns in the offshore Benin Basin (Figure 5.9). On the basis of the Moscardelli and Wood (2008), the mass-transport complexes can be grouped as slope attached mass-transport and levee-channel complexes.

5.8.1 Recognition of the mass-transport complexes (MTCs) on seismic data

The identification of MTCs was based on the recognition of some established key criteria put forward by various authors (e.g. Hampton et al., 1996; Lee et al., 2004; Frez-Martinez et al., 2005; Bull et al., 2008; 2009). The criteria are based on the seismic stratigraphic and morphology presented on seismic data (Figure 5.9). The criteria are summarised as follows:

- ❖ The MTCs may be identified by their characteristic seismic expression of transparent to chaotic seismic reflections that are bounded on top and base by distinctive and laterally correlatable surfaces. They have irregular geometries (Figure 5.9A).

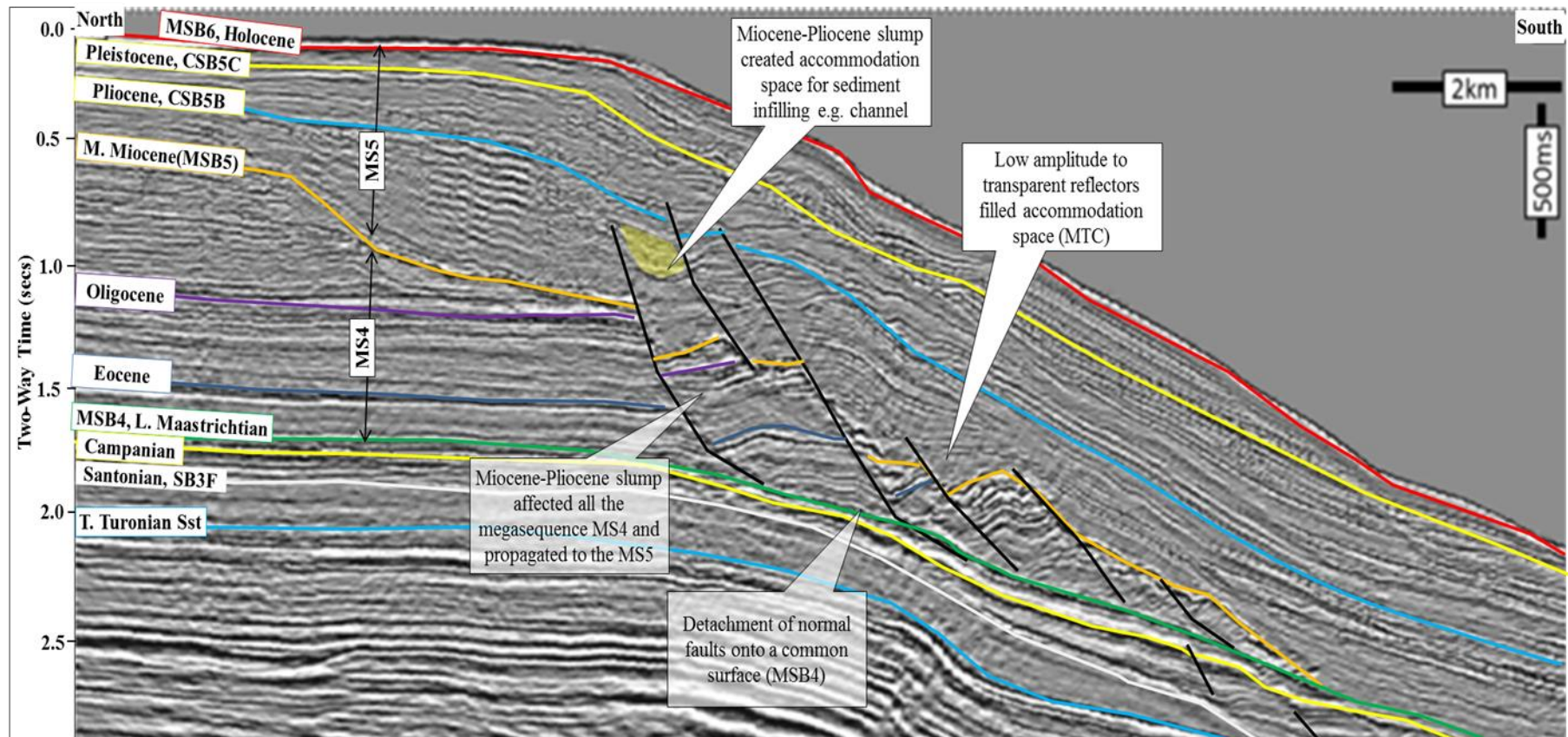


Figure 5.8: Crossline 4240 showing the Miocene-Pliocene slump and its diagnostic features. See Figure 5.11 for the location of the seismic section.

- ❖ The MTCs can be identified by the basal surface that is often conspicuous in seismic data. The basal surface forms laterally continuous reflections that are concordant to the underlying stratigraphy. The basal surface may sometimes have irregular topography due to their erosional ability during their formation (Figure 5.9B).
- ❖ The upper surface of the MTC consists of a laterally continuous or discontinuous and irregular reflection. This depends on internal deformation which the stratigraphic unit has undergone (Figure 5.9C).
- ❖ The MTC is usually characterised by a headwall scarp at the upslope end (Bull et al., 2009). This often occurs where the basal shear surface is steeply-dipping and cutting into shallower stratigraphy and may be exposed to the surface (Figure 5.9D). One of the main characteristics of headwall scarp is the occurrence of extensional structures (such as the presence of rotated blocks characterised by distinct detachment surfaces). The presence of contractional structures at the toe region. These structures are often thrust faults and their associated folds (Figure 5.9E).

5.9 Mass-transport complexes of the offshore Benin Basin

The submarine canyons along the offshore continental margin of Nigeria have not been well-developed (Burke, 1972; Mascle, 1976; Damuth, 1994). The submarine canyons in the offshore Benin Basin have received the least attention from authors (Burke, 1972; Billman, 1992; Olabode and Adekoya, 2008). The nearby Niger Delta (to eastern part of the study area) has received much attention probably due to its petroleum exploration activities (Petters and Ekweozor, 1982; Petters, 1984; Shanmugam et al., 1997; Nissen et al., 1999; Haack et al., 1999; Morgan, 2003; Apotria et al., 2004; Krueger and Grant, 2006; Deptuck et al., 2003; 2007; 2012). Olabode (2006) studied sedimentology using 13 lithofacies during an outcrop study of the Cretaceous Abeokuta Group when he inferred

that the lithofacies were deposited in a slope environment. Olabode and Adekoya (2008) investigated the origin, evolution and geological significance of Avon submarine canyon along the offshore Benin Basin.

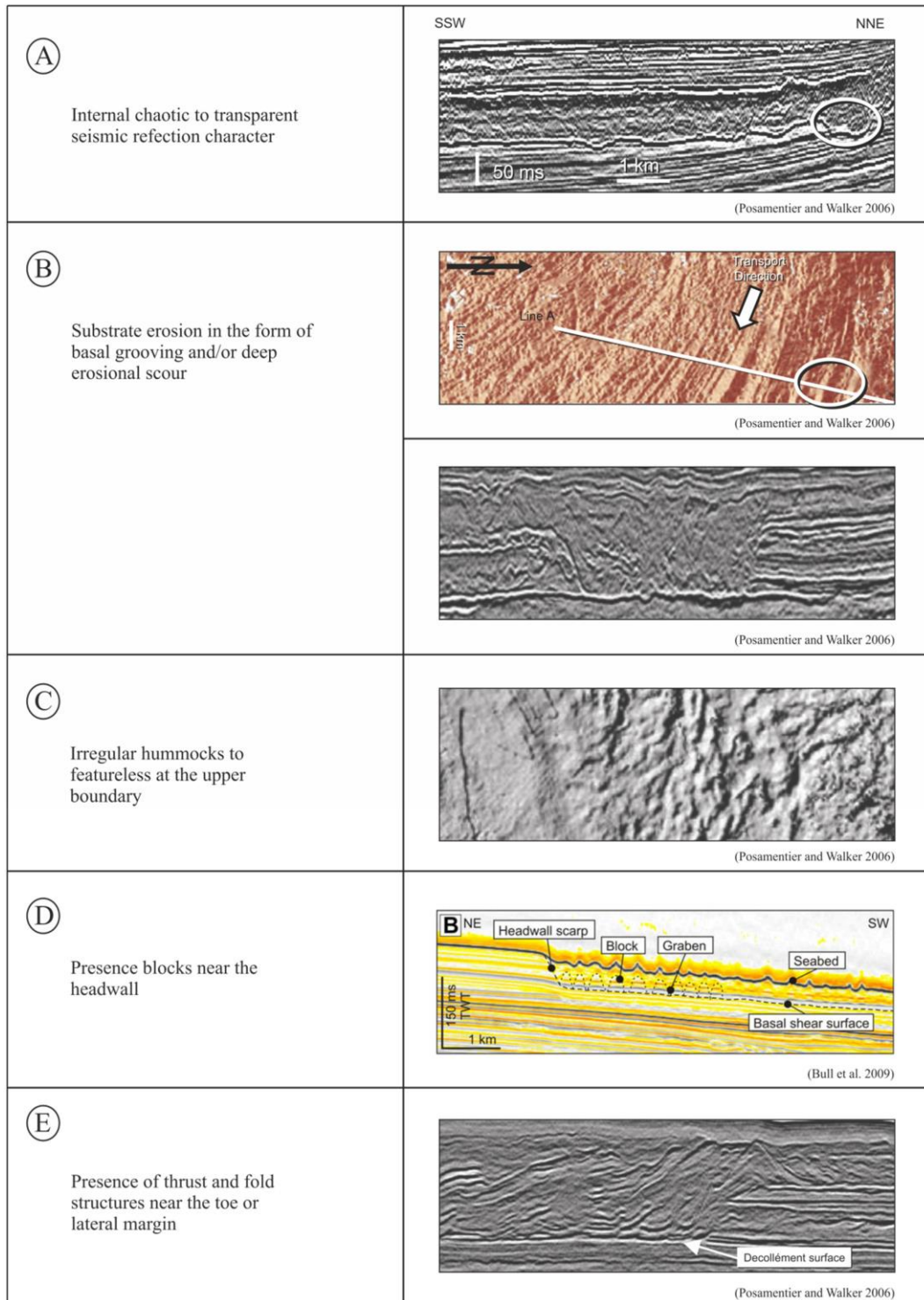


Figure 5.9: Diagnostic criteria of mass-transport complexes (MTCs) (after different authors indicated on them).

This study that is using both the 2D and the 3D seismic data will, therefore, better our understanding of the roles of the submarine canyons in the distribution of sediments in the offshore Benin Basin. Applying the criteria for the recognition of mass-transport complexes (e.g. Steckler et al., 1993; Posamentier and Walker, 2006; Bull et al., 2009; Alves and Cartwright, 2009; 2010; Alves, 2010; Alves et al., 2014) to the Cenozoic Benin Basin (offshore); two mass-transport complexes are associated with the regressive megasequence MS5 (Figure 5.10). They have been analysed and interpreted in this study:

- ❖ Mass-transport complex 1 (MTC1) (late Miocene-Pliocene)
- ❖ Mass-transport complex 2 (MTC2) (Pleistocene)

The mass-transport complexes in the study area show some level of recurrence, occurring in mainly regressive megasequence (MS5); they, however, range from middle Miocene (MSB5) to Holocene (MSB6). The internal character of the studied mass-transport complexes (MTC's) is obviously different from those of the slumped strata (Figure 5.10).

5.9.1 Mass-transport complex 1 (MTC1) (late Miocene-Pliocene)

The mass-transport complex 1 (hereafter refers to as MTC1) occurs in the sequence S5B of the regressive megasequence (MS5). The MTC1 is internally characterised by low to moderate amplitude chaotic reflections (Figure 5.10). Its basal surface is made up of a conspicuous sequence boundary marked by a sharp change in reflection characters from basal high amplitude, high-frequency parallel reflections (Figure 5.10). Occasionally, its seismic reflections are onlapping normal faults that bound MTC1 (Figure 5.10). MTC1 can be regarded as infilling into accommodation space created during the slope failure. Such infilling of chaotic reflections has been interpreted as channel infill.

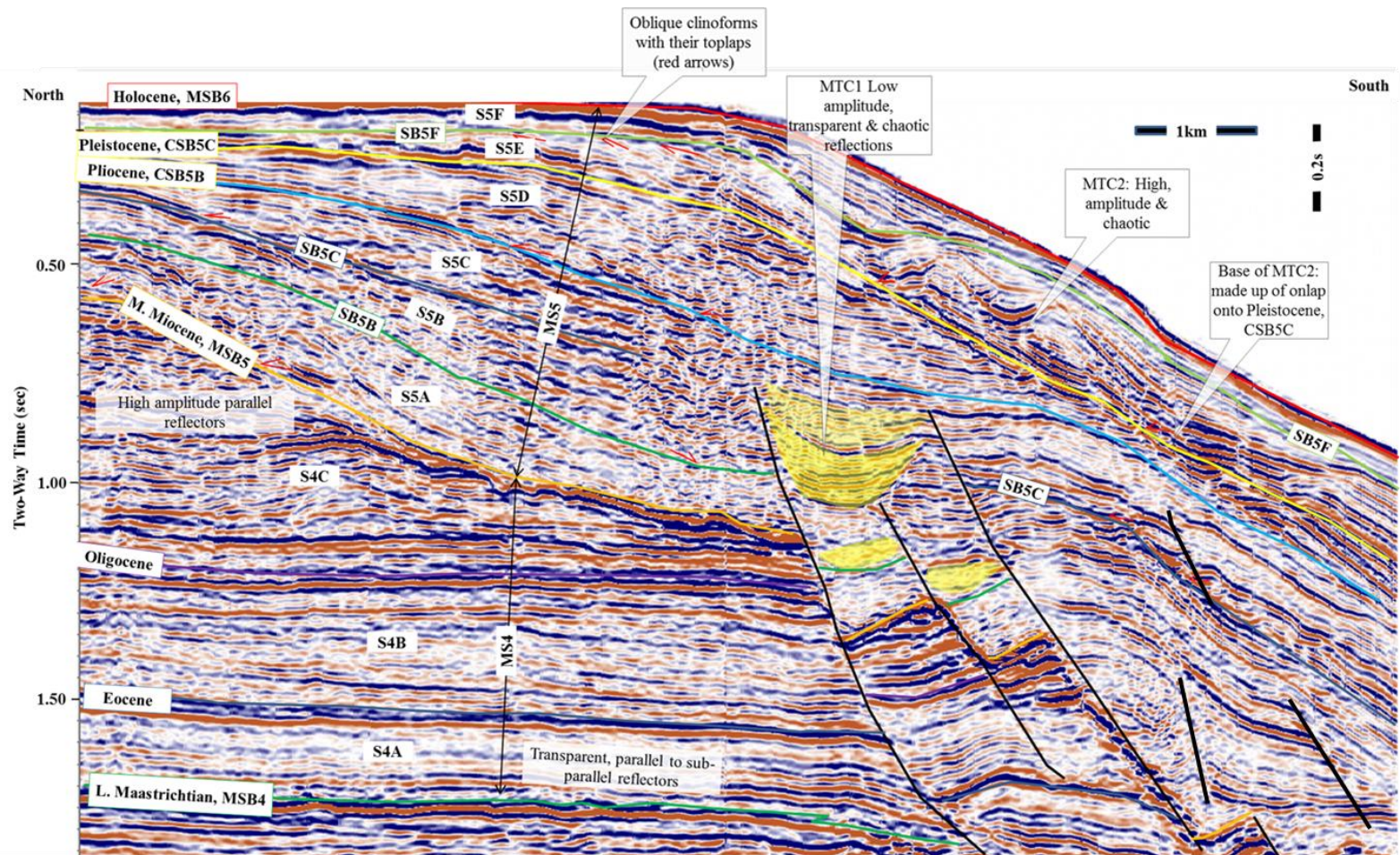


Figure 5.10: Examples of some MTCs in the study area. See Figure 5.11 for the location of the seismic section.

The channel infill associated with the MTC1 is made up of moderate amplitude reflections. These chaotic reflections appear to be deposited within depocentres as they onlap the normal faults. On the basis of Moscardelli and Wood (2008) classification, the MTC1 can be grouped as the channel-levee system (CLS) (Figure 5.1). This is because it is composed of chaotic reflections. The thickness of the MTC1 is variable but it ranges between 250 and 900 ms TWT. It decreases in thickness basinward. The basal boundary correlates with a major sequence boundary grouped as a megasequence boundary (i.e. MSB5, middle Miocene). Its top sequence boundary is characterised by onlapping surface which correlates with a composite sequence boundary (CSB5B, Pliocene).

5.9.2 Mass-transport complex 2 (MTC2) (Pleistocene)

The mass-transport complex 2 (hereafter MTC2) is internally composed of moderate to high amplitude chaotic reflections. MTC2 ranges from about 180 to 300 ms TWT, and it thins to the west. Some small-scale depocentres are present where the seismic reflections are also preserved. Another small-scale oblique reflections are preserved with clinofolds dipping NW (Figure 5.10). Its basal boundary is made up of onlap surface that correlates with a composite sequence boundary (CSB5C, Pleistocene). The CSB5C marks progressive onlapping of coastal onlap on top of one another, signifying aggradation on the continental shelf. Its top ties with the basal sequence boundary of the sequence S5F (Pleistocene). This top boundary is made up of toplap signifying a forced regression whereby sea level is at still standing. Lack of accommodation space at the continental shelf as result of a sea level fall that probably enhanced the deposition of the MTC2 in the continental slope of the offshore Benin Basin during the Pleistocene.

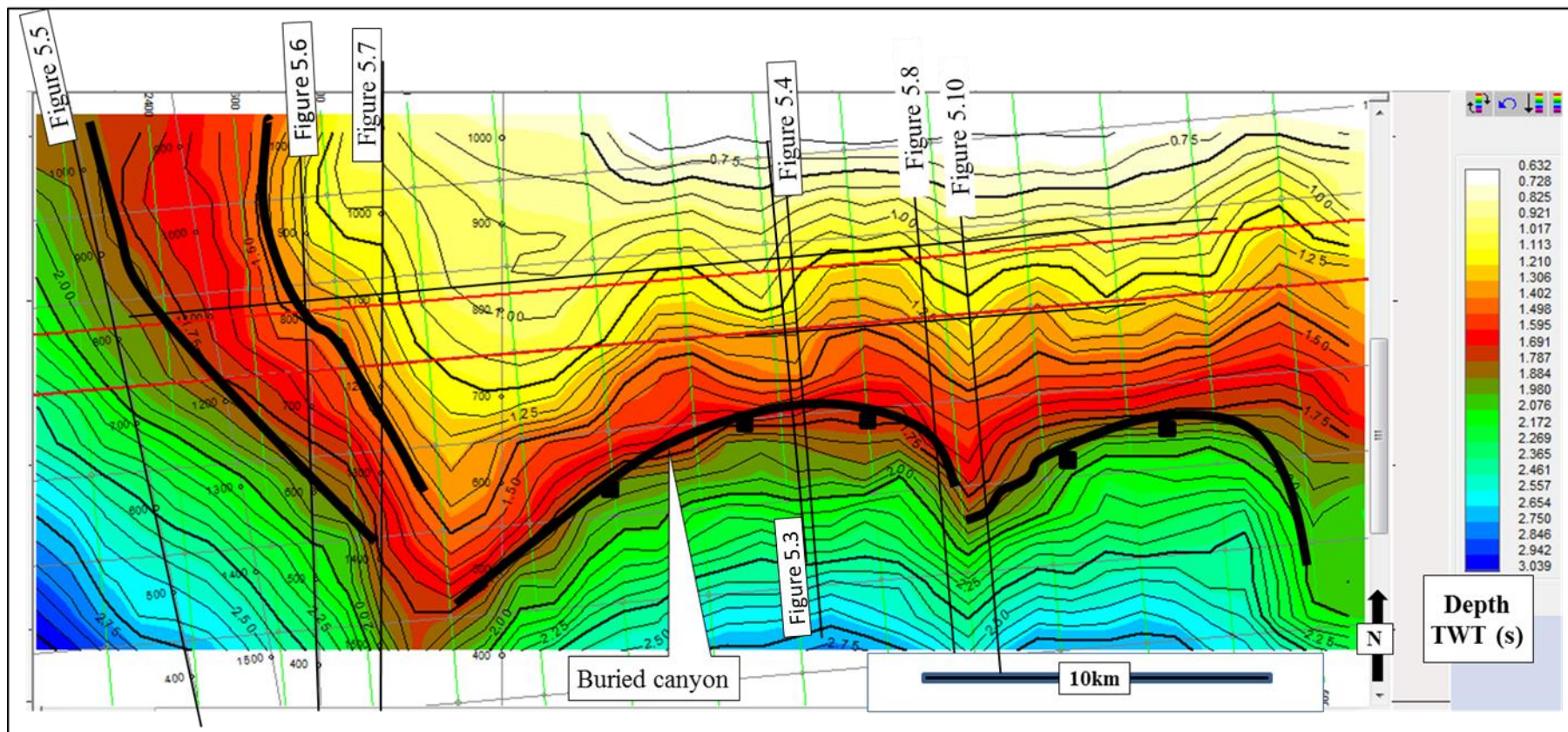


Figure 5.11: Isochron map to base of the transgressive megasequence boundary (MSB4, latest Maastrichtian). Evidence of the slumping and some ancient submarine canyons are eminent. The locations of some of the seismic sections cited in this chapter are indicated in this figure.

A third MTC that may be added is associated with a present-day marine environment in the offshore Benin Basin (Figure 5.10).

Classification of the mass-transport complexes (MTCs) in the offshore Benin Basin

The formation of most of the studied mass-transport complexes (MTC1 and MTC2) was enhanced by a post-slumping event (i.e. Miocene-Pliocene slump). Moscardelli and Wood (2008) classification of the MTCs, the studied MTCs can be grouped into either:

- ❖ Those associated with the slope-attached mass-transport with their sediments sourced from the catastrophic collapse of the upper slope area. This is the main cause of the MTCs in the study area because they are located very close to the head wall scarp and are attached to the continental slope.
- ❖ The studied MTCs can also be classified as detached mass-transport complex that may have originated from deposition through channel-levee systems (Moscardelli and Wood, 2008). The Miocene-Pliocene slumping event may have influenced other sediment transport systems as several active channel systems developed after the mass-transport event. This slumping event resulted in the accommodation creation in the basin, as it acted as a conduit for sediment transfer to the deeper basin.

5.10 Discussion

Both transgressive (MS4) and regressive (MS5) megasequences consist of evidence that suggest they were deposited under the control of sea level. These imply that there may no significant tectonic activities during the Cenozoic. The evidence includes slumping, submarine canyons, mass-transport complexes (MTCs). The transgressive megasequence (MS4) is characterised by slump which enhance its deepening of the environment during its deposition. The megasequence (MS4) was deposited under a significant rise in sea level (Figure 5.7). This, therefore, suggests that the geological period between the latest

Maastrichtian (MSB4) middle Miocene (MSB5) was typified by a relative rise in sea level in the offshore Benin Basin.

The regressive megasequence (MS5) is composed of evidence of submarine canyons, mass-transport complexes (MTCs); these are significant evidence of a relative sea level fall in the middle Miocene to Holocene.

5.11 Conclusions

The deposition of sediment in the Cenozoic Benin Basin (offshore) was enhanced by relative changes in sea level. These have led to the distribution of from the continental shelf, to the continental slope. Stratigraphically, the transgressive megasequence is made up of three sequences: sequence (S4A, S4B, and S4C). The regressive megasequence (MS5) consists of six sequences (S5A, S5B, S5C, S5D, S5E, and S5F).

Chapter Six

6.0 Discussion

6.1 Introduction

This chapter provides an integrated discussion of the key findings described in the preceding chapters, based on the concepts highlighted in the introductory chapter. It discusses the overall interpretations and deductions made in this study.

Section 6.2 discusses the rifting on the basis of the stratigraphic patterns and structural architecture observed in the northern and the southern half-grabens of the offshore Benin Basin (Chapters 2, and 3). The character of the syn-rift megasequence (MS2) seen on the seismic data has been used to reconstruct tectonic evolution model for this basin. It also involves the construction of different models that show how the different phases of rifting led to the evolution of the basin.

Sections 6.3 to 6.5 discuss the implications of the two phases of the post-rift deformation for the geodynamics of the SW Nigerian margin and Equatorial Atlantic margin. Palaeogeographic models of Guiraud et al. (1992), and Moulin et al. (2010) were adapted for this margin based on both the extensional and contractional structures.

Section 6.7 discusses the implications of the results presented in this study regarding hydrocarbon entrapment in the offshore Benin Basin.

6.2. Early Barremian (MSB2) to Late Aptian (MSB3) continental rifting

6.2.1 Lack of evidence for transform tectonics

The Equatorial Atlantic region is considered to be dominated by transform tectonics with the implication that the structural style of the margin will reflect an interplay of both strike-slip and extensional (normal) faulting (Matos, 2000; MacGregor et al., 2003; Basile et al., 2005; Brownfield and Charpentier, 2006; Anthobreh et al., 2009; Moulin et al., 2010; Nemčok et al., 2013a; 2013b; Fairhead et al., 2013; Heine and Brune, 2014). Matos (2000) observed that it is difficult to recognize typical syn-rift reflection geometries on seismic data acquired from the Equatorial Atlantic margin. The reason may be due to diffuse nature of deformation that is often associated with transform margin (Matos, 2000). However, in this study of the Benin Basin, two asymmetric half-grabens (northern and southern half-grabens), containing syn-rift megasequence (MS2) with a characteristic wedge geometry, controlled by planar basin-bounding normal faults (F1 and F2), are identified and these do not show features typically associated with transform faults.

6.2.2 Rifting of the offshore Benin Basin

Although direct correlation is not straightforward, the data suggests that there is no difference in age the rifting across the two half-grabens. Studies of other rift basins, notably the UK North Sea (Cowie et al., 2005) have demonstrated that the timing of the syn-rift phase migrates towards the rift centre as a result of strain localisation. Although earlier analysis of the data presented in this dissertation suggested this may be the case, more careful analysis has suggested that it is not the case for this study area, although it does only contain two half-grabens within the more extensive Benin Basin.

Rifting in the offshore Benin Basin started in the Barremian to late Aptian, implying that ocean crust began to form between Nigeria and Brazil no earlier than the late Aptian (age was based on biostratigraphic data). The N-S lithospheric extension is the direction proposed for the offshore Benin Basin occupying a region in the Equatorial Atlantic believed by some authors to be characterised by transform tectonism (e.g. Moulin et al., 2010; Heine and Brune, 2014). The basin does not show many relationships with other basins within the Equatorial Atlantic. The orthogonal extension implied that the African and South American Plates were stretching N-S in the Barremian-Aptian as transform tectonism was about to start in the Equatorial Atlantic. The N-S orthogonal extension in this basin may relate to basement reactivation that probably (and locally) created new E-W to ENE-WSW striking normal faults in the study area. Continuous N-S rifting of the two plates during the Barremian-Aptian created the asymmetric half-grabens of the offshore Benin Basin. There is no clear evidence for E-W or ENE-WSW transtension along proto-transform faults, because it is difficult to see how this would generate E-W striking dip-slip normal faults.

The Barremian-Aptian rift episode described as the time when rifting propagated northward towards the Equatorial Atlantic from the southern South Atlantic. The rifting is thought to be characterised by N-S lithospheric extension (Moulin et al., 2010; Fairhead et al., 2013; Heine and Brune, 2014). The N-S orthogonal extension proposed for the offshore Benin Basin is therefore consistent with those associated with the South Atlantic rifting. Prior to the Barremian-Aptian, Moulin et al., (2010) opined that some faults (e.g. Kandi/Sobral, Patos/Ngaoundere, Pernambuco/Sanaga lineaments and Demerara/Guinea plateaus; Figure 6.1) were aligned in the African and South American Plates respectively. From a regional or global point of view, the N-S orthogonal extension of the Benin Basin may be related to the basement reaction involving an N-S striking structure in the Barremian-Aptian.

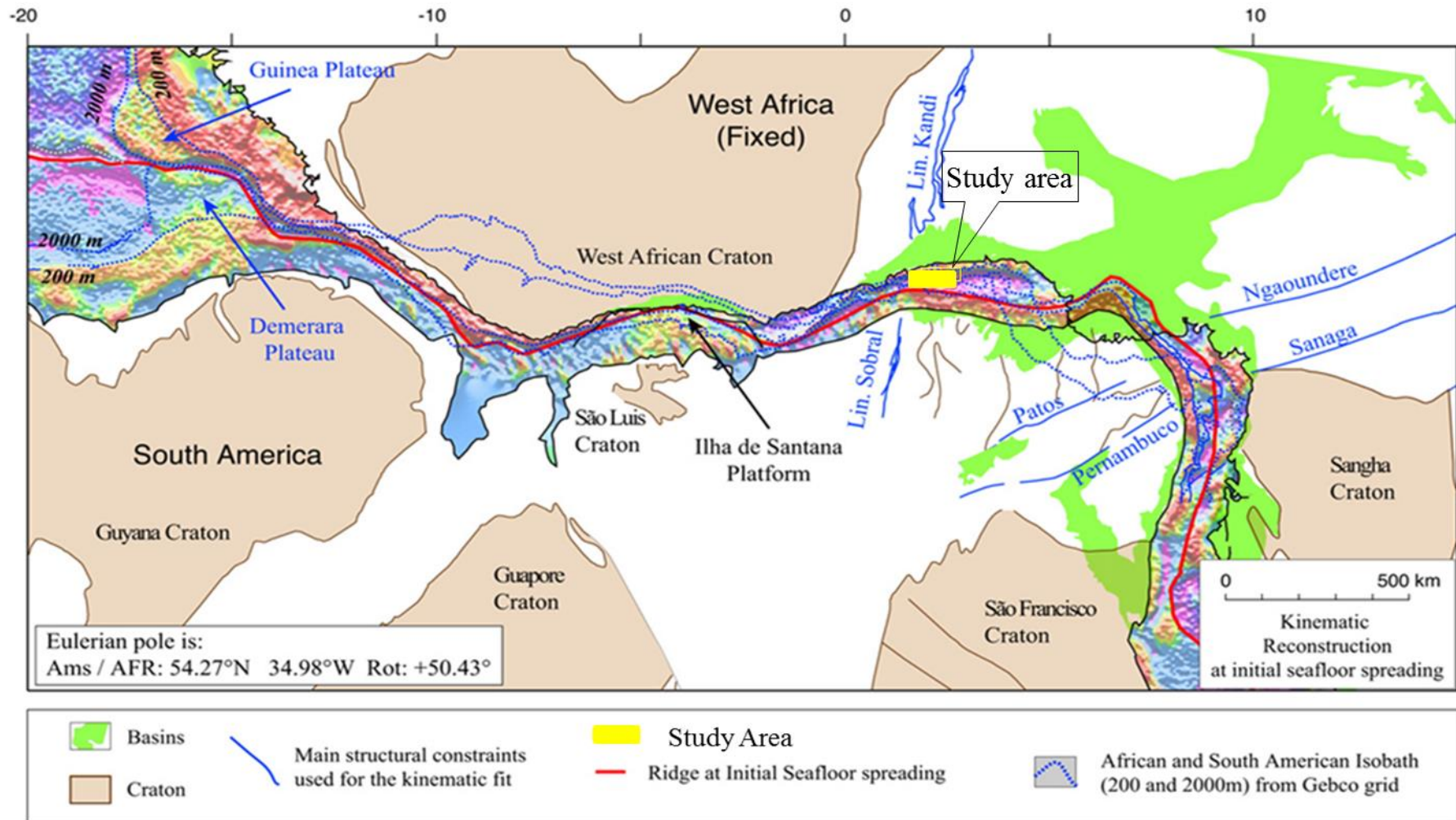


Figure 6.1: Palaeogeographic reconstruction of the Equatorial Atlantic Ocean. The figure shows, on each plate, gravity data from Sandwell and Smith (1997) between the coast and the area of continental breakup. The heavy red line shows the breakup separation between the plates by incipient seafloor spreading. Note the remarkable alignment of the conjugate pre-breakup fault systems (in blue: Kandi/ Sobral, Patos/Ngaoundere, Pernambuco/Sanaga lineaments and Demerara/Guinea plateaus). After Moulin et al. (2010).

Following Moulin et al. (2010), basement reactivation involving the Sobral Fault in the South American Plate is proposed for the N-S lithospheric rifting in the Benin Basin (Figure 6.2). During this rifting in the Benin Basin, it is thought that rifting was ongoing in some basins in the African intraplate region (e.g. Kantem, Bongor, Muglad Basins; Giedt, 1990; Mohamed et al., 2000; Fairhead et al., 2013). The movement along the N-S Sobral Fault caused the southern South American block to move relatively southward to its northern block. The relative movement between these blocks resulted in the initial N-S rifting of the southwestern Nigerian margin (Figure 6.3). Continental rifting in the study area is, therefore, unlikely to be associated with the subsequent development of the transform margin. However, the Equatorial Atlantic margin to the eastern parts of the study area had not fully opened for the North and South Atlantic to join (Figure 6.3; e.g. Moulin et al., 2010; Fairhead et al., 2013; Heine and Brune, 2014). The implication of this interpretation is that the Equatorial Atlantic that bridges the North Atlantic and the South Atlantic had not broken during the late Aptian (MSB3). The post-rift unconformity (MSB3) of late Aptian, therefore, suggests that rifting by orthogonal extension probably ceased in the Aptian as oblique rifting emerged on the eastern parts of the study area. This may account for the absence of the flower structures in the study area since flower structures are known to be characteristic structures of transform settings (e.g. Moulin et al., 2010; Basile, 2016; Mercer de Lépinay, 2016).

6.2.3 Significance of north-dipping normal faults

The basin-bounding normal faults (F1 and F2) in the Benin Basin dip to the north, away from the continental margin, a feature which is rare in passive margins. Could it be said that the landward dipping direction of this basin is linked to response to a change from N-S to NE-SW strike-slip movement that was set in the Aptian in the Equatorial

Atlantic? This would have as well changed the E-W to ENE-WSW strike of the Benin Basin. This is also consistent with the rifting described in this dissertation being related to phase of N-S lithospheric extension when the study area was located on the southern margin, or part of the greater Benin Basin. At that time, the half-graben bounding faults (F1 and F2) were dipping towards the rift access. This basin was presumably in the western part of the Benue Trough and Potiguar Basin (Brazil).

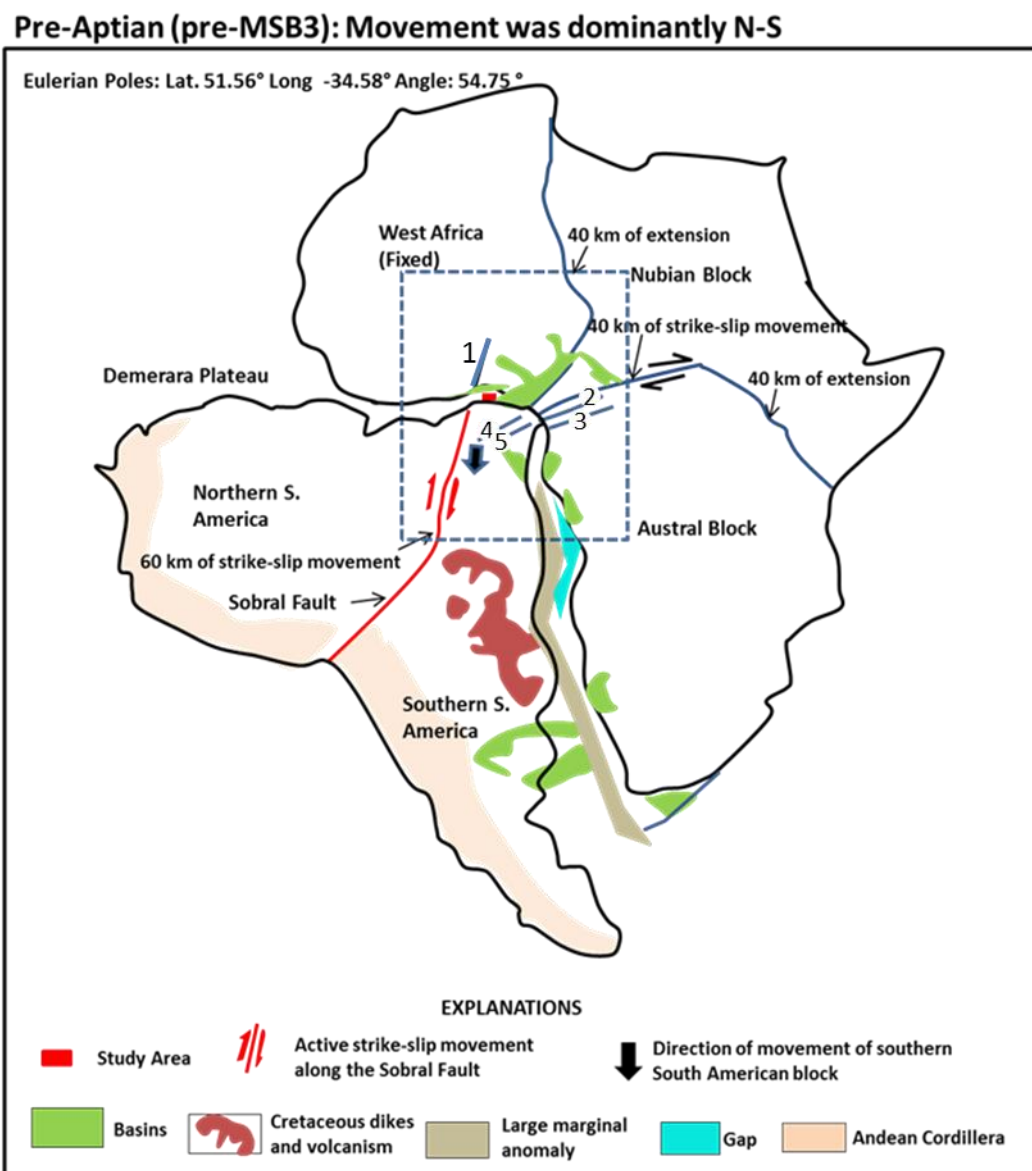


Figure 6.2: Paleogeographic reconstruction of the Equatorial Atlantic prior to the Aptian. African and South American Plates separation was dominantly in a N-S direction due to movement along the Sobral Fault (red line) in the South American Plate. Here, the southern South American block moved southward relative to a fixed northern South American block. Note the remarkable alignment of the conjugate pre-breakup fault lineaments: Sobral Fault / Kandi (1); Patos (4) / Ngaoundere (2); Pernambuco (5) / Sanaga (3). After Moulin et al. (2010).

The offshore Benin Basin became a ‘failed rift’ when rifting ceased at end of MS3 (late Aptian). Presumably extension leading to plate separation re-located somewhere to the south (close to the continent-ocean boundary) where the deformation was likely occurring/dominated by transform tectonics. Because of the rotation of the stress regime, this led to local inversion in the northern part of the study area, so that thermal subsidence was accompanied by local uplift. The Benin Basin could have failed as the Equatorial Atlantic began to open in the Albian. Its opening was by oblique rifting involving high angle faults. The failure of the offshore Benin Basin may be associated with the change in plate motion from N-S to NE-SW that marks the Equatorial Atlantic. The cessation of rifting in these basins has also been linked to the change in the plate motion (e.g. Guiraud et al., 1992; Moulin et al., 2010; Heine and Brune, 2014).

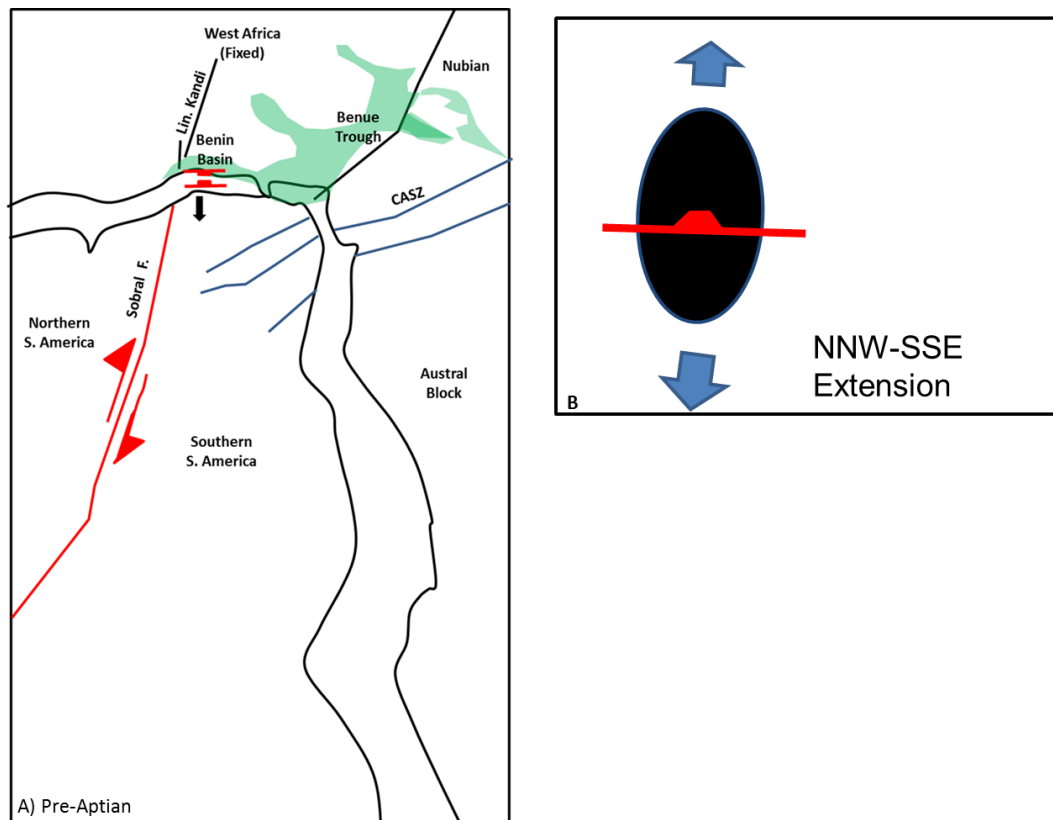


Figure 6.3: Geodynamic evolution of the Equatorial Atlantic margin based on the Benin Basin (offshore) during the Pre-Aptian times. A) Note that the Sobral Fault was active during the pre-Aptian. The southward movement of the southern South American block relative to the northern South American block. The West African remains fixed (modified after Moulin et al., 2010).

6.2.4 Significance of the breakup sequence

The post-rift unconformity (MSB3; late Aptian) suggests that the rifting in the Benin Basin did not coincide with the final breakup of the Africa and South America. From literature, the final breakup was reached in the middle Albian (Greenroyd, 2008; Greenhalgh et al., 2011), implying that the transition to breakup was recorded as the breakup sequence (Sequences S3A (early Albian) and Sequence S3B (middle Albian)). The transition phase can be tentatively dated as having occurred between the late Aptian (MSB3) and middle Albian. It may however be due to lack of accurate dating of the entire syn-rift megasequence (MS2). The breakup sequence is evidence that the Benin Basin experienced its initial continental crust breakup between the African and South American Plates when transform tectonism was still on-going in the Equatorial Atlantic. Perhaps the Equatorial Atlantic was already in its transform phase (e.g. Basile, 2016; Mercier de Lépinay et al., 2016). The dating problem is compounded as a result of the Cretaceous magnetic quiet time (125-84 Ma; e.g. Moulin et al., 2010) which affected the Equatorial Atlantic margin (e.g. Moulin et al., 2010; Fairhead et al., 2013; Basile, 2016; Mercier de Lépinay et al., 2016). The lack of magnetic reversal anomalies during the time rifting has made it difficult to estimate the continent-ocean boundary accurately (Moulin et al., 2010).

6.3 Late Aptian (MSB3) to Santonian (SB3F) tectonics

As noted above, the offshore Benin Basin also contains evidence for a major change in plate motion as it developed NE-SW striking shortening structures in the late Aptian/early Albian and in the Santonian (SB3F). These deformation events occurred after a time span of about 30 My. These, however, suggest that they are different tectonic phases that affected the Benin Basin. These structures strike differently from the ENE-WSW striking structures associated with the Equatorial Atlantic transform

margin, but are consistent with local NW-SE shortening within an ENE-WSW oriented dextral shear zone (Figures 6.4 and 6.5). The deformation event that immediately post-dated rifting in the late Aptian/early Albian can be linked to change in plate motion direction. This study also shows that the associated structures evolved due to basement reactivation that involved mild inversion. According to Matos (2000), Moulin et al. (2010), Fairhead et al. (2013), Heine and Brune (2014), Basile (2016), Mercier de Lapanay et al. (2016), the basins along the Equatorial transform margin are often characterised by prolonged propagation of their major strike-slip faults that often result in complex basin development on either side of the ocean (Figure 1.1). The thrust and folded structures studied in this dissertation are however not a result of prolonged propagation of strike-slip faulting. The Barremian - Aptian rifting episode in both the northern and the southern half-grabens is considered to be an earlier and separate tectonic event from those of the later deformation events. Such basin inversion is what Lowell (1995) described as selective basin inversion (McClay, 1995; Sibson, 1995; Glen et al., 2005; Grimaldi and Dorobek, 2011). The late Aptian/early Albian shortening in the offshore Benin Basin related to fault-related deformation that range from thrusting to inversion of transfer fault. Although the deformation did not invert the basin-bounding normal fault but the indirect intense buckling caused the thrusting on its hanging-wall.

Using the models of Guiraud et al. (1992) and Basile et al. (2005), the palaeogeography of the study area in the post-Aptian has been reconstructed (Figures 6.4 and 6.5). In order to accommodate the fault geometry and the NE-SW trend of the associated structures, in relation to the E-W to ENE-WSW trend of the major basin-bounding normal faults (F1 and F2), the hypothesis of intraplate deformation introduced by Burke and Dewey (1974) will be applied.

Post-Aptian reconstruction

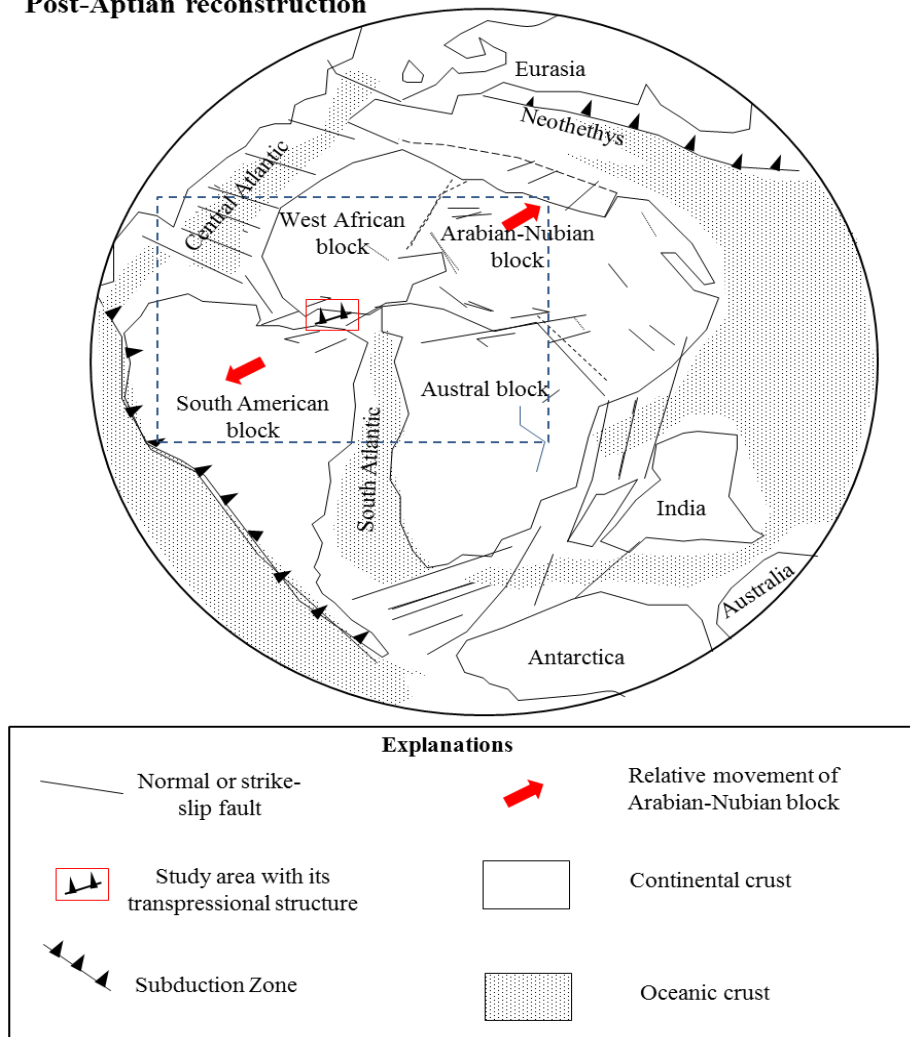


Figure 6.4: Reconstruction of the Early Cretaceous breakup of western Gondwana. Intraplate deformation emanating from the NE movement of the Arabian-Nubian block towards Eurasia, resulting in plate collision. The late Aptian/early Albian deformation recorded in the study area was possibly due to this collision. Blue dashed line rectangle is shown in Figure 6.5 (after Guiraud and Bellion, 1995; Bumby and Guiraud, 2005).

Since the introduction of the hypothesis of intraplate deformation in Africa at the Benue Trough by Burke and Dewey (1974), the hypothesis has been applied in order to close the Equatorial Atlantic and the South Atlantic Oceans by many authors (Pindell and Dewey, 1982; Fairhead, 1986; 1988; Guiraud and Maurin, 1991; 1992; Guiraud et al., 1992; Guiraud and Maurin, 1993; Guiraud and Bellion, 1995; Nilsen and Sylvester, 1995; Bosworth, 1995; Guiraud, 1998; Guiraud and Bosworth, 1997; 1999; Guiraud et

al., 2000; Basile et al., 2005; Moulin et al., 2010; Fairhead et al., 2013; Heine et al., 2013; Heine and Brune, 2014).

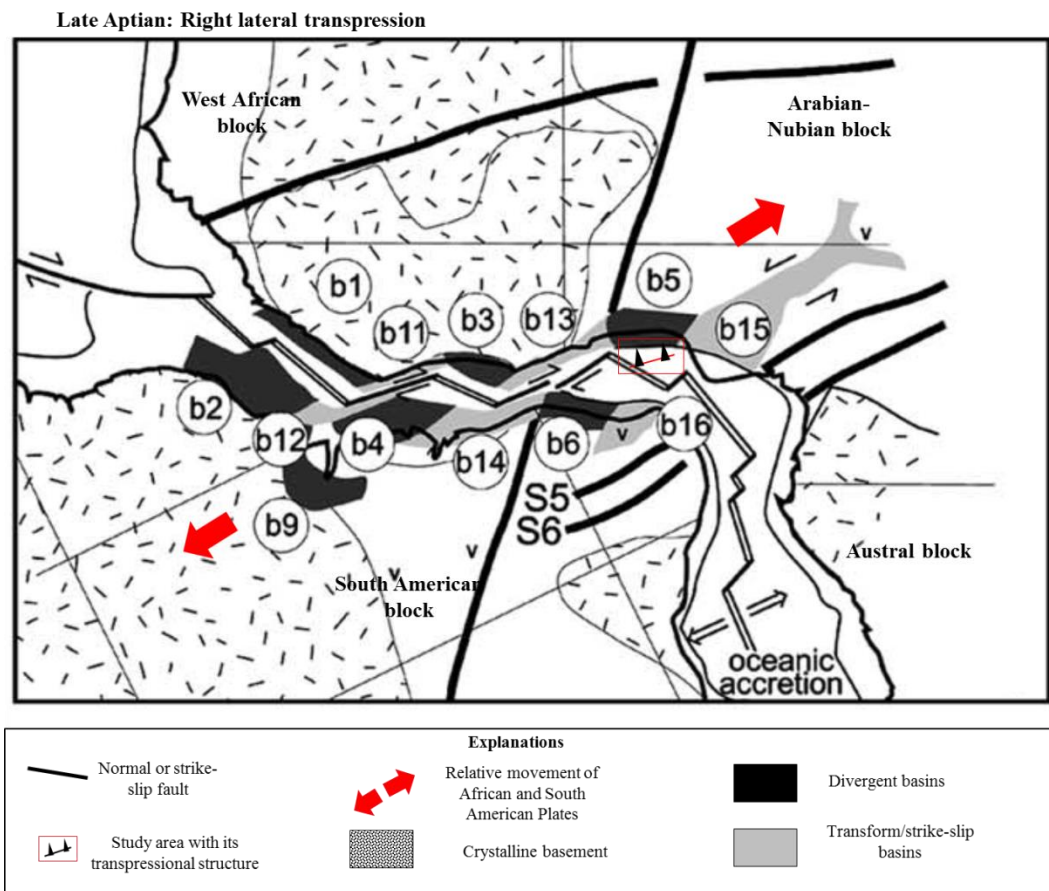


Figure 6.5: Geodynamic evolution of the Equatorial Atlantic margin based on the late Aptian/early Albian deformation in the Benin Basin (offshore). African Plate motion changed as the Nubian Block moved NE and was now stretching in the ENE-WSW direction. C1: West African craton; C2: Eburnean shield; C3: São Francisco craton; C4: São Luis craton; C5: Guyana craton. S1: Kandi lineament; S2: Guinean-Nubian lineaments; S3: South Adamaoua shear zone; S4: Sanaga shear zone; S5: Patos shear zone; S6: Pernambuco shear zone; S7: Trans-Brazilian fault zone. Conjugate divergent basins: b1 (Liberia) and b2 (Caciporè); b3 (deep Ivorian basin) and b4 (Barreirinhas); b5 (Benin) and b6 (Mundaú). Intracontinental divergent basins: b7 (Solimoes), b8 (Amazonas), b9 (Marajó), b10 (Tacutu). Conjugate transform continental margins: b11 (Côte d’Ivoire) and b12 (Pará-Maranhão); b13 (Ghana-Togo) and b14 (Ceará). Strike-slip basins: b15 (Benue), b16 (Potiguar) (after Basile et al., 2005).

According to Guiraud et al. (1992), Moulin et al. (2010), Fairhead et al. (2013), Heine and Brune (2014), intraplate rifting was transtensional. The late Aptian/early Albian deformation event could, therefore, be linked to the northeastward movement of the

Arabian-Nubian block. The motion was caused by the rejuvenation of the Central African Shear Zone (CASZ) in the Aptian (Guiraud and Maurin, 1992; Moulin et al., 2010). This shear zone divides the African Plate into the Arabian-Nubian and West African blocks. The reactivation of the Central African Shear Zone led to the movement of the Arabian-Nubian block towards the NE as the West African block remains fixed. This movement probably resulted to the Arabian-Nubian block moving northeasterly towards the Eurasian block. The collision between these blocks created these structures in the study area. The compressional stresses emanating from this collision may be transmitted through far-field stress (Guiraud et al., 1992). The World Stress map often shows that horizontal compressional stresses can be transmitted over great distances through the continental and oceanic lithosphere (Ziegler, 1989; Ziegler et al., 1995). This compressional stress possibly reactivated original structures and its deformation was subsequently accommodated by the folding on top of the fault tips. This deformation was therefore registered as inverted and thrust structures in the study area.

6.4 Santonian basin inversion

This Santonian deformation event in the offshore Benin Basin is related to southward propagation of deformation, although it still maintains its NW-SE compression. The Santonian deformation event has been well studied by many authors (e.g. Guiraud and Maurin, 1992; Moulin et al., 2010) in the passive margins and intraplate basins in the West and Central African rift systems (Figure 6.6). However, during the Santonian, the African Plate had started drifting in the NE direction (Figure 6.6; Brownfield and Charpentier, 2006; Moulin et al., 2010; Fairhead et al., 2013; Heine and Brune, 2014).

The implication of this study is that the opening of the Equatorial Atlantic Ocean did not only involve transpressional deformation widely believed by many authors (e.g. Heine and Brune, 2014). But its opening might have included orthogonal movement in

the passive margin as it has been revealed in this study. Intraplate deformation involving transtensional movement is well-known and reported in the African interior (e.g. Basile et al., 2005; Fairhead et al., 2013).

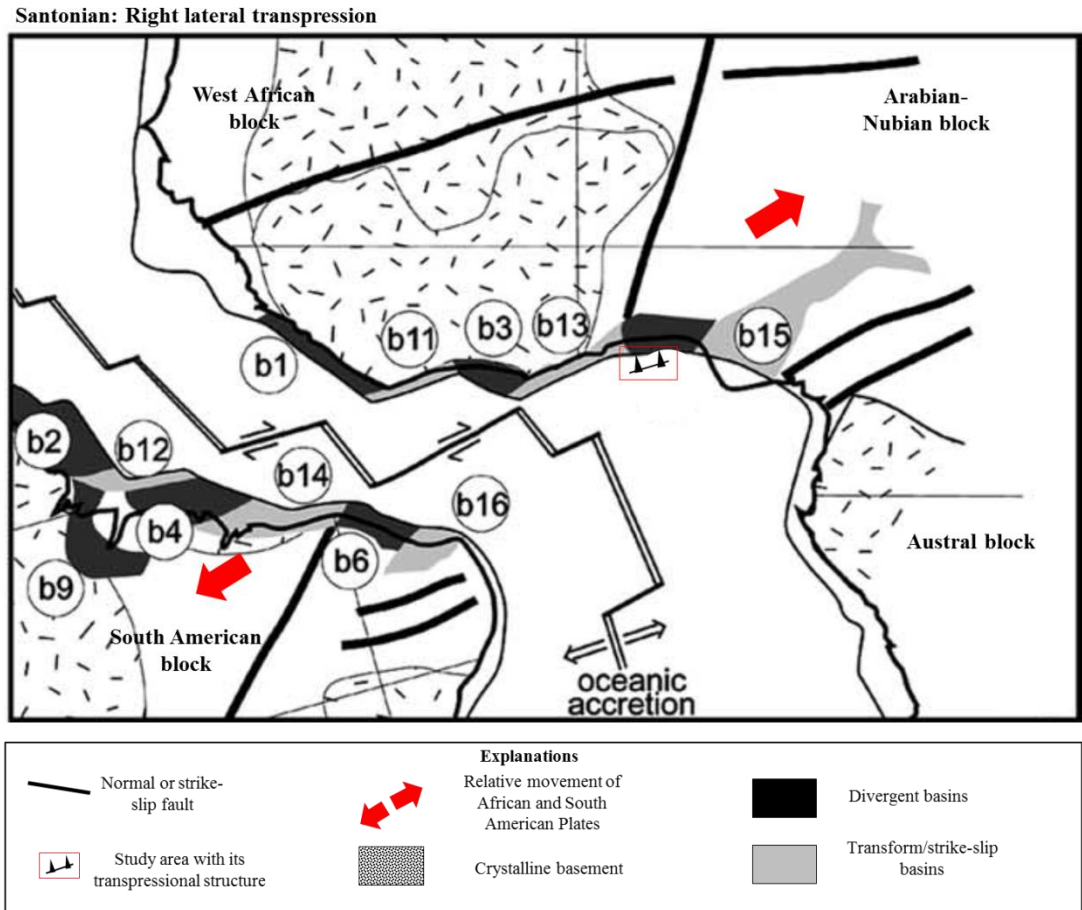


Figure 6.6: Santonian deformation of the study area thought to result from right-lateral transpression. Continued movement of the Arabian-Nubian block towards the European block in the Santonian. See legend used for Figure 6.5 (after Basile et al., 2005).

6.5 Opening models for the Equatorial Atlantic

The Equatorial Atlantic margin became passive in the Santonian as the offshore Benin Basin was being deformed by the Santonian contraction. The tectonic history of the offshore Benin Basin involves two important stages. These include the first N-S rifting and a NE-SW moving of the plates. The N-S movement is associated with N-S

orthogonal extension (Figure 6.7A) while the second stage involves an NE-SW transpressional movement (Figure 6.7B).

The 2-stage opening invoked for the Equatorial Atlantic was consistent with the models of some authors (e.g. Moulin et al. 2010; Fairhead et al., 2013). Many authors, however, believe the Equatorial Atlantic had maintained one stage movement involving ENE-WSW direction throughout its tectonic history (e.g. Heine and Brune, 2014; Basile, 2016).

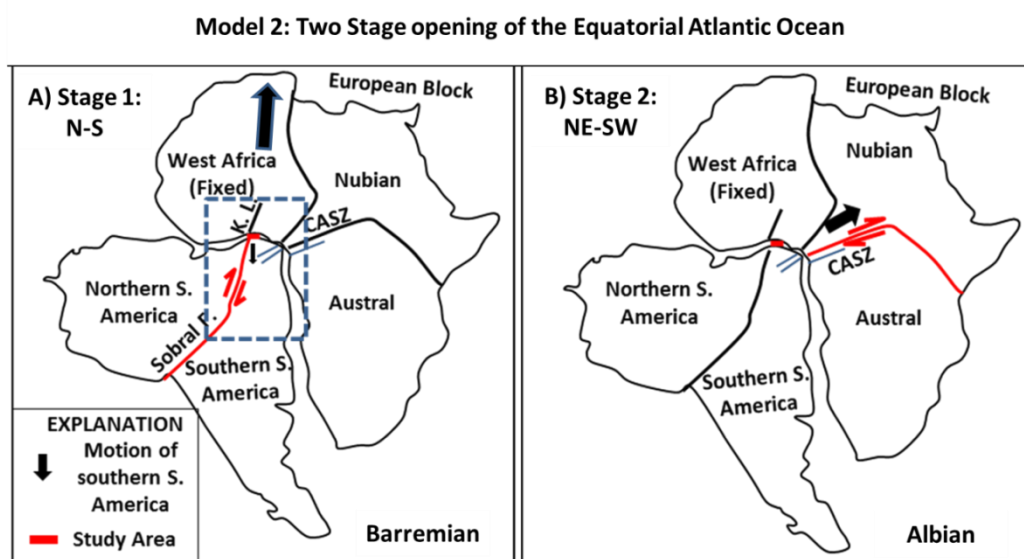


Figure 6.7: A two-stage opening model resulted in the opening of the Equatorial Atlantic Ocean. A) An initial opening involved the northward movement of the African Plate relative to the South American Plate in the Barremian. A northward movement of the African Plate occurred due to movement along the re-activated N-S Sobral Fault (the red line indicates active fault) (e.g. Moulin et al., 2010). B) Stage 2 NE-SW movement due to a change in the direction of movement of the African Plate in the Albian. The NE movement occurred through the reactivation of the Central African Shear Zone (red line) (CASZ; e.g. Fairhead et al., 2013).

6.6 Cenozoic sedimentation

The study shows that the Cenozoic is characterised by a period when sedimentation was largely controlled by relative sea level change. A plot of the sea level curve plotted for

the Cenozoic shows that the transgressive megasequence (MS4) was deposited under a relative sea level rise (Figure 5.7)

The regressive megasequence (MS5) is characterised by deposition under relative sea level fall. The regressive megasequence (MS5) is composed of some evidence of deposition under relative sea level fall such as the Miocene/Pliocene slump, submarine canyons, etc.

6.7 Implications of tectonics for the hydrocarbon entrapment in the offshore Benin Basin

Tectonics enhances the generation of structures such as folds and faults that can generally promote migration and accumulation of hydrocarbons. The mechanisms of a breakup, therefore, exert control on the distribution of petroleum in extensional basins and passive margins (including the intracontinental rift systems) (Magoon, 1988; Morley, 1995; Szatmari, 2000; Davison and Underhill, 2012).

A network of both shortening and extensional structures may form future hydrocarbons entrapment in the Equatorial Atlantic. The Eji anticline associated with the Santonian (SB3F) deformation event appears to have more potential as a trap than the one of the late Aptian/early Albian tectonic inversion. The reason is probably due to its fault (F3) associated with the Santonian (SB3F) deformation connects most of the pre-Santonian sedimentary strata and the basement (Figure 4.25). This study, therefore, reveals that the main hydrocarbon structure that is potentially viable in the offshore Benin Basin is the Santonian (SB3F) structure, that is, the fault-propagation fold (Figure 4.25). Its implication can be great on hydrocarbons accumulation.

The offshore Benin Basin may become a future hydrocarbon entrapment if the structural trends of the both extensional and shortening structures are studied in order to explore

for its hydrocarbons. However, shortening structures may post-date initial migration from source rocks, introduce some charge risk. Because the contraction modified the original extensional geometries there is also risk of loss of hydrocarbons during re-migration (Warren, 2009).

Chapter Seven

7.0 Summary, Conclusions, and Recommendations

7.1 Summary

This study describes and evaluates the seismic data tie to well data from four closely-spaced deviated wells (B-01 to B-04) to predict a tectonic evolution for the offshore Benin Basin. The study reveals the presence of both tectonic and non-tectonic structures. The tectonic structures include two half-grabens, two basin-bounding normal faults, inverted structure, thrust and folds, reverse fault, relay and transfer structures. The two half-grabens are synchronous and are characterised by E-W to ENE-WSW striking basin-bounding normal faults (F1 and F2). The basin-bounding normal faults (F1 and F2) are planar and dip northward at about 40° or sometimes less. The low dip of the basin-bounding normal faults may probably be related fault rotation during thermal subsidence. The non-tectonic structures comprise gravitational structures (mainly normal faulting). The study has shown that the study area is made up of five megasequences comprising: pre-rift (MS1), syn-rift (MS2), Cretaceous post-rift (MS3), transgressive (MS4), and regressive (MS5) megasequences.

The structural styles suggest a northward rifting-propagation for this basin. This corroborates with those E-W striking basins along the South Atlantic margin. It also validates the Barremian to Aptian age ascribed to the offshore Benin Basin in this study. The wedge geometry recorded on the seismic data suggests an 'Atlantic-type' of rifted basin. The syn-rift megasequence (MS2) suggests continental rifting by orthogonal extension.

The late Aptian/early Albian deformation event, which is restricted to the northern half-graben, is associated with the inverted structure, thrusting, and folding. Four structures have been studied representing the Aptian deformation: the Elo thrust, the Oga fold, the Iro transfer, and the Ore thrust. Another deformation phase prevailed in the Santonian (SB3F) and it is represented by the Eji anticline. The Santonian event involves basement-involved reverse fault (F3). Both events formed NE-SW striking structures. Both the late Aptian/early Albian and the Santonian events are mild and short-lived.

The implication of both the extensional and shortening structures for geodynamics of the southwestern Nigeria suggests that the African and South American Plates experienced changes in their direction of movement, thereby giving rise to a possible 2-stage opening of the Equatorial Atlantic:

- ❖ An initial N-S orthogonal extensional movement between the African and South American Plates in the Barremian to Aptian. This led to the formation of the E-W to ENE-WSW trending rifted basins or passive margin in the southwestern Nigeria. It has been proposed that the continental rifting could possibly be due to the reactivation of the N-S striking Sobral Fault (e.g. Moulin et al., 2010). The Sobral Fault subdivides the South American Plate into two parts: the northern and southern South American blocks. The southward movement of the southern South American block relative to a fixed northern South American block along the Sobral Fault probably led to the initial N-S opening of the SW Nigerian margin in the pre-Aptian time.
- ❖ A probable change in the direction of movement from N-S to NE-SW movement occurred in the post-Aptian. It is proposed in this study that the NE movement may be related to the movement along the Central African Shear Zone (CASZ) leading to the relative NE movement of the Nubian block

toward the European block. The West African block remains fixed (e.g. Guiraud et al., 1992; Fairhead et al., 2013). This movement may have emanated from the plate re-organisation leading to change in stress field (Janssen et al., 1995; Joshi and Hayashi, 2010).

The tectonic evolution of the offshore Benin Basin also has implication for sedimentation in this basin. The thick growth sequences in both northern and southern half-grabens represent the syn-tectonic deposition during the continental rifting. These thick growth sequences of the syn-rift phase comprising divergent reflections that thicken toward the basin-bounding normal fault, with their increasing dips- all suggest deposition due to block rotation as the African and South American Plates are extending.

Depending on the timing of hydrocarbon generation in this basin, both the extensional and shortening structures may enhance primary and secondary migration of hydrocarbons and consequently their accumulation in the structural trap. Secondary migration seems to be more probable, as the later developed faults (reverse/thrust faults) may permit re-migration and possible accumulation of hydrocarbons in their associated structural traps. This study has revealed that the Eji anticline of the Santonian deformation event is most viable hydrocarbons trap in the study area. The Eji anticline of the Santonian deformation correlates with the Aje structure that the Oil operator of the study area is prospecting for hydrocarbons.

The Cenozoic successions in the offshore Benin Basin have shown that their deposition was controlled, among other factors, by relative sea level change. The transgressive megasequence (MS4) is thought to be deposited during a relative sea level rise. The regressive megasequence (MS5) is made up of mainly prograding sequences suggesting sedimentation under relative sea level fall.

Two episodes of slumping were studied in this thesis: Campanian/Maastrichtian slump and late Miocene/Pliocene slump. The Campanian/Maastrichtian slump however affected the Late Cretaceous strata. Its growth sequence suggests that it prevailed in the Maastrichtian. The Miocene/Pliocene slump affected the Cenozoic successions and controls the distribution and transportation of post-failure strata (MTCs). The study reveals the presence of ancient submarine canyons. Both the MTCs and submarine canyons trend NE-SW similar to those of the Aptian and Santonian deformation events, these suggest that their evolution was probably enhanced by the deformation events.

The sequence stratigraphic models associated with the Cenozoic successions are conformable with those of Vail et al. (1977) and Neal and Abreu (2009) models.

7.2 Conclusions

The following conclusions emanated from the interpretations made in this study:

- ❖ The offshore Benin comprises classic wedge geometries that permit its classification as a passive rifted margin that evolved in the Barremian-Aptian rifting episode. An orthogonal extension is proposed in this study for the evolution of the E-W to ENE-WSW trending offshore Benin Basin.
- ❖ The study area is made up of two half-grabens separated by a ridge termed as Gaga ridge.
- ❖ Two northward-dipping basin-bounding normal faults (F1 and F2).
- ❖ The study area is made up of at least two episodes of tectonic compression namely the late Aptian/early Albian and the Santonian deformations. Both deformation events created structures that strike NE-SW.
- ❖ That the continental separation of the African and South American Plates along the SW Nigerian margin probably occurred in 2-stage: an initial N-S movement during the pre-Aptian; and an NE-SW movement in the post-Aptian.

- ❖ The deformation of the offshore Benin Basin introduces transpressional movement in the late Aptian/early Albian and in the Santonian.
- ❖ The deformation events did not only control the topography of the seafloor but it, however, enhances sedimentation since the late Aptian to Recent. They also enhance the evolution of the submarine canyons, incision and slumping (e.g. Blum and Aslan, 2006).
- ❖ The post-rift unconformity (MSB3) dated late Aptian suggests an onset of continental breakup since a final breakup is thought to have occurred in the middle Albian (e.g. Greenroyds et al., 2008; Greenhalgh et al., 2011) in the Equatorial Atlantic.
- ❖ The presence of the breakup sequence (late Aptian to early/middle Albian) implies that a transition phase exists between the start of oceanic spreading and the final continental separation (Greenhalgh et al., 2011).
- ❖ The Cenozoic successions comprise stacking patterns ranging from aggradation, retrogradation, progradation to degradation.
- ❖ Mass-transport complexes (MTCs) occur in the offshore Benin Basin that suggests evidence for sediment distribution under the influence of relative sea level change. These MTCs range from late Miocene to Pleistocene in age.

7.3 Recommendations

7.3.1 Limitations of this study

This study has been carried out on an integration of 2D and 3D seismic and well data of four closely-spaced wells. Despite the limited data size, this study has revealed some key issues on how and when the offshore Benin Basin probably evolved. These datasets, in addition to existing information and new results derived from these well data that accompanied these datasets, have provided an insight into the tectonic evolution and

geodynamic framework that explains the tectonic evolution of the offshore Benin Basin located on the Equatorial Atlantic margin.

One of the main limitations to this study is the location of the wells. Apart from them being closely-located, that permits detailed study; the exploratory wells are, however, located on the southern half-graben; with none on the northern half-graben. Correlation between the two half-grabens was compounded by the ridge (Gaga Ridge) that separates these half-grabens.

Another limitation is the lack of the well data coverage of the entire syn-rift megasequence (MS2). The wells did not penetrate the entire syn-rift phase. This, therefore, led to dating the rift-initiation stage by correlation with adjoining sedimentary basins. The lack of drilling of this interval has also led to uncertainty in terms of its hydrocarbon prospectively.

The 3D seismic data did not cover the entire areal extent of the two half-grabens studied in this thesis.

Most parts of the northern half-graben where the clinoforms concentrate were not covered by the 3D. This has however limited the detailed sequence stratigraphic study of the Cenozoic succession.

The resolution and quality of the seismic data are other factors limiting a more insightful analysis.

- ❖ The resolution and quality of the seismic data did not allow easy identification of the wedge geometry in the southern half-graben.
- ❖ The resolution and quality did not allow the analysis of the sequence stratigraphic study of the syn-rift megasequence.

7.3.2 Future Work

In spite of the results obtained in this study, there are a variety of puzzling areas that remain unclear or is mentioned here for the first time; these open for subsequent studies. Even some that are well-represented by their seismic geometries need regional studies in order to establish their extent. All these will better our understanding of the poorly-studied offshore Benin Basin located on the eastern border of the Equatorial Atlantic.

There is yet much work to be carried out especially in the dating of the syn-rift megasequence (MS2). A more detailed lithostratigraphic, chronostratigraphic, and palaeontological control that will allow dating of the rifting events especially the early rift sequence (S2A) which was not biostratigraphically dated. This may be achieved by drilling well(s) to the basement and acquire core samples from the syn-rift megasequences. Such core samples will provide both sedimentological and palaeontological information for the syn-rift intervals. This is very important because the syn-rift megasequence did not outcrop in any part of this basin. The problem of the dating of tectonic events is compounded by quiet magnetic zone known to be associated with the Equatorial Atlantic margin. This will, therefore, help to resolve the uncertainty that surrounds the age of the syn-rift as well as the post-rift megasequences.

Geophysical logging of such well(s) may also be included in order to provide the well-logs of the syn-rift intervals to compliment the seismic data and the core samples.

Further work is suggested by the analysis of the deformation events revealed in this study. This is particularly important for the late Aptian/early Albian structures, because basin inversion of this age has not been reported in the Equatorial Atlantic margin. This will enhance the conclusions made in this study with respect to the implications for the geodynamics of the SW Nigerian margin. It will also validate the orthogonal compression proposed for the both the Aptian and the Santonian structures.

The mass-transport complexes (MTCs) should be detail studied in the deep water environments in order to enhance their exploration for hydrocarbons.

A further regional study may be carried out on the entire offshore Benin Basin that extends from SW Nigeria to eastern Ghana; this will help to validate the inferences and deductions made in this study, as well as knowing the extent of orthogonal extension, transpressional deformation, and the geodynamics of the entire offshore Benin Basin.

References

- Abreu, V., Sullivan, M. D., Mohriak, D. and Pimez, C. (2003): Lateral accretion packages (LAPS): an important reservoir element in deep water sinuous channels. *Marine and Petroleum Geology*, 20, 631-648.
- Abreu, V., Neal, J. E., Bohacs, K. M. and Kalbas, J. L. (Eds) (2010) *Sequence Stratigraphy of Siliciclastic Systems - The Exxon Mobil Methodology. Atlas of Exercises*. Society of Economic Palaeontologists and Mineralogists, Concepts in Sedimentology and Paleontology. Oklahoma, USA. 226.
- Acocella, V., Morvillo, P. Funicello, R. (2005): What controls relay ramps and transfer faults within rift zones? Insights from analogue models. *Journal of Structural Geology*, 27, 397–408.
- Adegoke, O. S. (1969): The Eocene stratigraphy of Southern Nigeria. *Bulletin Bureau Research Geology Memoir*, 69, 23-48.
- Adeleye, D. R. (1975): Nigerian Late Cretaceous stratigraphy and paleogeography. Petrographical Study of Ewekoro Carbonate Rocks, in Ibese, South Western Nigeria Bulletin, 59 (12), 2302-2313.
- Adekeye, A. and Akande, S. O. (2010): The Principal source rocks for petroleum generation in the Dahomey Basin, southwestern Nigeria. *Continental Journal of Earth Sciences*, 5 (1), 42-55.
- Ajibade, A. C and Fitches W. R. (1988): The Nigerian Precambrian and the Pan-African Orogeny, *Precambrian Geology of Nigeria*, 45-53.
- Akinmosin, A. and Osinowo, O. O. (2010): Petrographical study of Ewekoro carbonate rocks, in Ibese, South Western Nigeria. *Earth Science Research Journal*, 14 (2), 187-196
- Akinmosin, A., Omosanya, K. O., Ariyo, S. O., Folorunsho, A. F. and Aiyeola, S. O. (2011): Structural control for bitumen seepages in Meri, Southwestern Nigeria. *International Journal of Basic and Applied Sciences*, 11 (1), 93-103.
- Ako, B. D., Adegoke, O. S. and Petters, S.W. (1980): Stratigraphy of Oshoshun Formation in South-western Nigeria. *Journal of Mining and Geology*, 17 (1), 97-106.
- Ala, M. A. and Selley, R. C. (1997): The West African Coastal Basins (Chapter 8). In: Selley, R.C. (Ed.), *Sedimentary Basins of the World*. Elsevier, 173-186.
- Allen, J. R. L. (1964): The Nigerian continental margin: *Marine Geology*, 1, 289-332.
- Allen, P. A. and Allen J. R. (2013): *Basin Analysis: Principles and application to petroleum assessment*. Willey-Blackwell, London.
- Alexander, J. and Leeder, M. R. (1986): Active tectonic control on alluvial architecture. In: Flores, R., Ethridge, F., and Harvey. M. (Eds), *Recent developments in fluvial*

- sedimentology. Society of Economic Paleontologists and Mineralogists Special Publications, 39, 243-252.
- Almagor, G., and Garfunkel, Z. (1979): Submarine Slumping in Continental Margin of Israel and Northern Sinai. American Association of Petroleum Geologists Bulletin 63 (3), 324-340.
- Alves, T. M., Manuppella, G., Gawthorpe, R. L., Hunt, D. W. and Monteiro, J. H. (2003): The depositional evolution of diapir-and fault-bounded rift basins: examples from the Lusitanian Basin of West Iberia. Sedimentary Geology, 162, 273-303.
- Alves, T. M., Moita, C., Sandnes, F., Cunha, T., Monteiro, J. H. and Pinheiro, L. M. (2006): Mesozoic-Cenozoic evolution of North Atlantic continental-slope basins: The Peniche basin, western Iberian margin. American Association Petroleum Geologists Bulletin, 90 (1), 31-60.
- Alves, T. M. (2010): 3D Seismic examples of differential compaction in mass-transport deposits and their effect on post-failure strata. Marine Geology, 271 (3-4), 212-224.
- Alves, T. M. and Cartwright, J. A. (2009): Volume balance of a submarine landslide in the Espírito Santo Basin, offshore Brazil: quantifying seafloor erosion, sediment accumulation and depletion. Earth and Planetary Science Letters, 288(3-4), 572-580.
- Alves, T. M. and Cartwright, J. A. (2010): The effect of mass-transport deposits on the younger slope morphology, offshore Brazil. Marine and Petroleum Geology, 27 (9), 2027-2036.
- Alves, T. M., Kurtev, K., Moore, G. F. and Strasser, M. (2014): Assessing the internal character, reservoir potential, and seal competence of mass-transport deposits using seismic texture: A geophysical and petrophysical approach. American Association of Petroleum Geologists Bulletin, 98 (4), 793-824.
- Alves, T. M. (2015): Submarine slide blocks and associated soft-sediment deformation in deep-water basins: A review. Marine and Petroleum Geology, 67, 262-285
- Anders, M. H., and Schlische, R. W. (1994): Overlapping faults, intrabasin highs and the growth of normal faults. The Journal of Geology, 102, 165-180
- Annor, A. E., Olobaniyi, S. B. and Mucke, A. (1997): Silicate facies iron-formation of the Egbe-Isanlu Palaeoproterozoic schist belt, Southwest Nigeria. Journal of African Earth Sciences, 24, 39-50.
- Antobreh, A. A., Faleide, J. I., Tsikalas, F. and Planke, S. (2009): Rift- shear architecture and tectonic development of the Ghana margin deduced from multichannel seismic reflection and potential field data. Marine and Petroleum Geology, 26, 345-368.
- Apotria, T., R. Lindholm, W. Metner, M. Eze1, D. Gunn, J. Geslin, P. Rumelhart, F.Goulding, and S.Mitchell (2004): Volume interpretation of shelf collapse processes and Biafra “disturbed” reservoirs, eastern Niger Delta joint venture: American Association of Petroleum Geologists, International Conference, Cancun, Mexico.

- Araripe, P. T. and Feijó, F. J. (1994): Bacia Potiguar. *B. Geoci. Petrobrás* 8 (1), 127–141.
- Aschoff, J. L. and Schmitt, J. G. (2008): Distinguishing syntectonic unconformity types to enhance analysis of growth Strata: An example from the Cretaceous, southeastern Nevada, U.S.A. *Journal of Sedimentary Research*, 78 (9), 608-623.
- Attoh, K., Brown, L., Guo, J. and Heanlein, J. (2004): Seismic stratigraphic record of transpression and uplift on the Romanche transform margin, offshore Ghana. *Tectonophysics* 378, 1-16.
- Austin, J. A. J. and Uchui, E. (1982): Continental-oceanic crustal transition off Southwest Africa. *American Association of Petroleum Geologists Bulletin*, 66 (9), 1328-1347.
- Austin, J., Bellahsen, N., Leroy, S., Husson, L., Beslier, M. and d'Acremont, E. (2013): The role of structural inheritance in oblique rifting: Insights from analogue models and application to the Gulf of Aden. *Tectonophysics*, 607, 51-64.
- Aydin, A. and Nur, A. (1982): Evolution of pull-apart basins and their scale independence. *Tectonics* 1/1, 91-105.
- Aydin, A. and Reches, Z. (1982): Number and orientation of fault sets in the field and in experiments. *Geology* 10, 107-112.
- Ayodele, O. S. (2013): Geology and structure of the Precambrian rocks in Ewekoro, Are and Afao, Southwestern Nigeria. *International Research Journal of Sciences*, 1(1), 14-29.
- Bacon, M., Simm, R. and Redshaw, T. (2009): 3-D Seismic interpretation. Cambridge University Press, Cambridge. 225.
- Basile, C., Mascle, J., Popoff, M., Bouillin, J. P. and Mascle, G. (1993): The Ivory Coast-Ghana transform margin - a marginal ridge structure deduced from seismic data. *Tectonophysics*, 59, 1-19.
- Basile, C., Mascle, J., Benkhelil, J. and Bouillin, J. P. (1998): Geodynamic evolution of the Côte d'Ivoire-Ghana transform margin: an overview of Leg 159 results. In: Mascle, J., Lohmann, G. P., Moullade, M. (Eds), *Proceedings Oil Drilling Programme, Scientific Results*, 159, 101-110.
- Basile, C. and Brun, J. P. (1999): Transtensional faulting patterns ranging from pull-apart basins to transform continental margins: an experimental investigation. *Journal of Structural Geology*, 21, 23-37.
- Basile, C., Mascle, J. and Guiraud, R. (2005): Phanerozoic geological evolution of the Equatorial Atlantic domain. *Journal of African Earth Sciences*, 43 (1-3): 275-282.
- Basile, C. (2016): Transform continental margins - part 1: Concepts and models. *Tectonophysics*, 661, 1-10.

- Baudin, F. and Berthou, P. Y. (1996): Environments de dépôt de la matière organique des sédiments aptiens-albiens du bassin d'Araripe (NE du Brésil). *Bull. Centres Rech. Exploration Production Elf Aquitaine* 20 (1), 213–227.
- Beauboeuf, R. T. and Friedmann, S. J. (2000): High-resolution seismic/sequence stratigraphic framework for the evolution of Pleistocene intra slope basins, Western Gulf of Mexico: depositional models and reservoir analogs. In: Weimer, P., Slatt, R. M., Coleman, J., Rosen, N. C., Nelson, H., Bouma, A. H., Styzen, M. J. and Lawrence, D. T. (Eds); *Deep-water reservoirs of the World: Gulf Coast Society of the Society of Economic Paleontologists and Mineralogists Foundation, 20th Annual Research Conference*, 40-60.
- Beauchamp, W., Barazangi, M., and Demnati, M., and Alji, M. E. (1996): Intracontinental rifting and inversion: Missouri Basin and Atlas Mountains, Morocco. *American Association of Petroleum Geologists Bulletin*, 80/9, 11459-1481.
- Beglinger, S. E., Doust, H., Cloetingh, S. (2012): Relating petroleum system and play development to basin evolution: West African South Atlantic basins. *Marine Petroleum Geology*, 30, 1-25.
- Benkhelil, J., Dainelli, P., Ponsard, J. F., Popoff, M. and Saugy, L. (1988): The Benue Trough: wrench fault related basins on the border of the Equatorial Atlantic. In: Manspeizer, W (Editor), *Triassic-Jurassic Rifting-Continental Breakup and the Origin of the Atlantic Ocean and Passive Margins. (Developments in Geotectonics, 22)*, Elsevier, Amsterdam, B, 787-820.
- Benkhelil, J., Mascle, J. and Tricart, P. (1995): The Guinea continental margin: an example of a structurally complex transform margin. *Tectonophysics*, 248, 117-137.
- Benkhelil, J., Giresse, P., Poumot, C. and Ngueutchoua, G. (2002): Lithostratigraphic, geophysical and morpho-tectonic studies of the South Cameroon shelf. *Marine and Petroleum Geology*, 19 (4), 499-517.
- Berg, O. R. (1982): Seismic detection and evaluation of delta and turbidite sequences: their application to the exploration for the subtle trap. In: Halbouty, M. T. (Ed.), *The Deliberate Search for the Subtle Trap. American Association of Petroleum Geologists Memoir*, 32, 57-75.
- Bernal, A. and Hardy, S. (2002): Syn-tectonic sedimentation associated with three-dimensional fault-bend fold structures: a numerical approach. *Journal of Structural Geology*, 24 (4), 609-635.
- Bigi, S. (2006): An example of inversion in a brittle shear zone. *Journal of Structural Geology* 28, 431-443.
- Billman, H. G. (1992): Offshore stratigraphy and paleontology of the Dahomey (Benin) Embayment, West Africa. *Nigerian Association of Petroleum Explorationists Bulletin*, 7 (2), 121-130.

- Bilotti, F. and Shaw, J. H. (2005): Deep-water Niger Delta folds and thrust belt modeled as a critical-taper wedge: The influence of elevated basal fluid pressure on structural styles. *American Association of Petroleum Geologists Bulletin*, 89, 1475-1491.
- Bilotti, F., Shaw, J. H., Cupich, R. M. and Lakings, R. M. (2005): Detachment fold, Niger Delta. In: Shaw, J. H., Connors, C. and Suppé, J. (Eds) *Seismic interpretation of contractional fault-related folds*. American Association of Petroleum Geologists, *Studies in Geology*, 53, 103-104.
- Binks, R. M. and Fairhead, J. D. (1992): A plate tectonic setting for Mesozoic rifts of West and Central Africa. *Tectonophysics*, 213 (1-2): 141-151.
- Bird, D. (2001): Shear margins: Continent-ocean transform and fracture zone boundaries. *The Leading Edge*, 20 (2), 150-159.
- Black, R., (1984): The Pan-African event in the geological framework of Africa. *Pangea* 2, 6–16.
- Blaich, O. A., Faleide, J. I. and Tsikalas, F. (2011): Crustal breakup and continent-ocean transition at South Atlantic conjugate margins. *Journal of Geophysical Research: Solid Earth*, 116 (B1), B01402.
- Blarez, E. and Mascle, J. (1988): Shallow structures and evolution of the Ivory Coast and Ghana transform margin. *Marine and Petroleum Geology*, 5, 54-64.
- Blum, M. D. and Aslan, A. (2006): Signatures of climate versus sea level change within incised valley-fill successions: Quaternary examples from the Texas Gulf Coast. *Sedimentary Geology*, 190, 177-211.
- Boillot, G. (1988): Rifting of the Galicia margin: crustal thinning and emplacement of mantle rocks on the seafloor. *Proceedings of the Ocean Drilling Program, Scientific Results*, 103, 741-756.
- Bonini, M., Souriot, T., Boccaletti, M. and Brun, J. P. (1997): Successive orthogonal and oblique extension episodes in a rift zone: Laboratory experiments with application to the Ethiopian Rift. *Tectonics*, 16(2), 347-362.
- Bosence, D., Cross, N. and Hardy, S. (1998): Architecture and depositional sequences of Tertiary fault-block carbonate platforms: an analysis from outcrop (Miocene, Gulf of Suez) and computer modeling. *Marine and Petroleum Geology*, 15 (3), 203-221.
- Bosworth, W. (1995): A high-strain rift model for the southern Gulf of Suez (Egypt). In: Lambiase, J. J. (Ed.), *Hydrocarbon Habitat in Rift Basins*. *Geology Society London, Special Publications*, 80: 75-102.
- Bourbié, T. Coussy, O. and Zinszner, B. (1987): *Acoustics of porous media*. Gulf Publishing, Houston.

- Bouriak, S., Vanneste, M. and Saoutkine, A. (2000): Inferred gas hydrates and clay diapirs near the Storegga slide on the Southern edge of the Voring Plateau, Offshore Norway. *Marine Geology*, 163:125-148.
- Braathen, A., Blikra, L. H., Berg, S. S. and Karlsen, F. (2004): Rock-slope failures in Norway; type, geometry, and hazard. *Norwegian Journal of Geology*, 84, 67-88.
- Braun, J. and Beaumont, C. (1989): A physical explanation of the relation between flank uplifts and the breakup unconformity at rifted continental margins. *Geology*, 17, 760-764.
- Briggs, S. E., Davies, R. J., Cartwright, J. A. and Morgan, R. (2006): Multiple detachment levels and their control on fold styles in the compressional domain of the deep-water west Niger Delta. *Basin Research*, 18: 435-450.
- Briggs, S. E., Davies, R. J., Cartwright, J. and Morgan, R. (2009): Thrusting in oceanic crust during continental drift offshore in the Niger Delta, Equatorial Africa. *Tectonics*, 28 (1), TC1004.
- Brown, A. R. (2004): *Interpretation of three-dimensional seismic data*. 6th edition. Tulsa: American Association of Petroleum Geologists; Society of Exploration Geophysicists.
- Brown, A. R. (2012): *Interpretation of three-dimensional seismic data*. 7th edition. Tulsa: American Association of Petroleum Geologists; Society of Exploration Geophysicists.
- Brown, L. F. and Fisher, W. L. (1977): Seismic stratigraphic interpretation of depositional systems: examples from Brazilian rift and pull-apart basins. In: Payton, C. E. (Ed), *Seismic stratigraphy - Applications to hydrocarbon exploration*: American Association of Petroleum Geologists 26, 213-248.
- Brown, A. (2008): Phase and polarity issues in modern seismic interpretation. American Association of Petroleum Geologists (Oral Presentation); International Conference and Exhibition, Cape Town, SA October 26-29, 2008
- Browne, S. E. and Fairhead, J. D. (1983): Gravity study of the Central African Rift System: a model of continental disruption. 1. The Ngaoundere and Abu Gabra Rifts. *Tectonophysics*, 94, 187-203.
- Brownfield, M. E. and Charpentier, R. R. (2006): Geology and total petroleum systems of the Gulf of Guinea Province of West Africa. U.S. Geological Survey, Bulletin, 2207-C: 32.
- Brun, J. P. and Nalpas, T. (1996): Graben inversion in nature and experiments. *Tectonics*, 15 (2), 677-687.
- Brune, S., Popov, A. A. and Sobolev, S. V. (2012): Modeling suggests that oblique extension facilitates rifting and continental breakup. *Journal of Geophysical Research: Solid Earth*, 117 (B8), B08402.

- Brune, S. and Autin, J. (2013): The rift to breakup evolution of the Gulf of Aden: Insights from 3D numerical lithospheric-scale modeling: *Tectonophysics*, 607, 65–79.
- Brunet, M., Dejax, J., Brillanceau, A., Congleton, J., Downs, W., Dupéron-Laudoueneix, M., Eisenmann, V., Flanagan, K., Flynn, L., Heintz, E., Hell, J., Jacobs, L., Jehenne, Y., Ndjeng, E., Mouchelin, G., and Pilbeam, D. (1988): Mise en évidence d'une sédimentation précoce d'âge Barrémien dans le fossé de la Bénoué en Afrique occidentale (Bassin du Mayo Oulo Léré, Cameroun), en relation avec l'ouverture de l'Atlantique sud. *C. R. Acad. Sci. Paris* 306, 1125–1130.
- Bryn, P., Berg, K., Stoker, M., Haflidason, H., and Solheim, A. (2005): Contourites and their relevance for mass wasting along the Mid-Norwegian Margin: *Marine and Petroleum Geology*, 22/1, 85-96.
- Buck, W. R. (1991): Modes of continental lithospheric extension. *Journal of Geophysical Research*, 96/B12, 20,161-20,178.
- Buck, W. R., (2007): The dynamics of continental breakup and extension. In: Watts, A.B., (Ed.) *The Treatise on Geophysics*, G. Schubert series editor, Volume 6: Crustal and Lithosphere Dynamics: Palisades, New York, Columbia University, 335-376.
- Bull, S., Cartwright, J. and Huuse, M. (2008): A subsurface evacuation model for submarine slope failure. *Basin Research*; 21, 433-443.
- Bull, S., Cartwright, J. and Huuse, M. (2009): A review of kinematic indicators from mass-transport complexes using 3D seismic data. *Marine and Petroleum Geology*, 26 (7), 1132-1151.
- Bumby, A. J. and Guiraud, R. (2005): The geodynamic setting of the Phanerozoic basins of Africa. *Journal of African Earth Sciences*, 43 (1-3), 1-12.
- Burke, K. C. B., Dessauvagie, T. F. J. and Whiteman, A. J. (1971): The opening of the Gulf of Guinea and geological history of the Benue Depression and Niger Delta. *Nature Physical Science*, 233 (38), 51-55.
- Burke, K. (1972): Offshore stratigraphy and paleontology of Dahomey (Benin) Embayment. *Nigerian Association of Petroleum Explorationists*, 70 (2): 121-130.
- Burke, K. and Dewey, J. F. (1974): Two plates in Africa during the Cretaceous? *Nature*, 249, 313-319.
- Burke, K., MacGregor, D. S. and Cameron, N. R. (2003): Africa's petroleum systems: four tectonic 'Aces' in the past 600 million years. In: Arthur, T. J., MacGregor, D. S. and Cameron, N. R. (Eds), *Petroleum Geology of Africa: New Themes and Developing Technologies*. London: The Geological Society, London. Special Publications, 207, 21-60.
- Busby, C. and Ingersoll, R. V. (1995): *Tectonics of sedimentary basins*. Blackwell Science, Cambridge.

- Caby, R. (1989): Precambrian terranes in Benin, Nigeria and northeast Brazil and the late Proterozoic south Atlantic fit. *Geological Society of America Special Paper* 230, 145–158.
- Caby, R. (2003): Terrane assembly and geodynamic evolution of central western Hoggar: a synthesis. *Journal of African Earth Science* 37, 133–159.
- Cainelli, C. and Mohriak, W. U. (1999): Some remarks on the evolution of sedimentary basins along the eastern Brazilian continental margin. *Episodes*, 22/3, 206-216.
- Canals, M., Lastras, G., Urgeles, R., Casamor, J. L., Mienert, J., Cattaneo, A., De Batist, M., Haflidason, H., Imbo, Y., Laberg, J. S., Locat, J., Long, D., Longva, O., Masson, D.G., Sultan, N., Tricardi, F. and Bryn, P. (2004): Slope failure dynamics and impact from seafloor and shallow sub-seafloor geophysical data: case studies from the COSTA project. *Marine Geology* 213, 9-72.
- Cande, S. C. LaBrecque, J. L. and Haxby, W. F. (1988): Plate kinematics of the South Atlantic: Chron C34 to Present. *Journal of Geophysical Research*, 93/811, 13479-13492.
- Carroll, A. R. and Bohacs, K. M. (1999): Stratigraphic classification of ancient lakes: Balancing tectonic and climatic controls. *Geology*, 27/2, 99-102.
- Cartwright, J., Mansfield, C. and Trudgill, B. (1996): The growth of normal faults by segment linkage. In: Buchanan, R. G. and Nieuwland, D. A. (Eds), *Modern developments in structural interpretation, validation and modelling*. Geological Society Special Publications 99, 163-177.
- Carvajal, C. R. and Steel, R. J. (2006): Thick turbidite successions from supply-dominated shelves during sea level highstand: *Geology*, 34, 665-668.
- Casas, A. M., Soto, R. and Martínez-Peña, B. (2002): Geometrical relationships between unconformities and subsequent folding: the Arro fold system (southern Pyrenees). *Comptes Rendus Geoscience*, 334 (10), 765-772.
- Casas-Sainz, A. M., Soto-Marín, R., González, Á. and José Villalaín, J. (2005): Folded onlap geometries: implications for recognition of syn-sedimentary folds. *Journal of Structural Geology*, 27 (9), 1644-1657.
- Castelltort, S., Pochat, S. and Van den Driessche, J. (2004): How reliable are growth strata in interpreting short-term (10 s to 100 s ka) growth structures kinematics? *Comptes Rendus Geoscience*, 336 (2), 151-158.
- Catuneanu, O., Khalifa, M. A. and Wanas, H. A. (2006): Sequence stratigraphy of the Lower Cenomanian Bahariya Formation, Bahariya Oasis, Western Desert, Egypt. *Sedimentary Geology*, 190 (1–4), 121-137.
- Catuneanu, O., Abreu, V., Bhattacharya, J. P., Blum, M. D., Dalrymple, R. W., Eriksson, P. G., Fielding, C. R., Fisher, W. L., Galloway, W. E., Gibling, M. R., Giles, K. A., Holbrook, J. M., Jordan, R., Kendall, C. G. S. C., Macurda, B., Martinsen, O. J., Miall,

- A. D., Neal, J. E., Nummedal, D., Pomar, L., Posamentier, H. W., Pratt, B. R., Sarg, J. F., Shanley, K. W., Steel, R. J., Strasser, A., Tucker, M. E. and Winker, C. (2009): Towards the standardization of sequence stratigraphy. *Earth-Science Reviews*, 92 (1-2), 1-33.
- Catuneanu, O., Martins-Neto, M. A. and Eriksson, P. G. (2012): Sequence stratigraphic framework and application to the Precambrian. *Marine and Petroleum Geology*, 33 (1), 26-33.
- Chang, K. H. (1975): Unconformity-bounded stratigraphic units. *Geological Society of America Bulletin*, 86 (11), 1544-1552.
- Channell, J. E. T., Erba, E., Nakanishi, M. and Tamaki, K. (1995): Late Jurassic–Early Cretaceous time scales and oceanic magnetic anomaly block models. In: Berggren, W. A., Kent, D. V., Aubry, M.-P., Hardenbol, J. (Eds), *Geochronology, time scales and global stratigraphic correlation*. Society of Economic Palaeontologists and Mineralogists Special Publications, 54, 51-64.
- Chemenda, A., Déverchère, J., and Calais, E. (2002): Three-dimensional laboratory modeling of rifting: Application to the Baikal Rift, Russia: *Tectonophysics*, 356, 253-273.
- Christie-Blick, N., and Biddle, K. T., (1985): Deformation and basin formation along strike-slip faults. In: Biddle, K. T., Christie-Blick N., (eds), *Strike-slip deformation, basin formation, and sedimentation*, Society of Economic Paleontologists and Mineralogists, Special Publication, 37, 1-35.
- Christie-Blick, N. (1991): Onlap, offlap, and the origin of unconformity-bounded depositional sequences. *Marine Geology*, 97 (1-2), 35-56.
- Claringbould, J. S., Bell, R. E., Jackson, C. A-L., Gawthorpe, R. L. and Odinsen, T. (2015): Diachronous growth of normal fault systems in multiphase rift basins: Structural evolution of the East Shetland Basin, Northern North Sea. EGU General Assembly, Geophysical Research Abstracts 17, EGU2015-5869.
- Clift, P. D., and Lorenzo, J. (1999): Flexural unloading and uplift along Côte d'Ivoire-Ghana transform margin, Equatorial Atlantic. *Journal of Geophysical Research* 104, 25257-25274.
- Clift, P. D., Lorenzo, J., Carter, A., Hurford, A. J. and Party, O. L. S. (1997): Transform tectonics and thermal rejuvenation on the Côte d'Ivoire-Ghana margin, West Africa. *Journal of the Geological Society*, 154 (3), 483-489.
- Cloetingh, S., Beekman, F., Ziegler, P. A., Van Wees, J-D. and Sokoutis, D. (2008): Post-rift compressional reactivation potential of passive margins and extensional basins. Johnson, H., Doré, A. G., Gatliff, R. W., Holdsworth, R., Lundin, E. R. and Ritchie, J. D. (Eds), *The nature and origin of compression in passive margins*. Geological Society, London, Special Publications, 306, 27-70.

- Cobbold, P. R., Meisling, K. E. and Mount, V. S. (2001): Reactivation of an obliquely rifted margin, Campos and Santos Basins, Southeastern Brazil. *American Association of Petroleum Geologists Bulletin*, 85 (11), 1925-1944.
- Cobbold, P. R., Clarke, B. J. and Loseth, H. (2009): Structural consequences of fluid overpressure and seepage forces in the outer thrust belt of the Niger Delta. *Petroleum Geoscience*, 15 (1), 3-15.
- Cohen, H. A. and McClay, K. (1996): Sedimentation and shale tectonics of the Northwestern Niger Delta front. *Marine and Petroleum Geology*, 13 (3), 313-328.
- Coker, S. J. L. and Ejedawe, J. E. (1987): Petroleum prospect of the Dahomey Embayment Nigeria. *Journal of Mining and Geology*, 23 (10), 27-43.
- Condie, K. C. (2003). *Plate Tectonics and Crustal Evolution* (Fourth edition). Butterworth-Heinemann, An imprint of Elsevier Science, 294.
- Cooper, M. A., Williams, G. D., de Graciansky, P. C., Murphy, R. W., Needham, T., de Paor, D., Stoneley, R., Todd, S. P., Turner, J. P. and Ziegler, P. A. (1989): Inversion tectonics - a discussion. In: Cooper, M. A. and Williams, G. D. (Eds), *Inversion tectonics*. Geological Society, London, Special Publications, 44 (1), 335-347.
- Cooper, M. and Warren, M. J. (2010): The geometric characteristic, genesis and petroleum significance of inversion structures. In: Law, R. D., Butler, R.W. H., Holdsworth, R. E., Krabbendam, M. and Strachan, A. (Eds), *Continental tectonics and mountain building*. Geological Society, London, Special Publications, 335, 827-846.
- Corfield, S., and Sharp, I. R. (2000): Structural style and stratigraphic architecture of fault-propagation folding in extensional settings: a seismic example from the Smorrbukk area, Halten Terrace, Mid-Norway. *Journal of Basin Research* 12, 329-341.
- Corredor, F., Shaw, J. H. and Bilotti, F. (2005): Structural styles in the deep-water fold and thrust belts of the Niger Delta. *American Association of Petroleum Geologists Bulletin*, 89 (6), 753-780.
- Corti, G., Bonini, M., Conticelli, S., Innocenti, F., Manetti, P. and Sokoutis, D. (2003): Analogue modelling of continental extension: a review focused on the relations between the patterns of deformation and the presence of magma. *Earth-Science Reviews* 63, 169 – 247.
- Corti, G., Carminati, E., Mazzarini, F. and Garcia, M. O. (2005): Active strike-slip faulting in El Salvador, Central America. *Geology* 33; no. 12, 989–992.
- Corti, G. (2012): Evolution and characteristics of continental rifting: Analog modeling-inspired view and comparison with examples from the East African Rift System. *Tectonophysics*, 522-523, 1-33.
- Coward, M. P. (1983): Thrust tectonics, thin-skinned or thick-skinned, and the continuation of thrusts to deep in the crust. *Journal of Structural Geology*, 5/2, 113-123.

- Coward, M. P. (1986): Heterogeneous stretching, simple shear and basin development. *Earth and Planetary Science Letters*, 80, 325-336.
- Cowie, P. A. (1998): A healing-reloading feedback control on the growth rate of seismogenic faults. *Journal of Structural Geology*, 20, 1075-1087.
- Cowie, P. A., Underhill, J. R., Behn, M. D., Lin, J. and Gill, C. E. (2005): Spatio-temporal evolution of strain accumulation derived from multi-scale observations of Late Jurassic rifting in the northern North Sea: A critical test of models for lithospheric extension. *Earth and Planetary Science Letters*, 23, 401-419.
- Crowell, J. C. (2003): Tectonics of Ridge Basin region, southern California. In: Crowell, J. C. (ed.), *An interplay of sedimentation and tectonics: Boulder, Colorado*, Geological Society of America Special Paper 367, 157-203.
- D'Almeida, G. A. F., Kaki, C. and Adeoye, J. A. (2016): Benin and Western Nigeria offshore basins: A stratigraphic nomenclature comparison. *International Journal of Geosciences*, 7, 177-188.
- Daly, M. C. Chorowicz, J. and Fairhead, J. D. (1989): Rift basin evolution in Africa: The influences of reactivated steep basement shear zones. In: Cooper, M. A. and Williams, G. D. (Eds), *Inversion tectonics*. Geological Society London, Special Publications 44, 309-334.
- Damuth, J. E. (1994): Neogene gravity tectonics and depositional processes on the deep Niger Delta continental margin. *Marine and Petroleum Geology*, 11 (3), 321-346.
- Davidson, I. (1987): Normal fault geometry related to sediment compaction and burial. *Journal of Structural Geology*, 9, 393-401.
- Davies, R. J., MacLeod, C. J., Morgan, R. and Briggs, S. E. (2005): Termination of a fossil continent-ocean fracture zone imaged with three-dimensional seismic data: The Chain Fracture Zone, eastern Equatorial Atlantic. *Geology*, 33 (8), 641-644.
- Davison, I. (1997): Wide and narrow margins of the Brazilian South Atlantic. *Journal of the Geological Society, London*, 154, 471-476
- Davison, I. and Underhill, J. R. (2012): Tectonic and sedimentation in extensional rifts: Implications for petroleum systems. In: Gao, D. (Ed.), *Tectonic and sedimentation in extensional rifts: Implications for petroleum systems*. American Association of Petroleum Geologists Memoir 100: 15-42.
- Dawers, N. H. and Underhill, J. R. (2000): The role of fault interaction and linkage in controlling syn-rift stratigraphic sequences: Late Jurassic, Statfjord east Area, Northern North Sea. *American Association of Petroleum Geologists Bulletin* 84/1, 45-64.
- Da Costa, I. G., Beltrami, C. V., and Alves, L. E. M. (1990): A evoluçãõ tectono-sedimentareo habitat do oleo da bacia do Ceará. *B. Geoci. Petrobrás* 4 (1), 65-74

- De Caprona, G. D. (1992): The continental margin of western Côte d'Ivoire: structural framework inherited from intra-continental shearing. Ph.D. Thesis, Göteborg Universitet, Geologiska Institutionen, 69, 150.
- De Graciansky, Y, P. C., Dardeau, G., Lemoine, M. and Tricart, P. (1989): The inverted margin of the French Alps and foreland basin inversion. In: Cooper, M. A. and Williams, G. D. (Eds). Inversion tectonics, Geological Society, London. Special Publications, 44: 87-104.
- De Polo, C. M., Clark, D. G., Siemmons, D. B. and Ramelli, A. R. (1991): Historical surface faulting in the Basin and Range province, western North America: implications for fault segmentation *Journal of Structural Geology* 13/2, 123-136.
- De Santis, V. (2013): UnconformityNext Hit-Previous HitBoundedNext Hit Previous HitStratigraphicNext Hit Previous HitUnitsNext Hit (Ubsus) In An Italian Alluvial-Plain Area: Recognizing and Dating. *Journal of Sedimentary Research*, 83 (1), 96-113.
- Delteil, J. R., Valvery, P., Fondeur, C., Patriat, P. and Mascle, J. (1974): Continental margin in the northern part of the Gulf of Guinea. In: Burk, C. A. and Drake, C. L (Eds), *The Geology of continental margins*. Berlin: Springer-Verlag.
- Delteil, J. R., Rivier, F., Montadert, L., Aostolesn, V., Didier, J., Goslin, M. and Patriat, M. (1976): Structure and sedimentation of the continental margin of the Gulf of Benin. *Anais Acad. Brasil, Ciencias Proc. Sao Paulo Conference*, 48 (Sulemento).
- DeVault, B. and Jeremiah, J. (2002): Tectono-stratigraphy of the Nieuwerkerk Formation (Delfland subgroup), West Netherlands Basin. *American Association of Petroleum Geologists Bulletin*, 86 (10), 1679-1707.
- Delvaux, D. (2016): Use of non-fault fractures in stress tensor reconstruction using the Mohr Circle with the Win-tensor program. *EGU General Assembly 2016*, 18-22 April 2016, Vienna, Austria. *Geophysical Research Abstracts*, 18, EGU2016-6345.
- Deptuck, M. E., Steffens, G. S., Barton, M. and Pirmez, C. (2003): Architecture and evolution of upper fan channel-belts on the Niger Delta slope and in the Arabian Sea. *Marine and Petroleum Geology*, 20 (6), 649-676.
- Deptuck, M. E., Sylvester, Z. Pirmez, C. and O'Byrne, C. (2007): Migration-aggradation history and 3D seismic geomorphology of submarine channels in the Pleistocene Benin-major Canyon, western Niger Delta slope. *Marine and Petroleum Geology*, 24, 406-433.
- Deptuck, M. E., Sylvester, Z. and O'Byrne, C. (2012): Pleistocene seascape evolution above a "Simple" Stepped Slope - Western Niger Delta. In: Prather, B. E., Deptuck, M. E., Mohrig, D., Van Hoorn, B. and Wynn, R. (Eds), *Application of the Principles of Seismic Geomorphology to Continental-Slope and Base-of-Slope Systems: Case studies from seafloor and near-seafloor analogues*. Society of Economic Paleontologists and Mineralogists Special Publications 99, 199-222.

- Destro, N., Szatmari, P., Alkmim, F. F. and Magnavita, L. P. (2003): Release faults, associated structures, and their control on petroleum trends in the Recôncavo rift, northeast Brazil. *American Association of Petroleum Geologists Bulletin*, 87/7, 1123-1144.
- Dewey, J. F. 1982. Plate tectonics and the evolution of the British Isles. *Journal of the Geological Society, London*, 139, 371-414.
- Dewey, J. F. (1989): Kinematics and dynamics of basin inversion. In: Cooper, M. A. and Williams, G. D. (Eds), *Inversion tectonics*, Geological Society, London, Special Publications 44 (1), 352.
- Dewey, J. F., Holdsworth, R. E. and Strachan, R. A. (1998): Transpression and transtension zones. In: Holdsworth, R. E., Strachan, R. A. & Dewey, J. E (Eds) *Continental transpressional and transtensional tectonics*. Geological Society, London, Special Publications, 135, 1-14.
- Dickson, W. G., Fryklund, R. E., Odegard, M. E. and Green, C. M. (2003): Constraints for plate reconstruction using gravity data—implications for source and reservoir distribution in Brazilian and West African margin basins. *Marine and Petroleum Geology*, 20 (3–4), 309-322.
- Doré A. G., Lundin, E. R. Fichler and Olsen, O. (1997): Patterns of basement structure and reactivation along the NE Atlantic margin. *Journal of the Geological Society, London*, 154, 85–92.
- Doré A. G., Lundin, E. R., Kusznir, N. J. and Pascal, C. (2008): Potential mechanisms for the genesis of Cenozoic domal structures on the NE Atlantic margin: pros, cons and some new ideas. In: Johnson, H., Doré A. G., Gatliff, R. W., Holdsworth, R., Lundin, E. and Ritchie, J. D. (Eds), *The nature and origin of compression in passive margins*. Geological Society, London, Special Publications, 306, 1–26.
- Doust, H. (1990) *Petroleum Geology of the Niger Delta*. In: Brooks, J. (Ed.), *Classic Petroleum Provinces*. Geological Society London, Special Publications 50, 365.
- Doyle, J.A., Jardiné, S., Doerekamp, A. (1982): *Afropollis*, a new genus of early angiosperm pollen, with notes on the Cretaceous palynostratigraphy and paleoenvironments of northern Gondwana. *Bull. Centres Rech. Exploration Production Elf-Aquitaine* 6 (1), 39–117.
- DPR (2003): *Business Opportunities in Nigeria and the E and P Environment*. International Oil and Gas Business days Conference. Holmen Fjord Hostel, Oslo Norway: August 26-28, 2003, 29.
- Driscoll, N. W., Hogg, J. R., Christie-Blick, N. and Karner, G. D. (1995): Extensional tectonics in the Jeanne d'Arc Basin, offshore Newfoundland: implications for the timing of break-up between Grand Banks and Iberia. In: R. A. Scrutton, M. S. Stoker, G. B. Shimmield and A. W. Tudhope (eds): *The tectonics, sedimentation, and palaeoceanography of the north Atlantic region*. Geological Society London, 90, 1-28.

- Du Chene, R. J. and Adegoke, O. S. (2006): Palynological and micropaleontological analyses of the 5900-8482 (MD) Cretaceous section of the Nigerian well Aje-3. Unpublished Report prepared for Lundin Petroleum AB.
- Duffy, O. B., Bell, R. E., Jackson, C. A-L., Gawthorpe, R. L., and Whipp, P. S. (2015): Fault growth and interactions in a multiphase rift fault network: Horda Platform, Norwegian North Sea. *Journal of Structural Geology*, 80, 99-119.
- Dumestre, M. A. (1985): Northern Gulf of Guinea shows promise. *Oil and Gas Journal*, 83 (18), 154-165.
- Eagles, G. (2007): New angles on South Atlantic opening. *Geophysical Journal International*, 168 (1), 353-361.
- Eagles, G. and Konig, M. (2008): A model of plate kinematics in Gondwana breakup. *Geophysical Journal International*, 173, 703-717.
- Ebinger, C., Petit, C. and Burov, E. (2002): Causes and consequences of lithospheric extension: The ups and downs of continental Rifts. In: Renaut, R. W. and Ashley, G. M. (Eds), *Sedimentation in continental rifts*. Society of Economic Paleontologists and Mineralogists, Special Publications 73, 11-23.
- Edwards, R. A., Whitmarsh, R. B. and Scrutton, R. A. (1997): The crustal structure across the transform continental margin off Ghana, eastern Equatorial Atlantic. *Journal of Geophysical Research*, 102, 747-772.
- Elueze, A. A. and Nton, M. E. (2004): Organic geochemical appraisal of limestones and shales in part of eastern Dahomey basin, southwestern Nigeria. *Journal of Mining and Geology*, 40 (1): 29-40.
- Embry, A. F. and Dixon, J. (1990): The breakup unconformity of the Amerasia Basin, Arctic Ocean: Evidence from Arctic Canada. *Geological Society of America Bulletin*, 102, 1526-1534.
- Embry, A. F., (1993): Transgressive-regressive (T-R) sequence analysis of the Jurassic succession of the Sverdrup Basin, Canadian Arctic Archipelago. *Canadian Journal of Earth Sciences*, 30, 301-320.
- Embry, A. F. (1995): Sequence boundaries and sequence hierarchies: problems and proposals. In: Steel, R. J., Felt, V. L., Johannessen, E. P. and Mathieu, C. (Eds), *Sequence Stratigraphy on the Northwest European Margin*. Norwegian Petroleum Society Special Publications 5, 1-11.
- Embry, A.F. (2002): Transgressive-Regressive (T-R) Sequence Stratigraphy. *Gulf Coast Association Geological Society Transactions* 52: 151-172.
- Embry, A. F. (2009): Practical sequence stratigraphy. *Canadian Society of Petroleum Geologists*, 79.

- Emery, K. O., Uchupi, E., Bowin, C. O., Phillips, J. and Simpson, S. W. (1975a): Continental margin off western Africa: Cape St Francis (South Africa) to Walvis Ridge (South-West Africa). *American Association of Petroleum Geologists Bulletin*, 59 (1), 3-59.
- Emery, K. O., Uchupi, E., Philips, J., Bowin, C. and Mascle, J. (1975b): Continental Margin Off Western Africa: Angola to Sierra Leone. *American Association of Petroleum Geologists Bulletin* 59 (12), 2209-2265.
- Emery, D., and Myers, K. J., eds. (1996): *Sequence Stratigraphy*: Blackwell, Oxford, 297.
- Enachescu, M. E. (1987): Tectonic and structural framework of the Northeast Newfoundland continental margin. In: Beaumont, C. and Tankard, A. J. (Eds), *Sedimentary Basins and Basin-forming Mechanisms*. Canadian Society of Petroleum Geologists Memoir, 12, 117-146.
- Etheridge, M. A. (1986): On the reactivation of extensional fault systems. *Philosophical Transactions of Royal Society*, 317/1539.
- Evamy, B. D; Haremboure, J., Kamerling, P., Knaap, W. A., Molloy, F. A. and Rowlands, P. H. (1978): Hydrocarbon Habitat of Tertiary Niger Delta. *American Association of Petroleum Geologists Bulletin* 62/1, 1-39.
- Eyal, Y. and Reches, Z. E. (1983): Tectonic analysis of the Dead Sea Rift Region since the Late-Cretaceous based on mesostructures. *Tectonics*, 2 (2), 167-185.
- Færseth, R. B. and Lien, T. (2002): Cretaceous evolution in the Norwegian Sea - a period characterised by tectonic quiescence. *Marine and Petroleum Geology*, 19 (8), 1005-1027.
- Fairhead, J. D. (1986): Geophysical controls on sedimentation within the African Rift Systems. In: Frostick, L. E., Renaut, R. W., Reid, I. and Tiercelin, J. J. (Eds), *Sedimentation in the African Rifts*, Geological Society London, Special Publication 25, 19-27.
- Fairhead, J. D. (1988): Mesozoic plate tectonic reconstructions of the central South Atlantic Ocean: The role of the West and Central African rift system. *Tectonophysics*, 155, 181-191.
- Fairhead, J. D. and Binks, R. M. (1991): Differential opening of the Central and South Atlantic Oceans and the opening of the West African Rift System. *Tectonophysics*, 187, 191-203.
- Fairhead, J. D., Green, C. M., Masterton, S. M. and Guiraud, R. (2013): The role that plate tectonics, inferred stress changes and stratigraphic unconformities have on the evolution of the West and Central African Rift System and the Atlantic continental margins. *Tectonophysics*, 594, 118-127.

- Faleide, J. I., Vagnes, E. and Gudlaugsson, S. T. (1993): Late Mesozoic-Cenozoic evolution of the south-western Barents Sea in a regional rift-shear tectonic setting. *Marine and Petroleum Geology*, 10, 186-214.
- Falvey, D. A. (1974): The development of continental margins in plate tectonic theory. *Australian Petroleum Exploration Association Journal*, 14, 95-106.
- Ferrill, D. A., Morris, A. P. and McGinnis, R. N. (2012): Extensional fault-propagation folding in mechanically layered rocks: The case against the frictional drag mechanism. *Tectonophysics*, 576-577, 78-85.
- Fidalgo, G., L. (2001): La cinématique de l'Atlantique Nord: la question de la déformation intraplaque. Brest, Univ. de Bretagne Occidentale: 260.
- Finch, E., Hardy, S. and Gawthorpe, R. (2003): Discrete element modeling of contractional fault-propagation folding above rigid basement fault blocks. *Journal of Structural Geology*, 25(4), 515-528.
- Ford, M., Williams, E. A., Artoni, A., Vergés, J. and Hardy, S. (1997): Progressive evolution of a fault-related fold pair from growth strata geometries, Sant Llorenç de Morunys, SE Pyrenees. *Journal of Structural Geology*, 19 (3-4), 413-441.
- Ford, M., Le Carlier de Veslud, C. and Bourgeois, O. (2007): Kinematic and geometric analysis of fault-related folds in a rift setting: The Dannemarie basin, Upper Rhine Graben, France. *Journal of Structural Geology*, 29 (11), 1811-1830.
- Fossen, H. and Tikoff, B. (1998): Extended models of transpression and transtension, and application to tectonic settings. In: Holdsworth, R. E., Strachan, R. A. and Dewey, J. E (eds), *Continental transpressional and transtensional tectonics*. Geological Society, London, Special Publications, 135, 15-33.
- Fossen, H. (2012): *Structural Geology*. Cambridge: Cambridge University Press.
- Fossen, H. and Rotevatn, A. (2016): Fault linkage and relay structures in extensional settings—A review. *Earth-Science Reviews*, 154, 14-28.
- Fox, P. J., and Gallo, D. G. (1984): A tectonic model for ridge-transform-ridge plate boundaries: implications for the structure of oceanic lithosphere. *Tectonophysics* 104, 205-242.
- Françolin, J. L. B., Cobbold, P. R., and Szatmari, P. (1994): Faulting in the Early Cretaceous Rio do Peixe Basin (NE Brazil) and its significance for the opening of the Atlantic. *Journal of Structural Geology* 16 (5), 647–661.
- Frey-Martinez, J., Cartwright, J. and Hall, B. (2005): 3D seismic interpretation of slump complexes: examples from the continental margin of Israel. *Basin Research*, 17, 83-108.
- Frey-Martinez, J., Cartwright, J. and James, D. (2006): Frontally confined versus frontally emergent submarine landslides: A 3D seismic characterisation. *Marine and Petroleum Geology*, 23, 585-604.

- Frostick, L. E. and Reid, I. (1987): Tectonic controls of desert sediments in rift basins ancient and modern. *In*: Frostick, L. E. and Rihd, I. (Eds), Desert Sediments: Ancient and Modern. Geological Society, London. Special Publications, 35, 53-68.
- Frostick, L. E., and Steel, R. J., (1993): Sedimentation in divergent plate margin basins. *In*: Frostick, L. E., Steel, R. J. (Eds); Tectonic controls and signatures in sedimentary successions. International Association of Sedimentologists Special Publications 20, 111-128.
- Gabrielsen, R. H. F., Erseth. R. B., Steel, R. J., Idil, S. and Klovjan. O. S. (1990): Architectural styles of basin fill in the northern Viking Graben. *In*: Blundell, D. J. and Gibbs, A. D. (Eds), Tectonic evolution of the North Sea Rifts. Oxford University Press. Oxford, 158-179.
- Galloway, W. E. (1998): Siliciclastic Slope and Base-of-Slope Depositional Systems: Component Facies, Stratigraphic Architecture, and Classification. American Association of Petroleum Geologists Bulletin, 82 (4), 569-595.
- Gamboa, D. A., Alves, T. M., Cartwright, J. A. and Temnha, P. (2010): MTD distribution on a 'passive' continental margin: The Espírito Santo Basin (SE Brazil) during the Palaeogene. *Petroleum Geology*, 27(7), 1311-1324.
- Gamboa, D. A. and Alves, T. M. (2015a): Three-dimensional fault meshes and multi-layer shear in mass-transport blocks: Implications for fluid flow on continental margins. *Tectonophysics*, 647, 21-32.
- Gamboa, D. and Alves, T. M. (2015b): Spatial and dimensional relationships of submarine slope architectural elements: A seismic scale analysis from the Espírito Santo Basin (SE Brazil). *Marine and Petroleum Geology*, 64, 43-57.
- Garrison, J. R. Jr. and van den Bergh, T. C. V. (2006): Effects of sedimentation rate, rate of relative rise in sea level, and duration of sea level cycle on the filling of incised valleys: examples of filled and "overfilled" incised valleys from the Upper Ferron Sandstone, Last Chance Delta, east-central Utah, USA. *In*: Dalrymple, R. W., Leckie, D. A and Tillman, R.W. (Eds): Incised Valleys in Time and Space. Society of Economic Palaeontologists and Mineralogists Special Publication, 85, 239-279.
- Gawthorpe, R. L. and Hurst, J. M. (1993): Transfer zones in extensional basins: Their structural style and influence on drainage development and stratigraphy: *Geological Society of London Journal*, 150, 1137-1152.
- Gawthorpe, R. L., Fraser, A. J. and Collier, R. E. L. (1994): Sequence stratigraphy in active extensional basins: implications for the interpretation of ancient basin-fills. *Marine and Petroleum Geology* 11/6, 642-658.
- Gawthorpe, R. L., Sharp, I., Underhill, J. R. and Gupta, S. (1997): Linked sequence stratigraphic and structural evolution of propagating normal faults. *Geology*, 25 (9), 795-798.

- Gawthorpe, R. L. and Leeder, M. R. (2000): Tectono-sedimentary evolution of active extensional basins. *Basin Research*, 12 (3-4): 195-218.
- Genik, G. J. (1992): Regional framework, structural and petroleum aspects of rift basins in Niger, Chad and the Central African Republic (C.A.R.). *Tectonophysics*, 213 (1-2), 169-185.
- Genik, G. J. (1993): Petroleum Geology of Cretaceous-Tertiary Rift basins in Niger, Chad, and Central African Republic. *American Association of Petroleum Geologists Bulletin*, 77 (8), 1405-1434.
- Geoffroy, L. (2005): Volcanic passive margins. *Comptes Rendus Geoscience*, 337 (16), 1395-1408.
- GETECH. (2002): Central African basins study. Unpublished report. 253.
- Gibbs, A. D. (1984): Structural evolution of extensional basin margins. *Journal of Geological Society London*, 141, 609-620.
- Gibbs, A. D. (1990): Linked faults in basin formation. *Journal of Structural Geology*, 12, 795-803.
- Gibson, J. R., Walsh, J. J. and Watterson, J. (1989): Modelling of bed contours and cross-sections adjacent to planar normal faults: *Journal of Structural Geology*, 11, 317-328.
- Giedt, N. R. (1990): Unity Field, Muglad Rift Basin, Upper Nile Province. In: Beaumont, E. A. & Foster, N. H. (Eds) *Structural Traps; III, Tectonic Fold and Fault Traps*. American Association of Petroleum Geologists *Treatise of Petroleum Geology, Atlas of Oil and Gas Fields*, A-019: 177-197.
- Girdler, R. W. and Styles, P. (1973): Two stage Red Seafloor spreading. *Nature* 247, 7-11.
- Glen, R. A., Hancock, P. L. and Whittaker, A. (2005): Basin inversion by distributed deformation: the southern margin of the Bristol Channel Basin, England. *Journal of Structural Geology*, 27 (12), 2113-2134.
- Gong, C., Wang, Y., Zh, W., Li, W., Xu, Q. and Zhan, J. (2011): The Central Submarine Canyon in the Qiongdongnan Basin, northwestern South China Sea: Architecture, sequence stratigraphy, and depositional processes. *Marine and Petroleum Geology*, 28, 1690-1702.
- Gong C., Wang, Y. Hodgson, D. M., Zhu, W., Li, W., Xu, C and Li, D. (2014): Origin and anatomy of two different types of mass-transport complexes: A 3D seismic case study from the northern South China Sea margin. *Marine and Petroleum Geology*, 54, 198-215.
- Granot, R. and Dymant, J. (2015): The Cretaceous opening of the South Atlantic Ocean. *Earth and Planetary Science Letters*, 414, 156–163.

- Grant, N. K. (1970): Geochronology of Precambrian basement rocks from Ibadan, Southwestern Nigeria. *Earth and Planetary Science Letters*, 10/1, 29-38.
- Greenhalgh, J., Wells, S., Borsato, R., Pratt, D., Martin, M., Roberson, R., Fontes, C. and Obaje, W. A. (2011): A fresh look at prospectivity of the Equatorial conjugate margin of Brazil and Africa. *First Break*, 29, 67-72.
- Greenroyd, C. J., Peirce, C., Rodger, M., Watts, A. B. and Hobbs, R. W. (2008): Do fracture zones define continental margin segmentation? Evidence from the French Guiana margin. *Earth and Planetary Science Letters*, 272, 553-566.
- Grimaldi, G. O. and Dorobek, S. L. (2011): Fault framework and kinematic evolution of inversion structures: Natural examples from the Neuquén Basin, Argentina. *American Association of Petroleum Geologists Bulletin*, 95, 27-60.
- Guiraud, R., Issawi, B., Bellion, Y. (1985): Les lineaments guino-nubiens: un trait structural majeur a l'échelle de la plaque africaine. *C. R. Acad. Sci. Paris* 300, 17-20.
- Guiraud, R. (1986): Correlations entre les principaux événements géodynamiques enregistrés du Trias à nos jours sur les marges alpine et atlantique de la plaque africaine. *Rev. Fac. Sci. Marrakech, Sect. Sci. Terre. No. Spec*, 2 PICG-Unesco 183, 313-338.
- Guiraud, R., Bellion, Y., Benkhelil, J., Moreau, C. (1987): Post-Hercynian tectonics in Northern and Western Africa. In: Bowden, E, Kinnaird, J. (Eds), *African Geology Reviews*. *Geology Journal*, 22, 433-466.
- Guiraud, R. and Maurin, J. C. (1991): Le rifting en Afrique au Crétacé inférieur: synthèse structurale, mise en évidence de deux étapes dans la genèse des bassins, relations avec les ouvertures océaniques périafricaines. *Bulletin Société Géologie France* 162, 811-823.
- Guiraud, R., Binks, R. M., Fairhead, J. D. and Wilson, M. (1992): Chronology and geodynamic setting of Cretaceous - Cenozoic rifting in West and Central Africa. In: Ziegler, P.A. (Ed.), *Geodynamics of rifting. Vol. II, Case History Studies on Rifts: North and South America, Africa-Arabia*. *Tectonophysics*, 213, 227-234.
- Guiraud, R. and Maurin, J. -C. (1992): Early Cretaceous rifts of Western and Central Africa: an overview. *Tectonophysics*, 213 (1-2), 153-168.
- Guiraud, R. and Maurin, J. -C. (1993): Cretaceous rifting and basin inversion in Central Africa. In: Thorweihe, U., Schandetmeier, H. (Eds), *Geoscientific Research in Northeast Africa*. Balkema, Rotterdam, 203-206.
- Guiraud, R. and Bellion, Y. (1995): Late Carboniferous to Recent geodynamic evolution of the West Gondwanan cratonic Tethyan margins. In: Nairn, A., Dercourt, J. and Vrielynck, B. (Eds), *The Ocean Basins and Margins, Vol. 8, The Tethys Ocean*, Plenum, New York, 101-124.

- Guiraud, M., Benkhelil, J., Mascle, J., Basile, C., Bouillin, J. P. and Cousin, M. (1997): Syn-rift to syn-transform deformation along the Côte d'Ivoire-Ghana transform margin: evidence from deep-sea dives. *Geo-Marine Letters*, 17, 70-78.
- Guiraud, R. and Bosworth, W. (1997): Senonian basin inversion and rejuvenation of rifting in Africa and Arabia: synthesis and implications to plate-scale tectonics. *Tectonophysics*, 28, 39-82.
- Guiraud, R. (1998): Mesozoic rifting and basin inversion along the northern African Tethyan margin: an overview. In: MacGregor, D.S., Moody, R. T. J. and Clark-Lowes, D. D. (Eds): *Petroleum Geology of North Africa*. London: Geological Society, 132, 217-229.
- Guiraud, R. and Bosworth, W. (1999): Phanerozoic geodynamic evolution of northeastern Africa and the northwestern Arabian platform. *Tectonophysics*, 315 (1-4), 73-104.
- Guiraud, R., Doumnang, J. -C., Mbaigane, C. S. and Dominguez, S. (2000): Evidence for a 6000 km length NW-SE-striking lineament in northern Africa: the Tibesti Lineament. *Journal of the Geological Society of London*, 157, 897-900.
- Guiraud, R., Bosworth, W., Thierry, J. and Delplanque, A. (2005): Phanerozoic geological evolution of Northern and Central Africa: An overview. *Journal of African Earth Sciences*, 43 (1-3), 83-143.
- Guiraud, M., Buta-Neto, A. and Quesne, D. (2010): Segmentation and differential post-rift uplift at the Angola margin as recorded by the transform-rifted Benguela and oblique-to-orthogonal-rifted Kwanza basins. *Marine and Petroleum Geology*, 27, (5), 1040-1068.
- Gupta, S., Cowie, P. A., Dawers, N. H. and Underhill, J. R. (1998): A mechanism to explain rift-basin subsidence and stratigraphic patterns through fault-array evolution. *Geology*, 26 (7), 595-598.
- Gupta, S., Underhill, J. R., Sharp, I., and Gawthorpe, R. L. (1999): Role of fault interactions in controlling syn-rift sediment dispersal patterns: Miocene, Abu Alaqa Group, Suez Rift, Sinai, Egypt. *Basin Research*, 11 (2), 167-189.
- Gutierrez-Alonso, G. and Gross, M. R. (1999): Structures and mechanisms associated with development of a fold in the Cantabrian Zone thrust belt, NW Spain. *Journal of Structural Geology*, 21, 653-670.
- Haack, R. C., Sundararaman, P., Diedjomahor, J. O., Xiao, H., Gant, N. J., May, E. D. and Kelsch, K. (2000): Niger Delta petroleum systems, Nigeria. In: M. R. Mello and B. J. Katz, (Eds), *Petroleum systems of South Atlantic margins*. American Association of Petroleum Geologists Memoir 73, 213-231.
- Haflidason, H., H. P. Sejrup, A. Nygård, J. Mienert, P. Bryn, R. Lien, C. F. Forsberg, K. Berg, and D. Masson (2004): The Storegga slide: Architecture, geometry, and slide development. *Marine Geology*, 213, 201-234.

- Hamblin, A. P. and Rust, B. R. (1989): Tectono-sedimentary analyses of alternate-polarity half-graben basin-fill successions: Late Devonian-Early Carboniferous Horton Group, Cape Breton Island, Nova Scotia. *Basin Research*, 2, 239-255.
- Hammuda, O. S., Van Hinte, J. E. and Nederbragt, S. (1992): Geohistory analysis mapping in central and southern Tarabulus Basin, northwestern offshore Libya. In: Salem, M. J., Hammuda, O. S. and Eliagoubi, B. A. (Eds): *The Geology of Libya*. Elsevier, 1657-1680.
- Hampton, M. A., H. J. Lee, and Locat, J. (1996): Submarine landslides: Reviews in *Geophysics*, 34, 33-59.
- Harding, T. P. and Lowell, J. D. (1979): Structural styles, their plate tectonic habitats, and hydrocarbon traps in petroleum provinces. *American Association of Petroleum Geologists Bulletin*, 63, 1016-1059.
- Harland, W. B. (1971): Tectonic transpression in Caledonian Spitsbergen. *Geological Magazine*, 108/1, 27-42.
- Hayward, A. B. and Graham, R. H. (1989): Some geometrical characteristics of inversion. In: Cooper, M.A., and Williams, G.D. (Eds), *Inversion Tectonics*. Geological Society, London, Special Publications, 44: 17-39.
- Heezen, B. C. (1974): Atlantic-type continental margins. In: Burk, C. A. and Drake, C. L. (Eds), *The Geology of continental margins*. Springer Science & Business Media, New York, 13-24.
- Heine, C. and Brune, S. (2014): Oblique rifting of the Equatorial Atlantic: Why there is no Saharan Atlantic Ocean. *Geology*, 42 (3), 211-214.
- Heine, C., Zoethout, J. and Muller, R. D. (2013): Kinematics of the South Atlantic rift. *Solid Earth*, 4: 1-46.
- Helland-Hansen, W. and Gjelberg, J. G. (1994): Conceptual basis and variability in sequence stratigraphy; a different perspective. *Sedimentary Geology*, 92, 31-52.
- Helland-Hansen, W. and Martinsen, O. J. (1996): Shoreline trajectories and sequences; description of variable depositional-dip scenarios. *Journal of Sedimentary Research*, 66: 670-688.
- Helle, K. and Helland-Hansen, W. (2009): Genesis of an over-thickened shoreface sandstone tongue: The Rannoch and Etive formations (Middle Jurassic Brent delta), North Sea. In: Henriksen, S. Hampson, G.J., Helland-Hansen, W., Johannessen, E. P. and Steel, R. J. (Eds) *Trajectory Analysis in Stratigraphy*, *Basin Research* 21(5), 620-643.
- Henriksen, S., Hampson, G. J., Helland-Hansen, W., Johannessen, E. P. and Steel, R. J. (2009): Shelf edge and shoreline trajectories, a dynamic approach to stratigraphic analysis. *Basin Research* 21, 445-453.

- Hesthammer, J. and Fossen, H. (1999): Evolution and geometries of gravitational collapse structures with examples from the Statfjord Field northern the North Sea. *Marine and Petroleum Geology*, 16, 259-281.
- Hinz, K. (1981): A hypothesis on terrestrial catastrophes. Wedges of very thick oceanward dipping layers beneath passive margins- thin origin and palaeoenvironment significance. *Geol. Jahrb., Reihe E., Geophysics*, H 22, 3-28.
- Hinz, K., Neben, S., Schreckenberger, B., Roeser, H. A., Block, M., Souza, K. G. D. and Meyer, H. (1999): The Argentine continental margin north of 48°S: sedimentary successions, volcanic activity during breakup. *Marine and Petroleum Geology*, 16 (1), 1-25.
- Howell, D. G. and Normark, W. R. (1982): Sedimentology of submarine fans. In: Scholle, P. A. and Spearing, D. (Eds); *Sandstone depositional environments*. American Association of Petroleum Geologists Memoir 31, 365-404.
- Hubbard, R. J., Pape, J., and Roberts, D. G. (1985): Depositional sequence mapping to illustrate the evolution of a passive continental margin. In: Berg, O. R. and Woolverton, D. G. (Eds); *Seismic stratigraphy II: An integrated approach to hydrocarbon exploration*. American Association of Petroleum Geologists Memoir, 39, 93–115.
- Hubbard, R. J. (1988): Age and significance of sequence boundaries on Jurassic and Early Cretaceous rifted continental margins. *American Association of Petroleum Geologists Bulletin*, 72, 49-72.
- Hunt, D. and Tucker, M. E. (1992): Stranded parasequences and the forced regressive wedge systems tract: deposition during base level fall. *Sedimentary Geology*, 81 (1–2), 1-9.
- Ingersoll, R. V. (1988): Tectonics of sedimentary basins. *Geological Society of America Bulletin*, 100, 1704-1719.
- Jabbour, M., Dhont, D., Hervouët, Y., and Deroin, J.-P. (2012): Geometry and kinematics of fault-propagation folds with variable interlimb angle. *Journal of Structural Geology*, 42, 212-226.
- Jackson, J. A., Gagnepain, J., Houseman, G., King, G. C. P., Papdimitriou, P., Soufleris, C. and Virieux, J. (1982): Seismicity, normal faulting, and the geomorphological development of the Gulf of Corinth (Greece): the Corinth earthquakes of February and March 1981. *Earth and Planetary Science Letters* 57: 377-397.
- Jackson, J. A. and White, N. J. (1989): Normal extension in the upper continental crust: observations from regions of active extension: *Journal of Structural Geology*, 11, 15–36.
- Jackson, J. and Leeder, M. (1994): Drainage systems and the development of normal faults: an example from Pleasant Valley, Nevada. *Journal of Structural Geology*, 16/8, 1041-1059.

- Jackson, J. and Blenkinsop, T. (1997): The Bilila-Mtakataka fault in Malaŵi: An active, 100 km long, normal fault segment in thick seismogenic crust. *Tectonics*, 16/1, 137-150.
- Jackson, C. A. L., Gawthorpe, R. L., Carr, I. D. and Sharp, I. R. (2005): Normal faulting as a control on the stratigraphic development of shallow marine syn-rift sequences: the Nukhul and Lower Rudeis Formations, Hammam Faraun fault block, Suez Rift, Egypt. *Sedimentology*, 52 (2), 313-338.
- Jackson, C.A.L, Gawthorpe, R.L., Sharp, I.R. (2006) Style and sequence of deformation during extensional fault-propagation folding: examples from the Hamman Faraun and ElQaa fault blocks, Suez Rift, Egypt. *Journal of Structural Geology*, 28, 519-535.
- Jamison, W. R. (1987): Geometric analysis of fold development in overthrust terranes. *Journal of Structural Geology*, 9 (2), 207-219.
- Jammes, S., Tiberi, C. and Manatschal, G. (2010): 3D architecture of a complex transcurrent rift system: The example of the Bay of Biscay - Western Pyrenees. *Tectonophysics*, 489 (1-4), 210-226.
- Janecke, S. U., Vandenburg, C. J. and Blankenau, J. J. (1998): Geometry, mechanisms, and significance of extensional folds from examples in the Rocky Mountain Basin and Range province, U.S.A. *Journal of Structural Geology*, 20/7, 841-856.
- Janssen, M. E., Stephenson, R. A. and Cloetingh, S. (1995): Temporal and spatial correlations between changes in plate motions and the evolution of rifted basins in Africa. *Bulletin, Geological Society of America*, 107: 1317-1332.
- Jones, H. A. and Hockey, R. D. (1964): The geology of southwestern Nigeria. *Bulletin 31, Geological Survey, Nigeria*, 101.
- Joshi, G. R. and Hayashi, D. (2010): Development of extensional stresses in the compressional setting of the Himalayan thrust wedge: inference from numerical modeling. *Natural Science*, 2, 667-680.
- Jungslager, E. A. (1999): Petroleum habitats of the Atlantic margin of South Africa. In: Cameron, N. R., Bate, R. H. and Clure, V. S. (Eds), *The Oil and Gas Habitats of the South Atlantic*. Geological Society, London, Special Publications, 153, 153-168.
- Kaki, C., d'Almeida, G. A. F., Yalo, N. and Amelina, S. (2012): Geology and petroleum systems of the Offshore Dahomey Embayment (Benin). *Oil Gas Science and Technology - Rev. IFP Energies Nouvelles*, 19.
- Karner, G. D. and Gamboa, L. A. P. (2007): Timing and origin of the South Atlantic pre-salt sag basins and their capping evaporites. In: Schreiber, B. C., Lugli, S. and Babel, M. (Eds); *Evaporites through space and time*. Geological Society, London, Special Publications, 285, 15-35.
- Katz, B. J., Ed. (1990): Controls on distribution of lacustrine source rocks through time and space. In Katz, B. J. (Ed.), *Lacustrine basin exploration - Case studies and modern analogs*. American Association of Petroleum Geologists Memoir 50: 132-139.

- Kearey, P., Brooks, M. and Hill, I. (2002): An introduction to Geophysical exploration. Blackwell Science Limited, Oxford.
- Keller, G. R., Wendlandt, R. F. and Bott, M. H. P. (1995): Chapter 13: West and Central African rift system. In: Olsen, K. H. (ed): Continental rifts: evolution, structure, tectonics. *Developments in Geotectonics* 25, 437-449.
- Kenyon, N. H. and Millington, J. (1995): Contrasting deep-sea depositional systems in the Bering Sea. In: Pickering, K. T., Hiscott, R. N., Kenyon, N. H., Ricci Lucchi, F. and Smith, R. D. A. (Eds): Atlas of deep-water environments; Architectural style in turbidity systems. Chapman & Hall, London, 89-93.
- Kenyon, N. H. (1987): Mass-wasting features on the continental slope of Northwest Europe. *Marine Geology*; 74: 57-77.
- Khalil, S. M. and McClay, K. R. (2002): Extensional fault-related folding, northwestern Red Sea, Egypt. *Journal of Structural Geology*, 24/4, 743-762.
- Kinabo, B. D., Atekwana, E. A., Hogan, J. P., Modisi, M. P., Wheaton, D. D., and Kampunzu, A. B. (2007): Early structural development of the Okavango rift zone, NW Botswana. *Journal of Earth Sciences*, 48, 125-136.
- Kogbe, C. A. (1974): The Upper Cretaceous Abeokuta Formation of Southwestern Nigeria. *Nigerian Field*, XXXIX, No 4.
- Kogbe, C. A. (1989): The Cretaceous and Paleogene sediments of Southern Nigeria. In: Kogbe, C. A. (Ed.) *Geology of Nigeria*. Rockview (Nigeria) Ltd, Jos, Nigeria; 325-334.
- Kornsawan, A. and Morley, C. K., (2002): The origin and evolution of complex transfer zones (graben shifts) in conjugate fault systems around the Funan Field, Pattani Basin, Gulf of Thailand. *Journal of Structural Geology*, 24, 435-449.
- Kroner, A. and Stern R. J. (2004): Pan-African Orogeny North African Phanerozoic Rift Valley. *Encyclopedia of Geology*, 1: 1-12.
- Krueger, S. W. and Grant, N. T. (2006): Evolution of fault-related folds in the contractional toe of the deep-water Niger Delta. Paper presented at the American Association of Petroleum Geologists Annual Convention, 9-12 April, Houston, Texas.
- Kyrkjebo, R., Gabrielsen, R. H. and Faleide, J. I. (2004): Unconformities related to the Jurassic-Cretaceous syn-rift-post-rift transition of the northern North Sea. *Journal of the Geological Society*, 161 (1): 1-17.
- Labails, C. (2007) La marge sud-marocaine et les premières phases d'ouverture de l'océan Atlantique Central,. Université de Bretagne Occidentale, Brest. 135
- Lambiase, J. J. (1990): A model for tectonic control of lacustrine stratigraphic sequences in continental rift basins. In: Katz, B. J. (Ed.) *Lacustrine Basin Exploration. Case studies and modern analogs*. American Association of Petroleum Geologists Memoir, 50: 265-276.

- Lambiase, J. J. and Bosworth, W. (1995): Structural controls on sedimentation in continental rifts. In: Lambiase, J. J. (Ed.), *Hydrocarbon habitat in rift basins*. Geological Society London, Special Publications, 80: 117-144.
- Lang, J., Anthony, E. J. and Oyede, L. M. (1995): Late Quaternary sediments in incised coastal valleys in Benin: A preliminary sequence stratigraphic interpretation. *Quaternary International*, 29/30: 31-39.
- Larsen, M., Rasmussen, T. and Hjelm, L. (2010): Cretaceous revisited: exploring the syn-rift play of the Faroe –Shetland Basin. In: Vining, B. A. and Pickering, S. C. (Eds), *Petroleum Geology: From Mature Basins to New Frontiers—Proceedings of the 7th Petroleum Geology Conference*, 7: The Geological Society, London; 953-962.
- Lastras, G., Canals, M., Urgeles, R., De Batis, M., Calafat, A., M. and Casamor, J. L. (2004): Characterisation of the recent BIG'95 debris flow deposit on the Ebro margin, Western Mediterranean Sea, after a variety of seismic reflection data. *Marine Geology*, 213, 235-255.
- Le Gall, B., Vétel, W. and Morley, C. K. (2005): Inversion tectonics during continental rifting: The Turkana Cenozoic rifted zone, northern Kenya. *Tectonics*, 24(2), 1-17.
- Lee, C., Nott, J. A., Keller, F. B. and Parrish, A. R. (2004): Seismic expression of the Cenozoic mass-transport complexes, deep-water Tarfaya-Agadir Basin, offshore Morocco. *Offshore Technology Conference*, Houston, TX.
- Leeder, M. R. and Gawthorpe, R. L. (1987): Sedimentary models for extensional tilt-block/half-graben basins. In: Coward, M. P., Dewey, J. F. and Hancock, P. L. (Eds), *Continental Extensional Tectonics*. Geological Society, London, Special Publications, 28: 139-152.
- Leeder, M. R. (1995): Continental rifts and proto-oceanic rift troughs. In: Busby-Spera, C. J. and Ingersoll, R. V. (Eds), *Tectonics of Sedimentary Basin*. Blackwell, Oxford, 119-148.
- Letouzey, J., Werner, P. and Marty, A. (1990): Fault reactivation and structural inversion. Backarc and intraplate compressive deformations. Example of the eastern Sunda shelf (Indonesia). *Tectonophysics*, 183: 341-362.
- Levy, F. and Jaupart, C. (2011): Folding in the region of extension. *Geophysical Journal International*, 185 (3): 1120-1134.
- Li, W., Alves, T.M., Wu, S., Völker, D., Zhao, F., Mi, L., Kopf, A., (2015): Recurrent slope failure and submarine channel incision as key factors controlling reservoir potential in the South China Sea (Qiongdongnan Basin, South Hainan Island). *Marine and Petroleum Geology*, 64, 17-30.
- Lister, G. S., Etheridge, M.A. and Symonds, P. A. (1986): Detachment faulting and the evolution of passive continental margins. *Geology*, 14: 246-250.

- López-Blanco, M. (2002): Sedimentary response to thrusting and fold growing on the SE margin of the Ebro basin (Paleogene, NE Spain). *Sedimentary Geology*, 146 (1-2): 133-154.
- Lowell, J. D. (1995): Mechanics of basin inversion from worldwide examples. In: Buchanan, J. G. and Buchanan, P. G. (Eds), *Basin Inversion*. Geological Society, London, Special Publications, 88 (1): 39-57.
- MacGregor, D. S., Robinson, J. and Spear, G. (2003): Play fairways of the Gulf of Guinea transform margin. In: Arthur, T. J., MacGregor, D. S. and Cameron, N. R. (Eds) *Petroleum geology of Africa - New themes and developing technologies*, 207: 131-150.
- Machette, M. N., Persounius, S. F. and Nelson, A. R. (1991): The Wasatch fault zone, Utah-segmentation and history of Holocene earthquakes. *Journal of Structural Geology*, 13, 137-149.
- Mack, G. H. and Seager, W. R. (1990): Tectonic control on facies distribution of the Camp Rice and Palomas Formations (Pliocene-Pleistocene) on the southern Rio Grande Rift. *Geological Society of America Bulletin*, 102: 45-53.
- Magoon, L. B. (1988): The Petroleum System- a classification scheme for research, exploration and resource assessment. In: Magoon, L. B. (Ed.), *Petroleum Systems of United States*, United States Geological Society Bulletin, 1870: 2-15.
- Maloney, D., Davies, R., Imber, J., Higgins, S. and King, S. (2010): New insights into deformation mechanisms in the gravitationally driven Niger Delta deep-water fold and thrust belt. *American Association of Petroleum Geologists Bulletin*, 94 (9): 1401-1424.
- Maloney, D., Davies, R., Imber, J. and King, S. (2012): Structure of the footwall of a listric fault system revealed by 3D seismic data from the Niger Delta. *Basin Research*, 24 (1), 107-123.
- Manatschal, G. (2004). New models for evolution of magma-poor rifted margins based on a review of data and concepts from West Iberia and the Alps. *International Journal of Earth Sciences*, 93 (3), 432-466.
- Manga, C. S., Loule, J-P. and Koum, J-J. (2001): Tectono-stratigraphic evolution and prospectivity of the Logone Birni Basin, North Cameroon – Central Africa. *American Association of Petroleum Geologists Bulletin*, 85, Supplement, 1-6.
- Mann P., Hempton M. R., Bradley D.C. and Burke K. (1983): Development of pull-apart basins. *Journal of Geology* 91 (5), 529-554.
- Mann, P. L. Gahaga, L. and Gordon, M. B. (2003): Tectonic setting of the World's oil and gas fields. In: Halbouty, (Ed.), *Giant oil and gas fields of decade 1990-1999*. American Association of Petroleum Geologists Memoir 78, 15-105.
- Mann, P. (2007): Global catalogue, classification and tectonic origins of restraining- and releasing-bends on active and ancient strike-slip fault systems. In: Cunningham W. D.

- and Mann, P. (Eds); Tectonics of strike-slip restraining and releasing bends. The Geological Society, London, Special Publications, 290, 13-142.
- Marrett, R. and Peacock, D. C. P. (1999): Strain and stress. *Journal of Structural Geology* 21, 1057-1063.
- Martinez, F., Arriagada, C., Mpodozis, C. and Pena, M. (2012): The Lautaro Basin: A record of inversion tectonics in northern Chile. *AndGeo[online]*. 39/2, 258-278.
- Martini, E. (1971): Standard Tertiary and Quaternary Calcareous Nannoplankton Zonation. *Proceedings of the II Planktonic Conference, Roma, 1970*, Farinacci, A. (Ed). *Tecnoscienza*, 739- 785.
- Mascle, J. (1976): Atlantic-type continental margins: Distinction of two basic structural types. *Ali. Açacl. bras. C~and*, 48, 149-155.
- Mascle, J. and Blarez, E. (1987): Evidence for transform margin evolution from the Ivory Coast–Ghana continental margin. *Nature* 326, 378–381.
- Mascle, J., Blarez, E. and Marinho, M. (1988): The shallow structures of the Guinea and Ivory Coast-Ghana transform margins: Their bearing on the Equatorial Atlantic Mesozoic evolution. *Tectonophysics*, 188: 193-209.
- Mascle, J., Lohman, G.P., Clift, P. (1995): La marge transformante de Côte d’Ivoire-Ghana: premiers résultants de la campagne ODP 159 (janvier-février 1995). 737–747 (Paris 320).
- Mascle, J., Lohmann, G. P., Clift, P. D. and Party, S. S. (1996): Geophysical and Geological Background. *Proceedings of the Ocean Drilling Program Initial Reports*, 159: 5-16.
- Masini, E., Manatschal, G., Mohn, G. and Unternehr, P. (2012): Anatomy and tectono-sedimentary evolution of a rift-related detachment system: The example of the Err detachment (central Alps, SE Switzerland). *Geological Society of America Bulletin*, 124 (9-10): 1535-1551.
- Maslin, M., Owen, M., Day, S., and Long, D. (2004): Linking continental-slope failures and climate change: testing the clathrate gun hypothesis: *Geology*, 32/ 1, 53–56.
- Masson, D. G., Harbitz, C. B., Wynn, R. B., Wynn, R. B., Pedersen, G. and Lovholt, F. (2006): Submarine landslides: processes, triggers, and hazard prediction. *Philosophical Transaction Royal Society A* 364: 2009-2039.
- Matos, R. M. D. (1992): The Northeast Brazilian Rift System. *Tectonics*, 11 (4): 766-791.
- Matos, R. M. D. (2000): Tectonic Evolution of the Equatorial South Atlantic. *Atlantic Rifts and Continental Margins, Geophysical Monograph* 115: 331-354.
- McClay, K. R. (1989): Analogue models of inversion tectonics. In: Cooper, M. A. and Williams, G.D. (Eds) *Inversion Tectonics*. Geological Society, London, Special Publications. 44: 41-59.

- McClay, K. R. (1995): The geometries and kinematics of inverted fault systems: a review of analogue models. In: Buchanan, J.G., Buchanan, P.G. (Eds), Basin Inversion. Geological Society London, Special Publications, 88, 97-118.
- McClay, K., and Khalil, S. (1998): Extensional hard linkages, eastern Gulf of Suez, Egypt. *Geology*, 26, 563–566.
- McHargue, T. R. Heidrick, T. L. and Livingston, J. E. (1992): Tectono-stratigraphic development of the interior Sudan rifts, Central Africa: *Tectonophysics*, 213, 187–202.
- McKenzie, D. (1978): Some remarks on the development of sedimentary basins. *Earth and Planetary Science Letters*, 40: 25-32.
- McLeod, A. E., Dawers, N. H. and Underhill, J. R. (2000): The propagation and linkage of normal faults: Insights from the Strathspey-Brent-Statfjord fault array, northern North Sea. *Basin Research*, 12: 263-284.
- Meador, K. J. and Austin, J. A. (1988): Seismic comparison of the early stratigraphic evolution of conjugate passive continental margins: the Newfoundland/Flemish basin and the eastern Iberian Abyssal plain south of Galicia Bank. In: Boillot, G., and Wintere, E. L. (Eds), *Proceedings of the ODP, Scientific Results*, 103, College Station, TX (Ocean Drilling Program), 777-786.
- Meador, K. J., Austin, J. A. and Dean, D. F. (1988): Shelf to basin correlations in the Newfoundland Basin. In: BALLY, A. W. (Ed.) *Atlas of Seismic Stratigraphy*. American Association Petroleum Geologists Studies in Geology, 27/2, 88-95.
- Mellere, D., Plink-Bjoklund, P., and Steel, R. (2002): Anatomy of shelf deltas at the edge of a prograding Eocene shelf margin, Spitsbergen. *Sedimentology* 49, 1181–1206.
- Mercier de Lépinay, M., Loncke, L., Basile, C., Roest, W.R., de Clarens, P., Maillard, A., Boukandou Sidi, C., and Patriat, M. (2016): Transform continental margins - part 2: A worldwide inventory. *Tectonophysics*, XXX.
- Merle, O. (2011): A simple continental rift classification. *Tectonophysics*, 513 (1-4), 88-95.
- Milani, E. J., and Davison, I. (1988): Basement control and transfer tectonics in the Reconcavo–Tucano–Jatoba rift, Northeast Brazil. *Tectonophysics*, 154, 41-70.
- Milia, A. and Torrente, M. M. (1999): Tectonics and stratigraphic architecture of a peri-Tyrrhenian half-graben (Bay of Naples, Italy). *Tectonophysics*, 315 (1-4): 301-318.
- Mitchum, R., Vail, P. R. and S. Thompson, (1977): Seismic stratigraphy and global changes in sea level, part 2: the depositional sequence as the basic unit for stratigraphic analysis: Section 2. Application of seismic reflection configuration to stratigraphic interpretation. In: Payton, C. E. (Ed.): *Seismic stratigraphy- Application to hydrocarbon exploration*. American Association of Petroleum Geologists Memoir, Tulsa; 26: 53-62.
- Mitchum, R. M. Jr. and Vail, P. R. (1977): Seismic stratigraphy and global changes of sea level: Part 7: Seismic stratigraphic interpretation procedure. In: Payton, C. E., (Ed.);

Seismic Stratigraphy - Applications to Hydrocarbon Exploration. American Association of Petroleum Geologists Memoir 26: 135-143.

Mitchum, R. M. and Van Wagoner, J. C. (1990): High-frequency sequences and their stacking patterns: sequence-stratigraphic evidence of high-frequency eustatic cycles. *Sedimentary Geology*, 70, 131-160.

Mitra, S. (1990): Fault-propagation folds: Geometry, kinematic evolution, and hydrocarbon traps. *American Association of Petroleum Geologists Bulletin*, 74(6): 921-945.

Mitra, S. (1993): Geometry and Kinematic evolution of Inversion Structures. *American Association of Petroleum Geologists Bulletin*, 77 (7): 1159-1191.

Mohamed, A. Y., Illiffe, J. E., Ashcroft, W. A. and Whiteman, A. J. (2000): Burial and maturation history of the Heglig field area, Muglad Basin, Sudan. *Journal of Petroleum Geology*, 23: 107-128.

Mohriak, W. U. and Talwani, M. (2000): Atlantic rifts and continental margins. *Geophysical Monograph*, American Geophysical Union, Washington D.C.

Mohriak, W. U., Mello, M. R., Bassetto, M., Vieira, I. S. and Koutsoukos, E. A. M. (2000): Crustal Architecture, Sedimentation, and Petroleum Systems in the Sergipe - Alagoas Basin, Northeastern Brazil. *American Association of Petroleum Geologists Memoir*, 73: 273-300.

Mohriak, W. U. and Rosendahl, B. R. (2003): Transform zones in the South Atlantic rifted continental margins. In: *Intraplate strike-slip deformation belts*, Geological Society, London, Special Publications, 210: 211-228.

Moore, J. G. (1992): A syn-rift to post-rift transition sequence in the Main Porcupine Basin, offshore western Ireland. In: Parnell, J. (ed.), *Basins on the Atlantic Seaboard: Petroleum Sedimentology and Basin Evolution*. Geological Society, London, Special Publications, 62, 333-349

Moores, E. M. and Twiss, R. J. (1995): *Tectonics*. W. H. Freeman and Company, New York.

Morgan, R. (2003): Prospectivity in ultradeep water: the case for petroleum generation and migration within the outer parts of the Niger Delta apron. In: Arthur, T. J., MacGregor, D. S. and Cameron, N. R. (Eds) *Petroleum Geology of Africa: new themes and developing technologies*. Geological Society, London, Special Publications, 207: 151-164.

Morley, C. K. (1989): Extension, detachments, and sedimentation in continental rifts (with particular reference to East Africa). *Tectonics*, 8: 1175-1192.

Morley, C. K. (1995): Developments in the structural geology of rifts over the last decade and their impact on hydrocarbon exploration. In: Lambiase, J. J. (Ed.) *Hydrocarbon Habitat in Rift Basins*. Geological Society, London, Special Publications, 80 (1): 1-32.

- Moscardelli, L., Wood, L. and Mann, P. (2006): Mass-transport complexes and associated processes in the offshore area of Trinidad and Venezuela. *American Association of Petroleum Geologists Bulletin* 90: 1059-1088.
- Moscardelli, L., and Wood, L. (2008): New classification system for mass-transport complexes in offshore Trinidad. *Basin Research* 20: 73–98.
- Mosunmolu Limited (2008): High-Resolution Biostratigraphic, Sequence stratigraphic and palaeoenvironmental analysis of the Aje-4 Well (2850-12625 feet). Unpublished Report submitted to Chevron Nigeria Limited. RPT. NO MOS/08/189.
- Moulin, M., Aslanian, D. and Unternehr, P. (2010): A new starting point for the South and Equatorial Atlantic Ocean. *Earth Science Review*, 98: 1-37.
- Mounguengui, M. M. and Guiraud, M. (2009): Neocomian to early Aptian syn-rift evolution of the normal to oblique-rifted North Gabon Margin (Interior and N’Komi Basins). *Marine and Petroleum Geology* 26, 1000–1017.
- Moustafa, A. R. (2014): Structural architecture and tectonic evolution of the Maghara inverted basin, Northern Sinai, Egypt. *Journal of Structural Geology*, 62, 80-96.
- Müller, R. D., Sdrolias, M., Gaina, C., Roest, W. R. (2008): Age, spreading rates, and spreading asymmetry of the world's ocean crust. *Geochem. Geophys. Geosyst.* 9, Q04006.
- Mutti, E. and Normark, W. R. (1991): An integrated approach to the study of turbidite systems. In: Weimer, P. and Link, M. H. (Eds); *Seismic Facies and Sedimentary Processes of Submarine Fans and Turbidite Systems*: New York, Springer-Verlag, 75-106.
- Narr, W. and Suppé, J. (1994): Kinematics of basement-involved compressive structures. *American Journal of Science*, 294, 802-860.
- Neal, J. and Abreu, V. (2009): Sequence stratigraphy hierarchy and the accommodation succession method. *Geology*; 37 (9): 779-782.
- Nemčok, M., Schamel, S. and Gayer, R. (2005): *Thrustbelts: Structural Architecture, Thermal Regimes, and Petroleum Systems*. Cambridge: Cambridge University Press.
- Nemčok, M., Stuart, C., Rosendahl, B. R., Welker, C., Smith, S., Sheya, C., Sinha, S. T., Chaudhuri, M., Allen, R., Reeves, C., Sharma, S. P., Venkatraman, S. and Sinha, N. (2013a): Continental breakup mechanism; lessons from intermediate- and fast-extension settings. In: Mohriak, W. U., Danforth, A., Post, P. J., Brown, D. E., Tari, G. C., Nemcok, M. and Sinha, S. T. (Eds): *Conjugate divergent margins*. Geological Society, London, Special Publications, 369: 373-401.
- Nemčok, M., Henk, A., Allen, R., Sikora, P. J. and Stuart, C. (2013b): Continental breakup along strike-slip fault zones; observations from the Equatorial Atlantic. In: Mohriak, W. U., Danforth, A., Post, P. J., Brown, D. E., Tari, G. C., Nemčok, M. and Sinha, S. T.

- (Eds), Conjugate Divergent Margins. Geological Society, London, Special Publications, 369: 537-556.
- Nigro, F. and Renda, P. (2004): Growth pattern of under lithified strata during thrust-related folding. *Journal of Structural Geology*, 26 (10): 1913-1930.
- Nilsen, T. H., and Sylvester, A. G. (1995): Strike-slip basins. In: Busby, C. J. and Ingersoll, R. V. (eds.), *Tectonics of sedimentary basins*: Cambridge, Massachusetts, Blackwell Science, 425-457.
- Nissen, S. E., Haskell, N. L., Steiner, C. T. and Cotterill, K. L. (1999): Debris flow outrunner blocks, glide tracks, and pressure ridges identified on the Nigerian Continental Slope using 3D seismic coherency. *The Leading Edge*, 18: 595-599.
- Normark, W. R. (1978): Fan valleys, channels and depositional lobes on modern submarine fans - characters for recognition of sandy turbidite environments: *American Association of Petroleum Geologists, Bulletin*, 62: 912-931.
- North, F. K. (1985): *Petroleum Geology*. Allen and Unwin, London.
- Nottvedt, A., Gabrielsen, R. H. and Steel, R. J. (1995): Tectono-stratigraphy and sedimentary architecture of rift basins, with reference to the northern North Sea. *Marine and Petroleum Geology*, 12 (8): 881-901.
- Nton, M. E., Eze, F. P. and Elueze, A. A. (2006): Aspects of source rock evaluation and diagenetic history of the Akinbo Shale, eastern Dahomey basin, southwestern Nigeria. *Nigerian Association of Petroleum Geologists Bulletin*, 19 (1): 35-49.
- Nton, M. E., Ikhane, P. R. and Tijani, M. N. (2009): Aspect of Rock-Eval Studies of the Maastrichtian-Eocene Sediments from Subsurface, in the Eastern Dahomey Basin Southwestern Nigeria'. *European Journal of Scientific Research*, 25 (3): 417-427.
- Nürnberg, D. and Müller, R. D. (1991): The tectonic evolution of the South Atlantic from Late Jurassic to Present. *Tectonophysics*, 191 (1-2): 27-53.
- Nwachukwu, S. O. (1972): The tectonic evolution of the southern portion of the Benue Trough, Nigeria. *Geological Magazine*, 109 (05): 411-419.
- Nyantakyi, E. K., Hu, W. S., Borkloe, J. K., Qin, G. and Han, M. C. (2013): Structural and Stratigraphic Mapping of Delta Field, Agbada Formation, Offshore Niger Delta, Nigeria. *American Journal of Engineering Research (AJER)*. 2(11): 204-215.
- Ogbe, F. G. A. (1970): Stratigraphy of strata exposed in the Ewekoro Quarry, Western Nigeria.
- Okosun, E. A. (1990): A review of the Cretaceous stratigraphy of the Dahomey Embayment, West Africa. *Cretaceous Research*, 11 (1): 17-27.
- Okosun, E. A. (1998): Review of the Early Tertiary Stratigraphy of southwestern Nigeria. *Journal of Mining and Geology*, 34 (1): 27-35.

- Olabode, S. O. (2006): Siliciclastic slope deposits from the Cretaceous Abeokuta Group, Dahomey (Benin) Basin, southwestern Nigeria. *Journal of African Earth Sciences*, 46: 187-200.
- Olabode, S. O. and Adekoya, J. A. (2008): Seismic stratigraphy and development of Avon canyon in Benin (Dahomey) basin, southwestern Nigeria. *Journal of African Earth Sciences*, 50: 286-304.
- Olabode, S. O. and Mohammed, M. Z. (2016): Depositional facies and sequence stratigraphic study in parts of Benin (Dahomey) Basin SW Nigeria: Implications on the re-interpretation of Tertiary sedimentary successions. *International Journal of Geosciences*, 7/2, 1-19.
- Olade, M. A. (1975): Evolution of Nigeria's Benue Trough (Aulacogen): A tectonic model. *Geological Magazine*, 112 (06): 575-583.
- Olsen, P. E. and Kent, D. V. (1999): Long-period Milankovitch cycles from the Late Triassic and Early Jurassic of eastern North America and their implications for the calibration of the early Mesozoic time scale and the long-term behavior of the planets. *Transactions, Royal Society of London, Series A*, 357: 1761-1786.
- Omatsola, M. A. and Adegoke, O. S. (1981): Tectonic evolution and Cretaceous stratigraphy of the Dahomey Basin. *Mining and Geology*, 18 (1): 130-137.
- Omosanya, K. O. and Alves, T. M. (2014): Mass-transport deposits controlling fault-propagation, reactivation and structural decoupling on continental margins (Espírito Santo Basin, SE Brazil). *Tectonophysics*, 628: 158-171
- Onuoha, K. M. (1999): Structural features of Nigeria's coastal margin: an assessment based on age data from wells. *Journal of African Earth Sciences*, 29 (3).
- Opara, A. I. (2011): Estimation of the Depth to Magnetic Basement in Part of the Dahomey Basin, Southwestern Nigeria. *Australian Journal of Basic and Applied Sciences*, 5 (9): 335-343.
- Oyinloye, A. O. (2004): Petrochemistry, Pb isotope systematic and geotectonic setting of granite gneisses in Ilesha schist belt southwestern Nigeria. *Global Journal of Geological Science*, 2(1): 1-13.
- Pacht, J. A., Bowen, B. E., Hall, D. J., Rosen, R., Shaffer, B. L. and Choudhury, A. (1994) Sequence stratigraphy of Neogene strata in offshore Nigeria. GCSSEPM Foundation 15th Annual Research Conference. December 4-7: 281-292.
- Park, R. G. (1997): Geological structures and moving plates. Chapman and Hall, London.
- Paton, D. A. and Underhill, J. R. (2004): Role of crustal anisotropy in modifying the structural and sedimentological evolution of extensional basins: the Gamtoos Basin, South Africa. *Basin Research*, 16/3, 339-359.

- Payton, C. E., (1977): Seismic Stratigraphy - Applications to Hydrocarbon Exploration. American Association of Petroleum Geologists Memoir 26: 135-143.
- Peacock, D. C. P. and Sanderson, D. J. (1991): Displacements, segment linkage and relay ramps in normal fault zones. *Journal of Structural Geology*, 13/6, 721-733.
- Peacock, D. C. P., Knipe, R. J., and Sanderson, D. J. (2000): Glossary of normal faults. *Journal of Structural Geology*, 22, 291–305.
- Peacock, D. C. P. (2002): Propagation, interaction and linkage in normal fault systems. *Earth-Science Reviews*, 58: 121-142.
- Pereira, R. and Alves, T. M. (2011): Margin segmentation prior to continental breakup: A seismic-stratigraphic record of multiphased rifting in the North Atlantic (Southwest Iberia). *Tectonophysics*, 505: 17-34.
- Péron-Pinvidic, G., Manatschal, G., Minshull, T. A., Sawyer, D. S. (2007): Tectono-sedimentary evolution of the deep Iberia–Newfoundland margins: evidence for a complex breakup history. *Tectonics* 26, TC2011.
- Petters, S. W. and Ekweozor, C. M. (1982): Petroleum Geology of Benue Trough and Southeastern Chad Basin, Nigeria. *American Association of Petroleum Geologists Bulletin*, 66: 1141-1149.
- Petters, S. W. (1984): An ancient submarine canyon in the Oligocene-Miocene of the western Niger Delta. *Sedimentology*, 31: 805-810.
- Pindell, J. and Dewey, J. F. (1982): Permo-Triassic reconstruction of western Pangea and the evolution of the Gulf of Mexico/Caribbean region. *Tectonics* 1, 2: 179-211.
- Piper, D.J.W., Pirmez, C., Manley, P.L., Long, D., Flood, R.D., Normark, W.R., Showers, W.J., Flood, R.D., Piper, D.J.W., Klaus, A., Burns, S.J., Busch, W.H., Cisowski, S.M., Cramp, A., Damuth, J.E., Goni, M.A., Haberle, S.G., Hall, F.R., Hinrichs, K.-U., Hiscott, R.N., Kowalski, R.O., Kronen, J.D., Long, D., Lopez, M., McDaniel, D.K., Manley, P.L., Maslin, M.A., Mikkelsen, N., Nanayama, F., Normark, W.R., Pirmez, C., dos Santos, J.R., Schneider, R.R., Showers, W.J., Soh, W. & Thibault, J. (1997): Mass-transport deposits of the Amazon fan. *Proceeding Ocean Drilling Programme Scientific Research*, 155, 109-146.
- Pirmez, C., Beaubouef, R. T., Friedman, S. J. and Mohrig, D. C. (2000): Equilibrium profile and base level in submarine channels: examples from Late Pleistocene systems and implications for the architecture of deep-water reservoirs. In: Weimer, P., Slatt, R. M., Coleman, J., Rosen, N. C., Nelson, H., Bouma, A. H., Styzen, M. J. and Lawrence, D.T., (Eds); *Deep-Water Reservoir of the World: Gulf Coast Society of the Society of Economic Paleontologists and Mineralogists Foundation, 20th Annual Research Conference*, 782-805.

- Pirmez, C., Pratson, L. F., and Steckler, M. S. (1998): Clinoform development by advection-diffusion of suspended sediment: Modeling and comparison to natural systems. *Journal of Geophysical Research*, 103, b10: 141-157.
- Plint, A. G. and Nummedal, D. (2000): The falling stage systems tract; recognition and importance in sequence stratigraphic analysis. In: Hunt, D. and Gawthorpe, R. I. (Eds): *Sedimentary response to forced regression*. Geological Society, London Special Publications; 172: 1-17.
- Poblet, J. and Lisle, R. J. (2011): Kinematic Evolution and Structural Styles of Fold-and-Thrust Belts. In: Poblet, J. and Lisle, R. J. (eds), *Kinematic Evolution and Structural Styles of Fold-and-Thrust Belts*. Geological Society, London, Special Publications, 349, 1-24.
- Pollard, D. D., and Aydin, A., (1988): Progress in understanding jointing over the past century. *Geological Society of America Bulletin* 100, 1181-1204.
- Popescu, I., Lericolais, G., Panin, N., Normand, A., Dinu, C. and Drezen, E. L. (2006): The Danube submarine canyon (Black Sea): morphology and sedimentary processes. *Marine Geology*, 206: 249-265.
- Posamentier, H. W., Jervey, M. T. and P. R. Vail, (1988): Eustatic controls on clastic deposition I: Conceptual framework. In: Wilgus, C. K., Hastings, B. S., Kendall, C. G., Posamentier, H. W., Ross, C. A. and van Wagoner, J. C. (Eds): *Sea level changes: An integrated approach*. Society of Economic Paleontologists and Mineralogists Special Publication 42: 109-124.
- Posamentier, H. W. and Vail, P. R. (1988): Eustatic controls on clastic deposition II: Sequence and systems tract models. In: Wilgus, C. K., Hastings, B. S., Kendall, C. G., Posamentier, H. W., Ross, C. A. and van Wagoner, J. C (Eds): *Sea level changes: An integrated approach*. Society of Economic Palaeontologists and Mineralogists Special Publication 42: 125-154.
- Posamentier, H. W., Erskine, R. D. and Mitchum, R. M. Jr. (1991): Submarine fan deposition in a sequence stratigraphic framework, in Weimer, P., and Link, M.H. (Eds); *Seismic Facies and Sedimentary Processes of Submarine Fans and Turbidite Systems*: New York, SpringerVerlag, 127-136.
- Posamentier, H. W. and Allen, G. P. (1993): Variability of the sequence stratigraphic model: Effects of local basin factors. *Sedimentary Geology*, 86, 91-109.
- Posamentier, H. W. and Allen, G. P. (1999): *Siliciclastic Sequence Stratigraphy - Concepts and Applications*: Society of Economic Paleontologists and Mineralogists, *Concepts in Sedimentology and Paleontology*, 7: 210.
- Posamentier, H. W., Meizarwin, N., Wisman, P. S., and Plawman, T. (2000): Deep water depositional systems- Ultra-deep Makassar Strait, Indonesia. In: Weimer, P., Slatt, R. M., Coleman, J., Rosen, N. C., Nelson, H., Bouma, A. H., Styzen, M. J. and Lawrence, D. T. (Eds); *Deep-Water Reservoirs of the World: Gulf Coast*. Society of Economic

Paleontologists and Mineralogists Foundation, 20th Annual Research Conference, 806-816.

- Posamentier, H. W. and Kolla, V. (2003): Seismic Geomorphology and Stratigraphy of Depositional Elements in Deep-Water settings. *Journal Sedimentary Research* 73(3), 367-388.
- Posamentier, H. W., and Walker, R. G., (2006): Deep-water turbidites and submarine fans. In: Posamentier, H.W., Walker, R.G. (Eds.), *Facies Models Revisited*. Society of Economic Paleontologists and Mineralogists Special Publications, Society for Sedimentary Geology 84, 397-520.
- Pratson, L. F., Ryan, W. B. F., Mountain, G. S. and Twichell, G. S., (1994): Submarine canyon initiation by downslope-eroding sediment flows: evidence in late Cenozoic strata on the New Jersey continental slope. *Geological Society America Bulletin* 106, 395-412.
- Pratson, L. F. (2001): A perspective on what is known and what is not known about seafloor instability in the context of continental margin evolution. *Marine Petroleum Geology*, 18: 499-501.
- Prosser, S. (1993): Rift-related linked depositional systems and their seismic expression. In: Williams G. D. and Dobb, A. (Eds) *Tectonics and seismic sequence stratigraphy*. Geological Society, London, Special Publications, 71 (1), 35-66.
- Qu, Y., Pan, J., Ma, S., Lei, Z., Li, L. and Wu, G. (2014): Geological characteristics and tectonic significance of unconformities in Mesoproterozoic successions in the northern margin of the North China Block. *Geoscience Frontiers*, 5 (1), 127-138.
- Rabinowitz, P. D. and Labrecque, J. (1979): The Mesozoic South Atlantic Ocean and evolution of its continental margins. *Journal of Geophysical Research*, 84/811, 5973-6002.
- Rahaman, M. A. (1989): Review of the Basement Geology of South-western Nigeria. In: Kogbe, C. A. (Ed.): *Geology of Nigeria*. Rockview (Nigeria) Limited, Jos, Nigeria, 39-56.
- Ravnås, R. and Bondevik, K. (1997): Architecture and controls on Bathonian-Kimmeridgian shallow-marine syn-rift wedges of the Oseberg-Brage area, northern North Sea. *Basin Research*, 9 (3), 197-226.
- Ravnås, R. and Steel, R. J. (1997): Contrasting styles of late Jurassic syn-rift turbidite sedimentation: A comparable study of the Magnus and Oseberg areas, northern North Sea. *Marine and Petroleum Geology*, 14, 417-449.
- Ravnås, R. and Steel, R. J. (1998): Architecture of marine rift-basin successions. *American Association of Petroleum Geologists Bulletin*, 82 (1), 110-146.
- Ravnås, R., Nøttvedt, A., Steel, R. J. and Windelstad, J. (2000): Syn-rift sedimentary architectures in the Northern North Sea. In: Nøttvedt, A, Larsen, B. T., Gabrielsen, R.

- H., Olausen, S., Brekke, H., Torudbakken, B., Brekke, H., Skogseid, J. and Birkeland, O. (Eds), Dynamics of the Norwegian Margin. Geological Society, London, Special Publications, 167 (1), 133-177.
- Reches, Z. (1978): Analysis of faulting in three-dimensional strain field. *Tectonophysics*, 47, 109-129.
- Remus, D., Webster, M. and Keawkan, K. (1993): Rift architecture and sedimentology of the Phetchabun Intermontane Basin, central Thailand. *Journal of Southeast Asian Earth Sciences*, 8 (1-4), 421-432.
- Reyment, R. A. (1965): Stratigraphy of some boreholes in Western Region of Nigeria. *Journal of Mining and Geology*, 2(1), 11.
- Riders, M. H. (1990): Gamma-ray log shape used as a facies indicator: critical analysis of an oversimplified methodology In: Hurst, A., Lovell, M. A. and Morton, A. C. (Eds), Geological Applications of wireline logs. Geological Society Special Publications. 48, 27-37.
- Rihm, R. and Henke, C. H. (1998): Geophysical studies on early tectonic controls on Red Sea rifting, opening and segmentation. In: Purser, B. H. and Bosence, D. W. J. (Eds): Sedimentation and tectonics of rift basins: Red Sea-Gulf of Aden. Chapman and Hall, London, 29-49.
- Robert-Charrue, C. and Burkhard, M. (2008): Inversion tectonics, interference pattern and extensional fault-related folding in the eastern Anti-Atlas, Morocco. *Journal of Geosciences*, 101, 397-408.
- Rogers, J. W., Unrug, R. A. and Sultan, M. (1995): Tectonic assembly of Gondwana. *Journal of Geodynamics*, 19, 1-34.
- Rohais, S., Eschard, R., Ford, M., Guillocheau, F., and Moretti, I. (2007): Stratigraphic architecture of the Plio-Pleistocene infill of the Corinth Rift: Implications for its structural evolution. *Tectonophysics*, 440 (1-4), 5-28.
- Rosenbaum, G., Gasparon, M., Lucente, F. P., Peccerillo, A. and Miller, M. S. (2008): Kinematics of slab tear faults during subduction segmentation and implications for Italian magmatism. *Tectonics*, 27/2, 1-16.
- Rosendahl, B. R (1987): Architecture of continental rifts with special reference to East Africa. (Annual Report). *Earth Planetary Science Letters* 15, 445-503.
- Rossetti, D. F. (2011): The role of tectonics on the preservation of incised-valley estuaries in areas with low accommodation rates: Examples from Upper Cretaceous and Miocene successions in Northern Brazil. In: Dalrymple, R. W., Leckie, D. A. and Tillman, R.W. (Eds), Incised valleys in time and space. Society of Economic Paleontologists and Mineralogists Special Publications 85, 199-217.
- Roy, S., Choudhuri, M. and Gupta, P. (2015): Rift Grabens and Crustal Architecture of the Offshore North East Coast-Mahanadi Basin, Eastern Continental Margin of India. In:

Mukherjee, S. (Ed.), *Petroleum Geosciences: Indian Contexts*. Springer International Publishing Switzerland, 63-85.

Sacchi, M., Horvath, E and Magyari, O. (1999): Role of unconformity-bounded units in the stratigraphy of the continental record: a case study from the Late Miocene of the western Pannonian Basin, Hungary. In: Durand, B., Jolivet, L., Horvath, E. and Seranne, M. (Eds): *The Mediterranean Basins: Tertiary extension within the Alpine Orogen*. Geological Society, London, Special Publications, 156, 357-390.

Sage, F., Basile, C., Mascle, J., Pontoise, B., Whitmarsh, R.B. (2000): Crustal structure of the continent-ocean transition off the Côte d'Ivoire–Ghana transform margin: implications for thermal exchanges across the palaeo-transform boundary. *Geophysical Journal International* 143, 662–678.

Sandwell, D. T. and Smith, W. H. F. (1997): Marine gravity anomaly from Geosat and ERS 1 satellite altimetry. *Journal of Geophysical Research: Solid Earth*, 102 (B5): 10039-10054.

Sangree, J. B. and Widmier, J. M. (1977): Seismic stratigraphy and global changes of sea level: Part 9. Seismic interpretation of clastic depositional facies: Section 2. Application of seismic reflection configuration to stratigraphic interpretation. In: Payton, C. E. (Ed.): *Seismic stratigraphy- Application to hydrocarbon exploration*. American Association of Petroleum Geologists Memoir, 26, 165-184.

Sangree, J. B. and Widmier, J. M. (1978): Seismic Stratigraphy and Global changes of sea level, Part 9: Seismic interpretation of clastic depositional facies. *American Association of Petroleum Geologists Bulletin*, 62 (5), 752-771.

Sangree, J. B. and Widmier, J. M. (1979): Interpretation of depositional facies from seismic data. *Geophysics*, 44 (2), 131-160.

Sawyer, D. E. (2006): Seismic geomorphology, lithology, and evolution of the Late Pleistocene Mars-Ursa Turbidite Region, Mississippi Canyon Area, Northern Gulf of Mexico. Unpublished M. Sc. Thesis, The Pennsylvania University, 37.

Schlische, R. W. and Olsen, P. E. (1990): Quantitative filling models for continental extensional basins with applications to Early Mesozoic rifts of eastern America. *Journal of Geology*, 98: 135-155.

Schlische, R. W. (1991): Half-graben basin filling models: new constraints on continental extensional basin development. *Basin Research*, 3, 123-141.

Schlische, R. W. (1993): Anatomy and evolution of the Triassic–Jurassic continental rift system, eastern North America: *Tectonics*, 12, 1026–1042.

Schlische, R. W. (1995): Geometry and Origin of Fault-Related Folds in Extensional Settings. *American Association of Petroleum Geologists Bulletin*, 79(11), 1661-1678.

Schlische, R. W. and Anders, M. H. (1996): Reconstructing the history of Basin and Range extension using sedimentology and stratigraphy. *Special Paper: Geological Society*,

- America, Chapter Stratigraphic effects and tectonic implications of the growth of normal faults and extensional basins, 303, 183-203.
- Schlische, R. W. and Withjack, M. O. (2009): Origin of fault domains and fault-domain boundaries (transfer zones and accommodation zones) in extensional provinces: Result of random nucleation and self-organized fault growth. *Journal of Structural Geology* 31, 910–925.
- Scholz, C. H. and Contreras, J. C. (1998): Mechanics of continental rift architecture. *Geology*, 26(11), 967-970.
- Scholz, C. A., Moore, T. C., Hutchinson, Jr. D. R., Golmshtok, A. J., Klitgord, K. D. and Kurotchkin, A. G. (1998): Comparative sequence stratigraphy of low-latitude versus high-latitude lacustrine rift basins: seismic data examples from the East African and Baikal rifts. *Palaeogeography, Palaeoclimatology, Palaeoecology* 140, 401-420.
- Schröder, B. (1987): Inversion tectonics along the western margin of the Bohemian Massif. *Tectonophysics*, 137 (1-4), 93-100.
- Selim, S. S. (2016): A new tectono-sedimentary model for Cretaceous mixed non-marine–marine oil-prone Komombo Rift, South Egypt. *International Journal of Earth Science*, 105, 1387-1415.
- Senant, J. and Popoff, M. (1991): Early Cretaceous extension in northeast Brazil related to the South Atlantic opening. *Tectonophysics* 198, 35–46.
- Sengor, A. M. C. and Bozkurt, E. (2013): Layer-parallel shortening and related structures in zones undergoing active regional horizontal extension. *International Journal of Earth Science*, 102, 101-119.
- Seranne, M. and Anka, Z. (2005): South Atlantic continental margins of Africa: A comparison of the tectonic vs climate interplay on the evolution of Equatorial West Africa and SW Africa margins. *Journal of African Earth Sciences*, 43, 283–300.
- Shanmugam, G., Famakinwa, S. B., Hodgkinson, R. J. Blundell, L. C. and Anonymous (1997): Deep-marine slump and debris-flow dominated reservoirs of the Zafiro Field, offshore Equatorial Guinea. *American Association of Petroleum Geologists Bulletin* 81, 1411.
- Shaw, J. H., Novoa, E. and Connors, C. D. (2004): Structural controls on growth stratigraphy in contractional fault-related folds. In: McClay, K. R. (Ed.), *Thrust tectonics and hydrocarbon systems: American Association of Petroleum Geologists Memoir* 82, 400-412.
- Shelton, J. W. (1984): Listric normal faults: an illustrated summary. *American Association of Petroleum Geologists Bulletin*, 68, 801–815.
- Shepard, F. P. (1934): Canyons off the New England Coast. *America Journal of Science*. 27: 24-36.

- Shepard, F. P. (1981): Submarine canyons: multiple cause and long-term persistence. *American Association of Petroleum Geologists Bulletin* 65, 1062-1077.
- Shipp, C., Nott, J. A. and Newlin, J. A. (2004): Physical characteristics and impact of mass-transport complexes on deep-water jetted conductors and suction anchor piles. *Offshore Technology Conference*, Houston, Texas.
- Short, K. C. and Stauble, A. J. (1967): Outline of Geology of Niger Delta. *American Association of Petroleum Geologists Bulletin*, 51/5, 761-779.
- Sibson, R. H. (1995): Selective fault reactivation during basin inversion: potential for fluid redistribution through fault-valve action. In: Buchanan, J. G. and Buchanan, P. G. *Basin Inversion*. Geological Society, London, Special Publications, 88 (1), 3-19.
- Sibuet, J.-C., Srivastava, S., Manatschal, G. (2007): Exhumed mantle-forming transitional crust in the Newfoundland-Iberia rift and associated magnetic anomalies. *Journal of Geophysical Research* 112, B06105.
- Sissingh, W. (1977): Biostratigraphy of Cretaceous calcareous nannoplankton. *Geology Mijnbouw* 57(3), 433- 440.
- Smith, M. and Mosley, P. (1993): Crustal heterogeneity and basement influence on the development of the Kenya Rift, East Africa. *Tectonics*, 12/2, 591-606.
- Smith, C., and Hatton, I. R. (1998): Inversion tectonics in the Lyme Bay-West Dorset area of the Wessex Basin UK, In: Underhill, J. R. (Ed.), *The Development, Evolution and Petroleum Geology of the Wessex Basin*. Geological Society Special Publications, 133, 267-288.
- Smith, G. A., McIntosh, W. and Kuhle, A. J. (2001): Sedimentologic and geomorphic evidence for seesaw subsidence of the Santo Domingo accommodation-zone basin, Rio Grande rift, New Mexico. *Geological Society America Bulletin*, 113, 561-574.
- Soares, D. M., Alves, T. M. and Terrinha, P. (2012): The breakup sequence and associated lithospheric breakup surface: their significance in the context of rifted continental margins (West Iberia and Newfoundland margins, North Atlantic). *Earth and Planetary Science Letters*, 355, 311-326.
- Soares, D. M., Alves, T. M. and Terrinha, P. (2014): Contourite drifts on early passive margins as an indicator of established lithospheric breakup. *Earth and Planetary Science Letters* 401, 116-131.
- Song, G., Wang, H., Gan, H., Sun, Z., Liu, X., Xu, M., Ren, J., Sun, M., and Sun, D. (2014): Paleogene tectonic evolution controls on sequence stratigraphic patterns in the central part of deep-water area of Qiongdongnan Basin, northern South China Sea. *Journal of Earth Science*, 25/2, 275-288.
- Spencer, E. W. (1969): *Introduction to the structure of the Earth*. McGraw-Hill Book Company, London.

- Steckler, M. S., D. J. Reynolds, D. J., Coakley, B. J., Swirl, B. A. and Jarrard, R. D. (1993): Modelling passive margin sequence stratigraphy; In: Posamentier, H. W., Summerhayes, C. P., Haq B. U. and Allen, G. P. (Eds): Sequence stratigraphy and facies associations. International Association of Sedimentology, Blackwell Publishing Ltd, Oxford; 19-41.
- Steel, R. J. and Olsen, T. (2002): Clinoforms, clinoform trajectories, and deep-water sands: Proceeding of the 22nd Annual Bob, F. Perkins Research Conference, 367-381.
- Stern, R. J. (1994): Arc Assembly and Continental collision in the Neoproterozoic East African orogen: implications for the consolidation of Gondwanaland. *Annual Review Earth and Planetary Sciences* 22, 319-351.
- Sun, J. and Zhang, Z. (2009): Syntectonic growth strata and implications for late Cenozoic tectonic uplift in the northern Tian Shan, China. *Tectonophysics*, 463(1-4), 60-68.
- Suppé, J. (1983): Geometry and kinematics of fault-bend folding. *American Journal of Science*, 283 (7), 684-721.
- Suppé, J. S., Chou, G. T. and Hook, S. C. (1992): Rates of folding and faulting determined from growth strata. In: McClay, K. R. (Ed.), *Thrust tectonics*. London: Chapman and Hall, 105-122.
- Suppé, J., Sàbat, F., Anton Muñoz, J., Poblet, J., Roca, E. and Vergés, J. (1997): Bed-by-bed fold growth by kink-band migration: Sant Illorenç de Morunys, eastern Pyrenees. *Journal of Structural Geology*, 19 (3-4), 443-461.
- Surlyk, F. (1978): Jurassic basin evolution of East Greenland. *Nature*, 274, 130-133.
- Surlyk, F. (1989): Mid-Mesozoic syn-rift turbidite systems: controls and predictions. In: Collinson, J. D. (Ed.) *Correlation in Hydrocarbon Exploration*. Norwegian Petroleum Society, Graham & Trotman, London, 231-241.
- Sykes, L. R. (1978): Intraplate seismicity, reactivation of pre-existing zones of weakness, alkaline magmatism and other tectonism post-dating continental fragmentation. *Reviews of Geophysics and Space Physics*, 16, 621-688.
- Szatmari, P. (2000): Habitat of Petroleum along the South Atlantic margins. In: Mello, M. R. and Katz, B. J. (Eds), *Petroleum Systems of South Atlantic margins*. American Association of Petroleum Geologists Memoir 73, 69-75.
- Tavani, S., Storti, F. and Salvini, F. (2007): Modeling growth stratal architectures associated with double edge fault-propagation folding. *Sedimentary Geology*, 196(1-4), 119-132.
- Teisserenc, P. and Villemin, J. (1990): Sedimentary basin of Gabon- Geology and oil systems. In: Edwards J. D., Santogrossi, P. A. (Eds), *Divergent/passive margin basins*. American Association of Petroleum Geologists Memoir 48, 177-199.

- Torsvik, T. H., Rouse, S., Labails, C. and Smethurst, M. A. (2009): A new scheme for the opening of the South Atlantic Ocean and the dissection of an Aptian salt basin. *Geophysical Journal International*, 177 (3), 1315-1333.
- Tucholke, B. E., Sawyer, D. S., Sibuet, J.-C. (2007): Breakup of the Newfoundland-Iberia rift. In: Karner, G.D., Manatschal, G., Pinheiro, L.M. (Eds.), *Imaging, Mapping and Modelling Continental Lithosphere Extension and Breakup*. Geological Society Special Publications, London, 9-46.
- Turner, J. P. and Williams, G. A. (2004): Sedimentary basin inversion and intraplate shortening. *Earth-Science Reviews*, 65 (3-4), 277-304.
- Trudgill, B. and Cartwright, J. (1994): Relay-ramp forms and normal-fault linkages, Canyonlands National Park, Utah Geological Society of America Bulletin, 106, 1143-1157.
- Trudgill, B. and Underhill, J. R. (2002): Introduction to the structure and stratigraphy of rift systems. *American Association of Petroleum Geologists Bulletin*, 86, 931-933.
- Twichell, D. C. and Roberts, D. G. (1982): Morphology, distribution, and development of submarine canyons on the US Atlantic Continental Slope between Hudson and Baltimore. *Geology* 10, 408-412.
- Twichell, D. C., Schwab, W. C., Nelson, C. H., Kenyon, N. H. and Lee, H. J. (1992): Characteristics of a sandy depositional lobe on the outer Mississippi fan from SeaMARC IA side scan sonar images. *Geology*, 20, 689-692.
- Unrug, R. (1996): The assembly of Gondwanaland. Scientific results of IGCP Project 288: Gondwanaland sutures and mobile belts. *Episodes* 19, 11-20.
- Unrug, R. (1997): Rodinia to Gondwana: The geodynamic map of Gondwana supercontinent assembly. *Geological Society of America Today* 7/1, 1-6.
- Untemehr, P., Curie, D., Olivet, J. L., Goslin, J. and Beuzart, P. (1988): South Atlantic fits and intraplate boundaries in Africa and South America. *Tectonophysics*, 155, 1-4, 169-179.
- Vail, P. R., Mitchum, R. M. Jr, and Thompson III, S. (1977): Seismic stratigraphy and global changes of sea level: Part 3: Relative changes of sea level from coastal onlap. In: Payton, C. E. (Ed.), *Seismic Stratigraphy-Applications to Hydrocarbon Exploration*: American Association of Petroleum Geologists Memoir 26, 63-81.
- Vail, P. R. (1987): Seismic stratigraphy interpretation using sequence stratigraphy: Part 1: Seismic stratigraphy interpretation procedure. In: Bally, A. W. (Ed.), *Atlas of Seismic Stratigraphy*. American Association of Petroleum Geologists Studies in Geology 27, Tulsa, 1-10.
- Vanneste, M., Mienert, J. and Bunz, S. (2006): The Hinlopen Slide: A giant, submarine slope failure on the northern Svalbard margin, Arctic Ocean. *Earth and Planetary Science Letters*, 245, 373-388.

- Van Wagoner, J. C., Posamentier, H. W., Mitchum, R. M., Vail, P. R., Sarg, J. F., Loutit, T. S. and Hardenbol, J. (1988): An overview of the fundamentals of sequence stratigraphy and key definitions. In: Wilgus, C. K., Hastings, B. S., Kendall, C. G., Posamentier, H. W., Ross, C. A. and Van Wagoner J. C. (Eds), Sea level changes: An integrated approach: Society of Economic Palaeontologists and Mineralogists Special Publication 42, 39-45.
- Van Wagoner, J. C., Mitchum, R. M., Campion, and K. M. Rahmanian, V. D. (1990): Siliciclastic sequence stratigraphy in well-logs, cores, and outcrops: Concepts for high-resolution correlation of time and facies. American Association of Petroleum Geologists Exploration Series, 7.
- Varnes, D. J. (1978): Chapter 2: Slope movement types and processes. In: Varnes D. J. (Ed.), Landslides: Analysis and control. Transportation Research Board Special Report 176, 11-33.
- Vergés, J., Marzo, M. and Muñoz, J. A. (2002): Growth strata in foreland settings. *Sedimentary Geology*, 146 (1-2), 1-9.
- Warren, M. J. (2009): Tectonic inversion and petroleum system implications in the rifts of Central Africa. *Frontiers Innovation*. Calgary Alberta Convention, 461-464.
- Watterson, J. (1986): Fault dimensions, displacements, and growth. *Pure and Applied Geophysics*, 124 (1-2), 365-373.
- Watts, A. B. and Stewart, J. (1998): Gravity anomalies and segmentation of the continental margin offshore West Africa. *Earth and Planetary Science Letters*, 156, 239-252.
- Weimer, P. (1989): Sequence stratigraphy of the Mississippi fan (Plio-Pleistocene), Gulf of Mexico. *Geo-Marine Letters* 9, 185–272.
- Weimer, P. (1990): Sequence stratigraphy, facies geometries, and depositional history of the Mississippi Fan, Gulf of Mexico (1). *American Association of Petroleum Geologists Bulletin*, 74/4, 425-453.
- Weimer, P. (1991): Seismic facies, characteristics, and variations in channel evolution, Mississippi Fan (Plio-Pleistocene), Gulf of Mexico. In: Weimer, P. and Link, M. H. (Eds); *Seismic Facies and Sedimentary Processes of Submarine Fans and Turbidite Systems*: New York, Springer-Verlag, 323-347.
- Weimer, P., and Shipp, C. (2004): Mass-transport complex: musing on past uses and suggestions for future directions, *in Proceedings Offshore Technology Conference*, 3-6 May 2004.
- Weimer, P., and Slatt, R. M. (2007): 7. Deep-water Reservoir Elements: Mass-transport complexes and slides, petroleum systems of deep-water settings. *Society of Exploration Geophysicists and European Association of Geoscientists and Engineers*, 7-1-7-32.
- Wernicke, B. (1981): Low-angle normal faults in the Basin and Range Province: Nappe tectonics in an extending orogen. *Nature*, 291/5817, 645-648.

- Wernicke, B. (1985): uniform-sense normal simple shear of continental lithosphere. *Canadian Journal of Earth Sciences*, 22, 108-125.
- White, N. J., Jackson, J. A. and Mckenzie, D. P. (1986): The relationship between the geometry of normal faults and that of the sedimentary layers in their hanging-walls. *Journal of Structural Geology*, 8(8), 897-909.
- Whiteman, A. (Ed.) (1982): *Nigeria: Its petroleum geology, resources, and potential*. London: Graham and Trotman, 394.
- Whitmarsh, R. B., Manatschal, G., Minshull, T. A., (2001): Evolution of magma-poor continental margins from rifting to seafloor spreading. *Nature* 413, 150-154.
- Whitmarsh, R. B. and Wallace, P. J. (2001): The rift-to-drift development of the West Iberia non-volcanic continental margin; a review of the contribution of Ocean Drilling Program Leg 173. In: Beslier, M-O., Whitmarsh, R. B. and Wallace, P. J. (Eds), *Proceedings of the ODP, Scientific Results. Vol. 173. Return to Iberia: covering Leg 173 of the cruises of the Drilling Vessel "Joides Resolution", Lisbon, Portugal, to Halifax, Nova Scotia, Sites 1065-1070, 15 April-15 June 1997*. Texas A & M University Ocean Drilling Program. 31, 1-36.
- Williams, G. D., Powell, C. M. and Cooper, M. A. (1989): Geometry and kinematics of inversion tectonics. In: Cooper, M. A. and Williams, G. D. (Eds), *Inversion Tectonics*, Geological Society, London, Special Publications, 44, 3-15.
- Williams, G. D. (1993): Tectonics and seismic sequence stratigraphy: an introduction. In: Williams, G. D. and Dobb, A. (Eds): *Tectonics and seismic sequence stratigraphy*: Geological Society, London, Special Publications, 71 (1), 1-13.
- Wilson, J. T. (1965): A new class of faults and their bearing on continental drift. *Nature*, 207, 343-347.
- Wilson, P. G., Turner, J. P. and Westbrook, G. K. (2003): Structural architecture of the ocean-continent boundary at an oblique transform margin through deep-imaging seismic interpretation and gravity modeling: Equatorial Guinea, West Africa. *Tectonophysics*, 374 (1-2), 19-40.
- Winterer, E. L. and Bosellini, A. (1981): Subsidence and sedimentation on Jurassic passive continental margin, Southern Alps, Italy. *American Association of Petroleum Geologists Bulletin*, 65 (3): 394-421.
- Withjack, M. O., and Drickman-Pollock, D. J. (1984): Synthetic seismic-reflection profiles and rift-related structures: *American Association of Petroleum Geologists Bulletin*, 68, 1160–1178.
- Withjack, M. O., Olson, J. and Peterson, E. (1990): Experimental models of extensional forced folds: *American Association of Petroleum Geologists Bulletin*, 74, 1038-1054.

- Withjack, M. O., Schlische, R. W. and Olsen, J. (1998): Diachronous Rifting, Drifting, and Inversion on the passive margin of Central Eastern North America: An analog for other passive margins. *American Association of Petroleum Geologists Bulletin*, 82, 817-835.
- Withjack, M. O., Schlische, R. W. and Olsen, P. E. (2002): Rift-basin structure and its influence on sedimentary systems. *Sedimentation in Continental Rifts*. Society of Economic Palaeontologists and Mineralogists Special Publications 73, 57-81.
- Withjack, M. O., Schlische, R. W. and Baum, M. S. (2009): The extensional development of the Fundy rift basin, southeastern Canada. *Geological Journal*, 44, 631-651.
- Withjack, M. O., Schlische, R. W., Malinconico, M. L. and Olsen, P. E. (2012): Rift-basin development: lessons from the Triassic-Jurassic Newark Basin of eastern North America. In: Mohriak, W. U., Danforth, A., Post, P. J., Brown, D. E., Tari, G. C., Nemcok, M. and Sinha, S. T. (Eds): *Conjugate Divergent Margins*. Geological Society, London, Special Publications, 369, 301-321.
- Woodcock, N. H. (1979): Sizes of submarine slides and their significance. *Journal of Structural Geology*, 1, 137-142.
- Young, M. J., R. L. Gawthorpe and Sharp, I. R. (2000): Sedimentology and sequence stratigraphy of a transfer zone coarse-grained delta, Miocene Suez Rift, Egypt. *Sedimentology*, 47, 1081-1104.
- Younes, A. I and McClay, K. (2002): Development of accommodation zones in the Gulf of Suez-Red Sea rift, Egypt. *American Association of Petroleum Geologists Bulletin*, 86, 1003-1026.
- Zalan, P. V., Nelson, E. P., Warme, J. E., and Davis, T. L. (1985): The Piauí basin: Rifting and wrenching in an Equatorial Atlantic transform basin. In: Biddle, K.T., Christie-Blick, N. (Eds), *Strike-slip deformation, basin formation, and sedimentation*. Special Publication Society of Economic Paleontologists and Mineralogists 37, 143-158.
- Zalan, P. V. (2011): Fault-related folding in the deep waters of the equatorial margin of Brazil. In: McClay, K., Shaw, J. and Suppé, J. (Eds), *Thrust fault-related folding*. *American Association of Petroleum Geologists Memoir* 94, 335-355.
- Zeng, H. (2013): Frequency-dependent seismic-stratigraphic and facies interpretation. *American Association of Petroleum Geologists Bulletin* 97 (2), 201-221.
- Zhang, G., Zhang, P., Min, W. and Chen, J. (2006): The identification and application of growth strata to the foreland fold- and thrust belt during mountain building. *Seismology and Geology*, 28 (2), 299-311.
- Ziegler, P. A. (1989): Geodynamic model for Alpine intraplate compressional deformation in Western and Central Europe. In: Cooper, M. A. and Williams, G. D. (Eds). *Inversion Tectonics*, Geological Society, London. Special Publications, 44, 63-85.

- Ziegler, P. A., Cloetingh, S. and Van Wees, J-D. (1995): Dynamics of intraplate compressional deformation: the Alpine foreland and other examples. *Tectonophysics* 252, 7-59.
- Ziegler, P. A. and Cloetingh, S. (2004): Dynamic processes controlling the evolution of rifted basins. *Earth- Science Reviews*, 64, 1-50.
- Ziesch, J., Aruffo, C. M., Tanner, D. C., Deilecke, T., Dance, T., Henk, A., Weber, B., Tenthorey, E., Lippmann, A., and Krawczyk, C. M. (2017): Geological structure and kinematics of normal faults in the Otway Basin, Australia.